0083994

DOE/ORP-2005-01

INITIAL SINGLE-SHELL TANK SYSTEM PERFORMANCE ASSESSMENT FOR THE HANFORD SITE

DATA PACKAGE

SECTION

2 OF 4

The SSTs were constructed in place with carbon steel (ASTM 2005) lining the bottom and sides of a reinforced concrete shell. The tanks have concave bottoms (i.e., center of tanks lower than the perimeter) and a curving intersection of the sides and bottom. The inlet and outlet lines are located near the top of the liners (Figure 2-64). The 100-Series tanks were constructed with cascade overflow lines in a 3-tank series that allowed gravity flow of liquid between tanks. The 200-Series tanks were connected and fed to diversion box C-252 (Crumpler 2004).

2.10.2.2 Ancillary Equipment

A complete listing of the WMA C ancillary equipment currently identified for inclusion in the SST system closure is provided in Lee (2004). As discussed in Section 2.5.4, the ancillary components included in the SST PA consist of the underground waste transfer lines and MUSTs located inside each WMA boundary. For WMA C, the ancillary components analyzed consist of the C tank farm waste transfer piping and five MUSTs. The MUSTs consist of one catch tank (241-C-301) and the four tanks in the 244-CR vault (244-CR-001, 244-CR-002, 244-CR-003, 244-CR-011).

Multiple levels of piping were installed over time in WMA C. A time line of piping installations is described in Williams (2001c). It is estimated that there are approximately 9.3 mi (+/- 2.7 mi) of waste transfer piping in the C tank farm (Field 2003a).

2.10.3 Geology

Following is an overview of the geology of WMA C summarized from the information provided in Reidel et al. (2006). Because WMAs A-AX and C are in close proximity (Figure 2-2 in Section 2.3) and have similar geologic conditions, they are discussed together in Reidel et al. (2006) and will be discussed together here. A generalized cross-section through WMAs A-AX and C is shown in Figure 2-65. Maps and cross-sections presented in Reidel et al. (2006) illustrate the distribution and thicknesses of these units in additional detail.

Figure 2-64. Typical Configuration and Dimensions of Single-Shell Tanks in Waste Management Area C

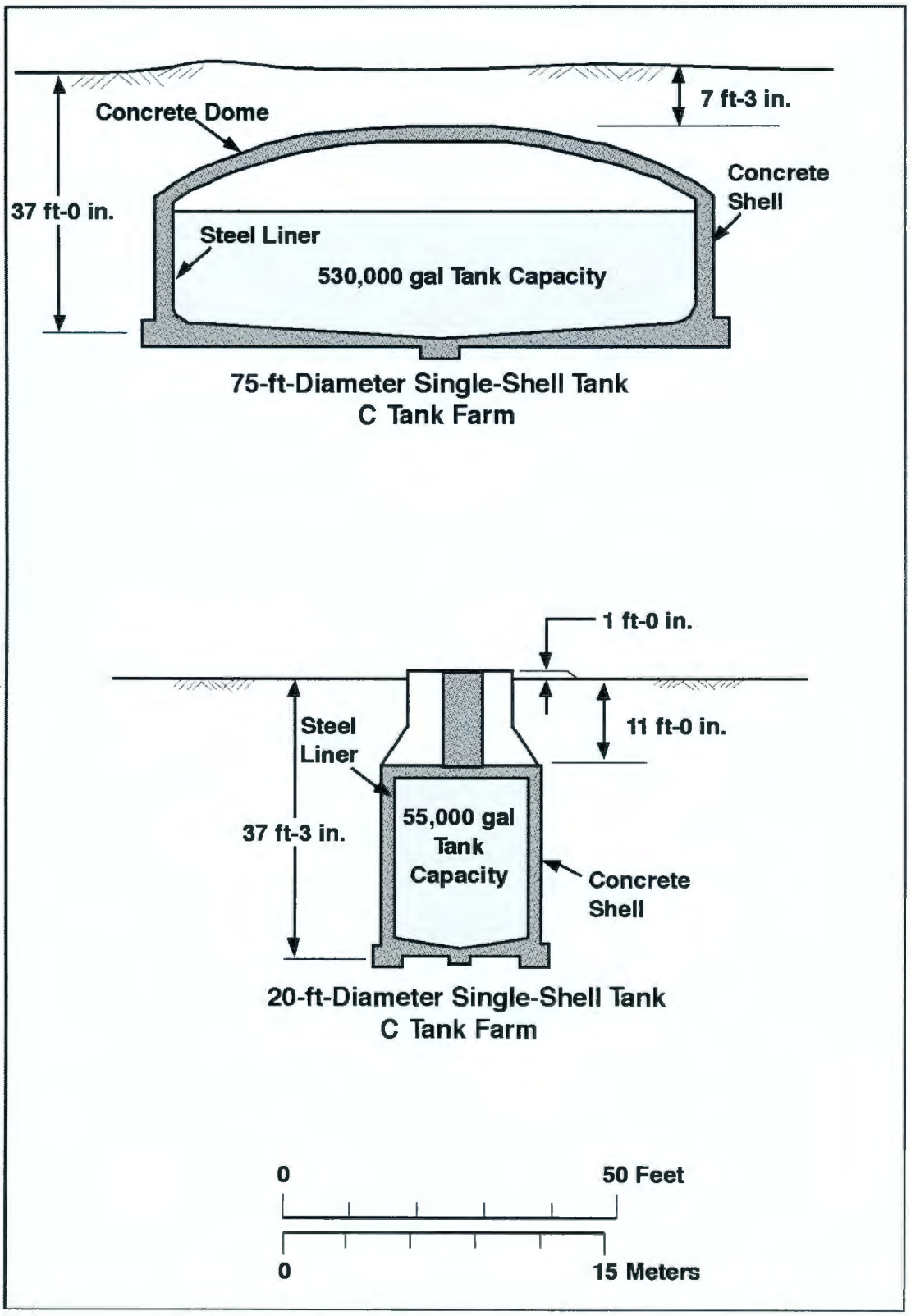

Figure 2-65. Fence Diagram Showing Cross-Sections through Waste Management Areas A-AX and C[a]

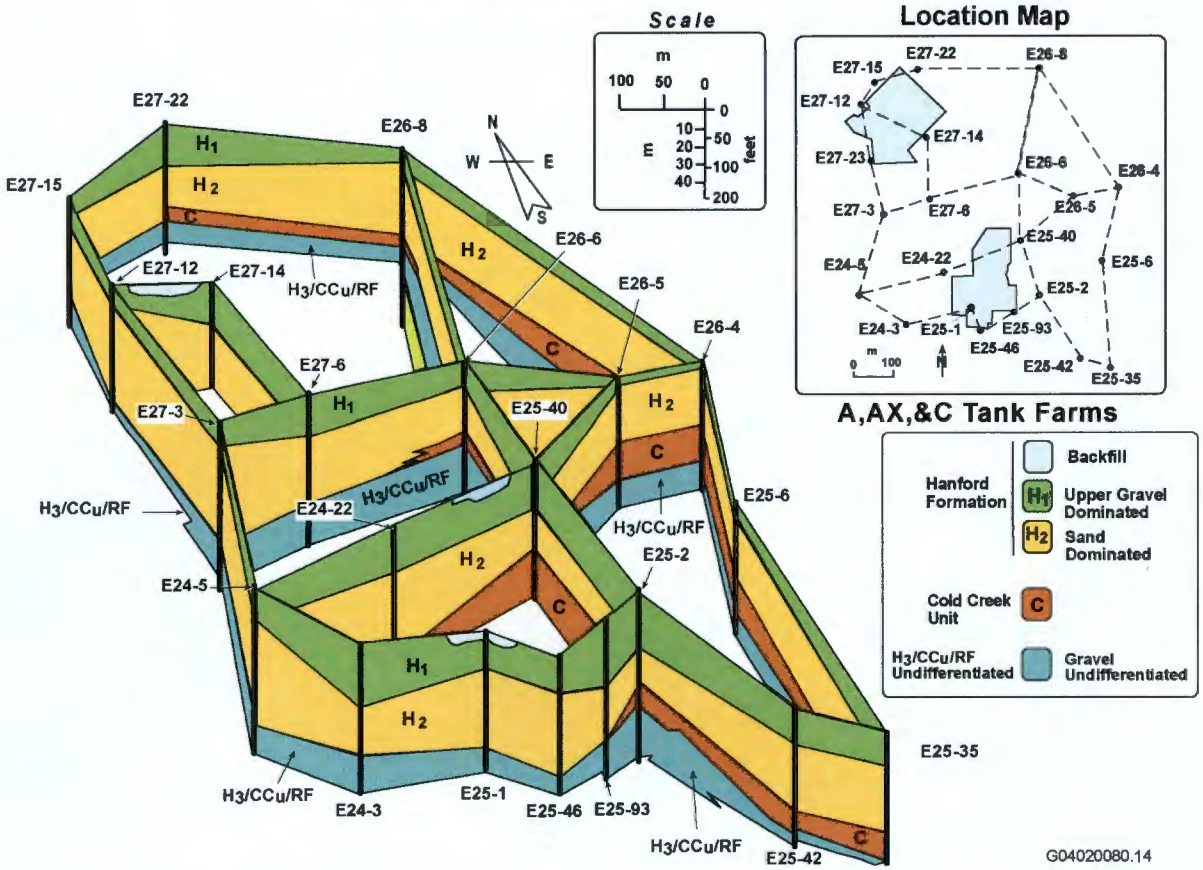

[a] *Reidel et al. (2006)*

Seven stratigraphic units lie within WMAs A-AX and C. From oldest to youngest, the primary geologic units are:

- Columbia River Basalt Group
- Undifferentiated Cold Creek unit fine unit and/or Ringold Formation
- Undifferentiated Cold Creek unit gravel and/or Ringold Formation Unit A?
- Hanford formation – lower gravelly sequence (H3 unit)
- Hanford formation – sand sequence (H2 unit)
- Hanford formation – upper gravelly sequence (H1 unit)
- Recent deposits.

The general characteristics of these units are described in Section 2.3.4.1 and in more detail in Reidel et al. (2006). The SSTs at WMAs A-AX and C were emplaced within the Hanford formation sediments of the upper, gravel-dominated (H1) unit, and may locally intercept the upper portions of the sand-dominated Hanford (H2) unit. The water table or potentiometric surface lies approximately 60 m (approximately 200 ft) below the bottom of the tank farms excavations at the basal portion of the Hanford formation (i.e., lower sand/silt dominated) H3 unit, or within the uppermost portions of the Cold Creek unit or Ringold Formation.

2.10.4 Hydrology

Following is an overview of the hydrology of the uppermost, unconfined aquifer beneath WMA C. The general geohydrology of the Hanford Site is summarized in Section 2.3.5.2. More detailed information supporting this section can be found in Reidel et al. (2006), Wood et al. (2003), and Hartman et al. (2004). Currently, the general groundwater flow direction in the unconfined aquifer beneath WMA C is to the southwest. The water table is very flat overall, with an estimated hydraulic gradient of 0.00033. The estimated groundwater flow velocity ranges from 1.2 to 2.3 m/day (Hartman et al. 2004).

The shift in discharge of large volumes of wastewater in the early 1950s to B Pond raised the water table in the vicinity of WMAs C and A-AX as much as 4.9 m (16 ft) above the pre-Hanford Site operations level (Hartman et al. 2004). Water levels began to decline in the late 1980s when wastewater discharges were reduced. The decline has become even more pronounced since other effluent discharges throughout the 200 Areas ceased in 1995. Water levels are expected to continue declining within the region surrounding WMAs A-AX and C. It is expected the water table will return to pre-Hanford Site conditions, the hydraulic gradient will decrease to 1.0E-5 m/m, and the flow direction will be to the east (Cole et al. 2001a)

Currently, the water table beneath WMA C lies 122 m (400 ft) amsl with about 77 m (255 ft) of vadose zone. The aquifer thickness, based on the top of basalt at 108 m (355 ft), is approximately 13.4 m (44 ft). The aquifer materials consist dominantly of sandy gravel or silty sandy gravel. Hydraulic conductivity values reported for the aquifer in this area vary considerably, ranging from 0.04 (silt lenses within the sandy gravel) to 6,900 m/day. Additional hydraulic property data from aquifer testing at wells near WMA C is provided in Reidel et al. (2006) and Hartman et al. (2004).

2.10.5 Vadose Zone Conditions

This section summarizes WMA C vadose zone monitoring and characterization activities and the current understanding of contamination in the vadose zone.

2.10.5.1 Monitoring and Characterization

WMA C has 70 leak detection wells (Figure 2-66) available for leak detection monitoring and to provide access for limited vadose zone characterization (e.g., geophysical logging). These drywells were drilled from 1944 to 1982. The depth ranges for most of these drywells is between 100 and 150 ft bgs.

In 1997, C farm drywells were logged using a high-resolution spectral gamma logging system. This effort was part of the baseline characterization for WMA C. Results are documented in DOE-GJO (1998c) and its associated addendum DOE-GJO (2000g).

The major gamma-emitting contaminants associated with WMA C are cesium-137 and cobalt-60 with lesser amounts of europium-154. These contaminants are located mostly in and around areas of confirmed or suspected tank and pipeline leaks. Although most of the drywells are deeper than the surrounding contamination, some zones of contamination extend deeper than nearby drywells. Consequently, the maximum depth of vadose zone contamination is not known in some areas of WMA C.

Figure 2-66. Vadose Zone Monitoring Network for Waste Management Area C

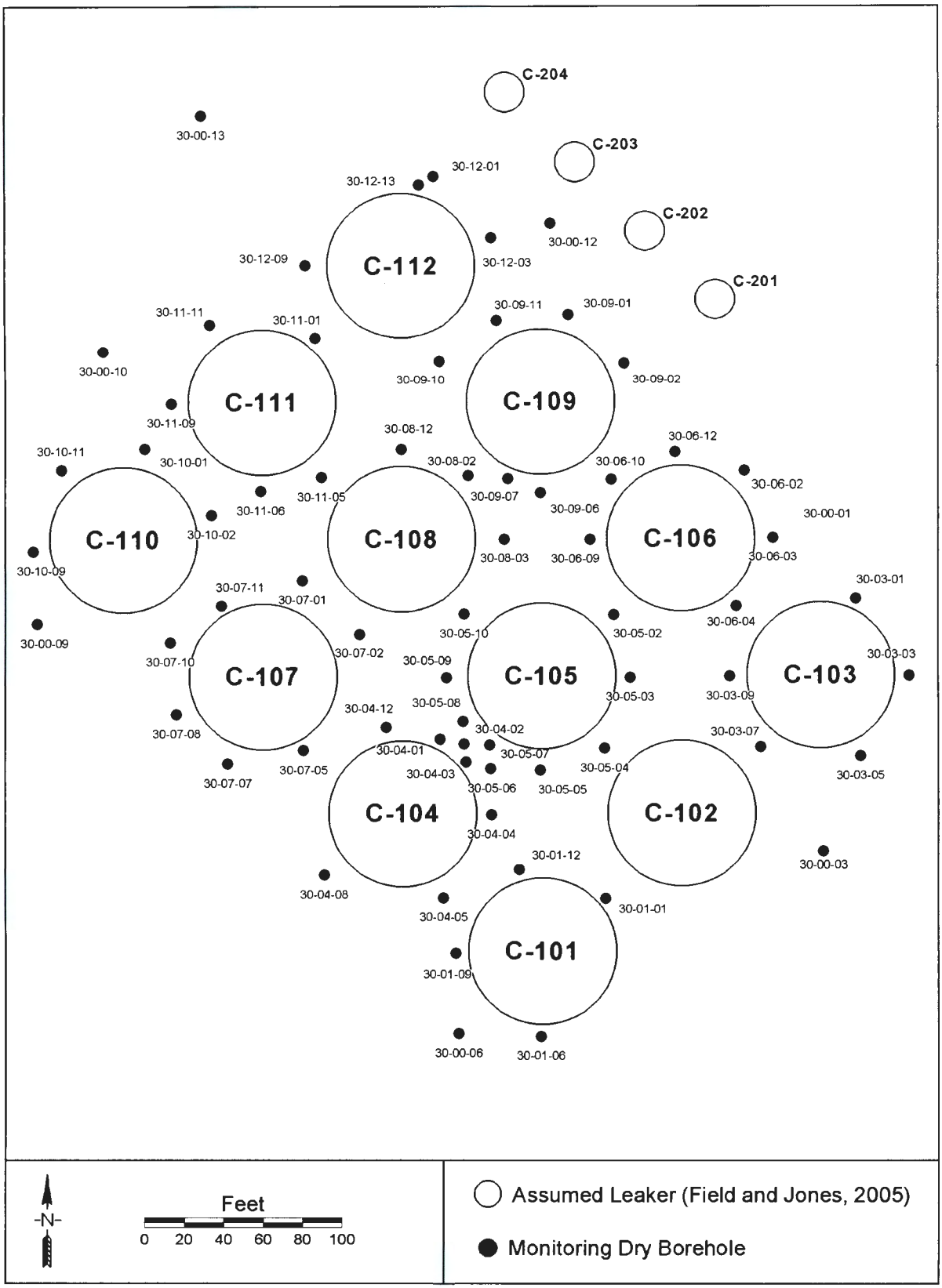

Limitations of estimates on the extent of contamination include the following:

- No data are available from directly under the tanks.
- No data are available below the bottoms of drywells. The deepest drywell in WMA C is 155 ft bgs (well 30-00-03), and the maximum logged depth is 143 ft bgs (well 30-04-08).

As part of the ongoing vadose zone characterization, a WMA C Phase I field investigation study is presently underway (Crumpler 2004). A FIR will document the results of the field characterization data. Additional information on manmade radionuclide distribution and movement with WMA C will be discussed in the FIR scheduled to be issued in fiscal year 2006.

2.10.5.2 Contamination

Figure 2-67 provides a visualization of the vadose zone contamination beneath WMA C as represented by cesium-137 data. This figure is a three-dimensional perspective of WMA C providing locations of tanks and associated drywells. Tanks considered to be assumed leakers based on information in Field and Jones (2005) are shown with darker shading. Each drywell is represented with a single vertical line. Shaded rings around the drywells indicate the level of vadose zone contamination based on spectral gamma logging results. Only the more significant soil contamination zones are shown. Zones with contamination levels less than 10 pCi/g are not shown.

An overall assessment of the spectral gamma logging data from C farm drywells indicates that, with the exception of contamination zones near tank C-105 and three unplanned pipeline releases, most vadose zone contamination originated from surface or near-surface contamination events that were not generally associated with particular recorded events and are not considered to be significant sources of vadose zone contamination (Wood et al. 2003).

Neither tank C-104 nor tank C-105 is listed as a confirmed or suspected leaker in Hanlon (2005). Spectral gamma logging data indicate the presence of contamination in the region between tanks C-104 and C-105. The most concentrated contamination occurs at drywell 30-05-07 on the southwest side of tank C-105 (Figures 2-66 and 2-67), where two high cesium-137 concentration zones occur at and below the tank bottom (Wood et al. 2003). The origin of the contamination has not been conclusively established and a leak from tank C-105 cannot be ruled out. A characterization borehole was drilled between tanks C-104 and C-105 during fiscal year 2004 (Crumpler 2004). Vadose zone sample data from that borehole will be incorporated into the analysis presented in the FIR for WMA C.

Evidence from the historical record indicates that three unplanned near-surface release events (UPR-200-E-81, UPR-200-E-82, UPR-20-E-86) occurred on the southwest side of the C tank farm (Figure 2-63). These events are known to have made relatively significant contributions to vadose zone contamination (Wood et al. 2003). The UPR-200-E-81 event occurred near the 241-CR-151 diversion box and involved the loss of approximately 36,000 gal of waste. The UPR-200-E-82 event occurred near the 241-C-152 diversion box and involved the loss of approximately 2,600 gal of waste. The UPR-200-E-86 event occurred in a pipeline break near the southwest corner of the C tank farm and involved the loss of approximately 17,400 gal of waste.

Figure 2-67. Three-Dimensional Perspective of Waste Management Area C Tanks and Drywells Showing Occurrence of Significant (>10 pCi/g) Cesium-137 Contamination in the Vadose Zone

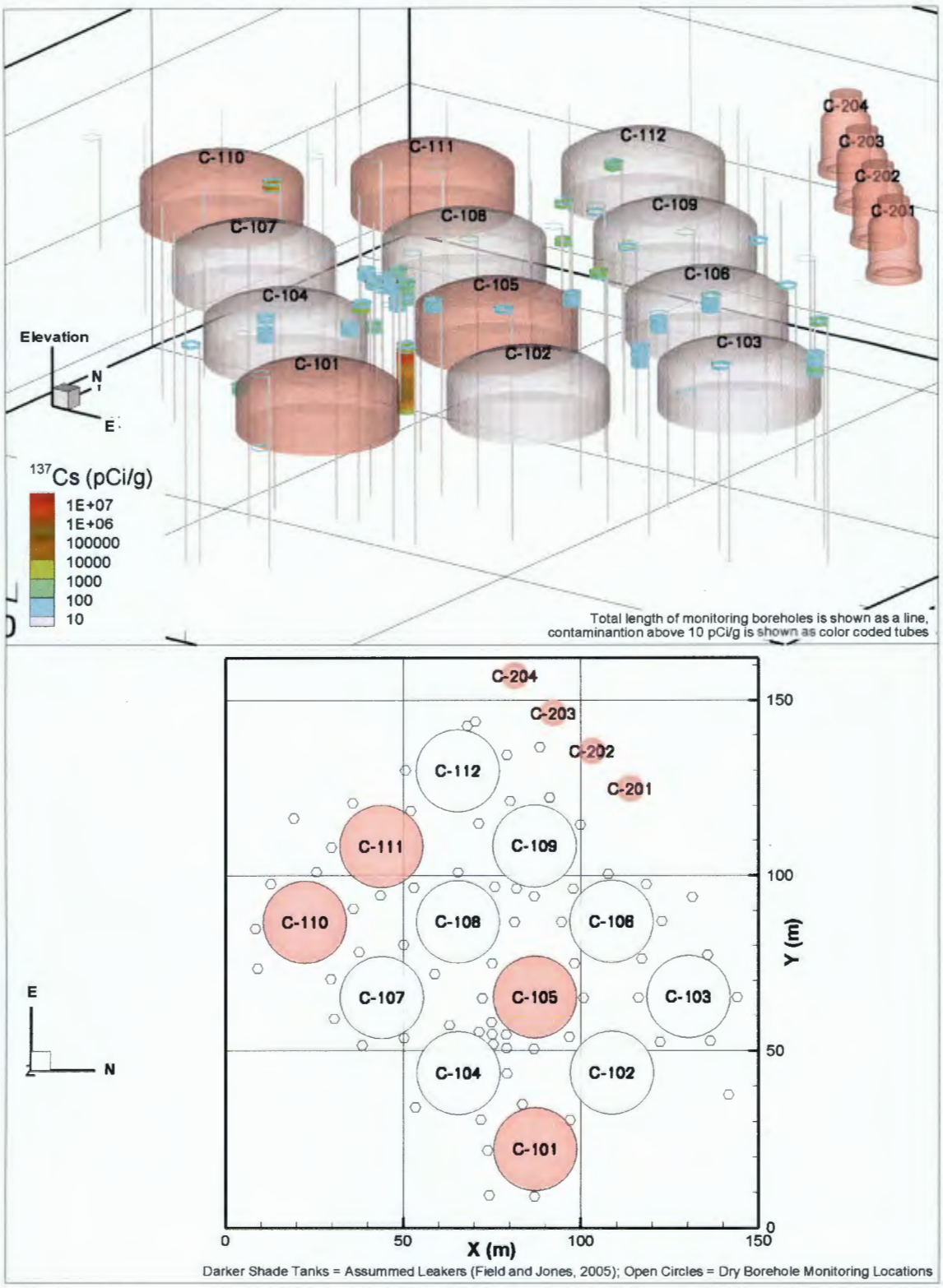

Spectral gamma logging data also indicate the presence of generalized near-surface contamination across WMA C. About a dozen of the drywells have elevated cesium-137 gamma activity in the upper 15 ft of the vadose zone. Two of these higher concentration zones, between tanks C-104 and C-105 and between tanks C-108 and C-109, are apparently related to small transfer line leaks (Wood et al. 2003).

2.10.6 Unconfined Aquifer Conditions

This section summarizes WMA C groundwater monitoring and characterization activities and the current understanding of contamination in the unconfined aquifer.

2.10.6.1 Monitoring and Characterization

The initial background-monitoring program for WMA C is complete; monitoring is currently conducted under an interim status indicator evaluation program as described in Horton and Narbutovskih (2001). The WMA C monitoring network currently consists of nine RCRA groundwater monitoring wells located outside the C tank farm fenceline. To date, monitoring results have not indicated that sources within WMA C have affected groundwater quality. The contaminant indicator parameters and statistical evaluation methodology for the WMA C groundwater indicator evaluation program are described in Horton and Narbutovskih (2001).

Three modifications to the monitoring plan have been issued through interim change notices (Horton and Narbutovskih 2002, 2003a, 2003b). Results of the groundwater detection indicator evaluation program are published annually.

When the monitoring network for WMA C was designed, flow was believed to be due west. A general flow direction to the southwest has subsequently been established based on direct flow measurements with a colloidal boroscope (Hartman et al. 2004). Three new downgradient wells and one new upgradient well were installed in fiscal year 2003 to improve the capability of the detection network to monitor the site.

During fiscal year 2003, the site was monitored with the original configuration of wells (Figure 2-63). Sampling data from the four new monitoring wells are expected to be available for inclusion in future annual groundwater monitoring reports. Monitoring under the indicator evaluation program will continue until the entire WMA is closed, or at such time as there is a shift to assessment monitoring as a result of statistically significant changes in indicator parameter concentrations in groundwater.

2.10.6.2 Contamination

Following is a summary of the fiscal year 2003 results adapted from Hartman et al. (2004). Additional detail on groundwater contamination and geochemistry at WMA C can be found in Hartman et al. (2004) and Reidel et al. (2006).

Wells were sampled quarterly during fiscal year 2003 at the request of Ecology due to rising trends in sulfate, nitrate, and calcium currently detected in both upgradient and downgradient wells. The critical mean values for the indicator parameters (i.e., pH, specific conductance, total organic carbon, and total organic halides) were not exceeded.

In 1999, technetium-99 began rising in upgradient well 299-E27-7, reaching a maximum in January 2002, then declining sharply to the current value of 39 pCi/L in September 2003 (Figure 2-68). Nitrate followed a similar trend to technetium-99 in this upgradient well. The current trend appears to be stable. Contamination sources both inside and outside of WMA C have been suggested but the origin of the concentration spike has not been conclusively established. Further insight into the source of the technetium-99 may be possible when data from the four new fiscal year 2003 wells are available.

Figure 2-68. Technetium-99 Concentrations Compared to Nitrate Concentrations for Upgradient Well 299-E27-7 at Waste Management Area C [a]

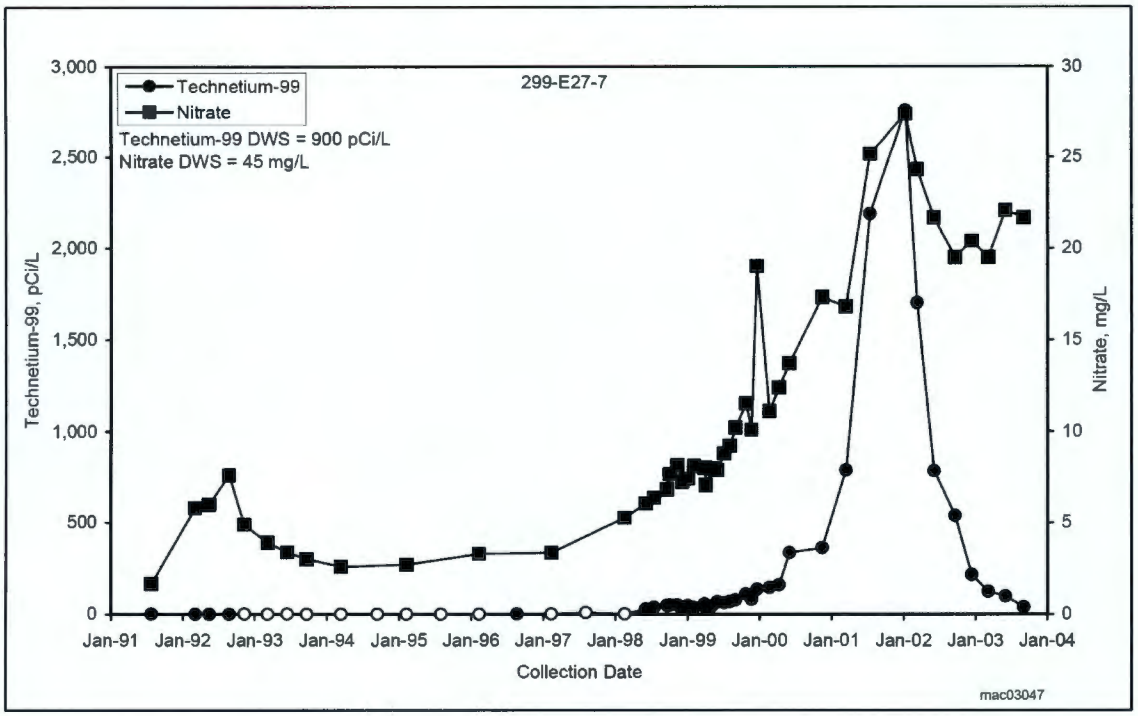

[a] *Hartman et al. (2004)*

2.10.7 Reference Case Source Terms

The reference case describes a set of assumed post-retrieval conditions that are based on current waste retrieval plans. The reference case analysis for WMA C includes three source terms consisting of past UPRs, residual SST waste, and residual ancillary equipment waste. Table 2-23 provides a listing of the reference case source terms for WMA C, and the inventory data source for that source term.

Source term inventories (reference case) for WMA C are provided in Table 2-24. To simplify the table, only the contaminants that dominate post-closure impacts are shown. All BBI contaminants are included in the reference case modeling analysis. Refer to Section 2.5 for a summary of source term inventory development methods. Complete source term inventory data are provided in Appendix C.

2.10.7.1 Past Unplanned Releases

The WMA C reference case includes eight past UPRs associated with SSTs (C-101, C105, C110, C-111, C-201, C-202, C-203, C-204) and four past UPRs associated with ancillary equipment (UPR-200-E-81, UPR-200-E-82, UPR-200-E-86, UPR-200-E-107). Volume estimates for those 12 waste loss events were developed by Field and Jones (2005) and vadose zone contaminant inventories were generated by Corbin et al. (2005) (Section 2.5.2).

2.10.7.2 Residual Single-Shell Tank Waste

The WMA C reference case includes residual waste in each of the 12 100-Series and four 200-Series SSTs in the C tank farm. Residual waste volume estimates for all tanks except C-106 were based on retrieving waste to the HFFACO Milestone M-45-00 goals (360 ft^3 for 100-Series tanks and 30 ft^3 for 200-Series tanks) (Ecology et al. 1989). Tank C-106 has been retrieved and is now undergoing an Appendix H exception request (Sams 2004b). Inventory estimates for tanks other than C-106 were generated with the use of the HTWOS model (Kirkbride et al. 2005), which accounts for the waste retrieval technology and tracks the fate of soluble and insoluble constituents in the waste (Section 2.5.3). Residual inventories for tank C-106 are based on post-retrieval sample analyses (Sams 2004a) rather than the HTWOS model.

2.10.7.3 Residual Ancillary Equipment Waste

The WMA C reference case includes the plugged and blocked piping in the C tank farm and the residual waste in five MUSTs consisting of one catch tank (241-C-301) and the four tanks in the 244-CR vault (244-CR-001, 244-CR-002, 244-CR-003, 244-CR-011) (Section 2.5.4). In the previous risk assessment for WMA C (Lee 2004), no information existed on the volume of plugged pipelines and a very conservative estimate was made. For that estimate, the length of all pipelines within WMA C was totaled (approximately 20,000 linear ft). It was assumed that 25% of those lines were blocked or plugged, which led to a volume of 250 ft^3 of blocked pipelines. Since that assumption was made, Lambert (2005) has developed a revised estimate (28 L) of the volume of plugged and blocked pipelines in WMA C. That estimate is much lower than the previous estimate but was based on information about the actual conditions of the pipeline systems in WMA C. The blocked pipeline, a cascade line, was designed to drain by gravity, as were most other pipelines. For this reason, most failed pipelines (i.e., failed pressure testing of the pipeline) are expected to have only a small inventory of residual waste.

Volume estimates for the residual waste in the WMA C MUSTs were calculated by assuming each tank would be retrieved to a residual volume proportional to that required under the HFFACO Milestone M-45-00 for 200-Series tanks (Ecology et al. 1989). Contaminant inventories associated with the residual ancillary equipment waste were estimated using the average chemical composition of the waste in the WMA C SSTs.

Table 2-23. Reference Case Analysis of Waste Management Area C (2 pages)

Inventory and Source Terms					
Sources	**Assumed Retrieval Method**	**Residual Volume**	**Volume Associated with Past Release [a] gal**	**Basis for Contaminant Inventory Estimate**	
				Residual Waste [b]	**Past Release**
241-C-101	Mobile retrieval system	360 ft^3	1,000	HTWOS	Corbin et al. 2005
241-C-102	Sluicing	360 ft^3	None	HTWOS	None
241-C-103	Sluicing	360 ft^3	None	HTWOS	None
241-C-104	Sluicing	360 ft^3	None	HTWOS	None
241-C-105	Mobile retrieval system	360 ft^3	1,000	HTWOS	Corbin et al. 2005
241-C-106	Retrieved	360 ft^3	None	HTWOS	None
241-C-107	Sluicing	360 ft^3	None	HTWOS	None
241-C-108	Sluicing	360 ft^3	None	HTWOS	None
241-C-109	Sluicing	360 ft^3	None	HTWOS	None
241-C-110	Mobile retrieval system	360 ft^3	2,000	HTWOS	Corbin et al. 2005
241-C-111	Mobile retrieval system	360 ft^3	5,500	HTWOS	Corbin et al. 2005
241-C-112	Sluicing	360 ft^3	None	HTWOS	None
241-C-201	Vacuum	30 ft^3	550	HTWOS	Corbin et al. 2005
241-C-202	Vacuum	30 ft^3	450	HTWOS	Corbin et al. 2005
241-C-203	Vacuum	30 ft^3	400	HTWOS	Corbin et al. 2005
241-C-204	Vacuum	30 ft^3	350	HTWOS	Corbin et al. 2005
UPR-200-E-81	NA	NA	36,000	NA	Corbin et al. 2005
UPR-200-E-82	NA	NA	2,600	NA	Corbin et al. 2005
UPR-200-E-86	NA	NA	18,500	NA	Corbin et al. 2005
UPR-200-E-107	NA	NA	5	NA	Corbin et al. 2005
241-C-302 catch tank [c]	TBD [c]	19 ft^3	None	Average	None
244-CR-001 vault tank [c]	TBD [c]	27 ft^3	None	Average	None
244-CR-002 vault tank [c]	TBD [c]	8 ft^3	None	Average	None

Table 2-23. Reference Case Analysis of Waste Management Area C (2 pages)

Inventory and Source Terms					
Sources	**Assumed Retrieval Method**	**Residual Volume**	**Volume Associated with Past Release [a] gal**	**Basis for Contaminant Inventory Estimate**	
				Residual Waste [b]	**Past Release**
244-CR-003 vault tank [c]	TBD [c]	8 ft^3	None	HTWOS	None
244-CR-011 vault tank [c]	TBD [c]	27 ft^3	None	Average	None
241-C tank farm pipelines [d]	TBD	28 L	None	Lambert 2005	NA

[a] Past leak volumes listed in Field and Jones (2005).

[b] Residual inventories from HTWOS model output (Kirkbride et al. 2005).

[c] TBD = to be determined. Final disposition of MUSTs not yet determined; however, MUSTs were carried forward in the assessment assuming MUSTs will be retrieved to at least the HFFACO goal (Ecology et al. 1989, Milestone M-45-00) equivalent to the 200-Series tanks. The residual volume is calculated by ratio of the total volume of the MUST to the 200-Series tanks (e.g., the retrieval goal for the 55,000-gal 200-Series tanks is 30 ft^3; thus, a MUST that is ⅔ the size of the 200-Series tank would have a residual volume of 20 ft^3). Inventory was calculated based on average waste per ft^3 within the WMA calculated from the HTWOS model (Kirkbride et al. 2005).

[d] Final disposition of pipelines is not yet determined; however, pipelines were carried forward in the assessment. Pipeline residual volumes shown represent the volume of waste in plugged or blocked pipelines as determined by Lambert (2005).

NA = not applicable

Table 2-24. Reference Case Inventory Estimates for Waste Management Area C

Source Type	Dominant Contaminants for Groundwater Pathway Impacts [a]							Dominant Contaminants for Inadvertent Intruder Impacts [a]						
	C-14 Ci	Tc-99 Ci	I-129 Ci	Cr(VI) kg	NO_3 kg	NO_2 kg	U kg	Sr-90 Ci	Tc-99 Ci	Sn-126 Ci	Cs-137 Ci	Pu-239 Ci	Pu-240 Ci	Am-241 Ci
Past releases [b]	3.46E-01	6.93E+00	3.02E-02	1.11E+02	1.07E+04	4.35E+03	7.88E+00	1.76E+03	6.93E+00	9.13E-02	2.19E+04	1.28E+00	2.89E-01	5.63E+00
Tank residuals	6.24E-02	2.72E+00	1.29E-02	9.96E+01	2.60E+03	1.04E+03	2.43E+03	1.70E+05	2.72E+00	2.15E+00	2.01E+04	2.00E+02	4.29E+01	2.30E+02
Ancillary equipment residuals [c]	1.52E-03	5.86E-02	2.78E-04	2.15E+00	5.93E+01	2.24E+01	5.22E+01	NA	NA	NA	NA	NA	NA	NA

[a] The reference case analysis included all BBI contaminants. As described in Bowen (2004), the standard analyte list tracked in the BBI contains **25 chemicals** including:

- aluminum
- bismuth
- calcium
- chlorine
- chromium
- fluorine
- total inorganic carbon as carbonate
- iron
- mercury
- potassium
- lanthanum
- manganese
- sodium
- nickel
- nitrite
- nitrate
- oxalate
- lead
- phosphate
- silicon
- sulfate
- strontium
- uranium total
- zirconium
- total organic carbon

and **46 radionuclides** including:

- tritium
- carbon-14
- nickel-59
- cobalt-60
- nickel-63
- selenium-79
- strontium-90
- yttrium-90
- zirconium-93
- niobium-93m
- technetium-99
- ruthenium-106
- cadmium-113m
- antimony-125
- tin-126
- iodine-129
- cesium-134
- cesium-137
- barium 137m
- samarium-151
- europium-152
- europium-154
- europium-155
- radium-226
- actinium-227
- radium-228
- thorium-229
- protactinium-131
- thorium-232
- uranium-232
- uranium-233
- uranium-234
- uranium-235
- uranium-236
- neptunium-237
- plutonium-238
- uranium-238
- plutonium-239
- plutonium-240
- americium-241
- plutonium-241
- curium 242
- plutonium-242
- americium-243
- curium-243
- curium-244

[b] Inventories shown are the combined inventories from SST past releases and ancillary equipment past releases. Both release types were considered for the groundwater pathway analysis; however, only the SST past releases were included in the inadvertent intruder analysis (along with SST residuals).

[c] NA indicates insufficient information is available to make estimates of intruder impacts into ancillary equipment (e.g., pipelines, diversion boxes).

2.11 DESCRIPTION OF WASTE MANAGEMENT AREA B-BX-BY

This section provides site-specific information for WMA B-BX-BY. It is a summary from numerous documents that describe present conditions (Hanlon 2005), geology and hydrology (Reidel et al. 2006), subsurface contamination (Wood et al. 2000; Knepp 2002b), and source terms (Kirkbride et al. 2005; Field and Jones 2005; Lambert 2005; Corbin et al. 2005).

2.11.1 Background

WMA B-BX-BY is located in the north central portion of the 200 East Area (Figure 2-69) and contains the B, BX, and BY tank farms. In general, WMA B-BX-BY is an L-shaped area where, in the southern edge of the BY tank farm, it is adjacent to the northern boundary of the BX tank farm, while the western edge of the B farm is next to the eastern edge of the BX tank farm, separated by Baltimore Avenue. BX and BY tank farms share an enclosing fence, while B tank farm has its own enclosing fence.

The current understanding of contaminant occurrences and environmental conditions at WMA B-BX-BY is described in Wood et al. (2000). Further information on subsurface contamination with in the WMA was provided by vadose zone field characterization activities conducted during fiscal year 2001 and documented in Knepp (2002b). Metal waste was the initial waste stream produced in the plutonium extraction process and contained the highest concentrations of radionuclide constituents. Field and Jones (2005) estimate this leak volume to be 91,000 gal. Groundwater contamination caused by tank leaks within the WMA is further complicated by large discharges of process waste (>10,000,000 gal) to nearby cribs and ditches.

Detailed discussion of WMA B-BX-BY farm construction and operations along with historical information on soil surface and vadose zone contamination in WMA B-BX-BY is provided in Williams (1999). Table 2-25 lists the estimated volume of waste stored in the WMA B-BX-BY tanks as of November 30, 2004.

Figure 2-69. General Configuration of Waste Management Area B-BX-BY [a]

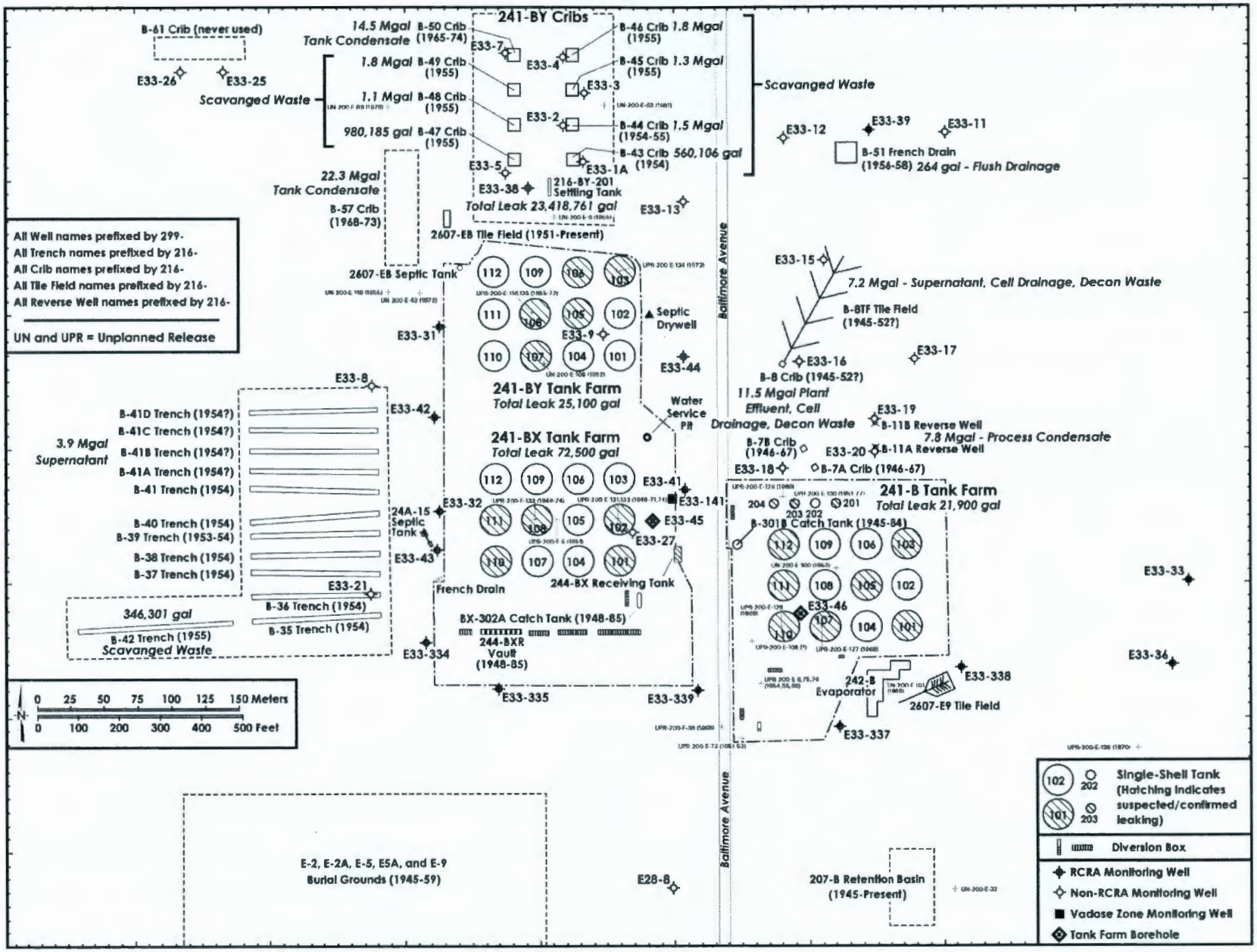

[a] *Knepp (2002b)*

Table 2-25. Waste Volume Estimates as of November 30, 2004, in Waste Management Area B-BX-BY Single-Shell Tanks [a] (2 pages)

Tank	Total Waste Volume gal × 1,000	Supernate gal × 1,000	Saltcake gal × 1,000	Sludge gal × 1,000
241-B-101	109	0	81	28
241-B-102	32	4	28	0
241-B-103	56	0	55	1
241-B-104	374	0	65	309
241-B-105	290	0	262	28
241-B-106	123	1	0	122
241-B-107	161	0	75	86
241-B-108	92	0	65	27
241-B-109	125	0	75	50
241-B-110	245	1	0	244
241-B-111	242	1	0	241
241-B-112	35	3	17	15
241-B-201	29	0	0	29
241-B-202	28	0	0	28
241-B-203	50	1	0	49
241-B-204	49	1	0	48
241-BX-101	48	0	0	48
241-BX-102	79	0	0	79
241-BX-103	74	12	0	62
241-BX-104	100	3	0	97
241-BX-105	72	5	0	68
241-BX-106	38	0	0	38
241-BX-107	347	0	0	347
241-BX-108	31	0	0	31
241-BX-109	193	0	0	193
241-BX-110	205	1	139	65
241-BX-111	189	0	157	32
241-BX-112	164	1	0	163
241-BY-101	370	0	333	37
241-BY-102	279	0	279	0
241-BY-103	417	00	408	9
241-BY-104	358	0	313	45
241-BY-105	481	0	433	48
241-BY-106	462	—	430	32
241-BY-107	272	0	256	16
241-BY-108	222	0	182	40

Table 2-25. Waste Volume Estimates as of November 30, 2004, in Waste Management Area B-BX-BY Single-Shell Tanks [a] (2 pages)

Tank	Total Waste Volume gal × 1,000	Supernate gal × 1,000	Saltcake gal × 1,000	Sludge gal × 1,000
241-BY-109	287	0	263	24
241-BY-110	366	0	323	43
241-BY-111	301	0	301	0
241-BY-112	286	0	284	2

[a] Hanlon (2005).

2.11.2 Infrastructure

This section describes the WMA B-BX-BY infrastructure components that were included in the SST PA and listed in Table 2-26. Reference case inventory development for those components is described in Section 2.11.7. Refer to Section 2.4 for generic infrastructure component descriptions and Section 2.5 for a summary of infrastructure inventory development methods.

2.11.2.1 Single-Shell Tanks

Two types of tanks (100-Series and 200-Series) are found in WMA B-BX-BY. The 100-Series tanks are 75 ft in diameter and 32 ft tall. The 200-Series tanks are 20 ft in diameter and 25 ft tall. The 100-Series tanks in B farm and all tanks in BX farm have a 16-ft operating depth, and an operating capacity of 530,000 gal each. All BY tanks have a 23-ft operating depth and an operating capacity of 758,000 gal each. The 200-Series tanks in B farm have a 24-ft operating depth, and an operating capacity of 55,000 gal each. Typical tank configuration and dimensions are shown in Figure 2-70. The tanks sit belowgrade with at least 7 ft of soil cover to provide shielding from radiation exposure to operating personnel. Tank pits are located on top of the tanks and provide access to the tank, pumps, and monitoring equipment. Additional details about tank construction can be found in Section 2.3.

The 100-Series tanks were constructed with cascade overflow lines in a 3-tank series that allowed gravity flow of liquid between tanks. The end of each cascade in BX tank farm is connected to the start of a cascade in the BY tank farm; therefore, a total of six tanks were connected. The current residual waste quantities in each tank farm are listed in Table 2-21.

The B tank farm contains twelve 100-Series SSTs and four 200-Series SSTs. These tanks were constructed between 1943 and 1944. The 100-Series tanks are arranged in four rows of three tanks each with cascade lines providing overflow. The 200-Series tanks are arranged in a straight line near the northern fenceline of the B tank farm. The B tank farm was built to provide storage for bismuth phosphate process waste (Wood et al. 2000). The B tank farm first received waste in April 1945 (Williams 1999).

The BX tank farm contains twelve 100-Series SSTs constructed between 1947 and 1949. The tanks are arranged in four rows of three tanks each with cascade lines providing overflow. The BX tank farm was built to provide storage capacity in addition to that of B tank farm for bismuth phosphate process waste (Wood et al. 2000). The BX tank farm first received waste in January 1948 (Williams 1999).

The BY tank farm contains twelve 100-Series SSTs constructed between 1947 and 1949. The tanks are arranged in four rows of three tanks each with cascade lines providing overflow. The BY tank farm was built to provide storage capacity in addition to that of B and BX tank farms for bismuth phosphate process waste (Wood et al. 2000). Each of the overflow cascades lines for each set of BY farm tanks are connected to the final cascade overflow from each set of BX tank cascades. The farm first received waste in March 1950 (Williams 1999).

Table 2-26. Operating Period and Capacities for Waste Management Area B-BX-BY Facilities Included in the Performance Assessment [a] (2 pages)

Facility	Removed From Service	Constructed	Operating Capacity gal
Single-Shell Tanks			
241-B-101	1974	1943 to 1944	530,000
241-B-102	1978		
241-B-103	1977		
241-B-104	1972		
241-B-105	1972		
241-B-106	1977		
241-B-107	1969		
241-B-108	1977		
241-B-109	1977		
241-B-110	1971		
241-B-111	1976		
241-B-112	1977		
241-B-201	1971	1943 to 1944	55,000
241-B-202	1977		
241-B-203	1977		
241-B-204	1977		
241-BX-101	1972	1946 to 1947	530,000
241-BX-102	1971		
241-BX-103	1977		
241-BX-104	1980		
241-BX-105	1980		
241-BX-106	1971		
241-BX-107	1977		
241-BX-108	1974		
241-BX-109	1974		
241-BX-110	1977		
241-BX-111	1977		
241-BX-112	1977		

Table 2-26. Operating Period and Capacities for Waste Management Area B-BX-BY Facilities Included in the Performance Assessment [a] (2 pages)

Facility	Removed From Service	Constructed	Operating Capacity gal
241-BY-101	1971	1948 to 1949	758,000
241-BY-102	1977		
241-BY-103	1973		
241-BY-104	1977		
241-BY-105	1974		
241-BY-106	1977		
241-BY-107	1974		
241-BY-108	1972		
241-BY-109	1979		
241-BY-110	1979		
241-BY-111	1977		
241-BY-112	1978		
Miscellaneous Underground Storage Tanks			
241-B-301B catch tank	1984	1945	36,400
241-BX-302A catch tank	1985	1948	11,389
244-BX-DCRT	Active	1983	31,000
244-BXR-001 vault tank	1951 (244-BXR vault)	1957	50,000
244-BXR-002 vault tank		1957	15,000
244-BXR-003 vault tank		1957	15,000
244-BXR-011 vault tank		1956	50,000
Underground Waste Transfer Lines			
241-B tank farm pipelines	NA	1943 to 1944	13,100 (+/-4,600)
241-BX tank farm pipelines	NA	1946 to 1947	15,000 (+/-4,600)
241-BY tank farm pipelines	NA	1948 to 1949	19,800 (+/-4,400)

[a] Data on the facilities is from DOE-RL (2005) and Field (2003a).

DCRT = double-contained receiver tank

NA = not applicable

Figure 2-70. Typical Configuration and Dimensions of Single-Shell Tanks in Waste Management Area B-BX-BY

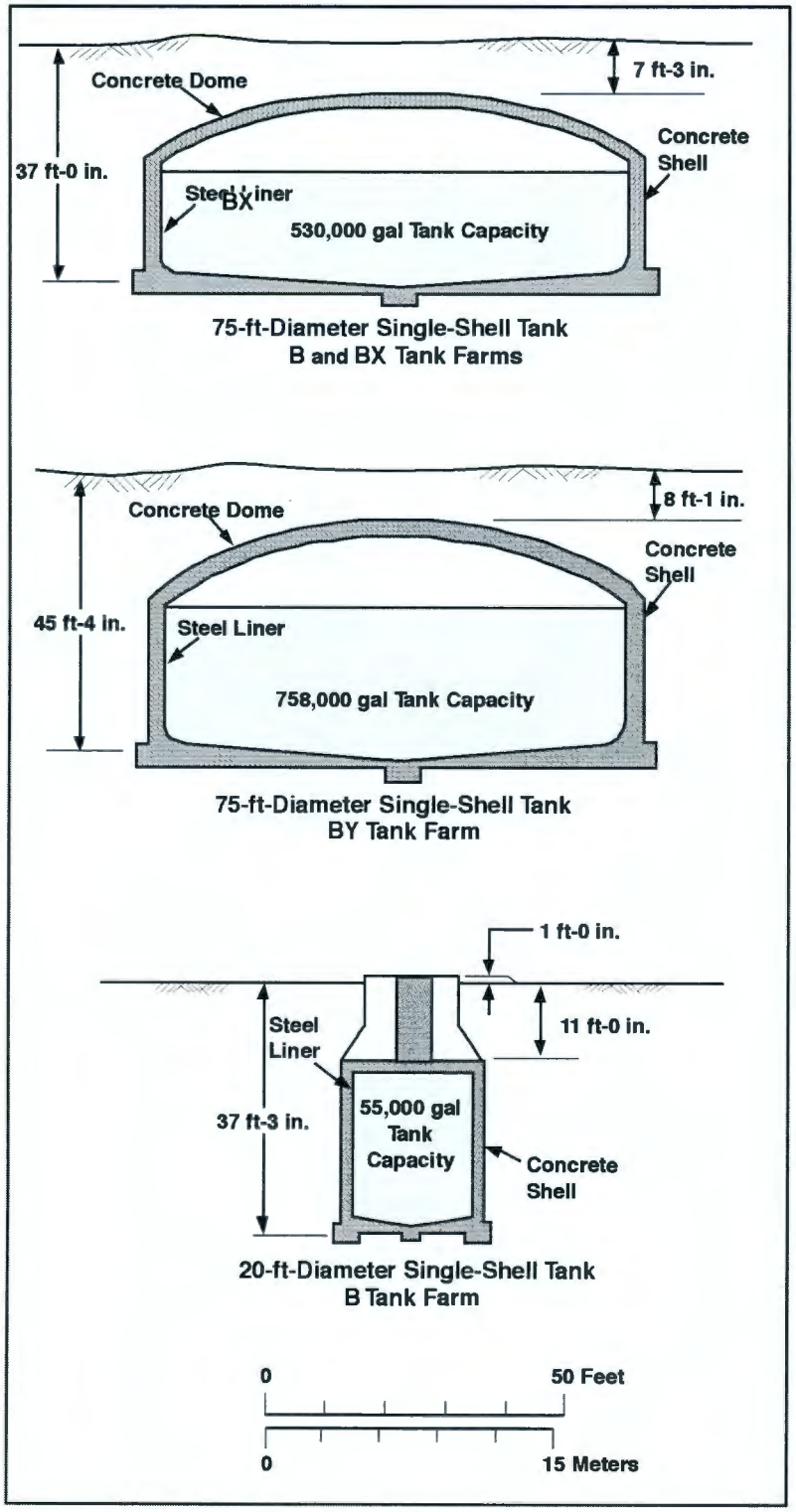

2.11.2.2 Ancillary Equipment

A complete listing of the WMA B-BX-BY ancillary equipment currently identified for inclusion in the SST system closure is provided in Lee (2004). As discussed in Section 2.5.4, the ancillary components included in the SST PA consist of the underground waste transfer lines and MUSTs located inside each WMA boundary. For WMA B-BX-BY, the ancillary components analyzed consist of the B, BX, and BY tank farms waste transfer piping and seven MUSTs. The MUSTs consist of two catch tanks (241-B-301B, 241-BX-302A), one double-contained receiver tank (244-BX DCRT), and the 244-BXR vault, which contains four tanks (244-BXR-001, 244-BXR-002, 244-BXR-003, 244-BXR-011).

Multiple levels of piping were installed over time in WMA B-BX-BY. A time line of piping installations is described in Williams (1999). It is estimated that there are approximately 6.7 mi (+/-2.4 mi) of waste transfer piping in the B tank farm, 7.7 mi (+/-2.4 mi) in the BX tank farm, and 10.2 mi (+/-2.3 mi) in the BY tank farm (Field 2003a).

2.11.3 Geology

Following is an overview of the geology of WMA B-BX-BY summarized from the information provided in Reidel et al. (2006). The generalized stratigraphy and thicknesses in the 200 East Area are shown in Section 2.3. A generalized cross-section through WMA B-BX-BY is shown in Figure 2-71. Maps and cross-sections presented in Reidel et al. (2006) illustrate the distribution and thicknesses of these units in additional detail.

Seven stratigraphic units lie within WMA B-BX-BY. From oldest to youngest, the primary geologic units are:

- Columbia River Basalt Group
- Undifferentiated Cold Creek unit fine unit and/or Ringold Formation
- Undifferentiated Cold Creek unit gravel and/or Ringold Formation Unit A?
- Hanford formation – lower gravelly sequence (H3 unit)
- Hanford formation – sand sequence (H2 unit)
- Hanford formation – upper gravelly sequence (H1 unit)
- Recent deposits (wind deposited material and backfill material placed during construction).

The general characteristics of these units are described in Section 2.3 and in more detail in Reidel et al. (2006). The SSTs at WMA B-BX-BY were emplaced within the Hanford formation sediments of the upper, gravel-dominated (H1) unit. The water table or potentiometric surface lies approximately 60 m (200 ft) below the bottom of the tank farms excavations within the Ringold Formation Unit E.

Figure 2-71. Fence Diagram Showing Cross-Sections through Waste Management Area B-BX-BY [a]

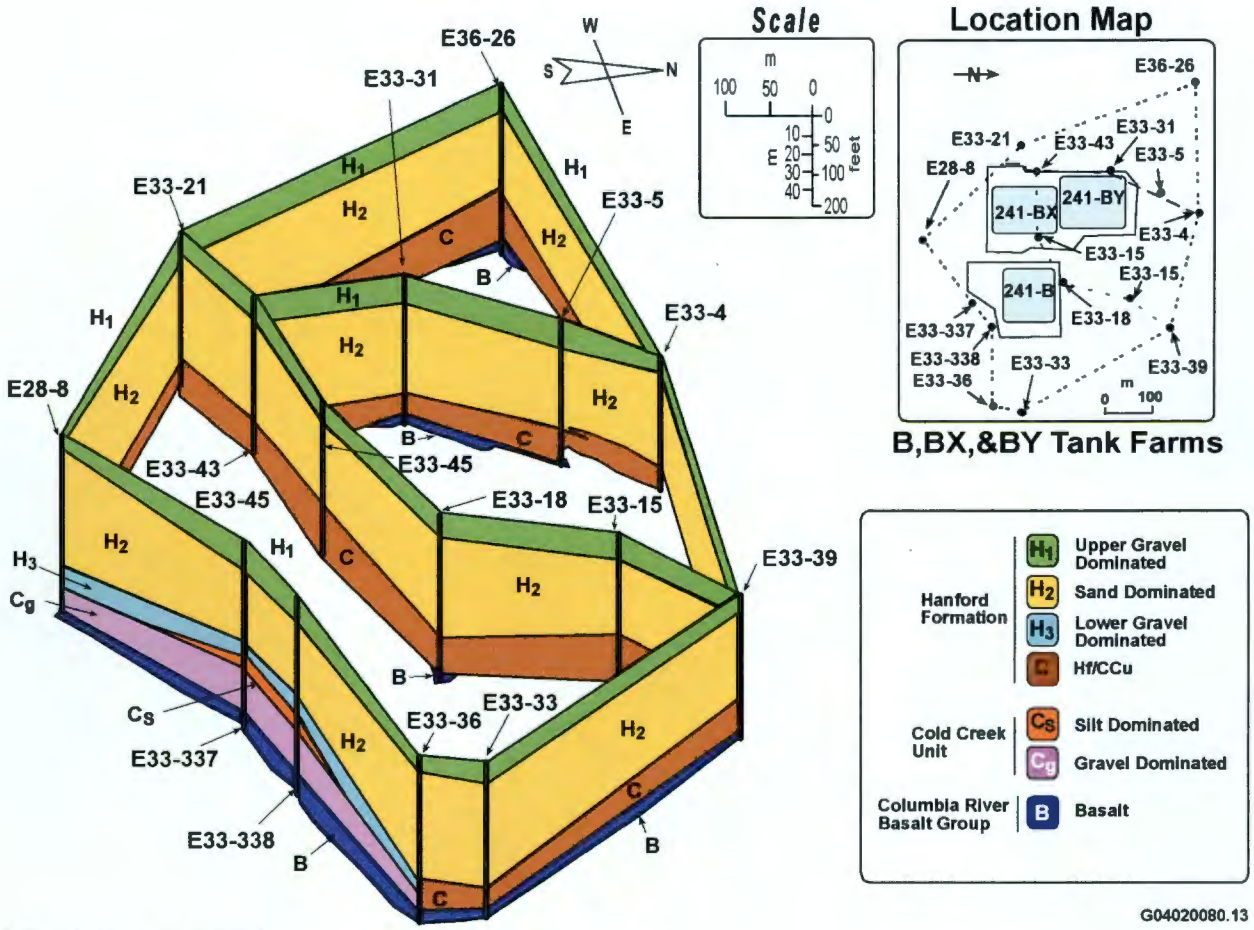

[a] *Reidel et al. (2006)*

2.11.4 Hydrology

Following is an overview of the hydrology of the uppermost, unconfined aquifer beneath WMA B-BX-BY. More detailed information supporting this section can be found in Reidel et al. (2006), Wood et al. (2000), and Hartman et al. (2004). Currently, the general groundwater flow direction in the unconfined aquifer beneath WMA B-BX-BY ranges from south-southwest to west-southwest (Wood et al. 2000). This is based on observations of contaminant movement because the water table is very flat overall, with an estimated hydraulic gradient of only 0.00017. This extremely small gradient makes it difficult to define the direction of groundwater flow. The estimated groundwater flow velocity is approximately 0.9 m/day (Wood et al. 2000).

Water levels stopped declining across the site during fiscal year 2003 (Hartman et al. 2004). However, some sampling wells in the area began showing an increase in water levels. This phenomenon is under further investigation. Currently, the water table beneath WMA B-BX-BY lies 122 m (400 ft) amsl with about 77 m (255 ft) of vadose zone. The aquifer thickness, based on the top of basalt at 108 m (355 ft), is approximately 13.4 m (44 ft). The aquifer materials

consist dominantly of unconsolidated gravels. Hydraulic conductivity values reported for the aquifer in this area is approximately 1,600 m/day (5,300 ft/day). Additional hydraulic property data from aquifer testing at wells near WMA B-BX-BY are provided in Wood et al. (2000), Reidel et al. (2006), and Hartman et al. (2004).

2.11.5 Vadose Zone Conditions

This section summarizes WMA B-BX-BY vadose zone monitoring and characterization activities and the current understanding of contamination in the vadose zone.

2.11.5.1 Monitoring and Characterization

The B tank farm has 52 leak detection wells (Figure 2-72) available for leak detection monitoring and to provide access for limited vadose zone characterization (e.g., geophysical logging). These drywells were drilled from 1944 to 1974. The depth ranges for most of these drywells is between 18.6 m (61 ft) and 45.7 m (150 ft) bgs.

The BX tank farm has 76 leak detection wells (Figure 2-73) available for leak detection monitoring and to provide access for limited vadose zone characterization (e.g., geophysical logging). These drywells were drilled from 1947 to 1977. The depth ranges for most of these drywells is between 22.9 m (75 ft) and 45.7 m (150 ft) bgs.

The BY tank farm has 70 leak detection wells (Figure 2-74) available for leak detection monitoring and to provide access for limited vadose zone characterization (e.g., geophysical logging). These drywells were drilled from 1949 to 1974. The depth ranges for most of these drywells is between 30.5 m (100 ft) and 45.7 m (150 ft) bgs.

Gamma logging took place in WMA B-BX-BY over two decades allowing evaluation of the time-dependent behavior of the gamma-emitting radionuclides. Between 1997 and 1999, spectral gamma logging was used to evaluate WMA B-BX-B-BY. This effort was part of the baseline characterization for WMA B-BX-BY. Results are documented in DOE-GJO (1997c, 1998d, 2000h). The baseline reports are further supplemented by their associated addenda reports (DOE-GJO 2000i, 2000j, 2000k).

The major gamma-emitting contaminants associated with WMA B-BX-BY are cesium-137, cobalt-60, ruthenium-106, antimony-125, and strontium-90. These contaminants are located mostly in and around areas of confirmed or suspected tank and pipeline leaks. However, the evaluation of time-dependent behavior indicates that the more mobile radionuclides have migrated away from their locations of emplacement (Wood et al. 2000). Although most of the drywells are deeper than the surrounding contamination, some zones of contamination extend deeper than nearby drywells. Consequently, the maximum depth of vadose zone contamination is not known in some areas of WMA B-BX-BY.

During fiscal year 2001, field characterization efforts were conducted at WMA B-BX-BY in support of RCRA Corrective Action process requirements. The investigative approach for this work is described in Rogers and Knepp (2000b). A detailed discussion of these investigations and an analysis of the results are included in the WMA B-BX-BY FIR (Knepp 2002b).

Figure 2-72. Vadose Zone Monitoring System for the B Tank Farm within Waste Management Area B-BX-BY

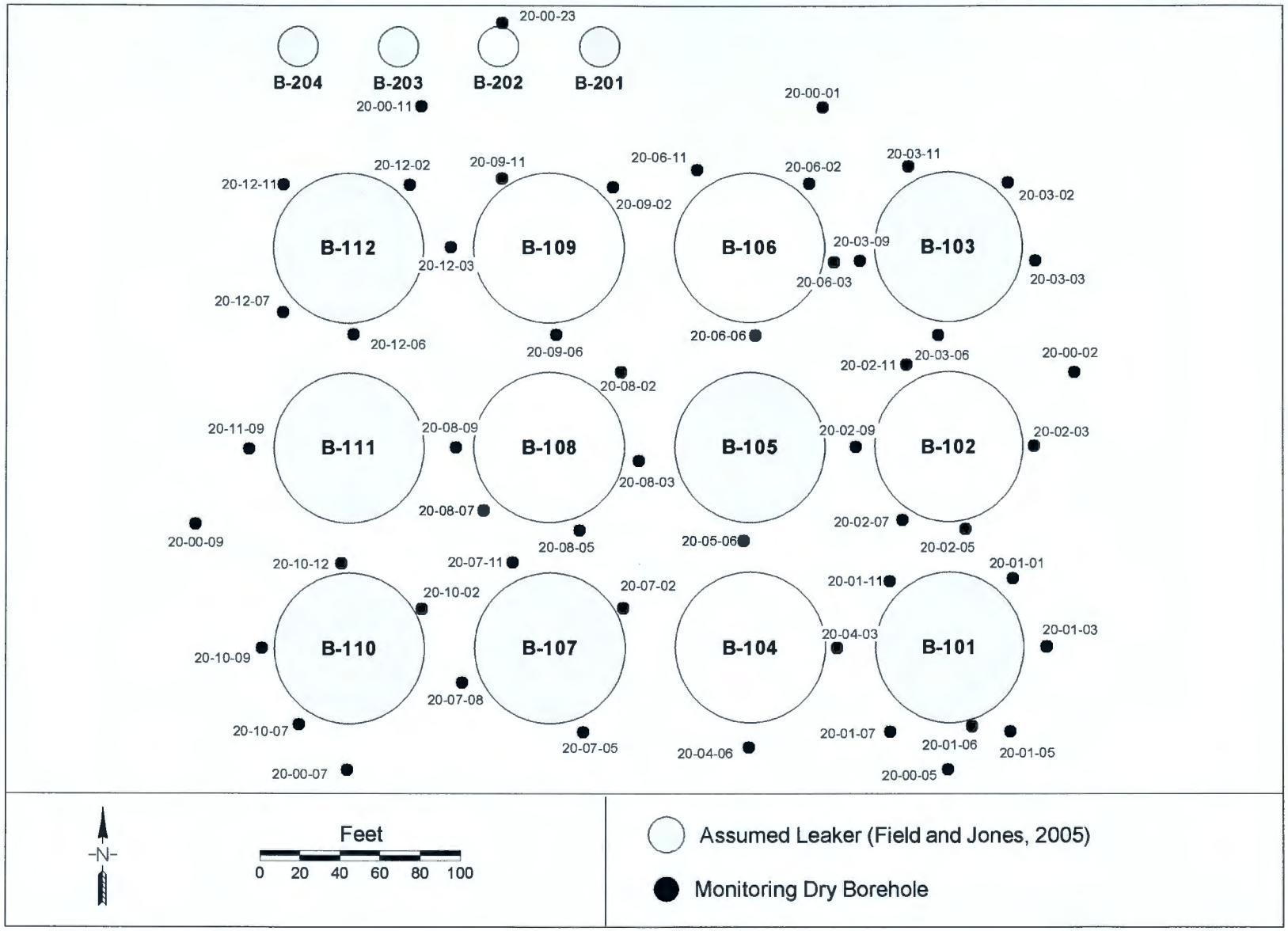

Figure 2-73. Vadose Zone Monitoring System for the BX Tank Farm within Waste Management Area B-BX-BY

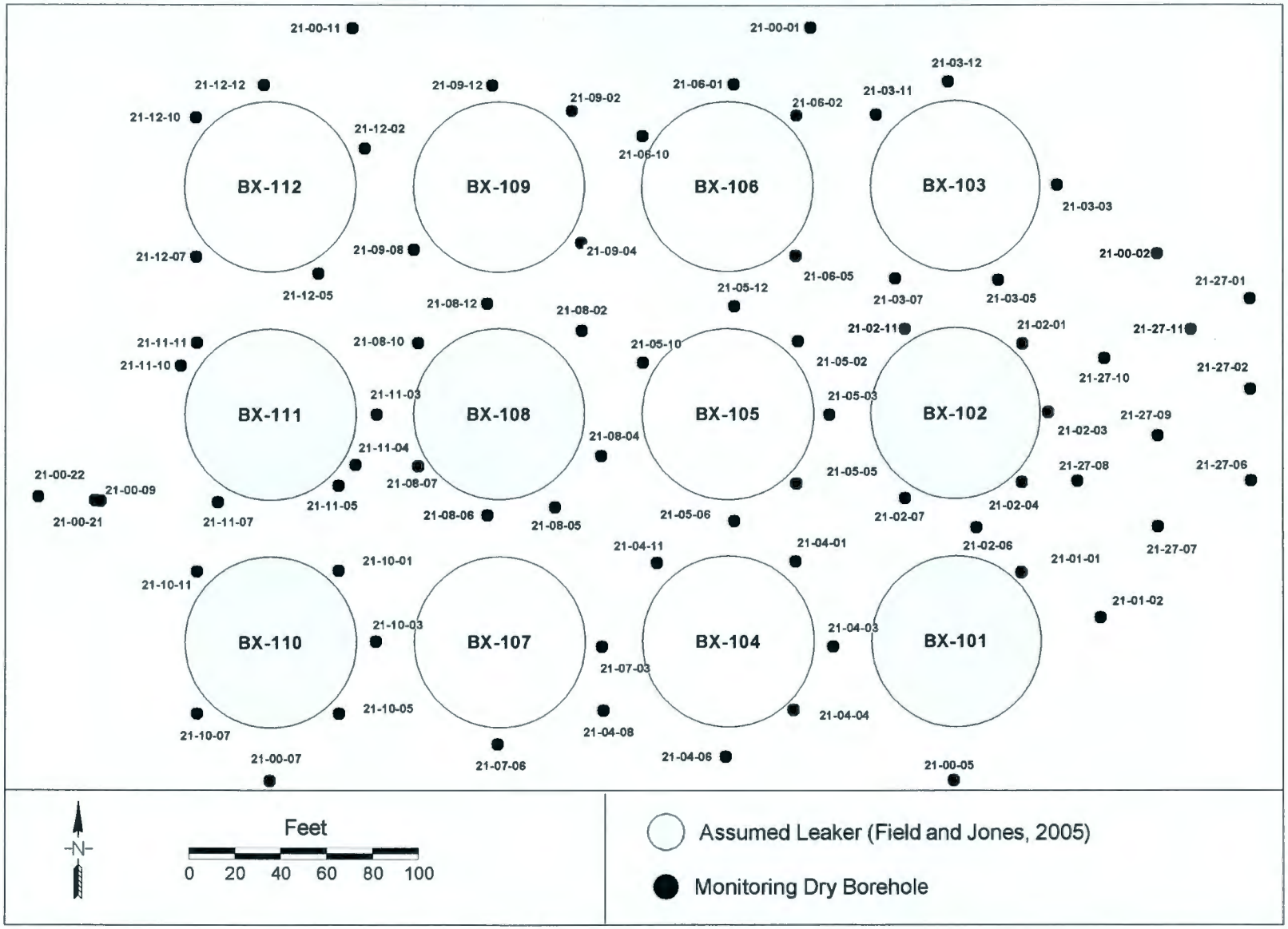

Figure 2-74. Vadose Zone Monitoring System for the BY Tank Farm within Waste Management Area B-BX-BY

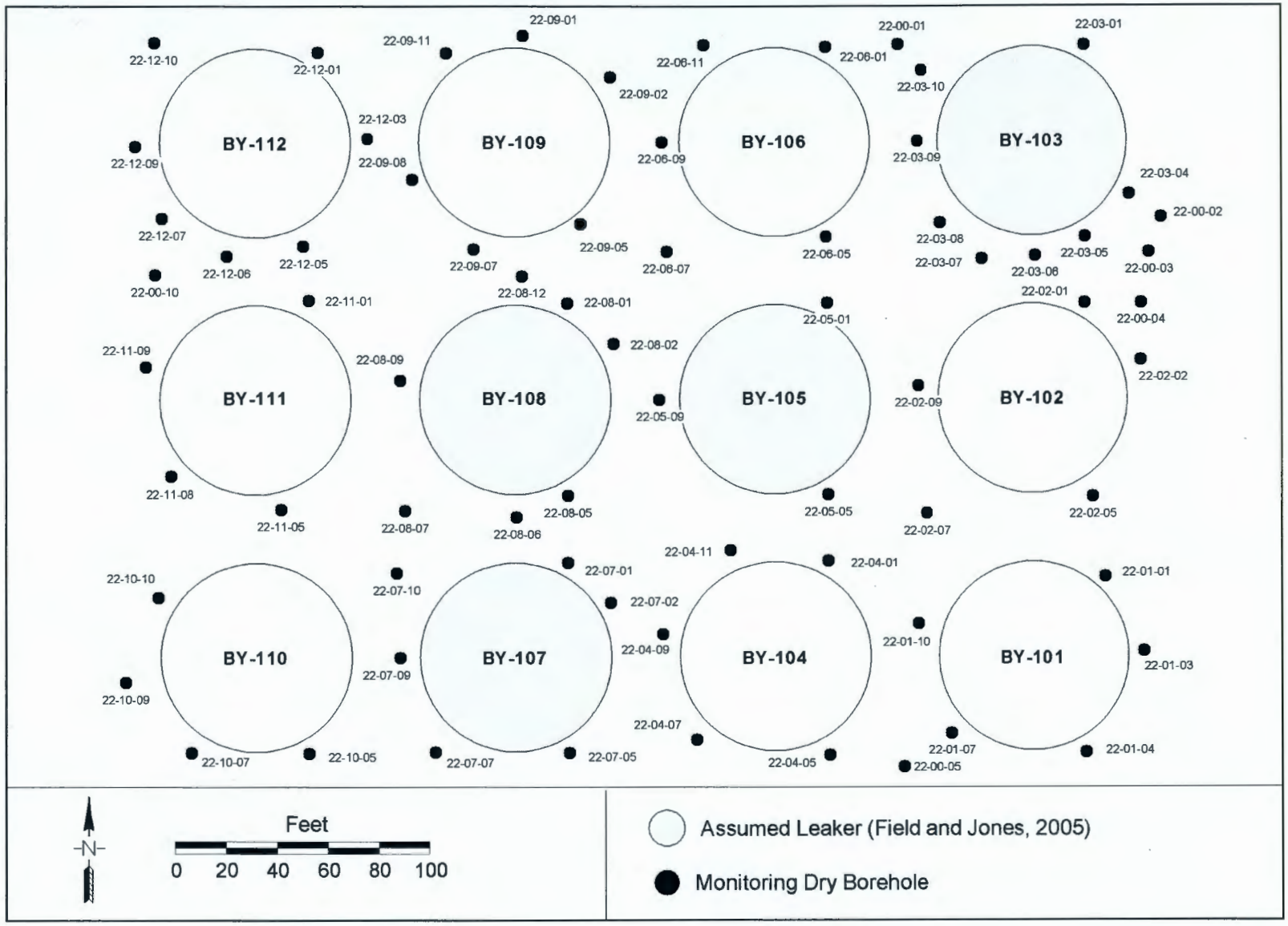

2.11.5.2 Contamination

Figures 2-75 through 2-77 provide a visualization of the vadose zone contamination beneath WMA B-BX-BY. These figures show a three-dimensional perspective of radioactive contamination levels observed in the boreholes in WMA B-BX-BY. Tanks considered to be assumed leakers based on information in Field and Jones (2005) are shown with darker shading. Each drywell is represented with a single vertical line. Shaded rings around the drywells indicated the level of vadose zone contamination based on spectral gamma logging results. Only the more significant soil contamination zones (>10 pCi/g) are shown. Zones with contamination levels less than 5 pCi/g are not shown for B and BX tank farms, and for BY tank farm, levels less than 10 pCi/g are not shown.

The primary areas of elevated gamma readings for WMA B-BX-BY occur in the drywells located around tanks (B-101, B-103, B-105, B-107, B-110, B-111, B-112, BX-101, BX-102, BX-108, BX-110, BX-111, BY-103, BY-105, BY-106, BY-107, BY-108). The presence of contamination in these areas has provided or supported the determinations of postulated leaks based on the WMA B-BX-BY historical record (Wood et al. 2000). The major gamma-emitting contaminants associated with WMA B-BX-BY are cesium-137, cobalt-60, ruthenium-106, antimony-125, and strontium-90.

As there are two decades of temporal distribution of gamma activity data available, it is possible to evaluate any changes in estimated distributions. Six BX tank farm drywells and 26 drywells in BY tank farm show "instability," changes over the duration of the monitoring activity (Wood et al. 2000). The evaluation for B tank farm is ongoing. It is believed that the areas of instability in WMA B-BX-BY are associated with the postulated leaks from tanks B-110, BX-102, BX-108, BX-110, and BX-111 (Wood et al. 2000).

Logging data in the drywells surrounding B-110 are unique in that they show the presence of significant quantities of strontium-90. Drywell 20-10-12 shows a large strontium-90 contamination zone from 8 to 30 m (25 to 100 ft) bgs, with the region from 18 to 30 m (60 to100 ft) bgs believed to contain a large inventory of strontium-90. The 8 to 30 m (25 to 100 ft) bgs zone also contains cesium-137 at concentrations that saturate the detector. The cesium-137 concentrations then decrease from 5,000 pCi/l to 100 pCi/L. Drywell 20-10-02 also shows a zone of strontium-90 contamination from 23 to 24 m (75 to 80 ft) bgs (Wood et al. 2000).

The most extensive region of contaminated vadose zone is found adjacent to and to the east of tank BX-102. The drywell logging data indicate the primary contaminants are cesium-137, uranium-235, and uranium-238, with smaller amount of cobalt-60 and antimony-125. Drywell 20-02-04 shows cesium-137 contamination starting at 8 m (25 ft) bgs and continuing to the bottom of the drywell at 70 m (230 ft) (Wood et al. 2000).

Several drywells associated with tanks BX-108 and BX-111 support the identification of these tanks as leakers. Numerous drywells show elevated cesium-137 contamination in a zone from 11 to 14 m (35 to 45 ft) bgs. Drywells 21-11-03 and 21-11-04 show gamma activity that is above the saturation level of the logging tool. The concentration in drywell 21-08-07 goes from a maximum of 80 pCi/g at a depth of 11 m (35 ft) below the surface to 1 pCi/g at a depth of 12 m (40 ft). Drywell 21-10-05 has cesium-137 concentrations above the gamma logging tool saturation point from 12 to 15 m (40 to 48 ft).

Figure 2-75. Three-Dimensional Perspective of B Tank Farm Tanks and Drywells Showing Occurrence of Significant (>5 pCi/g) Cesium-137 Contamination in the Vadose Zone

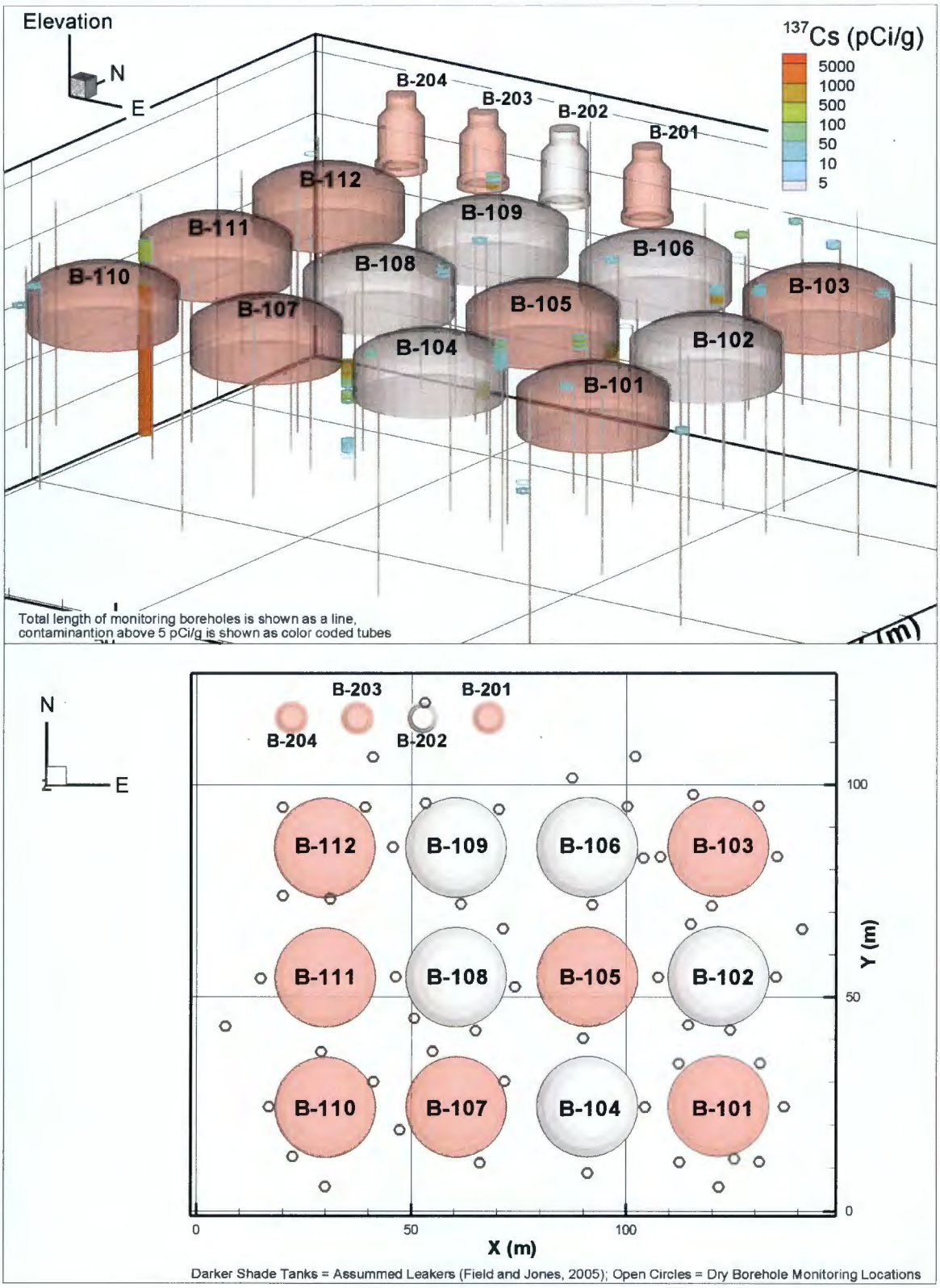

Figure 2-76. Three-Dimensional Perspective of BX Tank Farm Tanks and Drywells Showing Occurrence of Significant (>5 pCi/g) Cesium-137 Contamination in the Vadose Zone

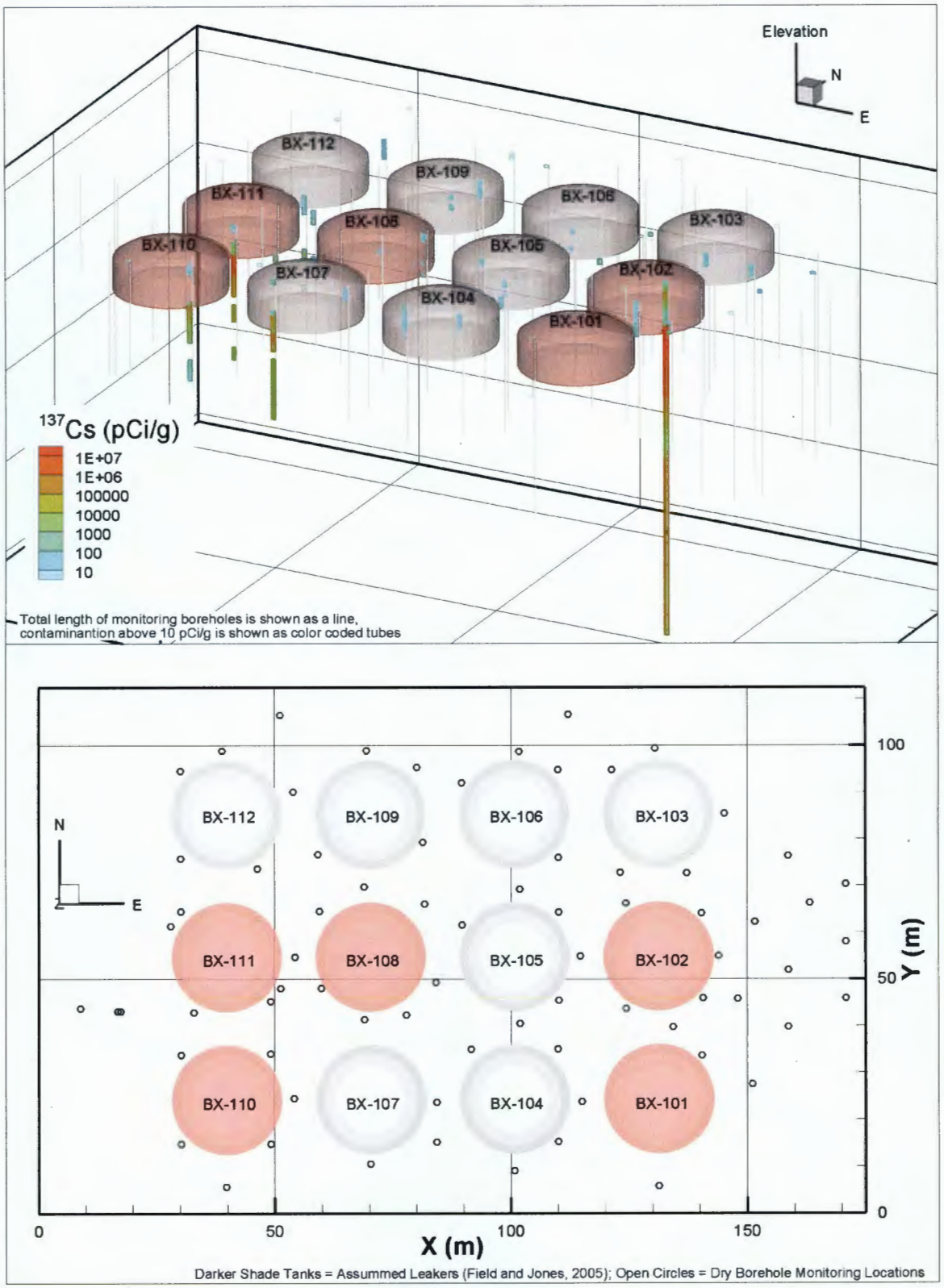

Figure 2-77. Three-Dimensional Perspective of BY Tank Farm Tanks and Drywells Showing Occurrence of Significant (>10 pCi/g) Cesium-137 Contamination in the Vadose Zone

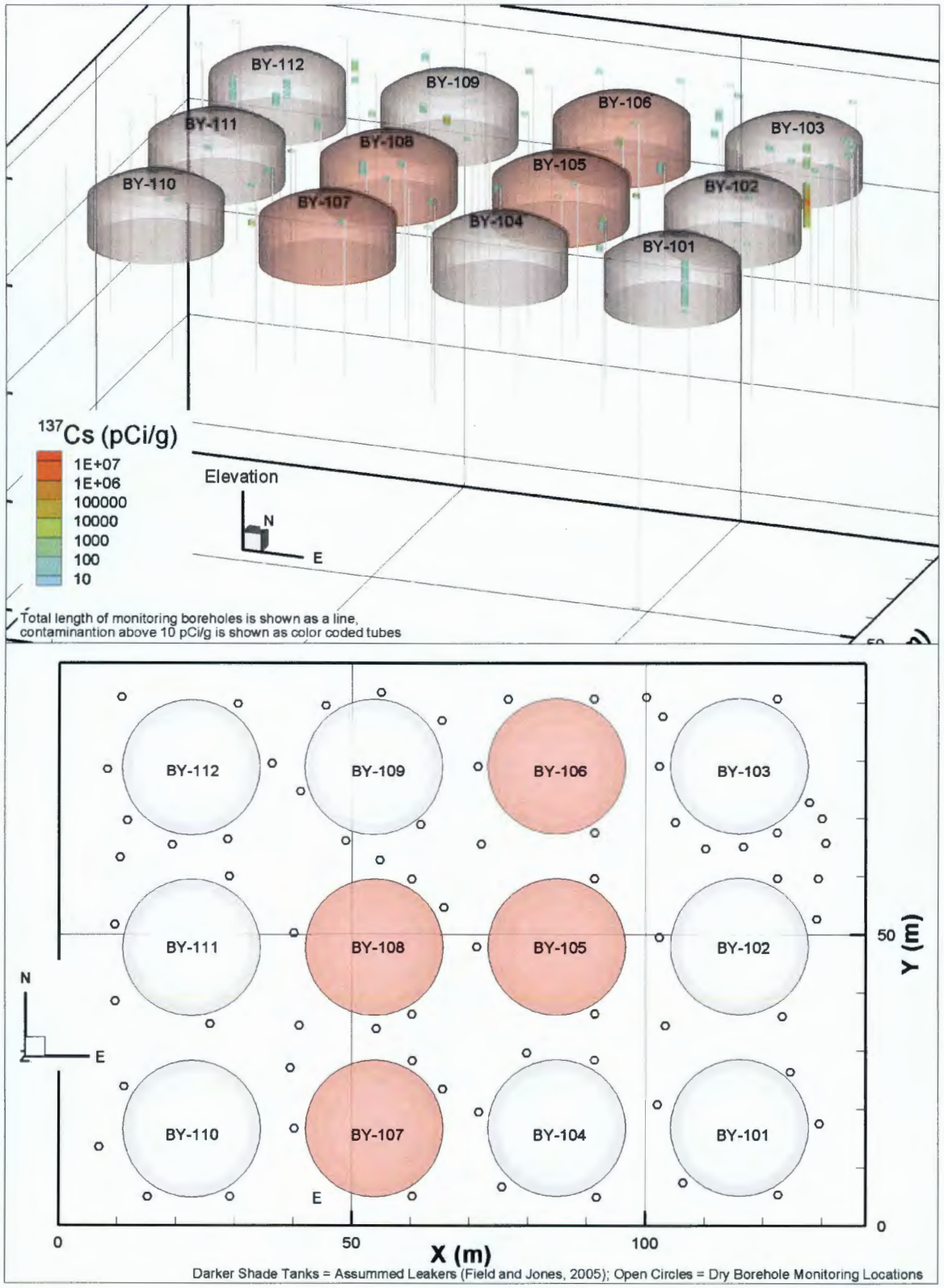

Drywells 20-10-03 and 20-10-05 show evidence of tank leaks from tank BX-110. Cesium-137 concentrations in drywell 20-10-03 are above the logging tool saturation point in three zones, 3 to 12 m (10 to 40 ft), 14 to 15 m (45 to 50 ft), and 24 to 25 m (80 to 82 ft) bgs. Uranium-235 was identified in drywell 21-10-05 with a concentration of approximately 100 pCi/L at a depth between 15 and 18 m (50 and 60 ft).

Although it is believed that five tanks in the BY tank farm leaked, the gamma logging records along with waste transfer records do not support this position. Spectral gamma logging data also indicate the presence of generalized surface contamination across the BY tank farm in the range of 100 pCi/g of cesium-137 (Wood et al. 2000), in most cases decreasing with depth. Cobalt-60 is often found from 12 m (40 ft) to the bottom of the drywells. High levels of cesium-137 are reported in the first 1.2 m (6 ft) for drywells 22-00-01, 22-05-04, 22-08-02, and 22-12-03. Appreciable cesium-137 is reported because depths greater than 1.2 m (6 ft) are reported for three drywells. Drywell 22-03-05 shows gamma activity high enough to saturate the detector between 7 and 14 m (24 and 47 ft) and drywells 22-02-01 and 22-03-06 show levels of approximately 100 pCi/g at a depth between 14 and 15 m (45 and 50 ft). No uranium isotopes were reported in any BY tank farm drywell. The significance of the gamma activity within the drywells with respect to actual tank leak volumes is discussed further in Section 2.12.7.1. Detailed discussions on this topic are found in Wood et al. (2000) and Field and Jones (2005).

2.11.6 Unconfined Aquifer Conditions

This section summarizes WMA B-BX-BY groundwater monitoring and characterization activities and the current understanding of contamination in the unconfined aquifer.

2.11.6.1 Monitoring and Characterization

Thirteen RCRA groundwater monitoring wells associated with WMA B-BX-BY are shown in Figure 2-78. Twelve wells are located outside the tank farm fencelines. The wells are intended to monitor groundwater contamination attributable to the entire WMA rather than individual components. The initial background-monitoring program for WMA B-BX-BY is complete and monitoring is currently conducted under an interim status assessment monitoring program.

The parameters and the statistical evaluation methodology for the WMA B-BX-BY groundwater assessment program are described in Narbutovskih (2000). Two modifications to the monitoring plan have been issued to document changes in the monitoring program status (Narbutovskih 2002, 2003). Results of the groundwater detection indicator evaluation program are published annually. The most recently published data are for fiscal year 2003 (Hartman et al. 2004).

When the monitoring network for WMA B-BX-BY was designed, flow was believed to be toward the east. A general flow direction to the southwest has subsequently been established. Three new downgradient wells and one new upgradient well were installed in fiscal year 2003 to improve the capability of the detection network to monitor the site.

During fiscal year 2003, the site was monitored with the original configuration of wells (Figure 2-78). Sampling data from the four new monitoring wells are included in the groundwater monitoring report for fiscal year 2004 (Hartman et al. 2005). Monitoring under the groundwater assessment program will continue until the entire WMA is closed.

Figure 2-78. Ground Water Monitoring Network for Waste Management Area B-BX-BY [a]

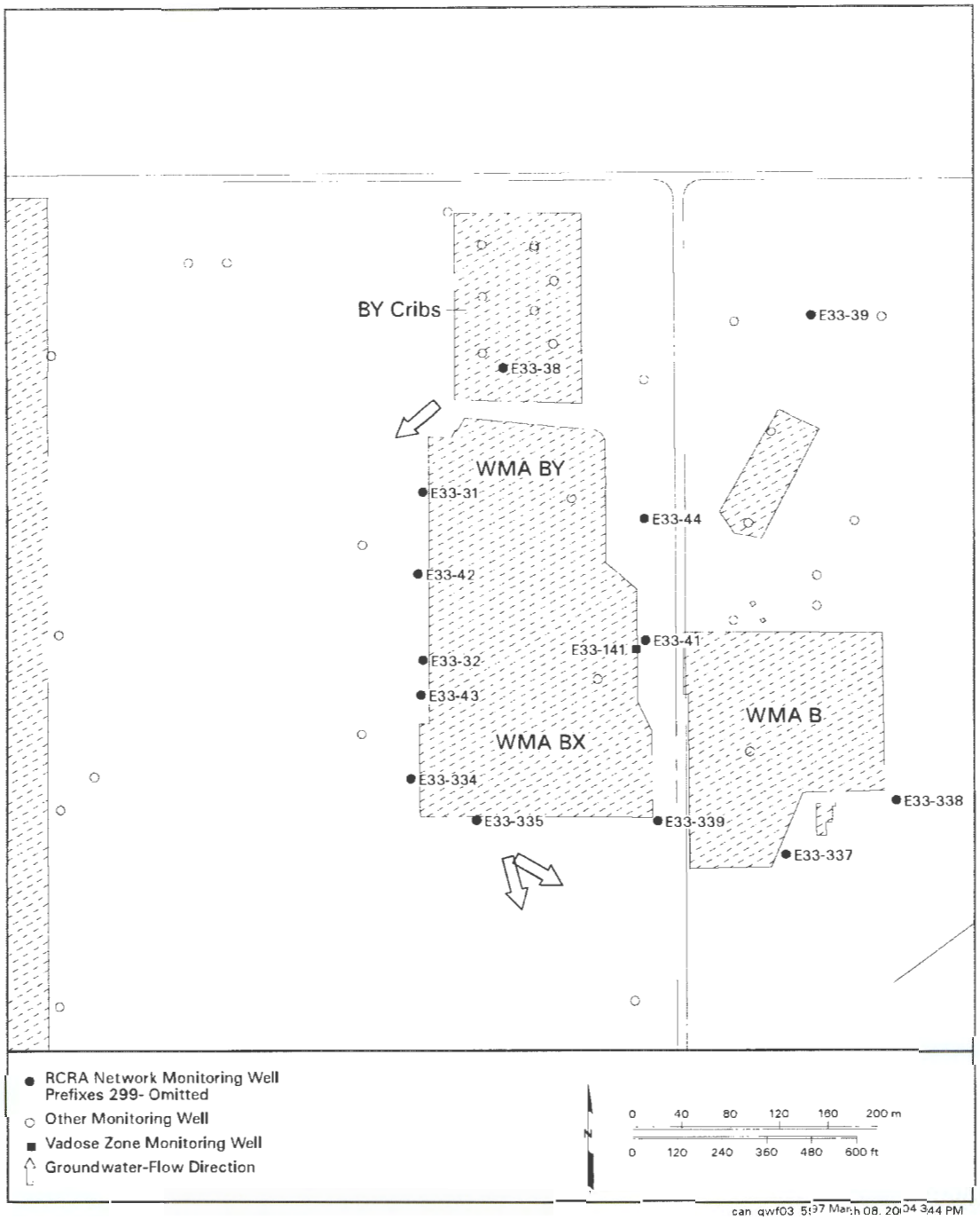

[a] *Appendix B of Hartman et al. (2004)*

2.11.6.2 Contamination

The most recently published groundwater monitoring results for WMA B-BX-BY are for fiscal year 2003 (Hartman et al. 2004). Following is a summary of the fiscal year 2003 results adapted from Hartman et al. (2004). Additional detail on groundwater contamination and geochemistry at WMA B-BX-BY can be found in Hartman et al. (2004) and Reidel et al. (2006).

Wells were sampled quarterly during fiscal year 2003. A number of contaminants were detected at or above their respective DWS levels. A summary of these contaminants follows. Details regarding the measurements, levels found, and the wells showing contamination can be found in Hartman et al. (2004).

- Tritium contamination is widespread throughout the northwest part of the 200 East Area. Tritium values have increased recently at the south end of WMA B-BX-BY. The tritium is believed to have originated in the southern portion of the 200 East Area (Figure 2-20).
- One lobe of the nitrate plume beneath the 200 East Area originates in the vicinity of the BY and 216-B-8 cribs. This lobe joins the other lobe of nitrate contamination in moving northwest (Figure 2-20).
- A band of elevated iodine-129 concentrations extends through WMA B-BX-BY to the northeast corner of Low-Level Waste Management Area 1 (Figure 2-20).
- A plume of technetium-99 extends from the area of the BY cribs and WMA B-BX-BY to beyond the 200 East Area north boundary to the northwest. This plume is believed to have originated from early releases of technetium-99 to the BY cribs. Monitoring data indicates the plume is continuing to move northward (Figure 2-20).
- Cobalt-60 and cyanide are found to the north of WMA B-BX-BY in the monitoring wells associated with the BY cribs.
- There is a uranium plume found within the BY tank farm and on the east side of the tank farm. This plume is moving southward and is believed to have originated from a release at tank BX-102 (Figure 2-20).
- There is some localized cesium-137 and strontium-90 near their source as these contaminants are fairly immobile. These contaminants are believed to be from the 216-B-5 injection well (Figure 2-20).

2.11.7 Reference Case Source Terms

The reference case describes a set of assumed post-retrieval conditions that are based on current waste retrieval plans. The reference case analysis for WMA B-BX-BY includes three source terms consisting of past UPRs, residual SST waste, and residual ancillary equipment waste. Table 2-27 provides a listing of the reference case source terms for WMA B-BX-BY, and the inventory data source for that source term.

Source term inventories (reference case) for WMA B-BX-BY are provided in Table 2-28. To simplify the table, only the contaminants that dominate post-closure impacts are shown. All BBI contaminants are included in the reference case modeling analysis. Refer to Section 2.5 for a summary of source term inventory development methods. Complete inventory data are provided in Appendix C.

2.11.7.1 Past Unplanned Releases

The WMA B-BX-BY reference case include 12 past UPRs associated with SSTs (B-107, B-110, B-112, B-201, B-203, B-204, BX-101, BX-102, BX-108, BY-103, BY-107, BY-108) and nine past UPRs associated with ancillary equipment (UPR-200-E-6, UPR-200-E-38, UPR-200-E-73, UPR-200-E-74, UPR-200-E-75, UPR-200-E-105, UPR-200-E-108, UPR-200-E-109, UPR-200-E-110). Volume estimates for those 21 waste loss events were developed by Field and Jones (2005) and vadose zone contaminant inventories were generated by Corbin et al. (2005) (Section 2.5.2). No volume or inventory estimates were assigned to the waste loss events associated with tanks B-101, B-103, B-105, B-111, BX-110, BX-111, BY-105, and BY-106 because of insufficient information to quantify or verify the releases (Field and Jones 2005). If new information becomes available to quantify the waste loss events from those tanks, the data will be evaluated under the integrated regulatory closure process described in Chapter 1.0.

2.11.7.2 Residual Single-Shell Tank Waste

The WMA B-BX-BY reference case includes residual waste in each of the 36 100-Series and four 200-Series SSTs in the B, BX, and BY tank farms. The HFFACO Milestone M-45-00 goal allows up to 360 ft^3 of waste to remain in the 100-Series tanks after retrieval in the event that retrieval beyond that level becomes impracticable (Ecology et al. 1989). Thus, the analysis includes a 360 ft^3 source term associated with residual waste remaining in each of the tanks after retrieval. The inventory estimates were generated with the use of the HTWOS model (Kirkbride et al. 2005), which accounts for the waste retrieval technology and tracks the fate of soluble and insoluble constituents in the waste (Section 2.5.3).

2.11.7.3 Residual Ancillary Equipment Waste

The WMA B-BX-BY reference case includes the plugged and blocked piping in the B, BX, and BY tank farms and the residual waste in seven MUSTs consisting of two catch tanks (241-B-301, 241-BX-302A), one double-contained receiver tank (244-BX DCRT), and the four tanks in the 244-BXR vault (244-BXR-001, 244-BXR-002, 244-BXR-003, 244-BXR-011) (Section 2.5.4). Volume and inventory estimates for the waste in the plugged and blocked piping (none in B tank farm, 28 L in BX tank farm, none in BY tank farm) were developed by Lambert (2005). Volume estimates for the residual waste in the MUSTs were calculated by assuming each tank would be retrieved to a residual volume proportional to that required under the HFFACO Milestone M-45-00 for 200-Series tanks (Ecology et al. 1989). Contaminant inventories associated with the residual ancillary equipment waste were estimated using the average chemical composition of the waste in the WMA B-BX-BY SSTs.

Table 2-27. Reference Case Analysis of Waste Management Area B-BX-BY (3 pages)

Inventory and Source Terms					
Sources	**Assumed Retrieval Method**	**Residual Volume**	**Volume Associated with Past Release [a] gal**	**Basis for Contaminant Inventory Estimate**	
				Residual Waste [b]	**Past Release**
241-B-101 [c]	Mobile retrieval system	360 ft^3	NSI [c]	HTWOS	None
241-B-102	Sluicing	360 ft^3	None	HTWOS	None
241-B-103 [c]	Mobile retrieval system	360 ft^3	NSI [c]	HTWOS	None
241-B-104	Sluicing	360 ft^3	None	HTWOS	None
241-B-105 [c]	Mobile retrieval system	360 ft^3	NSI [c]	HTWOS	None
241-B-106	Sluicing	360 ft^3	None	HTWOS	None
241-B-107	Mobile retrieval system	360 ft^3	14,000	HTWOS	Corbin et al. 2005
241-B-108	Sluicing	360 ft^3	None	HTWOS	None
241-B-109	Sluicing	360 ft^3	None	HTWOS	None
241-B-110	Mobile retrieval system	360 ft^3	10,000	HTWOS	Corbin et al. 2005
241-B-111 [c]	Mobile retrieval system	360 ft^3	NSI [c]	HTWOS	None
241-B-112	Mobile retrieval system	360 ft^3	2,000	HTWOS	Corbin et al. 2005
241-B-201	Vacuum	30 ft^3	1,200	HTWOS	Corbin et al. 2005
241-B-202	Vacuum	30 ft^3	None	HTWOS	None
241-B-203	Vacuum	30 ft^3	300	HTWOS	Corbin et al. 2005
241-B-204	Vacuum	30 ft^3	400	HTWOS	Corbin et al. 2005
241-BX-101	Mobile retrieval system	360 ft^3	4,000	HTWOS	Corbin et al. 2005
241-BX-102	Mobile retrieval system	360 ft^3	91,600	HTWOS	Corbin et al. 2005
241-BX-103	Sluicing	360 ft^3	None	HTWOS	None
241-BX-104	Sluicing	360 ft^3	None	HTWOS	None
241-BX-105	Sluicing	360 ft^3	None	HTWOS	None
241-BX-106	Sluicing	360 ft^3	None	HTWOS	None
241-BX-107	Sluicing	360 ft^3	None	HTWOS	None
241-BX-108	Mobile retrieval system	360 ft^3	2,500	HTWOS	Corbin et al. 2005
241-BX-109	Sluicing	360 ft^3	None	HTWOS	None
241-BX-110 [c]	Mobile retrieval system	360 ft^3	NSI [c]	HTWOS	None

Table 2-27. Reference Case Analysis of Waste Management Area B-BX-BY (3 pages)

Inventory and Source Terms					
Sources	**Assumed Retrieval Method**	**Residual Volume**	**Volume Associated with Past Release [a] gal**	**Basis for Contaminant Inventory Estimate**	
				Residual Waste [b]	**Past Release**
241-BX-111 [c]	Mobile retrieval system	360 ft^3	NSI [c]	HTWOS	None
241-BX-112	Sluicing	360 ft^3	None	HTWOS	None
241-BY-101	Sluicing	360 ft^3	None	HTWOS	None
241-BY-102	Sluicing	360 ft^3	None	HTWOS	None
241-BY-103	Mobile retrieval system	360 ft^3	400	HTWOS	None
241-BY-104	Sluicing	360 ft^3	None	HTWOS	None
241-BY-105 [c]	Mobile retrieval system	360 ft^3	NSI [c]	HTWOS	None
241-BY-106 [c]	Mobile retrieval system	360 ft^3	NSI [c]	HTWOS	None
241-BY-107	Mobile retrieval system	360 ft^3	1,200	HTWOS	None
241-BY-108	Mobile retrieval system	360 ft^3	400	HTWOS	None
241-BY-109	Sluicing	360 ft^3	None	HTWOS	None
241-BY-110	Sluicing	360 ft^3	None	HTWOS	None
241-BY-111	Sluicing	360 ft^3	None	HTWOS	None
241-BY-112	Sluicing	360 ft^3	None	HTWOS	None
UPR-200-E-6	NA	NA	1,017	NA	Corbin et al. 2005
UPR-200-E-38	NA	NA	5,400	NA	Corbin et al. 2005
UPR-200-E-73	NA	NA	92.5	NA	Corbin et al. 2005
UPR-200-E-74	NA	NA	10	NA	Corbin et al. 2005
UPR-200-E-75	NA	NA	1,017	NA	Corbin et al. 2005
UPR-200-E-105	NA	NA	23,000	NA	Corbin et al. 2005
UPR-200-E-108	NA	NA	196	NA	Corbin et al. 2005
UPR-200-E-109	NA	NA	150	NA	Corbin et al. 2005
UPR-200-E-110	NA	NA	5,085	NA	Corbin et al. 2005
241-B-301 catch tank [d]	TBD [d]	20 ft^3	None	Average	None
241-BX-302A catch tank [d]	TBD [d]	6.4 ft^3	None	Average	None
244-BX DCRT [d]	TBD [d]	17 ft^3	None	Average	None

Table 2-27. Reference Case Analysis of Waste Management Area B-BX-BY (3 pages)

Inventory and Source Terms					
Sources	**Assumed Retrieval Method**	**Residual Volume**	**Volume Associated with Past Release [a] gal**	**Basis for Contaminant Inventory Estimate**	
				Residual Waste [b]	**Past Release**
244-BXR-001 vault tank [d]	TBD [d]	27 ft^3	None	Average	None
244-BXR-002 vault tank [d]	TBD [d]	8 ft^3	None	Average	None
244-BXR-003 vault tank [d]	TBD [d]	8 ft^3	None	Average	None
244-BXR-011 vault tank [d]	TBD [d]	17 ft^3	None	Average	None
241-B tank farm pipelines [e]	TBD	None	None	Lambert 2005	NA
241-BX tank farm pipelines [e]	TBD	28.0 L	None	Lambert 2005	NA
241-BY tank farm pipelines [e]	TBD	None	None	Lambert 2005	NA

[a] Past leak volumes listed in Field and Jones (2005).

[b] Residual inventories from HTWOS model output (Kirkbride et al. 2005).

[c] NSI = not sufficient information. Tanks B-101, B-103, B-105, B-111, BX-110, BX-111, BY-105, and BY-106 are identified as a "confirmed or suspected" leaker in Hanlon (2005) but Field and Jones (2005) state there is insufficient information for developing a leak volume at this time. As information becomes available, a leak volume will be developed.

[d] TBD = to be determined. Final disposition of MUSTs not yet determined; however, MUSTs were carried forward in the assessment assuming MUSTs will be retrieved to at least the HFFACO goal (Ecology et al. 1989, Milestone M-45-00) equivalent to the 200-Series tanks. The residual volume is calculated by ratio of the total volume of the MUST to the 200-Series tanks (e.g., the retrieval goal for the 55,000-gal 200-Series tanks is 30 ft^3; thus, a MUST that is ⅔ the size of the 200-Series tank would have a residual volume of 20 ft^3). Inventory was calculated based on average waste per ft^3 within the WMA calculated from the HTWOS model (Kirkbride et al. 2005).

[e] Final disposition of pipelines is not yet determined; however, pipelines were carried forward in the assessment. Pipeline residual volumes shown represent the volume of waste in plugged or blocked pipelines as determined by Lambert (2005).

NA = not applicable

Table 2-28. Reference Case Inventory Estimates for Waste Management Area B-BX-BY

Source Type	Dominant Contaminants for Groundwater Pathway Impacts [a]							Dominant Contaminants for Inadvertent Intruder Impacts [a]						
	C-14 Ci	Tc-99 Ci	I-129 Ci	Cr(VI) kg	NO_3 kg	NO_2 kg	U kg	Sr-90 Ci	Tc-99 Ci	Sn-126 Ci	Cs-137 Ci	Pu-239 Ci	Pu-240 Ci	Am-241 Ci
Past releases [b]	3.98E-01	1.00E+01	1.53E-02	1.99E+02	2.44E+04	3.98E+03	1.01E+04	3.53E+03	1.00E+01	1.19E-01	9.30E+03	1.91E+00	2.23E-01	1.98E+00
Tank residuals	6.00E-01	3.92E+01	9.98E-02	1.80E+03	2.09E+04	2.33E+03	6.54E+03	8.71E+04	3.92E+01	7.14E-01	2.84E+04	1.45E+02	2.27E+01	5.14E+01
Ancillary equipment residuals [c]	2.27E-03	1.05E-01	2.47E-04	9.62E+00	1.33E+02	1.52E+01	5.51E+01	NA	NA	NA	NA	NA	NA	NA

[a] The reference case analysis included all BBI contaminants. As described in Bowen (2004), the standard analyte list tracked in the BBI contains **25 chemicals** including:

- aluminum
- bismuth
- calcium
- chlorine
- chromium
- fluorine
- total inorganic carbon as carbonate
- iron
- mercury
- potassium
- lanthanum
- manganese
- sodium
- nickel
- nitrite
- nitrate
- oxalate
- lead
- phosphate
- silicon
- sulfate
- strontium
- uranium total
- zirconium
- total organic carbon

and **46 radionuclides** including:

- tritium
- carbon-14
- nickel-59
- cobalt-60
- nickel-63
- selenium-79
- strontium-90
- yttrium-90
- zirconium-93
- niobium-93m
- technetium-99
- ruthenium-106
- cadmium-113m
- antimony-125
- tin-126
- iodine-129
- cesium-134
- cesium-137
- barium 137m
- samarium-151
- europium-152
- europium-154
- europium-155
- radium-226
- actinium-227
- radium-228
- thorium-229
- protactinium-131
- thorium-232
- uranium-232
- uranium-233
- uranium-234
- uranium-235
- uranium-236
- neptunium-237
- plutonium-238
- uranium-238
- plutonium-239
- plutonium-240
- americium-241
- plutonium-241
- curium 242
- plutonium-242
- americium-243
- curium-243
- curium-244

[b] Inventories shown are the combined inventories from SST past releases and ancillary equipment past releases. Both release types were considered for the groundwater pathway analysis; however, only the SST past releases were included in the inadvertent intruder analysis (along with SST residuals).

[c] NA indicates insufficient information is available to make estimates of intruder impacts into ancillary equipment (e.g., pipelines, diversion boxes).

2.12 DESCRIPTION OF WASTE MANAGEMENT AREA A-AX

This section provides site-specific information for WMA A-AX. It is a summary from numerous documents that describe present conditions (Hanlon 2005), geology and hydrology (Reidel et al. 2006), subsurface contamination (Wood et al. 2003), and source terms (Kirkbride et al. 2005; Field and Jones 2005; Lambert 2005; and Corbin et al. 2005).

2.12.1 Background

WMA A-AX is located in the south central portion of 200 East Area (Figure 2-79). WMA A-AX contains the A tank farm and AX tank farm. The A tank farm contains six SSTs that were constructed in 1954, put into service in 1955, and used to store and transfer waste until 1980. The AX tank farm contains four tanks that were constructed in 1963, put into service in 1964, and used to store and transfer waste until 1980. The A and AX tank farms received waste generated by PUREX Plant operations. The PUREX process produced three major waste streams: PUREX coating waste, PUREX acid waste which contained about 99% of the fission products, and organic wash waste.

During its operational history, there were a number of confirmed or suspected waste loss events in WMA A-AX. These included suspected tank leaks and known waste losses from piping systems. Currently, the pumpable liquid wastes have been removed from the WMA A-AX tanks and all tanks have been interim stabilized (Hanlon 2005). Table 2-29 lists the estimated volume of waste stored in the WMA A-AX tanks as of November 30, 2004.

The current understanding of contaminant occurrences and environmental conditions at WMA A-AX is described in Wood et al. (2003). Historical information on soil surface and vadose zone contamination in WMA A-AX is provided in Williams (2001c). The primary contamination zones currently identified in WMA A-AX are a localized cesium-137 activity zone near the bottom of tanks A-104 and A-105 and three UPRs near pipelines and diversion boxes.

A FIR for WMA A-AX is scheduled to be issued in fiscal year 2006. Field characterization data to support the FIR is scheduled to be collected in fiscal year 2005 as outlined in Crumpler (2004). Planned WMA A-AX closure and post-closure actions identified at the present time are described in Lee (2004).

Figure 2-79. Location Map of Waste Management Area A-AX and Surrounding Facilities [a]

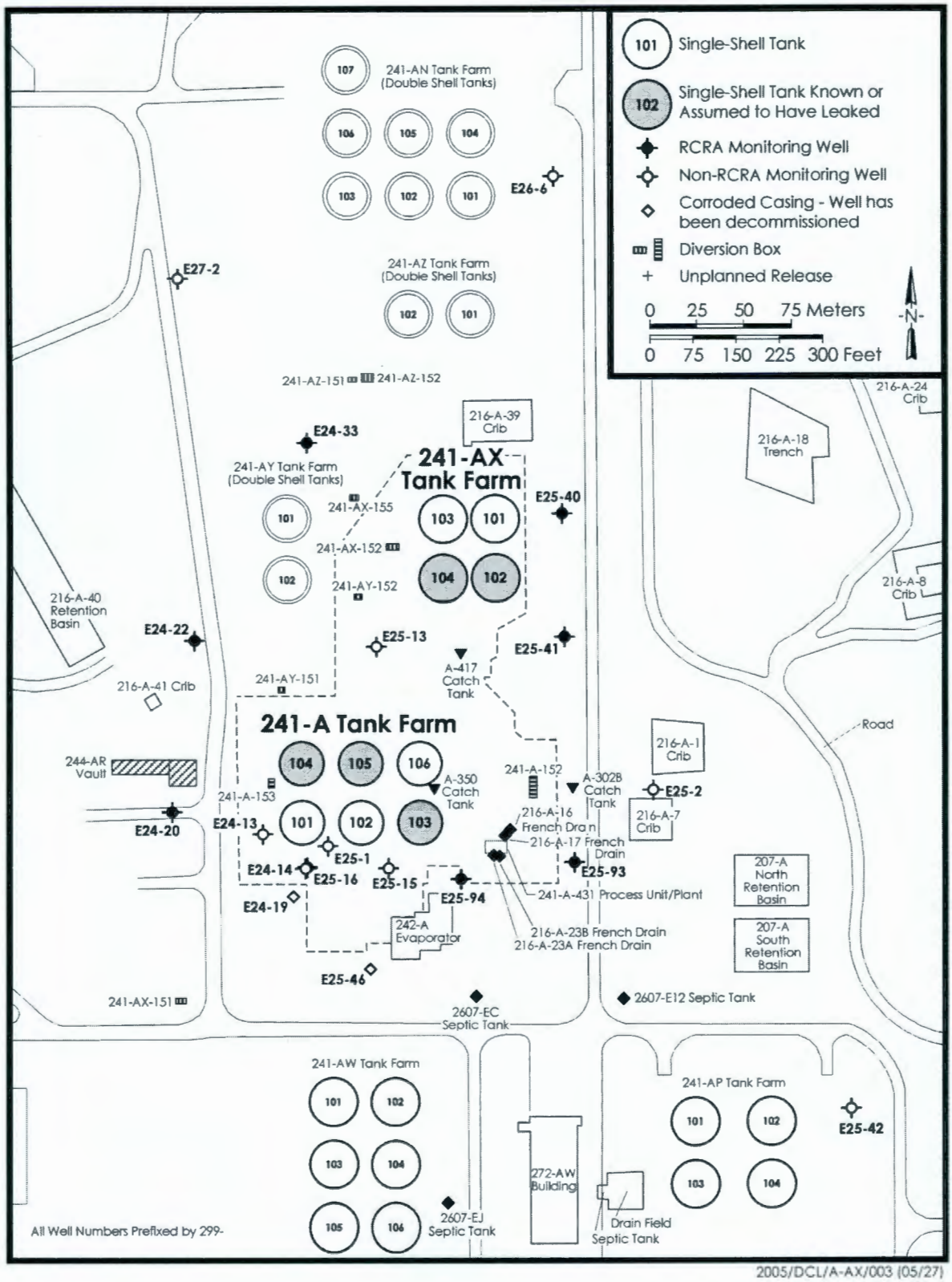

[a] *Crumpler (2004)*

Table 2-29. Waste Volume Estimates as of November 30, 2004, in Waste Management Area A-AX Single-Shell Tanks [a]

Tank	Total Waste Volume kgal	Supernate kgal	Saltcake kgal	Sludge kgal
241-A-101	320	0	317	3
241-A-102	40	3	37	0
241-A-103	370	4	364	2
241-A-104	28	0	0	28
241-A-105	37	0	0	37
241-A-106	79	0	29	50
241-AX-101	358	0	355	3
241-AX-102	30	0	24	6
241-AX-103	107	0	99	8
241-AX-104	7	0	0	7

[a] Hanlon (2005).

2.12.2 Infrastructure

This section describes the WMA A-AX infrastructure components that were included in the SST PA and are listed in Table 2-30. Reference case inventory development for those components is described in Section 2.12.7. Refer to Section 2.4 for generic infrastructure component descriptions and Section 2.5 for a summary of infrastructure inventory development methods.

2.12.2.1 Single-Shell Tanks

The A and AX series tanks are 75 ft in diameter and 44 ft tall from base to dome. The A tank farm contains six SSTs with a capacity of 1,000,000 gal each, and the AX tank farm contains four SSTs with a capacity of 1,000,000 gal each. Typical tank configuration and dimensions are shown in Figure 2-80. The tanks sit belowgrade with a 6.0 ft soil cover to provide shielding from radiation exposure to operating personnel. Tank pits are located on top of the tanks and provide access to the tank, pumps, and monitoring equipment.

The SSTs were constructed in place with carbon steel (ASTM 2005) lining the bottom and sides of a reinforced concrete shell. The tanks in the A and AX tank farms have a flat bottom. In addition, the A tank farm was underlain by laterals connected to caissons as a leak detection system because the tank farm was designed to store boiling waste. The AX farm tanks included a grid of drain slots beneath the steel liner bottom and a leak detection well that could collect potential leakage. The tanks in WMA A-AX were connected by overflow lines but did not cascade.

Table 2-30. Operating Period and Capacities for Waste Management Area A-AX Facilities Included in Performance Assessment [a]

Facility	Removed From Service	Constructed	Operating Capacity gal
Single-Shell Tanks			
241-A-101	1980	1954 to 1955	1,000,000
241-A-102	1980	1954 to 1955	
241-A-103	1980	1954 to 1955	
241-A-104	1975	1954 to 1955	
241-A-105	1963	1954 to 1955	
241-A-106	1980	1954 to 1955	
241-AX-101	1980	1963 to 1964	
241-AX-102	1980	1963 to 1964	
241-AX-103	1980	1963 to 1964	
241-AX-104	1978	1963 to 1964	
Miscellaneous Underground Storage Tanks			
241-A-350 catch tank	1985	1956	800
241-A-417 catch tank	1985	1956	44,2000
241-AX-152 catch tank [b]	1985	1965	NA
244-AR vault [c]	1985	1976	NA
Underground Waste Transfer Lines			
241-A tank farm pipelines	NA	1954 to 1955	17,600 (+/-5,800)
241-AX tank farm pipelines	NA	1963 to 1964	15,300 (+/-4,400)

[a] Data on the facilities is from DOE-RL (2005).

[b] Catch tank 241-AX-152 was stabilized and isolated in 2002 (Allen 2002) and has a reported waste level of 0 in.

[c] The 244-AR vault is located outside the WMA A-AX boundary and was not included in the analysis.

NA = not applicable

Figure 2-80. Typical Configuration and Dimensions of Single-Shell Tanks in Waste Management Area A-AX

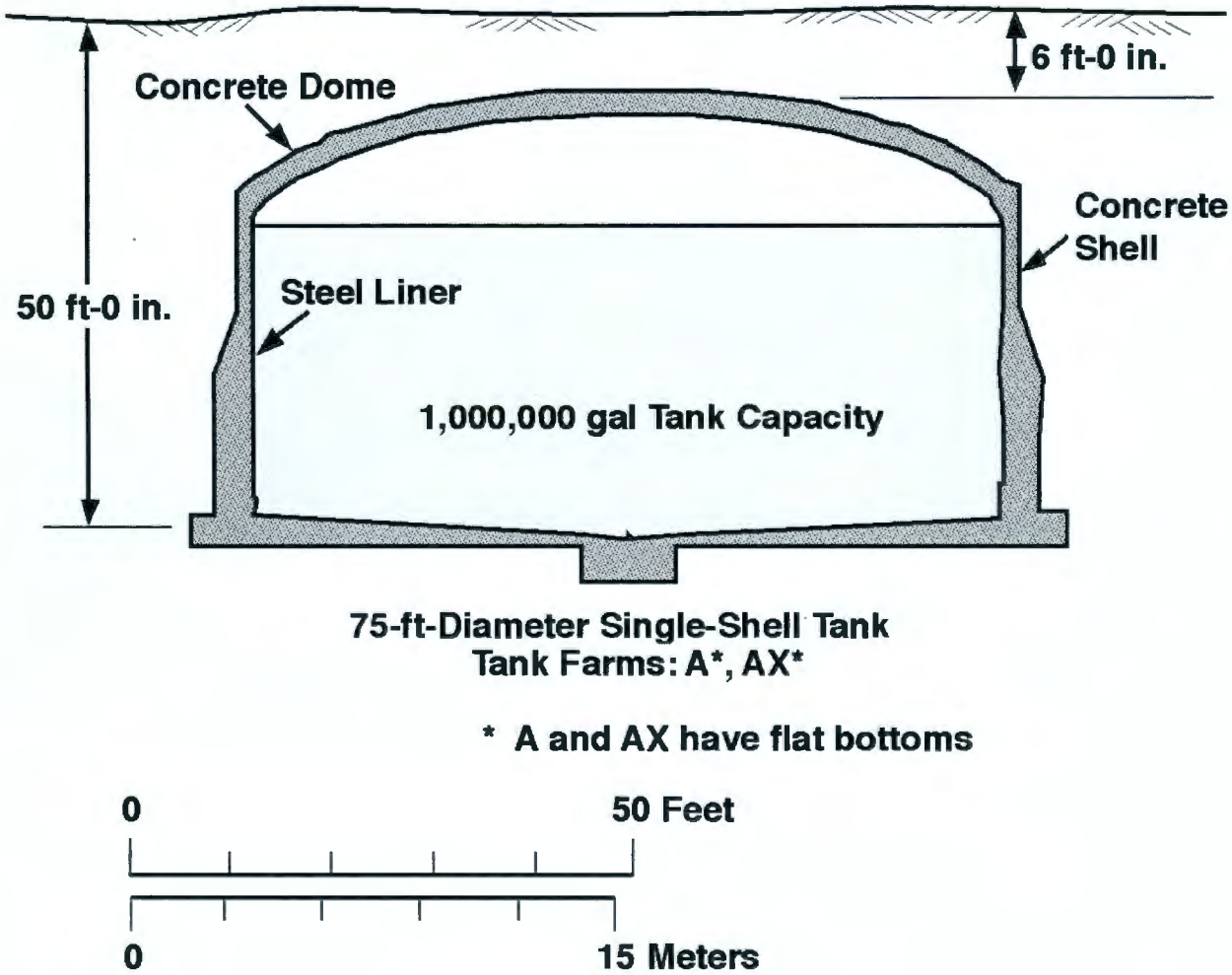

2.12.2.2 Ancillary Equipment

A complete listing of the WMA A-AX ancillary equipment currently identified for inclusion in the SST system closure is provided in Lee (2004). As discussed in Section 2.5.4, the ancillary components included in the SST PA consist of the underground waste transfer lines and MUSTs located inside each WMA boundary. For WMA A-AX, the ancillary components analyzed consist of the A and AX tank farms waste transfer piping and two MUSTs (241-A-350 and 241-A-417 catch tanks).

The 241-AX-152 catch tank is located inside the WMA A-AX boundary and is not included in the analysis because it was stabilized and isolated in 2002 (Allen 2002) and has a reported waste level of 0 in. The 244-AR vault is located outside the WMA A-AX boundary (Figure 2-79) and is not included in the analysis. That facility will be evaluated in the future under the integrated regulatory closure process described in Chapter 1.0.

Multiple levels of piping were installed over time in WMA A-AX. A time line of piping installations is described in Williams (2001c). It is estimated that there are approximately 9.1 mi (+/-3.0 mi) of waste transfer piping in the A tank farm and 7.9 mi (+/-2.3 mi) in the AX tank farm (Field 2003a).

Four intentional discharge facilities (216-A-16, 216-A-17, 216-A-23A, 216-A-23B French drains) are located inside the WMA A-AX boundary (Figure 2-79). As discussed in Section 2.5.2, intentional discharge facilities are not included in the SST PA. Those facilities will be evaluated in the future under the integrated regulatory closure process described in Chapter 1.0.

2.12.3 Geology

Following is an overview of the geology of WMA A-AX summarized from the information provided in Reidel et al. (2006). Because WMA A-AX and WMA C are in close proximity and have similar geologic conditions, they are discussed together in Reidel et al. (2006) and will be discussed together here. The generalized stratigraphy and thicknesses in the 200 East Area are shown in Section 2.3. A generalized cross-section through WMAs A-AX and C is shown in Figure 2-81. Maps and cross-sections presented in Reidel et al. (2006) illustrate the distribution and thicknesses of these units in additional detail.

Seven stratigraphic units lie within WMAs A-AX and C. From oldest to youngest, the primary geologic units are:

- Columbia River Basalt Group
- Undifferentiated Cold Creek unit fine unit and/or Ringold Formation
- Undifferentiated Cold Creek unit gravel and/or Ringold Formation Unit A?
- Hanford formation – lower gravelly sequence (H3 unit)
- Hanford formation – sand sequence (H2 unit)
- Hanford formation – upper gravelly sequence (H1 unit)
- Recent deposits.

The general characteristics of these units are described in Section 2.3 and in more detail in Reidel et al. (2006). The SSTs at WMAs A-AX and C were emplaced within the Hanford formation sediments of the upper, gravel-dominated (H1) unit, and may locally intercept the upper portions of the sand-dominated Hanford (H2) unit. The water table or potentiometric surface lies approximately 200 ft below the bottom of the tank farms excavations at the basal portion of the Hanford formation (i.e., lower sand/silt dominated) H3 unit, or within the uppermost portions of the Cold Creek unit or Ringold Formation.

Figure 2-81. Fence Diagram Showing Cross-Sections through Waste Management Areas A-AX and C [a]

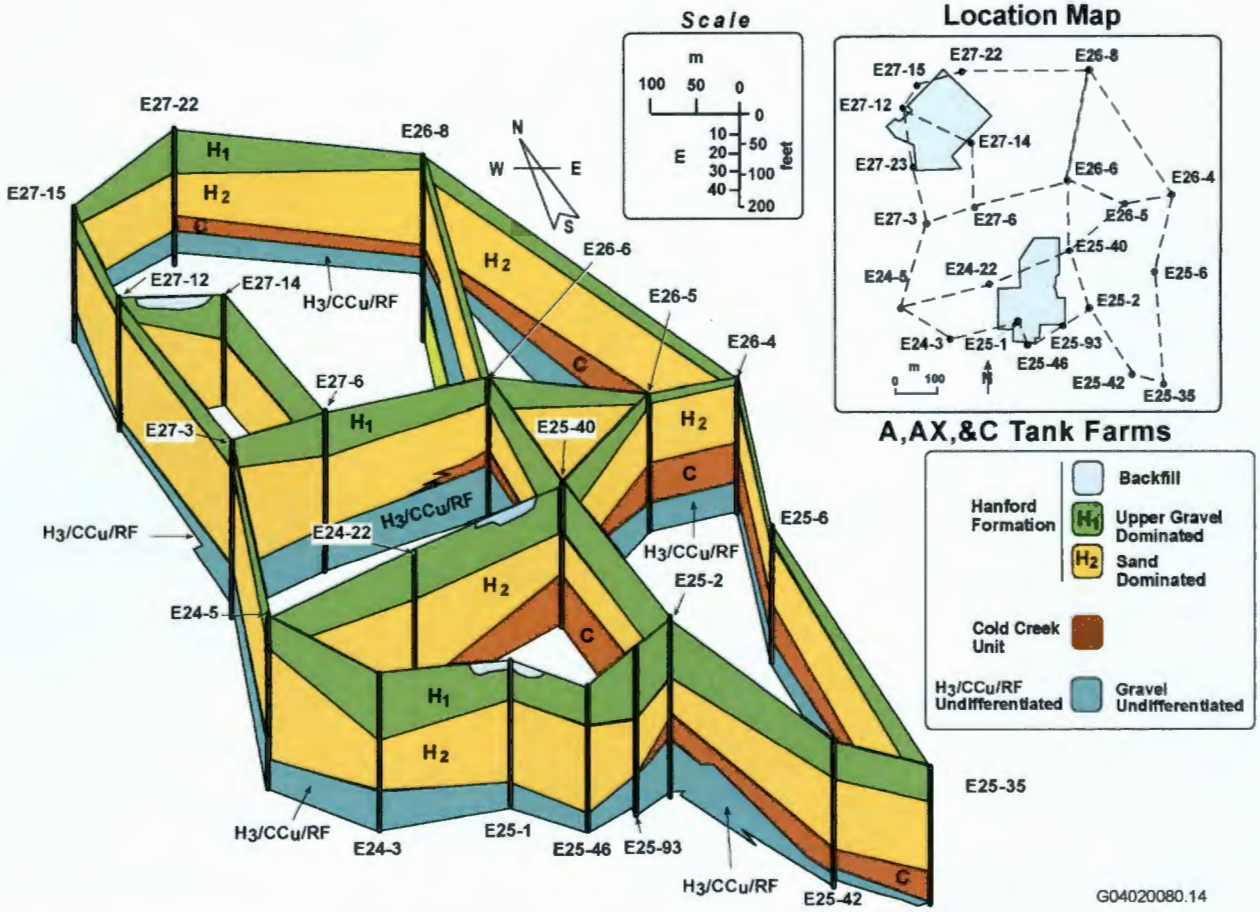

[a] *Reidel et al. (2006)*

2.12.4 Hydrology

Following is an overview of the hydrology of the uppermost, unconfined aquifer beneath WMA A-AX. More detailed information supporting this section can be found in Reidel et al. (2006), Wood et al. (2003), and Hartman et al. (2004). Currently, the general groundwater flow direction in the unconfined aquifer beneath WMA A-AX is to the southeast.

The shift in discharge of large volumes of wastewater in the early 1950s to B Pond raised the water table in the vicinity of WMAs C and A-AX as much as 16 ft above the pre-Hanford Site operations level (Hartman et al. 2004). Water levels began to decline in the late 1980s when wastewater discharges were reduced. The decline has become even more pronounced since other effluent discharges throughout the 200 Areas ceased in 1995. Water levels are expected to continue declining within the region surrounding WMAs A-AX and C.

The vadose zone extends to a depth of 295 ft around WMA A-AX (Narbutovskih and Horton 2001). The unconfined aquifer is relatively thin (60 to 90 ft) and resides mostly within the undifferentiated Cold Creek unit gravels and/or Ringold Formation Unit A? sequence.

2.12.5 Vadose Zone Conditions

This section summarizes WMA A-AX vadose zone monitoring and characterization activities, and the current understanding of contamination in the vadose zone.

2.12.5.1 Monitoring and Characterization

The A tank farm has 53 leak detection drywells available for leak detection monitoring (Figure 2-82). These drywells were drilled from 1955 to 1981. The depth ranges for most of these drywells are between 80 and 150 ft bgs, except for drywell 10-06-18, which is 180 ft bgs. Gamma logging data from the drywells from 1974 through 1993 were used to ascertain the integrity of the associated tanks.

The AX tank farm has 33 leak detection drywells available for leak detection monitoring and that provide access for limited vadose zone characterization (e.g., geophysical logging) (Figure 2-83). These drywells were drilled from 1974 to 1981. The depth ranges for most of these drywells are between 75 and 150 ft bgs.

A high-resolution spectral gamma logging system was used in 1997 to log AX tank farm drywells and in 1998 and 1999, to log A tank farm drywells. This effort was part of the baseline characterization for WMA A-AX. Results are documented in DOE-GJO (1997d, 1999b). The addendum report for A tank farm is DOE-GJO (2000L); the addendum report for AX tank farm is DOE-GJO (2000m).

The major gamma-emitting contaminant associated with WMA A-AX is cesium-137. Historical gross gamma evaluations also indicated the presence of ruthenium-106 in the 1970s, which has since decayed to negligible quantities. Contaminants are located mostly in and around areas of confirmed or suspected tank and pipeline leaks.

Additional information on manmade radionuclide distribution and movement will be discussed in the FIR resulting from the WMA A-AX Phase I field investigation. Collection of field characterization data to support the FIR is scheduled to begin in fiscal year 2005 (Crumpler 2004). The draft FIR for WMA A-AX is scheduled to be issued in fiscal year 2006.

Figure 2-82. Vadose Zone Monitoring Network for the A Tank Farm

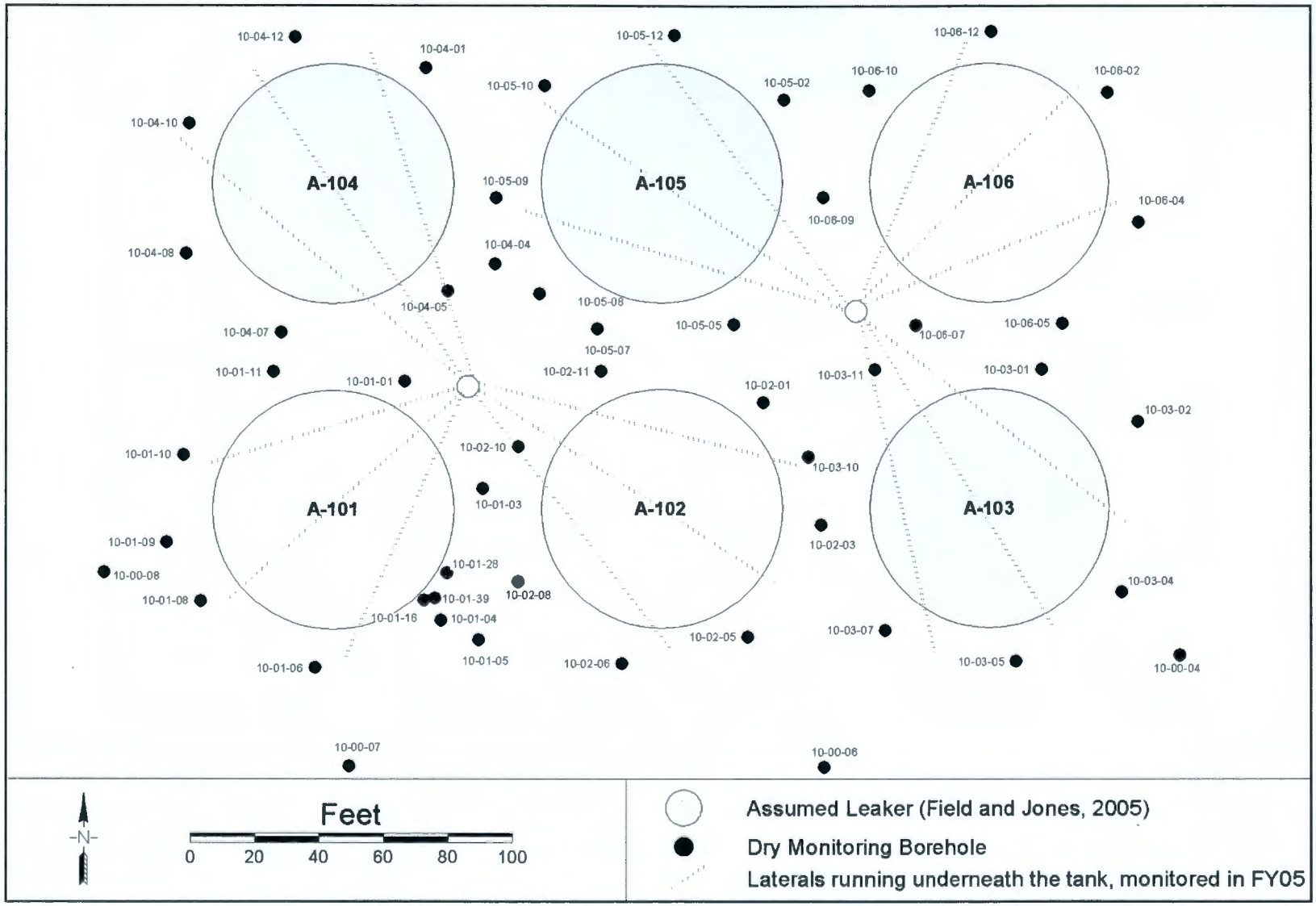

Figure 2-83. Vadose Zone Monitoring Network for the AX Tank Farm

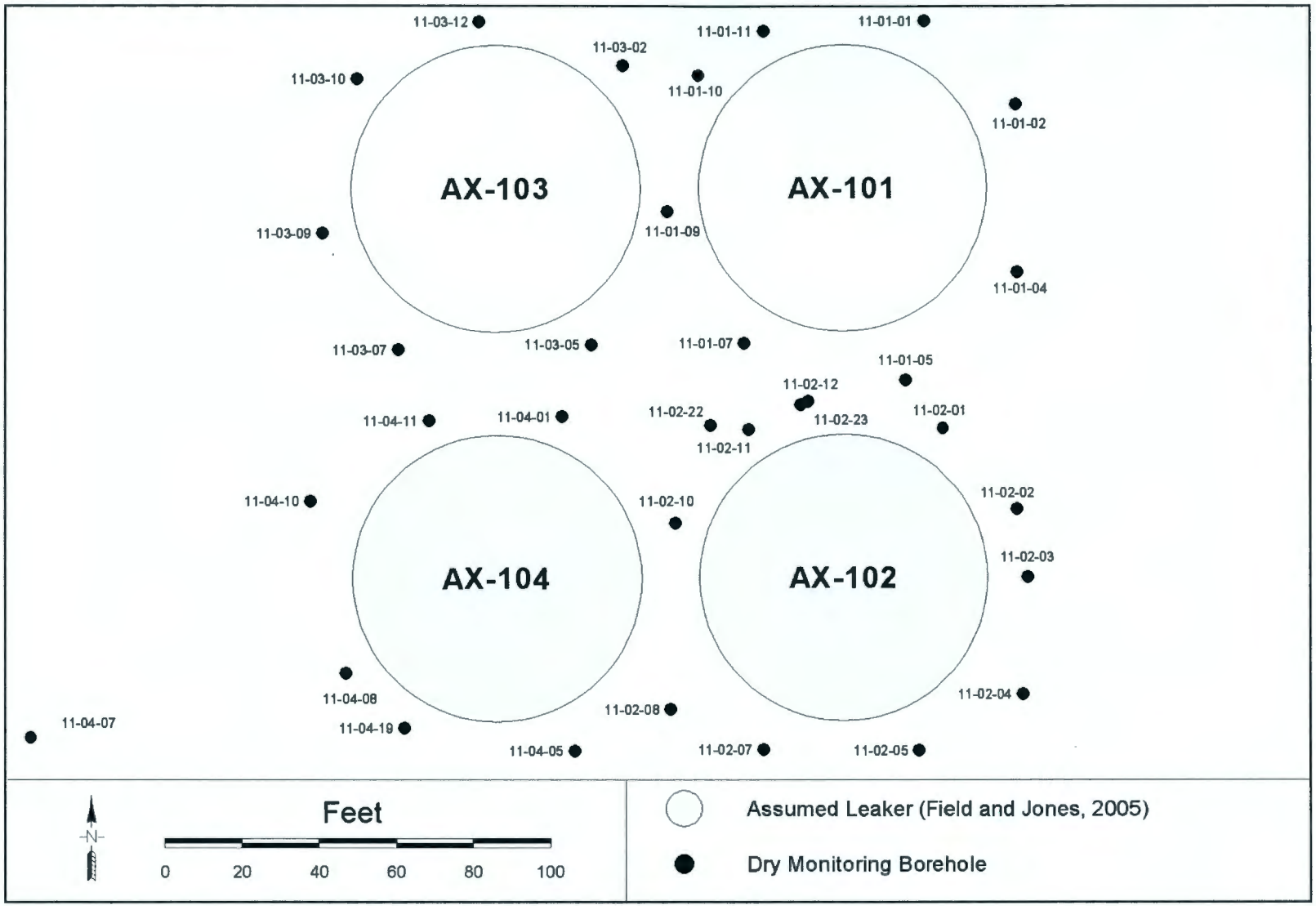

2.12.5.2 Contamination

An overall assessment of the spectral gamma logging data from WMA A-AX drywells indicates minimal tank waste contamination in the vadose zone (Wood et al. 2003). Figures 2-84 and 2-85 are three-dimensional perspectives of A and AX tank farms providing locations of tanks and associated drywells. Tanks considered to be leakers based on information in Field and Jones (2005) are shown with darker shading. Each drywell is represented with a single vertical line. Shaded rings around the drywells indicate the level of vadose zone contamination based on spectral gamma logging results. Only the more significant soil contamination zones are shown. Zones with contamination levels less than 10 pCi/g are not shown.

Cesium-137 concentrations have been measured at several drywells (10-05-02, 10-05-05, 10-05-07, 10-05-09, 10-06-09, 10-05-12) at the tank bottom and lower depths. However, many of these drywells were constructed in two stages and drag-down contamination is likely in most of them. One drywell (10-05-10) may contain cesium-137 contamination from the tank A-105 leak (between 23 and 26 m [75 and 86 ft] bgs) but the complicated drilling process may have shifted the cesium-137 from its original location. The historical gross gamma log shows a shift in cesium-137 contamination levels around 1978; this is probably related to the second-stage drilling that occurred then.

2.12.6 Unconfined Aquifer Conditions

This section summarizes WMA A-AX groundwater monitoring and characterization activities and the current understanding of contamination in the unconfined aquifer.

2.12.6.1 Monitoring and Characterization

Seven RCRA groundwater monitoring wells are associated with WMA A-AX. The wells are intended to monitor groundwater contamination attributable to the entire WMA rather than individual components. There are four downgradient wells (299-E24-19, 299-E24-20, 299-E25-46, 299-E25-93) and three upgradient wells (299-E24-22, 299-E25-40, 299-E25-41). Wells 299-E24-22 and 299-E25-93 were both installed in fiscal year 2003 (Hartman et al. 2004). The initial background-monitoring program for WMA A-AX is complete and monitoring is currently conducted under an interim status indicator evaluation program.

The contaminant indicator parameters and the statistical evaluation methodology for the WMA A-AX groundwater indicator evaluation program are described in Narbutovskih and Horton (2001). Results of the groundwater detection indicator evaluation program are published annually. The most recently published data are for fiscal year 2003 (Hartman et al. 2004).

2.12.6.2 Contamination

The most recently published groundwater monitoring results for WMA A-AX are for fiscal year 2003 (Hartman et al. 2004). Following is a summary of the fiscal year 2003 results adapted from Hartman et al. (2004). Additional detail on groundwater contamination and geochemistry at WMA A-AX can be found in Hartman et al. (2004) and Reidel et al. (2006).

Technetium-99 levels have increased slightly across WMA A-AX, with the highest value of 234 pCi/L (in fiscal year 2003) found to the northeast in well 299-E25-41. The technetium-99 concentration in this well was 220 pCi/L in fiscal year 2002. Well 299-E25-41 is downgradient from the AX tank farm, which currently has no upgradient coverage. This slight rise means technetium-99 is probably moving into the area from farther north.

Figure 2-84. Three-Dimensional Perspective of A Tank Farm Tanks and Drywells Showing Occurrence of Significant (>10 pCi/g) Cesium-137 Contamination in the Vadose Zone

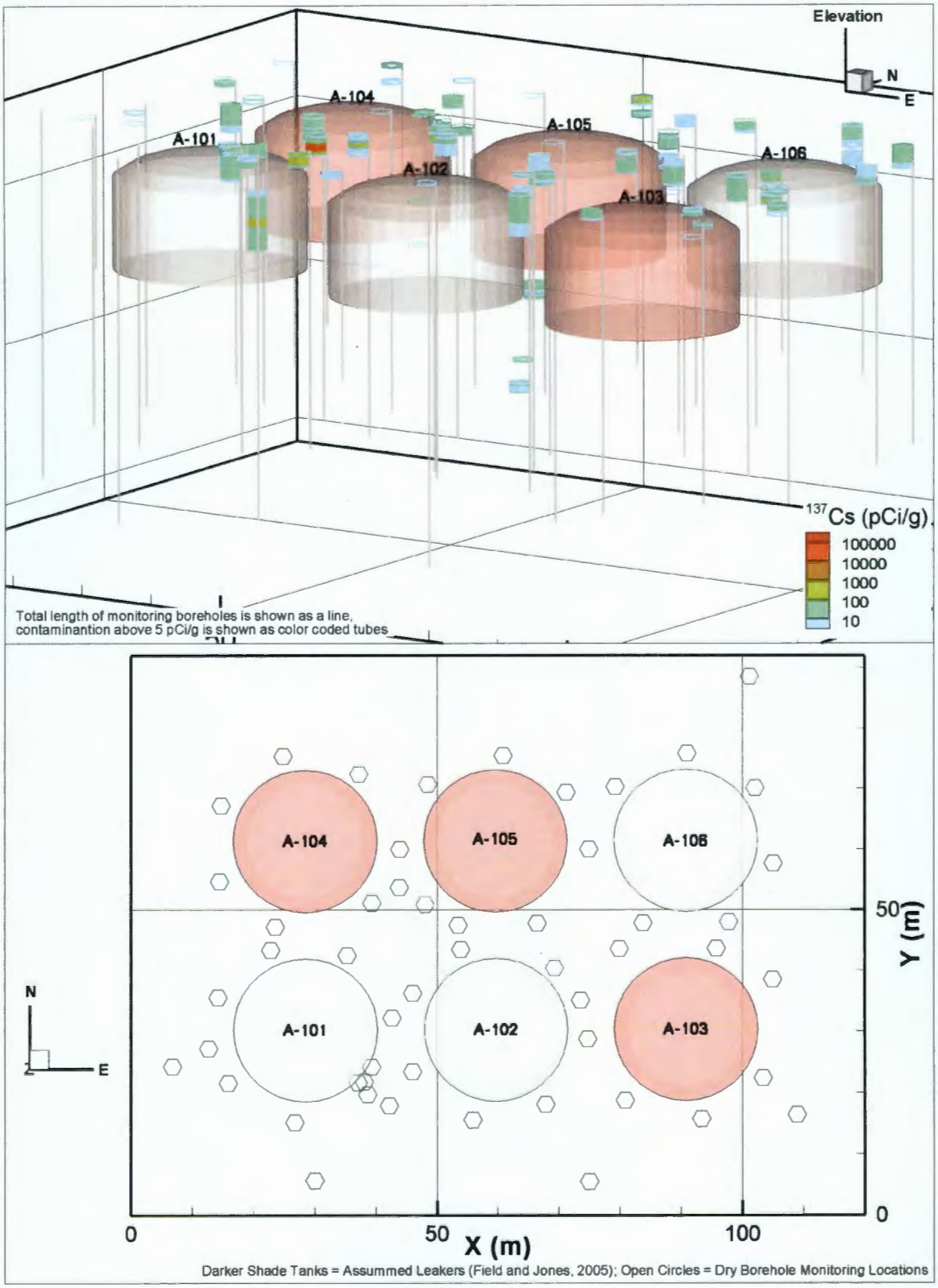

Figure 2-85. Three-Dimensional Perspective of AX Tank Farm Tanks and Drywells Showing Occurrence of Significant (>10 pCi/g) Cesium-137 Contamination in the Vadose Zone

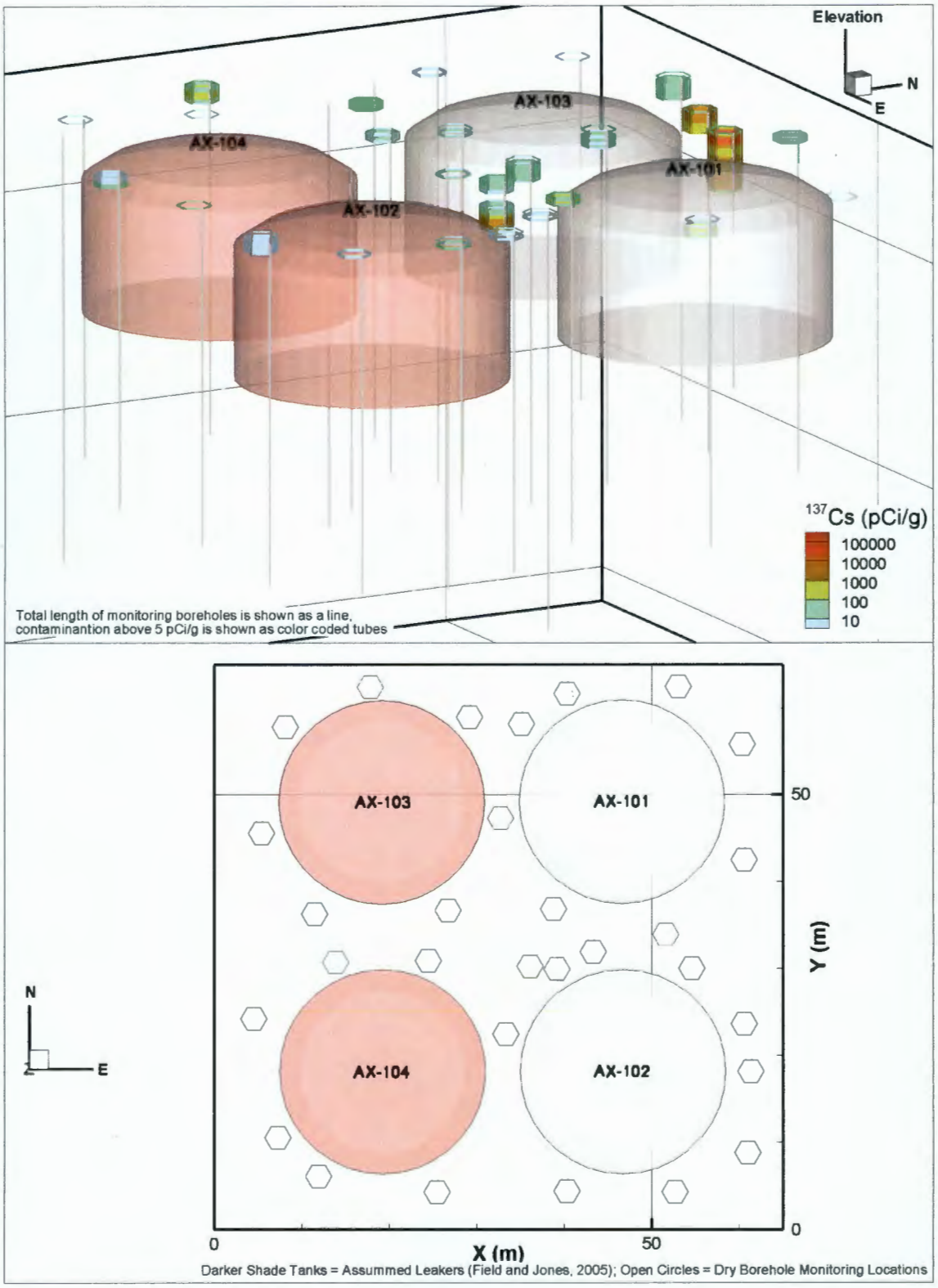

Tritium values across WMA A-AX have increased from a range of 4,150 to 8,750 pCi/L reported for June 2002 to a range of 5,060 to 12,200 pCi/L in fiscal year 2003. The drinking water standard for tritium is 20,000 pCi/L. The highest value of 12,200 pCi/L is seen upgradient of the site. This local region had higher values of tritium (over 200,000 pCi/L) in the late 1960s when the PUREX Plant was operating. The rising tritium does not appear to be related to WMA A-AX and is, most likely, part of a regional trend.

In filtered samples from well 299-E24-19, chromium continued to be detected at values above the drinking water standard of 100 µg/L, ranging from 462 to 2,510 µg/L in fiscal year 2003. Historically, manganese and nickel also exceed the DWS levels when chromium concentrations are high (manganese, 50 µg/L; nickel, 100 µg/L). The elevated concentrations of metals are associated with the corrosion of stainless steel and not with any tank-associated waste as shown by comparing chromium concentrations to technetium-99 levels in this well (Figure 2-86). Sampling results from purge testing showed that the chromium is from a source close to the well and is not moving through the aquifer. Furthermore, the inverse relationship between chromium concentrations and pH observed during extended purge tests supports a chromium source based on a reduction-oxidation reaction of stainless steel.

Figure 2-86. Chromium and Technetium-99 Trends at Well 299-E24-19

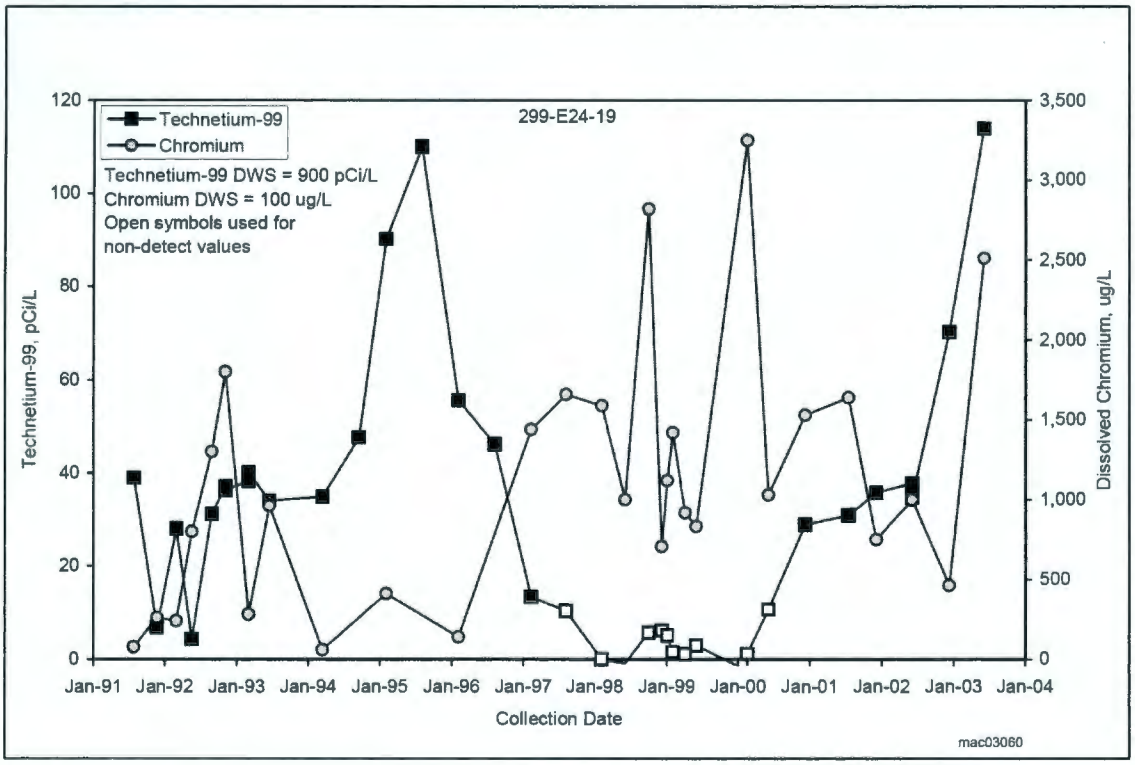

2.12.7 Reference Case Source Terms

The reference case describes a set of assumed post-retrieval conditions that are based on current waste retrieval plans. The reference case analysis for WMA A-AX includes three source terms consisting of past UPRs, residual SST waste, and residual ancillary equipment waste. Table 2-31 provides a listing of the reference case source terms for WMA A-AX, and the inventory data source for those source terms.

Source term inventories (reference case) for WMA A-AX are provided in Table 2-32. To simplify the table, only the contaminants that dominate post-closure impacts are shown. All BBI contaminants are included in the reference case modeling analysis. Refer to Section 2.5 for a summary of source term inventory development methods. Source data are provided in Appendix C.

2.12.7.1 Past Unplanned Releases

The WMA A-AX reference case includes past UPRs associated with four SSTs (A-103, A-104, A-105, AX-102). Volume estimates for those four waste loss events were developed by Field and Jones (2005) and vadose zone contaminant inventories were generated by Corbin et al. (2005) (Section 2.5.2). No volume or inventory estimates were assigned to the waste loss event associated with tank AX-104 because of insufficient information to quantify or verify the releases (Field and Jones 2005). If new information becomes available to quantify the waste loss events from those tanks, the data will be evaluated under the integrated regulatory closure process described in Chapter 1.0.

2.12.7.2 Residual Single-Shell Tank Waste

The WMA A-AX reference case includes residual waste in each of the ten 100-Series SSTs in the A and AX tank farms. The HFFACO Milestone M-45-00 goal allows up to 360 ft^3 of waste to remain in the 100-Series tanks after retrieval in the event that retrieval beyond that level becomes impracticable (Ecology et al. 1989). Thus, the analysis includes a 360 ft^3 source term associated with residual waste remaining in each of the tanks after retrieval. The inventory estimates were generated with the use of the HTWOS model (Kirkbride et al. 2005), which accounts for the waste retrieval technology and tracks the fate of soluble and insoluble constituents in the waste (Section 2.5.3).

2.12.7.3 Residual Ancillary Equipment Waste

Lambert (2005) identified no plugged and blocked piping in the A and AX tank farms. Therefore, the reference case ancillary equipment source term for WMA A-AX includes only two ancillary components, the 241-A-350 and 241-A-417 catch tanks (Section 2.5.4). The estimated volume of residual waste in those tanks was calculated by assuming the tanks would be retrieved to a residual volume proportional to that required under the HFFACO Milestone M-45-00 for 200-Series tanks (Ecology et al. 1989). Contaminant inventories for the tanks were estimated using the average chemical composition of the waste in WMA T SSTs.

Table 2-31. Reference Case Analysis of Waste Management Area A-AX

Inventory and Source Terms					
Sources	**Assumed Retrieval Method**	**Residual Volume**	**Volume Associated with Past Release [a] gal**	**Basis for Contaminant Inventory Estimate**	
				Residual Waste [b]	**Past Release**
241-A-101	Sluicing	360 ft^3	None	HTWOS	None
241-A-102	Sluicing	360 ft^3	None	HTWOS	None
241-A-103	Mobile retrieval system	360 ft^3	5,500	HTWOS	Corbin et al. 2005
241-A-104	Mobile retrieval system	360 ft^3	2,000	HTWOS	Corbin et al. 2005
241-A-105	Mobile retrieval system	360 ft^3	1,000	HTWOS	Corbin et al. 2005
241-A-106	Sluicing	360 ft^3	None	HTWOS	None
241-AX-101	Sluicing	360 ft^3	None	HTWOS	None
241-AX-102	Mobile retrieval system	360 ft^3	3,000	HTWOS	Corbin et al. 2005
241-AX-103	Sluicing	360 ft^3	None	HTWOS	None
241-AX-104 [c]	Mobile retrieval system	360 ft^3	NSI [c]	HTWOS	None
241-A-350 catch tank [d]	TBD [d]	0.5 ft^3	NA	Average	None
241-A-417 catch tank [d]	TBD [d]	24.1 ft^3	NA	Average	None
241-A tank farm pipelines [e]	TBD	0	None	Lambert 2005	NA
241-AX tank farm pipelines [e]	TBD	0	None	Lambert 2005	NA

[a] Past leak volumes listed in Field and Jones (2005).

[b] HTWOS = Hanford Tank Waste Operation Simulator. Residual inventories from HTWOS model output (Kirkbride et al. 2005).

[c] NSI = not sufficient information. Tank AX-104-114 is identified as a "confirmed or suspected" leaker in Hanlon (2005) but both Hanlon (2005) and Field and Jones (2005) state there is insufficient information for developing a leak volume at this time. As information becomes available, a leak volume will be developed.

[d] TBD = to be determined. Final disposition of MUSTs not yet determined; however, MUSTs were carried forward in the assessment assuming MUSTs will be retrieved to at least the HFFACO goal (Ecology et al. 1989, Milestone M-45-00) equivalent to the 200-Series tanks. The residual volume is calculated by ratio of the total volume of the MUST to the 200-Series tanks (e.g., the retrieval goal for the 55,000-gal 200-Series tanks is 30 ft^3; thus, a MUST that is ⅔ the size of the 200-Series tank would have a residual volume of 20 ft^3). Inventory was calculated based on average waste per ft^3 within the WMA calculated from the HTWOS model (Kirkbride et al. 2005).

[e] Final disposition of pipelines is not yet determined; however, pipelines were carried forward in the assessment. Pipeline residual volumes shown represent the volume of waste in plugged or blocked pipelines as determined by Lambert (2005).

NA = not applicable

Table 2-32. Reference Case Inventory Estimates for Waste Management Area A-AX

Source Type	Dominant Contaminants for Groundwater Pathway Impacts [a]							Dominant Contaminants for Inadvertent Intruder Impacts [a]						
	C-14 Ci	Tc-99 Ci	I-129 Ci	Cr(VI) kg	NO_3 kg	NO_2 kg	U kg	Sr-90 Ci	Tc-99 Ci	Sn-126 Ci	Cs-137 Ci	Pu-239 Ci	Pu-240 Ci	Am-241 Ci
Past releases [b]	2.13E-01	6.98E+00	5.71E-03	6.97E+01	4.89E+03	2.86E+03	1.39E+00	1.06E+02	6.98E+00	9.09E-02	1.13E+04	2.17E-01	5.59E-02	2.88E-01
Tank residuals	7.81E-02	7.25E+00	2.41E-03	2.06E+03	2.54E+03	1.36E+03	1.88E+03	6.78E+05	7.25E+00	1.05E+00	6.13E+03	2.50E+02	6.19E+01	1.18E+03
Ancillary equipment residuals [c]	5.18E-04	6.18E-02	1.58E-05	1.31E+01	1.42E+01	9.15E+00	1.74E+01	3.31E+03	6.18E-02	4.48E-03	4.53E+01	1.77E+00	4.10E-01	4.61E+00

[a] The reference case analysis included all BBI contaminants. As described in Bowen (2004), the standard analyte list tracked in the BBI contains **25 chemicals** including:

- aluminum
- bismuth
- calcium
- chlorine
- chromium
- fluorine
- total inorganic carbon as carbonate
- iron
- mercury
- potassium
- lanthanum
- manganese
- sodium
- nickel
- nitrite
- nitrate
- oxalate
- lead
- phosphate
- silicon
- sulfate
- strontium
- uranium total
- zirconium
- total organic carbon

and **46 radionuclides** including:

- tritium
- carbon-14
- nickel-59
- cobalt-60
- nickel-63
- selenium-79
- strontium-90
- yttrium-90
- zirconium-93
- niobium-93m
- technetium-99
- ruthenium-106
- cadmium-113m
- antimony-125
- tin-126
- iodine-129
- cesium-134
- cesium-137
- barium 137m
- samarium-151
- europium-152
- europium-154
- europium-155
- radium-226
- actinium-227
- radium-228
- thorium-229
- protactinium-131
- thorium-232
- uranium-232
- uranium-233
- uranium-234
- uranium-235
- uranium-236
- neptunium-237
- plutonium-238
- uranium-238
- plutonium-239
- plutonium-240
- americium-241
- plutonium-241
- curium 242
- plutonium-242
- americium-243
- curium-243
- curium-244

[b] Inventories shown are the combined inventories from SST past releases and ancillary equipment past releases. Both release types were considered for the groundwater pathway analysis; however, only the SST past releases were included in the inadvertent intruder analysis (along with SST residuals).

[c] NA indicates insufficient information is available to make estimates of intruder impacts into ancillary equipment (e.g., pipelines, diversion boxes).

2.13 REFERENCES

64 FR 61615, 1999. "Record of Decision: Hanford Comprehensive Land-Use Plan Environmental Impact Statement (HCP EIS)," *Federal Register*, Vol. 64, No. 218, pp. 61615-61625, November 12.

65 FR 37253, 2000. "Establishment of the Hanford Reach National Monument," *Federal Register*, Vol. 65, No. 114, pp. 37253-37257, June 13.

Alexander et al. 1995. D.J. Alexander, S.D. Evelo, V.G. Johnson, and M.D. Sweeney, *Groundwater Impact Assessment Report for the 216-T-4-2 Ditch,* WHC-EP-0815, Westinghouse Hanford Company, Richland, Washington.

Allen 1982. J.R.L Allen, 1982, "Developments in Sedimentology," in *Sedimentary Structures, their Character and Physical Basis*, Elsevier Scientific Publications, Amsterdam, New York, pp. 30A-30B.

Allen 2002. "Contract Number DE-AC27-99RL14047; Stabilization and Isolation of Catch Tank 241-AX-152," letter CHG-0200089 from D.I. Allen, CH2M HILL Hanford Group, Inc., Richland, Washington, to J.H. Swailes, U.S. Department of Energy, Office of River Protection, Richland, Washington, dated January 17.

Alwin 1970. J.A. Alwin, 1970, *Clastic Dikes of the Touchet Beds, Southeastern Washington*, M.S. thesis, Washington State University, Pullman, Washington.

Anderson 1990. J.D. Anderson, 1990, *A History of the 200 Area Tank Farms*, WHC-MR-0132, Westinghouse Hanford Company, Richland, Washington.

ARHCO 1973. *241-T-106 Tank Leak Investigation*, ARH-2874, ARHCO Research Department Staff, Atlantic Richfield Hanford Company, Richland, Washington.

ASTM 2005. "Standard Specification for Low and Intermediate Tensile Strength Carbon Steel Plates," A283/A283M-03, American Society for Testing and Materials, ASTM International.

Baker and Bunker 1985. V.R. Baker and R.C. Bunker, 1985, "Cataclysmic late Pleistocene flooding from glacial Lake Missoula: A review," *Quat. Sci. Rev.* Vol. 4, No. 1, pp. 1-41.

Berger et al. 1991. A. Berger, H. Gallee, and J.L. Melice, 1991, "The Earth's Future Climate at the Astronomical Timescale," in *Future Climate Change and Radioactive Waste Disposal: Proceedings of International Workshop*, G.M. Goodess and J.P. Palutikof (editors), NSS/R257, U.K. Nirex Radioactive Waste Disposal, Ltd., Harwell, OX11 ORH, United Kingdom, pp. 148-165.

Bergeron and Wurstner 2000. M.P. Bergeron and S.K. Wurstner, 2000, *Groundwater Flow and Transport Calculations Supporting the Immobilized Low-Activity Waste Disposal Facility Performance Assessment,* PNNL-13400, Pacific Northwest National Laboratory, Richland, Washington.

Bjornstad et al. 2001. B.N. Bjornstad, K.R. Fecht, and C.J. Pluhar, 2001, "Long History of Pre-Wisconsin, Ice Age Cataclysmic Floods: Evidence from Southeastern Washington State," *Journal of Geology*, Vol. 109, pp. 695-713.

Bowen 2004. K.M. Bowen, 2004, *Best Basis Inventory Process Requirements*, RPP-7625, Rev. 5, CH2M HILL Hanford Group, Inc., Richland, Washington.

Bretz et al. 1956. J.H. Bretz, H.T.U. Smith, and G.E. Neff, 1956, "Channeled Scabland of Washington: New Data and Interpretations," *Geol. Soc. of Am. Bul.*, Vol. 67, No. 8, pp. 957-1049.

Caggiano 1996. J.A. Caggiano, 1996, *Assessment Groundwater Monitoring Plan for Single-Shell Tank Waste Management Area S-SX*, WHC-SD-EN-AP-191, Rev. 0, Westinghouse Hanford Company, Richland, Washington.

Caggiano and Chou 1993. J.A. Caggiano and C.J. Chou, 1993, *Interim-Status Groundwater Quality Assessment Plan for the Single-Shell Tank Waste Management Areas T and TX-TY*, WHC-SD-EN-AP-132, Rev. 0, Westinghouse Hanford Company, Richland, Washington.

Cantrell et al. 2003. K.J. Cantrell, R.J. Serne, and G.V. Last, 2003, *Hanford Contaminant Distribution Coefficient Database and Users Guide,* PNNL-13895, Rev. 1, Pacific Northwest National Laboratory, Richland, Washington.

Chatters 1991. J.C. Chatters, 1991, "Long-Term Climate Change Effects," in *Hanford Site Protective Barrier Development Program: Fiscal Year 1990 Highlights*, L.L. Cadwell (editor), PNL-7831, Pacific Northwest Laboratory, Richland, Washington, pp. 2.23-3.1.

Chatters and Hoover 1992. J.C. Chatters and K.A. Hoover, 1992, "Response of the Columbia River Fluvial System to Holocene Climatic Change," *Quaternary Research*, Vol. 37, No. 1, pp. 42-59.

CNSS 2001. Composite Earthquake Catalog, Council of the National Seismic System. Online at: http://www.quake.geo.berkeley.edu/cnss

Cole et al. 2001a. C.R. Cole, M.P. Bergeron, C.J. Murray, P.D. Thorne, S.K. Wurstner, and P.M. Rogers, 2001, *Uncertainty Analysis Framework – Hanford Site-Wide Groundwater Flow and Transport Model*, PNNL-13641, Pacific Northwest National Laboratory, Richland, Washington.

Connelly 2004. M.P. Connelly, 2004, *Risk Assessment for Waste Management Area S-SX Closure Plan*, RPP-21596, Rev. 0, CH2M HILL Hanford Group, Inc., Richland, Washington.

Connelly et al. 1992a. M.P. Connelly, B.H. Ford, and J.V. Borghese, 1992, *Hydrogeologic Model for the 200 West Groundwater Aggregate Area*, WHC-SD-EN-TI-014, Rev. 0, Westinghouse Hanford Company, Richland, Washington.

Connelly et al. 1992b. M.P. Connelly, J.V. Borghese, C.D. Delaney, B.H. Ford, J.W. Lindberg, and S.J. Trent, 1992, *Hydrogeologic Model for the 200 East Groundwater Aggregate Area*, WHC-SD-EN-TI-019, Rev. 0, Westinghouse Hanford Company, Richland, Washington.

Corbin et al. 2005. R.A. Corbin, B.C. Simpson, M.A. Anderson, W. Danielson III, J.G. Field, T.E. Jones, M.D. Freshley, and C.T. Kincaid, 2005, *Hanford Soil Inventory Model, Rev. 1*, RPP-26744, Rev. 0, CH2M HILL Hanford Group, Inc., Richland, Washington.

Cropper et al. 1986. J.P. Cropper, H.C. Fritts, and M.G. Foley, 1986, *A 360 Year Temperature and Precipitation Record for the Pasco Basin Derived from Tree-Ring Data*, DOE/RL-01830-T46, U.S. Department of Energy, Richland, Washington.

Crumpler 2001. J.D. Crumpler, 2001, *Site-Specific SST Phase 1 RFI/CMS Work Plan Addendum for WMAs T and TX-TY*, RPP-7578, Rev. 1, CH2M HILL Hanford Group, Inc., Richland, Washington.

Crumpler 2004. J.D. Crumpler, 2004, *Site-Specific Single-Shell Tank Phase 1 RCRA Facility Investigation/Corrective Measures Study Work Plan Addendum for Waste Management Areas C, A-AX, and U*, RPP-16608, Rev. 1, CH2M HILL Hanford Group, Inc., Richland, Washington.

Dietz 1999. L.A. Dietz, 1999, *Waste Information Data System Data Field Definitions and Criteria*, BHI-00933, Vol. 1, Rev. 1, Bechtel Hanford, Inc. Richland, Washington. Database available online at: http://www.hanford.gov/cp/gpp/modeling/databases.cfm

DOE 1986. *Environmental Assessment, Reference Repository Location, Hanford Site, Washington*, DOE/RW-0070, U.S. Department of Energy, Washington, D.C.

DOE 1987. *Final Environmental Impact Statement: Disposal of Hanford Defense High-Level, Transuranic and Tank Wastes*, DOE/EIS-0113, U.S. Department of Energy, Washington, D.C.

DOE 1988. *Consultation Draft: Site Characterization Plan, Reference Repository Location, Hanford Site, Washington*, DOE/RW-0164, U.S. Department of Energy, Washington, D.C.

DOE 1999b. *Final Hanford Comprehensive Land-Use Plan Environmental Impact Statement*, DOE/EIS-0222-F, U.S. Department of Energy, Richland Operations Office, Richland, Washington. (The Record of Decision was published in the *Federal Register* on November 12, 1999. See 64 FR 61615).

DOE 1999d. *Format and Content Guide for U.S. Department of Energy Low-Level Waste Disposal Facility Performance Assessments and Composite Analyses*, U.S. Department of Energy, Washington, D.C.

DOE-GJO 1996. *Vadose Zone Characterization Project at the Hanford Tank Farms: SX Tank Farm Report*, DOE/ID/12584-268, GJPO-HAN-4, U.S. Department of Energy, Grand Junction Office, Grand Junction, Colorado.

DOE-GJO 1997a. *Hanford Tank Farms Vadose Zone: TX Tank Farm Report*, GJO-97-13-TAR, GJO-HAN-11, U.S. Department of Energy, Grand Junction Office, Grand Junction, Colorado.

DOE-GJO 1997b. *Vadose Zone Characterization Project at the Hanford Tank Farms: U Tank Farm Report*, GJO-97-1-TAR, GJO-HAN-8, U.S. Department of Energy, Grand Junction Office, Grand Junction, Colorado.

DOE-GJO 1997c. *Vadose Zone Characterization Project at the Hanford Tank Farms: BY Tank Farm Report*, GJO-96-2-TAR, GJO-HAN-6, U.S. Department of Energy, Grand Junction Office, Grand Junction, Colorado.

DOE-GJO 1997d. *Vadose Zone Characterization Project at the Hanford Tank Farms: AX Tank Farm Report*, GJO-97-14-TAR, GJO-HAN-12, U.S. Department of Energy, Grand Junction Office, Grand Junction, Colorado.

DOE-GJO 1998a. *Hanford Tank Farms Vadose Zone: S Tank Farm Report*, GJO-97-31-TAR, GJO-HAN-17, U.S. Department of Energy, Grand Junction Office, Grand Junction, Colorado.

DOE-GJO 1998b. *Hanford Tank Farms Vadose Zone: TY Tank Farm Report*, GJO-97-30-TAR, GJO-HAN-16, U.S. Department of Energy, Grand Junction Office, Grand Junction, Colorado.

DOE-GJO 1998c. *Hanford Tank Farms Vadose Zone: C Tank Farm Report*, GJO-98-39-TAR, GJO-HAN-18, U.S. Department of Energy, Grand Junction Office, Grand Junction, Colorado.

DOE-GJO 1998d. *Hanford Tank Farms Vadose Zone: BX Tank Farm Report*, GJO-98-40-TAR, GJO-HAN-19, U.S. Department of Energy, Grand Junction Office, Grand Junction, Colorado.

DOE-GJO 1999a. *Hanford Tank Farms Vadose Zone: T Tank Farm Report*, GJO-99-101-TAR, GJO-HAN-27, U.S. Department of Energy, Grand Junction Office, Grand Junction, Colorado.

DOE-GJO 1999b. *Hanford Tank Farms Vadose Zone: A Tank Farm Report*, GJO-98-64-TAR, GJO-HAN-23, U.S. Department of Energy, Grand Junction Office, Grand Junction, Colorado.

DOE-GJO 2000a. *Hanford Tank Farms Vadose Zone: Addendum to the S Tank Farm Report,* GJO-97-31-TARA, GJO-HAN-17, U.S. Department of Energy, Grand Junction Office, Grand Junction, Colorado.

DOE-GJO 2000b. *Hanford Tank Farms Vadose Zone: Addendum to the SX Tank Farm Report* DOE/ID/12584-268A, GJO-HAN-4, U.S. Department of Energy, Grand Junction Office, Grand Junction, Colorado.

DOE-GJO 2000c. *Hanford Tank Farms Vadose Zone: Addendum to the T Tank Farm Report,* GJO-99-101-TARA, GJO-HAN-27, U.S. Department of Energy, Grand Junction Office, Grand Junction, Colorado.

DOE-GJO 2000d. *Hanford Tank Farms Vadose Zone: Addendum to the TX Tank Farm Report,* GJO-97-13-TARA, GJO-HAN-11, U.S. Department of Energy, Grand Junction Office, Grand Junction, Colorado.

DOE-GJO 2000e. *Hanford Tank Farms Vadose Zone: Addendum to the TY Tank Farm Report,* GJO-97-30-TARA, GJO-HAN-16, U.S. Department of Energy, Grand Junction Office, Grand Junction, Colorado.

DOE-GJO 2000f. *Hanford Tank Farms Vadose Zone: Addendum to the U Tank Farm Report,* GJO-97-1-TARA, GJO-HAN-8, U.S. Department of Energy, Grand Junction Office, Grand Junction, Colorado.

DOE-GJO 2000g. *Hanford Tank Farms Vadose Zone: Addendum to the C Tank Farm Report,* GJO-98-39-TARA, GJO-HAN-18, U.S. Department of Energy, Grand Junction Office, Grand Junction, Colorado.

DOE-GJO 2000h. *Hanford Tank Farms Vadose Zone: B Tank Farm Report*, GJO-99-113-TAR, GJO-HAN-28, U.S. Department of Energy, Grand Junction Office, Grand Junction, Colorado.

DOE-GJO 2000i. *Hanford Tank Farms Vadose Zone: Addendum to the B Tank Farm Report*, GJO-99-113-TARA, GJO-HAN-28, U.S. Department of Energy, Grand Junction Office, Grand Junction, Colorado.

DOE-GJO 2000j. *Hanford Tank Farms Vadose Zone: Addendum to the BX Tank Farm Report,* GJO-98-40-TARA, GJO-HAN-19, U.S. Department of Energy, Grand Junction Office, Grand Junction, Colorado.

DOE-GJO 2000k. *Hanford Tank Farms Vadose Zone: Addendum to the BY Tank Farm Report*, GJO-96-2-TARA, GJO-HAN-6, U.S. Department of Energy, Grand Junction Office, Grand Junction, Colorado.

DOE-GJO 2000L. *Hanford Tank Farms Vadose Zone: Addendum to the A Tank Farm Report*, GJO-98-64-TARA, GJO-HAN-23, U.S. Department of Energy, Grand Junction Office, Grand Junction, Colorado.

DOE-GJO 2000m. *Hanford Tank Farms Vadose Zone: Addendum to the AX Tank Farm Report,* GJO-97-14-TARA, GJO-HAN-12, U.S. Department of Energy, Grand Junction Office, Grand Junction, Colorado.

DOE-RL 1992. *Hanford Site Groundwater Background*, DOE/RL-92-23, U.S. Department of Energy, Richland Operations Office, Richland, Washington.

DOE-RL 1997a. *Waste Site Grouping for 200 Areas Soil Investigations*, DOE/RL-96-81, Rev. 0, U.S. Department of Energy, Richland Operations Office, Richland, Washington.

DOE-RL 1997b. *Hanford Site Background: Part 3, Groundwater Background*, DOE/RL-96-61, Rev. 0, U.S. Department of Energy, Richland Operations Office, Richland, Washington.

DOE-RL 2002. *Standardized Stratigraphic Nomenclature for the Post-Ringold-Formation Sediments Within the Central Pasco Basin*, DOE/RL-2002-39, Rev. 0, U.S. Department of Energy, Richland Operations Office, Richland, Washington.

DOE-RL 2005. *Hanford Site Waste Management Units Report*, DOE/RL-88-30, Rev. 14, U.S. Department of Energy, Richland Operations Office, Richland, Washington.

Ecology et al. 1989. Ecology, EPA, and DOE, 1989, *Hanford Federal Facility Agreement and Consent Order*, as amended, Washington State Department of Ecology, Olympia, Washington, U.S. Environmental Protection Agency, and U.S. Department of Energy, Washington D.C.

ERDA 1975. *Final Environmental Impact Statement: Waste Management Operations, Hanford Reservation, Richland, Washington*, ERDA-1538, Energy, Research, and Development Administration, Richland, Washington.

Fayer et al. 1996. M.J. Fayer, G.W. Gee, M.L. Rockhold, M.D. Freshley, and T.B. Walters, 1996, "Estimating Recharge Rates for a Groundwater Model using a GIS," *Journal of Environmental Quality*, Vol. 25, pp. 510-518.

Fayer et al. 1999. M.J. Fayer, E.M. Murphy, J.L. Downs, F.O. Khan, C.W. Lindenmeier, and B.N. Bjornstad, 1999, *Recharge Data Package for the Immobilized Low-Activity Waste 2001 Performance Assessment,* PNNL-13033, Pacific Northwest National Laboratory, Richland, Washington.

Fecht et al. 1987. K.R. Fecht, S.P. Reidel, and A.M. Tallman, 1987, "Paleodrainage of the Columbia River System on the Columbia Plateau of Washington State – A Summary," Washington Division of Geology and Earth Resources Bulletin 77, Washington State Department of Natural Resources, Olympia, Washington.

Fecht et al. 1999. K.R. Fecht, K.A. Lindsey, B.N. Bjornstad, D.G. Horton, G.V. Last, and S.P. Reidel, 1999, *Clastic Injection Dikes of the Pasco Basin and Vicinity – Geologic Atlas Series,* BHI-01103, Rev. 0, Bechtel Hanford, Inc., Richland, Washington.

Field 2003a. J.G. Field, 2003, *Single-Shell Tank System Description,* RPP-15043, Rev. 0, CH2M HILL Hanford Group, Richland, Washington.

Field and Jones 2005. J.G. Field and T.E. Jones, 2005, *Tank Farm Vadose Zone Contamination Volume Estimates,* RPP-23405, Rev. 1, CH2M HILL Hanford Group, Inc., Richland, Washington.

Freeman-Pollard 1994. J.R. Freeman-Pollard, 1994, *Engineering Study of 50 Miscellaneous Inactive Underground Radioactive Waste Storage Tanks Located at the Hanford Site, Washington,* WHC-SD-EN-ES-040, Rev. 0, Westinghouse Hanford Company, Richland, Washington.

Freshley and Graham 1988. M.D. Freshley and M.J. Graham, 1988, *Estimation of Ground-Water Travel Time at the Hanford Site: Description, Past Work, and Future Needs*, PNL-6328, Pacific Northwest National Laboratory, Richland, Washington.

Gee et al. 1992. G.W. Gee, M.J. Fayer, M.L. Rockhold, and M.D. Campbell, 1992, "Variations in Recharge at the Hanford Site," *Northwest Sci.* Vol. 66, No. 4, pp. 237-250.

Geomatrix 1996. *Probabilistic Seismic Hazard Analysis DOE Hanford Site, Washington*, WHC-SD-W236A-TI-002, Rev. 1, Westinghouse Hanford Company, Richland, Washington.

Gephart 1999. R.E. Gephart 1999, *A Short History of Plutonium Production and Nuclear Waste Generation, Storage, and Release at the Hanford Site*, PNNL-SA-32152, Pacific Northwest National Laboratory, Richland, Washington.

Gephart et al. 1976. R.E. Gephart, P.A. Eddy, R.C. Arnett, and G.A. Robinson, 1976, *Geohydrologic Study of the West Lake Basin,* ARH-CD-775, Atlantic Richfield Hanford Company, Richland, Washington.

Gerber 1992. M.S. Gerber, 1992, *Legend and Legacy: Fifty Years of Defense Production at the Hanford Site,* WHC-MR-0293, Rev. 2, Westinghouse Hanford Company, Richland, Washington.

Graham et al. 1984. M.J. Graham, G.V. Last, and K.R. Fecht, 1984, *An Assessment of Aquifer Intercommunication in the B Pond-Gable Mountain Pond Area of the Hanford Site*, RHO-RE-ST-12P, Rockwell Hanford Operations, Richland, Washington.

Gramulich 1987. L.H. Gramulich 1987, "Precipitation Variation in the Pacific Northwest (1675-1975) as Reconstructed from Tree Rings," *Annals of the Association of American Geographers*, 77:19-29.

Hajek 1966. B.F. Hajek, 1966, *Soil Survey: Hanford Project in Benton County, Washington*, BNWL-243, Pacific Northwest Laboratory, Richland, Washington.

Hanlon 2005. B.M. Hanlon, 2005, *Waste Tank Summary Report for Month Ending November 30, 2004*, HNF-EP-0182, Rev. 200, CH2M HILL Hanford Group, Inc., Richland, Washington.

Hartman 2000. M.J. Hartman (editor), 2000, *Hanford Site Groundwater Monitoring Setting, Sources and Methods,* PNNL-13080, Pacific Northwest National Laboratory, Richland, Washington.

Hartman et al. 2003. M.J. Hartman, L.F. Morasch, and W.D. Webber, (editors), 2003, *Hanford Site Groundwater Monitoring for Fiscal Year 2002*, PNNL-14187, Pacific Northwest National Laboratory, Richland, Washington.

Hartman et al. 2004. M.J. Hartman, L.F. Morasch, and W.D. Webber (editors), 2004, *Hanford Site Groundwater Monitoring for Fiscal Year 2003*, PNNL-14548, Pacific Northwest National Laboratory, Richland, Washington.

Hartman et al. 2005. M.J. Hartman, L.F. Morasch, and W.D. Webber (editors), 2005, *Hanford Site Groundwater Monitoring for Fiscal Year 2004*, PNNL-15070, Pacific Northwest National Laboratory, Richland, Washington.

Henderson 1999. J.C. Henderson, 1999, *Preliminary Site-Specific SST Phase 1 RFI/CMS Work Plan Addendum for WMA S-SX*, HNF-4380, Rev. 1B, Lockheed Martin Hanford Corporation, Richland, Washington.

HFSUWG 1992a. *The Future for Hanford: Uses and Cleanup, Summary of the Final Report of the Hanford Future Site Uses Working Group*, Hanford Future Site Uses Working Group, Westinghouse Hanford Company, Richland, Washington.

HFSUWG 1992b. *The Future for Hanford: Uses and Cleanup, the Final Report of the Hanford Future Site Uses Working Group*, Hanford Future Site Uses Working Group, Westinghouse Hanford Company, Richland, Washington.

Hodges 1998. F.N. Hodges, 1998, *Results of Phase I Groundwater Quality Assessment for Single-Shell Tank Waste Management Areas T and TX-TY at the Hanford Site*, PNNL-11809, Pacific Northwest National Laboratory, Richland, Washington.

Hodges and Chou 2000a. F.N. Hodges and C.J. Chou, 2000, *Groundwater Quality Assessment for Waste Management Area U: First Determination*, PNNL-13282, Pacific Northwest National Laboratory, Richland, Washington.

Hodges and Chou 2000b. F.N. Hodges and C.J. Chou, 2000, *Groundwater Quality Assessment Plan for Single-Shell Tank Waste Management Area U at the Hanford Site*, PNNL-13185, Pacific Northwest National Laboratory, Richland, Washington.

Hodges and Chou 2001a. F.N. Hodges and C.J. Chou, 2001, *RCRA Assessment Plan for Single-Shell Tank Waste Management Area T at the Hanford Site*, PNNL-12057, Pacific Northwest National Laboratory, Richland, Washington.

Hodges and Chou 2001b. F.N. Hodges and C.J. Chou, 2001, *RCRA Assessment Plan for Single-Shell Tank Waste Management Area TX-TY at the Hanford Site*, PNNL-12072, Pacific Northwest National Laboratory, Richland, Washington.

Hodges and Chou 2002. F.N. Hodges and C.J. Chou, 2002, *RCRA Assessment Plan for Single-Shell Tank Waste Management Area T at the Hanford Site, Interim Change Notice 1*, PNNL-12057-ICN-1, Pacific Northwest National Laboratory, Richland, Washington.

Hoitink et al. 2004. D.J. Hoitink, K.W. Burk, J.V. Ramsdell, Jr., and W.J. Shaw, 2004, *Hanford Site Climatological Data Summary 2003 with Historical Data,* PNNL-14616, Pacific Northwest National Laboratory, Richland, Washington.

Horton 2002. D.G. Horton, 2002, *RCRA Assessment Plan for Single-Shell Tank Waste Management Area TX-TY at the Hanford Site, Interim Change Notice 1*, PNNL-12072-ICN-1, Pacific Northwest National Laboratory, Richland, Washington.

Horton and Narbutovskih 2001. D.G. Horton and S.M. Narbutovskih, 2001, *RCRA Groundwater Monitoring Plan for Single-Shell Tank Waste Management Area C at the Hanford Site*, PNNL-13024, Pacific Northwest National Laboratory, Richland, Washington.

Horton and Narbutovskih 2002. D.G. Horton and S.M. Narbutovskih, 2002, *RCRA Groundwater Monitoring Plan for Single-Shell Tank Waste Management Area C at the Hanford Site, Interim Change Notice 1*, PNNL-13024-ICN-1, Pacific Northwest National Laboratory, Richland, Washington.

Horton and Narbutovskih 2003a. D.G. Horton and S.M. Narbutovskih, 2003, *RCRA Groundwater Monitoring Plan for Single-Shell Tank Waste Management Area C at the Hanford Site, Interim Change Notice 2*, PNNL-13024-ICN-2, Pacific Northwest National Laboratory, Richland, Washington.

Horton and Narbutovskih 2003b. D.G. Horton and S.M. Narbutovskih, 2003, *RCRA Groundwater Monitoring Plan for Single-Shell Tank Waste Management Area C at the Hanford Site, Interim Change Notice 3*, PNNL-13024-ICN-3, Pacific Northwest National Laboratory, Richland, Washington.

Horton et al. 2002. D.G. Horton, F.N. Hodges, V.G. Johnson, and CJ Chou, 2002, *RCRA Groundwater Quality Assessment Report for Single-Shell Tank Waste Management Area T (January 1998 through December 2001),* PNNL-13929, Pacific Northwest National Laboratory, Richland, Washington.

Jensen 1987. E.J. Jensen, 1987, *An Evaluation of Aquifer Intercommunication Between the Unconfined and Rattlesnake Ridge Aquifers on the Hanford Site*, PNL-6313, Pacific Northwest Laboratory, Richland, Washington.

Johnson and Chou 1998. V.G. Johnson and C.J. Chou, 1998, *Results of Phase I Groundwater Quality Assessment for Single-Shell Tank Waste Management Area S-SX at the Hanford Site*, PNNL-11810, Pacific Northwest National Laboratory, Richland, Washington.

Johnson and Chou 1999. V.G. Johnson and C.J. Chou, 1999, *RCRA Assessment Plan for Single-Shell Tank Waste Management Area S-SX at the Hanford Site*, PNNL-12114, Pacific Northwest National Laboratory, Richland, Washington.

Johnson and Chou 2001. V.G. Johnson and C.J. Chou, 2001, *RCRA Groundwater Quality Assessment Report for Waste Management Area S-SX (November 1997 through April 2000)*, PNNL-13441, Pacific Northwest National Laboratory, Richland, Washington.

Johnson and Chou 2002. V.G. Johnson and C.J. Chou, 2002, *Groundwater Quality Assessment Report for Waste Management Area S-SX (April 2000 through December 2001)*, PNNL-13801, Pacific Northwest National Laboratory, Richland, Washington.

Johnson et al. 1992. V.G. Johnson, F.N. Hodges, and S.P. Reidel, "Arid Environment Aquifers: An Example from South Central Washington," *Geological Society of America* (ABS) 24(5):36.

Johnson et al. 1999. V.G. Johnston, T.E. Jones, S.P. Reidel, and M.I. Wood, 1999, *Subsurface Conditions Description for the S-SX Waste Management Area*, HNF-4936, Rev. 0, Lockheed Martin Hanford Company, Richland, Washington.

Kaplan and Serne 2000. D.I. Kaplan and R.J. Serne, 2000, *Geochemical Data Package for the Hanford Immobilized Low-Activity Tank Waste Performance Assessment (ILAW PA)*, PNNL-13037, Rev. 1, Pacific Northwest National Laboratory, Richland, Washington.

Khaleel et al. 2006b. R. Khaleel, M.P. Connelly, and W.J. McMahon, 2006, *Modeling Data Package for an Initial Assessment of Closure of the S and SX Tank Farms*, RPP-17209, Rev. 1, CH2M HILL Hanford Group, Inc., Richland, Washington.

Kincaid et al. 1998. C.T. Kincaid, M.P. Bergeron, C.R. Cole, M.D. Freshley, N.L. Hassig, V.G. Johnson, D.I. Kaplan, R.J. Serne, G.P. Streile, D.L. Strenge, P.D. Thorne, L.W. Vail, G.A. Whyatt, and S.K. Wurstner, 1998, *Composite Analysis for Low-Level Waste Disposal in the 200 Area Plateau of the Hanford Site*, PNNL-11800, Pacific Northwest National Laboratory, Richland, Washington.

Kipp and Mudd 1973. K.L. Kipp and R.D. Mudd, 1973, *Collection and Analysis of Pump Test Data for Transmissivity Values*, BNWL-1709, Pacific Northwest Laboratory, Richland, Washington.

Kipp and Mudd 1974. R.L. Kipp and R.D. Mudd, 1974, *Selected Water Table Contour Maps and Well Hydrographs for the Hanford Reservation, 1944-1973,* BNWL-B-360, Pacific Northwest Laboratory, Richland, Washington.

Kirkbride et al. 2005. R.A. Kirkbride. P.J. Certa, T.M. Hohl, A.M. Johnson, and R.S. Wittman, 2005, *Hanford Tank Waste Operations Simulator Model Data Package for the Development Run for the Refined Target Case,* RPP-RPT-23412, Rev. 0A, CH2M HILL Hanford Group, Inc., Richland, Washington.

Knepp 2002a. A.J. Knepp, 2002, *Field Investigation Report for Waste Management Area S-SX*, RPP-7884, Rev. 0, CH2M HILL Hanford Group, Inc., Richland, Washington.

Knepp 2002b. A.J. Knepp, 2002, *Field Investigation Report for Waste Management Area B-BX-BY*, RPP-10098, Rev. 0, CH2M HILL Hanford Group, Inc., Richland, Washington.

Lambert 2005. S.L. Lambert, 2005, *Residual Waste Inventories in the Plugged and Abandoned Pipelines at the Hanford Site*, RPP-25113, Rev. 0, CH2M HILL Hanford Group, Inc., Richland, Washington.

Last et al. 1994. G.V. Last, D.W. Duncan, M.J. Graham, M.D. Hall, V.W. Hall, D.S. Landeen, J.G. Leitz, and R.M. Mitchell, 1994, *216-U-10 Pond and 216-Z19 Ditch Characterization Studies,* WHC-EP-0707 (formerly RHO-ST-45), Westinghouse Hanford Company, Richland, Washington.

Last et al. 2004a. G.V. Last, E.J. Freeman, K.J. Cantrell, M.J. Fayer, G.W. Gee, W.E. Nichols, B.N. Bjornstad, and D.G. Horton, 2004, *Vadose Zone Hydrogeology Data Package for the 2004 Composite Analysis*, PNNL-14702, Rev. 0, Pacific Northwest Laboratory, Richland, Washington.

Lee 2004. T.A. Lee, 2004, *Single-Shell Tank System Closure Plan*, RPP-13774, Rev. 2, CH2M HILL Hanford Group, Inc., Richland, Washington.

Lindsey 1991. K.A Lindsey, 1991, *Revised Stratigraphy for the Ringold Formation, Hanford Site, South-Central Washington*, WHC-SD-EN-EE-004, Westinghouse Hanford Company, Richland, Washington.

Lindsey 1995. K.A. Lindsey, 1995, *Miocene- to Pliocene-Aged Suprabasalt Sediments of the Hanford Site, South-Central Washington*, BHI-00184, Rev. 00, Bechtel Hanford, Inc., Richland, Washington.

Lindsey 1996. K.A. Lindsey, 1996, "The Miocene to Pliocene Ringold Formation and Associated Deposits of the Ancestral Columbia River System, South-Central Washington and North-Central Oregon," Washington Division of Geology and Earth Resources Open File Report 96-8, Washington State Department of Natural Resources, Olympia, Washington.

Lindsey et al. 2000. K.A. Lindsey, S.E. Kos, and K.D. Reynolds, 2000, *Vadose Zone Geology of Boreholes 299-W22-50 and 299-W23-19 S-SX Waste Management Area Hanford Site, South-Central Washington*, RPP-6149, Rev. 0, CH2M HILL Hanford Group, Inc., Richland, Washington.

Lupher 1944. R.L. Lupher, 1944, "Clastic Dikes of the Columbia Basin Region, Washington and Idaho," *Geological Society of America Bulletin*, Vol. 55, pp. 1431-1462.

Malde 1968. H.E. Malde, 1968, *The Catastrophic Late Pleistocene Bonneville Flood in the Snake River Plain, Idaho,* Professional Paper 596, U.S. Geological Survey, Washington, D.C.

Mann et al. 2001. F.M. Mann, K.C. Burgard, W.R. Root, R.J. Puigh, S.H. Finfrock, R. Khaleel, D.H. Bacon, E.J. Freeman, B.P. McGrail, S.K. Wurstner, and P.E. LaMont, 2001, *Hanford Immobilized Low-Activity Tank Waste Performance Assessment: 2001 Version,* DOE/ORP-2000-24, Rev. 0, U.S. Department of Energy, Office of River Protection, Richland, Washington.

Martin 2002. Hanford Advisory Board Consensus Advice #132, "Exposure Scenarios Task Force on the 200 Area" letter from T. Martin, Chair, Hanford Advisory Board, Richland, Washington, to K. Klein, Manager, U.S. Department of Energy, Richland Operations Office, H. Boston, Manager, U.S. Department of Energy, Office of River Protection, J. Iani, Regional Administrator, U.S. Environmental Protection Agency, Region 10, and T. Fitzsimmons, Director, Washington State Department of Ecology, dated June 7. Online at: http://www.hanford.gov/public/boards/hab/?hab=advice

Myers 2005. D.A. Myers, 2005, *Field Investigation Report for Waste Management Areas T and TX-TY*, RPP-23752, Rev. 0-A, CH2M HILL Hanford Group, Inc., Richland, Washington.

Naiknimbalkar 2005a. A.N. Naiknimbalkar, 2005, *Software Verification and Validation Plan and Results for Hanford Tank Waste Operations Simulator Model Reference Version 1.1*, RPP-18592, Rev. 2, CH2M HILL Hanford Group, Inc., Richland, Washington.

Narbutovskih 2000. S.M. Narbutovskih, 2000, *Groundwater Quality Assessment Plan for Single-Shell Waste Management Area B-BX-BY at the Hanford Site*, PNNL-13022, Pacific Northwest National Laboratory, Richland, Washington.

Narbutovskih 2002. S.M. Narbutovskih, 2002, *Groundwater Quality Assessment Plan for Single-Shell Tank Waste Management Area B-BX-BY at the Hanford Site, Interim Change Notice 1,* PNNL-13022-ICN-1, Pacific Northwest National Laboratory, Richland, Washington.

Narbutovskih 2003. S.M. Narbutovskih, 2003, *Groundwater Quality Assessment Plan for Single-Shell Tank Waste Management Area B-BX-BY at the Hanford Site, Interim Change Notice 2,* PNNL-13022-ICN-2, Pacific Northwest National Laboratory, Richland, Washington.

Narbutovskih and Horton 2001. S.M. Narbutovskih and D.G. Horton, 2001, *RCRA Groundwater Monitoring Plan For Single-Shell Tank Waste Management Area A-AX at the Hanford Site*, PNNL-13023, Pacific Northwest National Laboratory, Richland, Washington.

Neitzel et al. 2004. D.A. Neitzel (editor), A.L. Bunn, S.D. Cannon, J.P. Duncan, R.A. Fowler, B.G. Fritz, D.W. Harvey, P.L. Hendrickson, D.J. Hoitink, D.G. Horton, G.V. Last, T.M. Poston, E.L. Prendergast-Kennedy, S.P. Reidel, A.C. Rohay, M.J. Scott, and P.D. Thorne, 2004, *Hanford Site National Environmental Policy Act (NEPA) Characterization,* PNNL-6415, Rev. 16, Pacific Northwest National Laboratory, Richland, Washington.

Newcomb 1958. R.C. Newcomb, 1958, "Ringold Formation of Pleistocene Age in Type Locality, the White Bluffs," Washington, *American Journal of Science*, Vol. 256, pp. 328-340.

Newcomb 1962. R.C. Newcomb, 1962, "Hydraulic Injection of Clastic Dikes in the Touchet Beds, Washington, Oregon, and Idaho," *Geological Society of the Oregon Country Geological Newsletter*, Vol. 28(10), p. 70.

Newcomb et al. 1972. R.C. Newcomb, J.R. Strand, and F.J. Frank, 1972, *Geology and Ground-Water Characteristics of the Hanford Reservation of the U.S. Atomic Energy Commission, Washington*, Professional Paper 717, U.S. Geological Survey, Washington, D.C.

O'Connor 1993. J.E. O'Connor, 1993, "Hydrology, Hydraulics, and Geomorphology of the Bonneville Flood," *Geol. Soc. Am. Spec. Paper*; Vol. 274. p.83.

O'Connor and Baker 1992. J.E. O'Connor and V.R. Baker, 1992, "Magnitudes and Implications of Peak Discharges from Glacial Lake Missoula," *Geol. Soc. of Am. Bul.*, Vol. 104, No. 3, pp. 267-279.

Obermeier 1996. S.F. Obermeier, 1996, "Use of Liquefaction-Induced Features for Seismic Analysis – An Overview of How Seismic Liquefaction Features Can be Distinguished from Other Features and How Their Regional Distribution and Properties of Source Sediment Can be Used to Infer the Location and Strength of Holocene Paleo-Earthquakes," *Engineering Geology*, Vol. 44, pp. 1-76.

OFM 2002. "Population of Cities, Towns and Counties: April 1, 2000 to April 1, 2002," Office of Financial Management, Forecasting Division, Olympia, Washington. Online at: http://www.ofm.wa.gov/pop/poptrends/index.htm

Petersen 2005. S.W. Petersen, 2005, *Silt Borrow Source Field Investigation Report*, D&D-25575, Rev. 0, Fluor Hanford, Inc., Richland Washington.

Pogue 1998. K.R. Pogue, 1998, "Earthquake-generated (?) structures in Missoula flood slackwater sediments (Touchet Beds) of southeastern Washington," *Geological Society of America Abstracts with Programs*, Vol. 30, No. 7, pp. 398-399.

Poston et al. 1991. T.M., K.R. Price, and D.R. Newcomer, 1991, *An Evaluation of the Chemical, Radiological, and Ecological Conditions of West Lake on the Hanford Site,* PNL-7662, Pacific Northwest Laboratory, Richland, Washington.

Poston et al. 2004. T.M. Poston, R.W. Hanf, R.L. Dirkes, and L.F. Morasch (editors), 2004, *Hanford Site Environmental Report for Calendar Year 2003*, PNNL-14687, Pacific Northwest National Laboratory, Richland, Washington.

PSPL 1982. *Preliminary Safety Analysis for Skagit/Hanford Nuclear Project*, Amendment 29, Puget Sound Power and Light Company, Bellevue, Washington.

Reidel and Hooper 1989. S.P. Reidel and P.R. Hooper (editors), 1989, "Volcanism and Tectonism in the Columbia River Flood-Basalt Province," Special Paper 239, *Geological Society of America*, Boulder, Colorado, p. 386, plate 1.

Reidel et al. 1992. S.P. Reidel, K.A. Lindsey, and K.R. Fecht, 1992, *Field Trip Guide to the Hanford Site,* WHC-MR-0391, Westinghouse Hanford Company, Richland, Washington.

Reidel et al. 1994. S.P. Reidel, N.P. Campbell, K.R. Fecht, and K.A. Lindsey, 1994, "Late Cenozoic Structure and Stratigraphy of South-Central Washington," in *Regional Geology of Washington State*, E. Cheney, and R. Lasmanis (editors), Washington Division of Geology and Earth Resources, Bulletin 80, Washington State Department of Natural Resources, pp. 159-180.

Reidel et al. 2006. S.P. Reidel, D.G. Horton, Y.J. Chien, D.B. Barnett, and K. Singleton, 2006, *Geology, Hydrogeology, Geochemistry, and Mineralogy Data Package for the Single-Shell Tank Waste Management Areas at the Hanford Site*, RPP-23748, Rev. 0, CH2M HILL Hanford Group, Inc., Richland, Washington.

Rogers and Knepp 2000a. P.M. Rogers and A.J. Knepp, 2000, *Site-Specific SST Phase 1 RFI/CMS Work Plan Addendum for WMA S-SX*, HNF-5085, Rev. 1, CH2M HILL Hanford Group, Inc., Richland, Washington.

Rogers and Knepp 2000b. P.M. Rogers and A.J. Knepp, 2000, *Site-Specific SST Phase 1 RFI/CMS Work Plan Addendum for WMA B-BX-BY*, RPP-6072, Rev. 1, CH2M HILL Hanford Group, Inc., Richland, Washington.

Rohay 1989. A.C. Rohay, 1989, *Earthquake Recurrence Rate Estimates for Eastern Washington and the Hanford Site*, PNL-6956, Pacific Northwest Laboratory, Richland, Washington.

Routson et al. 1979. R.C. Routson, W.H. Price, D.J. Brown, and K.R. Fecht, 1979, *High-Level Waste Leakage from the 241-T-106 Tank at Hanford*, RHO-ST-14, Rockwell Hanford Operations, Richland, Washington.

Sams 2004a. T.L. Sams, 2004, *Stage II Retrieval Data Report for Single-Shell Tank 241-C-106*, RPP-20577, Rev. 0, CH2M HILL Hanford Group, Inc. Richland, Washington.

Sams 2004b. T.L. Sams, 2004, *Basis for Exception to the Hanford Federal Facility Agreement and Consent Order Waste Retrieval Criteria for Single-Shell Tank 241-C-106*, RPP-20658, Rev. 0, CH2M HILL Hanford Group, Inc., Richland, Washington.

Serne et al. 2002. R.J. Serne, B.N. Bjornstad, H.T. Schaef, B.A. Williams, D.C. Lanigan, D.G. Horton, R.E. Clayton, A.V. Mitroshkov, V.L. LeGore, M.J. O'Hara, C.F. Brown, K.E. Parker, I.V. Kutnyakov, J.N. Serne, G.V. Last, S.C. Smith, C.W. Lindenmeier, J.M. Zachara, and D.B. Burke, 2002, *Characterization of Vadose Zone Sediment: Uncontaminated RCRA Borehole Core Samples and Composite Samples,* PNNL-13757-1, Pacific Northwest National Laboratory, Richland, Washington.

Shaw et al. 1999. J. Shaw, M. Munro-Stasuik, B. Sawyer, C. Beaney, J.-E. Lesemann, A. Musacchio, B. Rains, and R.R. Young, 1999, "The Channeled Scabland: Back to Bretz?," *Geology,* Vol. 27, No. 7, pp. 605-608.

Simpson et al. 2001. B.C. Simpson, R.A. Corbin, and S.F. Agnew, 2001, *Groundwater/Vadose Zone Integration Project, Hanford Soil Inventory Model*, BHI-01496, Rev. 0, Bechtel Hanford, Inc., Richland, Washington.

Singleton and Lindsey 1994. K.M. Singleton and K.A. Lindsey, 1994, *Groundwater Impact Assessment Report for the 216-U-14 Ditch*, WHC-EP-0698, Westinghouse Hanford Company, Richland, Washington.

Slate 1996. J.L Slate, 1996, "Buried Carbonate Paleosols Developed in Pliocene-Pleistocene Deposits of the Pasco Basin, South-Central Washington, U.S.A.," *Quaternary International*, Vol. 34-36, pp. 191-196.

Smith et al. 2001. R.M. Smith, F.N. Hodges, and B.A. Williams, 2001, *Groundwater Quality Assessment Plan for Single-Shell Tank Waste Management Area U*, PNNL-13612, Pacific Northwest National Laboratory, Richland, Washington.

Smith et al. 2003. R.M. Smith, F.N. Hodges, and B.A. Williams, 2003, *Groundwater Quality Assessment Plan for Single-Shell Tank Waste Management Area U, Interim Change Notice 1*, PNNL-13612-1, Pacific Northwest National Laboratory, Richland, Washington.

Spane and Thorne 1995. F.A. Spane, Jr. and P.D. Thorne, 1995, *Comparison of Constant-Rate Pumping Test and Slug Interference Test Results at the Hanford Site B Pond Multilevel Test Facility*, PNL-10835, Pacific Northwest National Laboratory, Richland, Washington.

Spane and Thorne 2000. F.A. Spane, Jr. and P.D. Thorne, 2000, *Analysis of the Hydrologic Response Associated with Shutdown and Restart of the 200-ZP-1 Pump-and-Treat System*, PNNL-13342, Pacific Northwest National Laboratory, Richland, Washington.

Spane et al. 2001a. F.A. Spane, Jr., P.D. Thorne, and D.R. Newcomer, 2001, *Results of Detailed Hydrologic Characterization Tests – Fiscal Year 1999*, PNNL-13378, Pacific Northwest National Laboratory, Richland, Washington.

Spane et al. 2001b. F.A. Spane, Jr., P.D. Thorne, and D.R. Newcomer, 2001, *Results of Detailed Hydrologic Characterization Tests – Fiscal Year 2000*, PNNL-13514, Pacific Northwest National Laboratory, Richland, Washington.

Spane et al. 2002. F.A. Spane, Jr., P.D. Thorne, and D.R. Newcomer, 2002, *Results of Detailed Hydrologic Characterization Tests – Fiscal Year 2001*, PNNL-14113, Pacific Northwest National Laboratory, Richland, Washington.

Swanson et al. 1979a. D.A. Swanson, J.L. Anderson, R.D. Bentley, G.R. Byerly, V.E. Camp, J.N. Gardner, and T.L. Wright, 1979, "Reconnaissance Geologic Map of the Columbia River Basalt Group in Eastern Washington and Northern Idaho," Open-File Report 79-1363, U.S. Geological Survey, Washington, D.C.

Swanson et al. 1979b. D.A. Swanson, T.L. Wright, P.R. Hooper, and R.D. Bentley, 1979, *Revisions in Stratigraphic Nomenclature of the Columbia River Basalt Group,* Bulletin 1457-G, U.S. Geological Survey, Boulder, Colorado.

Tallman et al. 1981. A.M. Tallman, J.T. Lillie, and K.R. Fecht, 1981, "Suprabasalt Sediments of the Cold Creek Syncline Area," in *Subsurface Geology of the Cold Creek Syncline*, C.W. Myers and S.M. Price (editors), RHO-BW1-ST-14, Rockwell Hanford Operations, Richland, Washington.

Thorne 2004. P.D. Thorne, 2004, *Groundwater Data Package for the 2004 Composite Analysis*, PNNL-14753, Rev. 0, Pacific Northwest National Laboratory, Richland, Washington.

Thorne and Newcomer 1992. P.D. Thorne and D.R. Newcomer, 1992, *Summary and Evaluation of Available Hydraulic Property Data for the Hanford Site Unconfined Aquifer System*, PNL-8337, Pacific Northwest Laboratory, Richland, Washington.

Thorne and Newcomer 2002. P.D. Thorne and D.R. Newcomer, 2002, *Prototype Database and User's Guide of Saturated Zone Hydraulic Properties for the Hanford Site*, PNNL-14058, Pacific Northwest National Laboratory, Richland, Washington.

Thorne et al. 1994. P.D. Thorne, M.A. Chamness, Q.C. MacDonald, S.E. Schubert, and V.R. Vermeul, 1994, *Three-Dimensional Conceptual Model for the Hanford Site Unconfined Aquifer System: FY 1994 Status Report*, PNL-10195, Pacific Northwest Laboratory, Richland, Washington.

TWINS 2005. *Tank Waste Information Network System (TWINS) 3*. Online at http://twins.pnl.gov/twins.htm.

USGS 1987. "Subsurface Transport of Radionuclides in Shallow Deposits of the Hanford Nuclear Reservation, Washington – Review of Selected Previous Work and Suggestions for Further Study," U.S. Geological Survey, Open File Report 87-222, Tacoma, Washington.

USGS 1996. *National Seismic-Hazard Maps: Documentation June 1996*, U.S. Geological Survey Open-File Report 96-532, Denver, Colorado.

UWGP 2001. Online Earthquake Catalog. University of Washington Geophysics Program, Seattle, Washington.. Online at http://www.geophys.washington.edu/SEIS

Vaughan 2002. R.L. Vaughan, 2002, *Virtual Library Design Document*, BHI-01535, Rev. 2, Bechtel Hanford, Inc., Richland, Washington.

WAC 173-201A, "Water Quality Standards for Surface Waters of the State of Washington," *Washington Administrative Code*, as amended.

WAC 173-216, "State Waste Discharge Permit Program," *Washington Administrative Code*, as amended.

Waitt 1980. R.B. Waitt, 1980, "About Forty Last-Glacial Lake Missoula Jökulhlaups through Southern Washington," *Journal of Geology*, Vol. 88, pp. 653-679.

Ward et al. 2002a. A.L. Ward, G.W. Gee, Z.F. Zhang, and J.M. Keller, 2002, *Vadose Zone Transport Field Study: FY 2002 Status Report*, PNNL-14150, Pacific Northwest National Laboratory, Richland, Washington.

Ward et al. 2002b. A.L. Ward, G.W. Gee, and Z.F. Zhang, 2002, "Hydrologic Tests of Lateral Flow and Transport in the Hanford Vadose Zone," Appendix D.4.1 (pp. D-223 – D-233), in A.J. Knepp, *Field Investigation Report for Waste Management Area B-BX-BY*, RPP-10098, Rev. 0, CH2M HILL Hanford Group, Inc., Richland, Washington.

Williams 1999. J.C. Williams, 1999, *Historical Vadose Zone Contamination from B, BX, and BY Tank Farm Operations*, HNF-5231, Rev. 0, Lockheed Martin Hanford Corporation, Richland, Washington.

Williams 2000. J.C. Williams, 2000, *Historical Vadose Zone Contamination from T, TX, and TY Tank Farm Operations*, RPP-5957, Rev. 0, CH2M HILL Hanford Group, Inc., Richland, Washington.

Williams 2001a. J.C. Williams, 2001, *Historical Vadose Zone Contamination from S and SX Tank Farm Operations*, HNF-SD-WM-ER-560, Rev. 1, CH2M HILL Hanford Group, Inc., Richland, Washington.

Williams 2001b. J.C. Williams, 2001, *Historical Vadose Zone Contamination from U Farm Operations*, RPP-7580, Rev. 0, CH2M HILL Hanford Group, Inc.,, Richland, Washington.

Williams 2001c. J.C. Williams, 2001, *Historical Vadose Zone Contamination from the A, AX and C Tank Farm Operations*, RPP-7494, Rev. 0, CH2M HILL Hanford Group, Inc., Richland, Washington.

Wimett et al. 2004. J.M. Wimett, L.M. Sasaki, and P.A. Kabage, 2004, *Calculation for the Post-Retrieval Volume Determination for Tank 241-C-106,* RPP-19866, Rev. 1, CH2M HILL Hanford Group, Inc., Richland, Washington.

Wood and Jones 2003. M.I. Wood and T.E. Jones, 2003, *Subsurface Conditions Description of the U Waste Management Areas*, RPP-15808, Rev. 0, CH2M HILL Hanford Group, Inc., Richland, Washington.

Wood et al. 2000. M.I. Wood, T.E. Jones, R. Schalla, B.N. Bjornstad, and S.M. Narbutovskih, 2000, *Subsurface Conditions Description of the B-BX-BY Waste Management Area*, HNF-5507, Rev. 0A, CH2M HILL Hanford Group, Inc., Richland, Washington.

Wood et al. 2001. M.I. Wood, T.E. Jones, R. Schalla, B.N. Bjornstad, and F.N. Hodges, 2001, *Subsurface Conditions Description of the T and TX-TY Waste Management Areas*, RPP-7123, Rev. 0, CH2M HILL Hanford Group Inc., Richland, Washington.

Wood et al. 2003. M.I. Wood, T.E. Jones, B.N. Bjornstad, D.G. Horton, S.M. Narbutovskih, and R. Schalla, 2003, *Subsurface Conditions Description of the C and A-AX Waste Management Area*, RPP-14430, Rev. 0, CH2M HILL Hanford Group, Inc., Richland, Washington.

Zhang et al. 2003. Z.F. Zhang, A.L. Ward, and G.W. Gee, 2003, "A Tensorial Connectivity-Tortuosity Concept to Describe the Unsaturated Hydraulic Properties of Anisotropic Soils," *Vadose Zone Journal*, Vol. 2, pp. 313-321.

Zimmerman et al. 1986. D.A. Zimmerman, A.E. Reisenauer, G.D. Black, and M.A. Young, 1986, *Hanford Site Water Table Changes, 1950 Through 1980 – Data Observations and Evaluation*, PNL-5506, Pacific Northwest Laboratory, Richland, Washington.

The largest grouping of WMA T drywells containing elevated gamma contamination is in the vicinity of tank T-106. The presence of extensive vadose zone contamination in this area is consistent with a 1973 supernate leak from tank T-106 that is the largest (115,000 gal) and most thoroughly documented SST leak in Hanford Site history. The first extensive study of the tank T-106 leak was done shortly after it occurred (ARHCO 1973), and a followup study was completed in 1978 (Routson et al. 1979). In 1994, to provide greater understanding of the nature and extent of vadose contamination, an extensive sampling and analysis program was completed on soil samples taken from a borehole near the center of the tank T-106 leak (Freeman-Pollard et al. 1994). A synthesis of available vadose zone contamination data related to the tank T-106 leak is provided in Wood et al. (2001). These data along with additional data from two soil characterization boreholes installed around tank T-106 during WMA T field characterization efforts was analyzed in depth in Myers (2005).

A large number of drywells contain contamination from the tank T-106 leak because of the large extent of the leak and the high density of drywells constructed to quantify the soil column contamination caused by this leak. Historical gross gamma and spectral gamma data collected in these wells provide the most complete characterization data set of any tank farm leak on the Hanford Site. The gamma data reveal zones of different gamma signatures with increasing distance from the leak source, indicating that extensive lateral as well as vertical spreading of the leak occurred (Wood et al. 2001).

The location of the tank T-106 leak appears to be on the southeast part of the tank wall near the bottom of the tank (Wood et al. 2001). Two drywells adjacent to tank T-106 in this area (50-06-05 and 50-06-17) have zones of very high cesium-137 concentration (10^8 pCi/g) beginning near the tank bottom at 35 ft and extending to a depth of about 100 ft. Cesium-137 concentrations decrease with increasing distance from the inferred source. At the outer margins of the inferred leak area, no cesium-137 is detected. Gamma ray activity in drywells located at the outer margins of the leak is primarily from cobalt-60, which frequently extends to the drywell bottoms (Wood et al. 2001).

Interpretation of the historical gamma data collected from 1975 through 1994 indicates ruthenium-106 and cobalt-60 migration in most of the drywells that intercepted the tank T-106 leak plume (Wood et al. 2001). Downward migration of ruthenium-106 and cobalt-60 at drywells 50-00-09 and 50-09-10 appears to have occurred near the tank bottom around 1980 and again at greater depths (about 60 to 100 ft) in the late 1980s. Cesium-137 migration is indicated in the leak location area in the late 1970s.

Spectral gamma logging data also indicate the presence of generalized near-surface contamination across WMA T. The contamination is typically 1 to 10 pCi/g or less and is largely constrained to the first 10 ft of the soil column (Wood et al. 2001). The contamination is related to minor releases of contaminated fluids during tank farm operations that made relatively insignificant contributions to vadose zone contamination.

2.7.6 Unconfined Aquifer Conditions

This section summarizes WMA T groundwater monitoring and characterization activities and the current understanding of contamination in the unconfined aquifer.

2.7.6.1 Monitoring and Characterization

A detection level RCRA groundwater monitoring program for WMA T was initiated in 1989, and the WMA was placed into assessment status in 1993 because specific conductance limits were exceeded in downgradient monitoring well 299-W10-15 (Caggiano and Chou 1993). Specific conductance values in well 299-W10-15 dropped below the critical mean in 1994; however, before the WMA could be returned to a detection level monitoring program, specific conductance in well 299-W11-27 started a rapid increase in late 1995 and exceeded the critical mean in early 1996. Accordingly, WMA T continues to be monitored under a groundwater quality assessment program.

The increased specific conductance in well 299-W11-27 was accompanied by elevated technetium-99, tritium, nitrate, calcium, magnesium, sulfate, chromium, cobalt-60, and total organic carbon. Results of the initial groundwater quality assessment at WMA T found evidence linking the contaminants in groundwater to the WMA (Hodges 1998). The groundwater monitoring plan governing activities at WMA T is contained in Hodges and Chou (2001a) and its revision (Hodges and Chou 2002). RCRA groundwater assessment monitoring results are included in quarterly reports to Ecology and annually, as required, in the groundwater monitoring annual reports. Monitoring under the assessment-monitoring program will continue until the entire WMA is closed and post-closure monitoring is implemented, or until such time that there is a shift in the monitoring status of the WMA. Changes in the monitoring program status will be documented in an approved groundwater monitoring plan.

2.7.6.2 Contamination

Groundwater beneath WMA T is contaminated with technetium-99, carbon tetrachloride, trichloroethene, chromium, nitrate, and fluoride (Hartman et al. 2004). Horton et al. (2002) also lists concentrations of gross beta, tritium, and manganese as exceeding the respective MCLs in the groundwater around WMA T. Hartman et al. (2004) provides data for fiscal year 2003 and states that WMA T does not appear to be the source of most of the contamination, except for technetium-99 (and by inference gross beta), in the uppermost aquifer. Carbon tetrachloride and trichloroethene contamination is attributed to Plutonium Finishing Plant operations. Nitrate contamination also is attributed to Plutonium Finishing Plant operations as well as past-practice disposal to cribs and trenches near WMA T. Chromium, fluoride, and tritium contamination is attributed to cribs and trenches upgradient of WMA T. The elevated manganese concentrations are believed to be a consequence of reducing conditions around the monitoring wells. The exceptionally high concentration measured at well 299-W11-24 is believed to have been caused by the very fine particulates in the mud at the bottom of well, which had less than 1 m of water in the well when the sample was taken.

Since late 2000 and early 2001, technetium-99 concentrations in the area have increased substantially. During fiscal year 2003, the highest technetium-99 concentration in those wells was 2,600 pCi/L in well 299-W11-41 (Hartman et al. 2004). Apparently, technetium-99 is migrating toward the south along the east edge of WMA T from the northeast corner of the

WMA (Figure 2-49). This migration is coincident with a shift in groundwater flow direction from northeastward before 1996 to 1997 to eastward or slightly southeastward after 1997 (Hartman et al. 2004). Technetium-99 is also increasing upgradient of WMA T, with corresponding increases in chromium and nitrate, near the 216-T-36 crib, but this increase is attributed to the 216-T-5, 216-T-7, or 216-T-36 cribs.

Figure 2-49. Technetium-99 Distribution in Groundwater at Waste Management Area T [a]

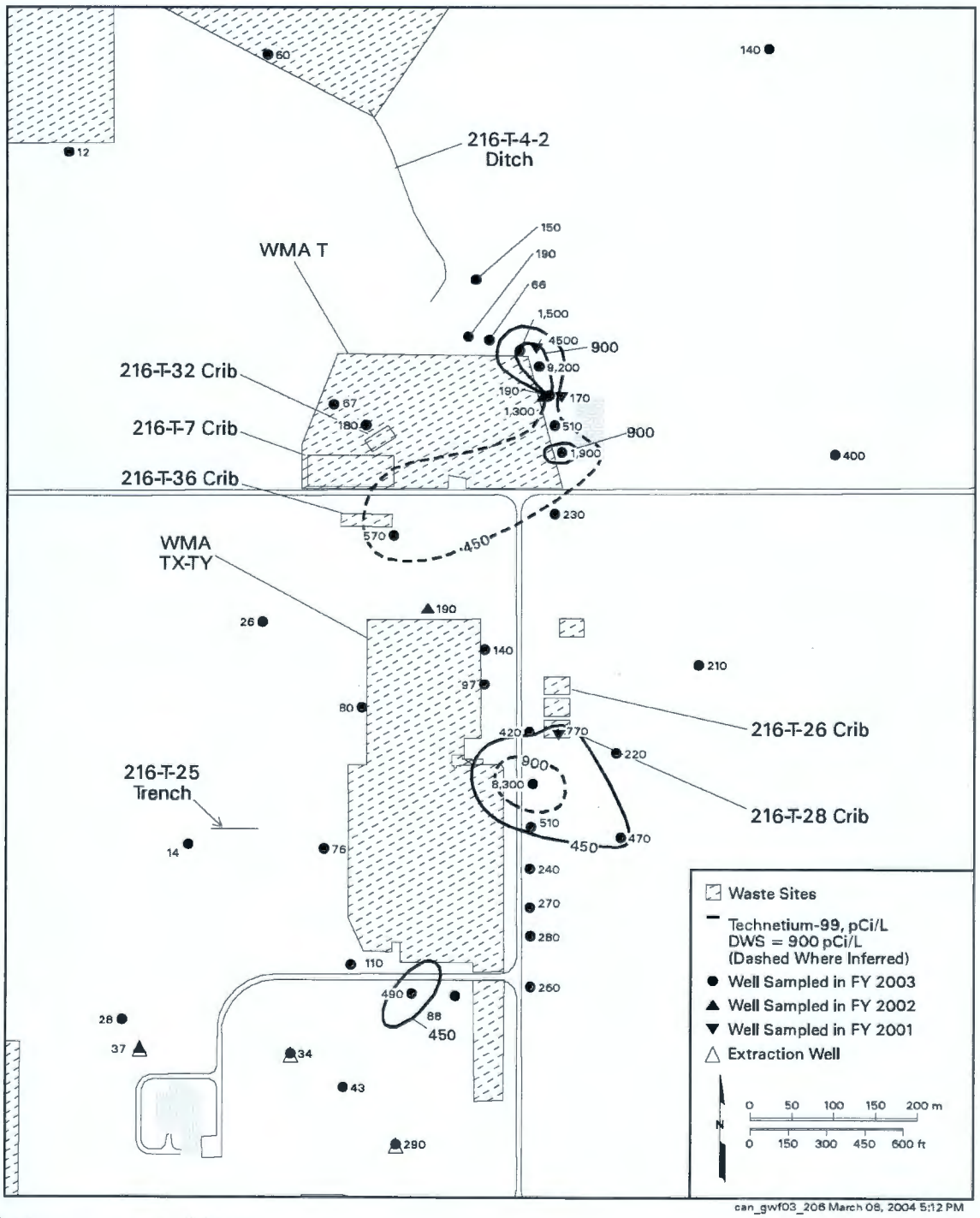

[a] *Hartman et al. (2004)*

2.7.7 Reference Case Source Terms

The reference case describes a set of assumed post-retrieval conditions that are based on current waste retrieval plans. The reference case analysis for WMA T includes three source terms consisting of past UPRs, residual SST waste, and residual ancillary equipment waste. Table 2-11 provides a listing of the reference case source terms for WMA T, and the inventory data source for that source term.

Source term inventories (reference case) for WMA T are provided in Table 2-12. To simplify the table, only the contaminants that dominate post-closure impacts are shown. All BBI contaminants are included in the reference case modeling analysis. Refer to Section 2.5 for a summary of source term inventory development methods. Complete source term inventory data are provided in Appendix C.

2.7.7.1 Past Unplanned Releases

The WMA T reference case includes six past UPRs associated with SSTs (T-101, T-103, T-106, T-108, T-109, T-111). Volume estimates for those six waste loss events were developed by Field and Jones (2005) and vadose zone contaminant inventories were generated by Corbin et al. (2005) (Section 2.5.2). No volume or inventory estimates were assigned to the waste loss event associated with tank T-107 because of insufficient information to quantify or verify the release (Field and Jones 2005). If new information becomes available to quantify the waste loss event from that tank, the data will be evaluated under the integrated regulatory closure process described in Chapter 1.0.

2.7.7.2 Residual Single-Shell Tank Waste

The WMA T reference case includes residual waste in each of the twelve 100-Series and four 200-Series SSTs in the T tank farm. The HFFACO Milestone M-45-00 goal allows up to 360 ft^3 of waste to remain in the 100-Series tanks after retrieval in the event that retrieval beyond that level becomes impracticable (Ecology et al. 1989). Thus, the analysis included a 360 ft^3 source term associated with residual waste remaining in each of the tanks after retrieval. The inventory estimates were generated with the use of the HTWOS model (Kirkbride et al. 2005), which accounts for the waste retrieval technology and tracks the fate of soluble and insoluble constituents in the waste (Section 2.5.3).

2.7.7.3 Residual Ancillary Equipment Waste

Lambert (2005) identified no plugged and blocked piping in the T tank farm. The reference case ancillary equipment source term for WMA T therefore included one ancillary component, the 241-T-301B catch tank (Section 2.5.4). The estimated volume of residual waste in that tank was calculated by assuming the tank would be retrieved to a residual volume proportional to that required under the HFFACO Milestone M-45-00 for 200-Series tanks (Ecology et al. 1989). Contaminant inventories for the tank were estimated using the average chemical composition of the waste in WMA T SSTs.

Table 2-11. Reference Case Analysis of Waste Management Area T (2 pages)

Inventory and Source Terms					
Sources	**Assumed Retrieval Method**	**Residual Volume**	**Volume Associated with Past Release [a] gal**	**Basis for Contaminant Inventory Estimate**	
				Residual Waste [b]	**Past Release**
241-T-101	Mobile retrieval system	360 ft^3	10,000	HTWOS	Corbin et al. 2005
241-T-102	Sluicing	360 ft^3	None	HTWOS	None
241-T-103	Mobile retrieval system	360 ft^3	3,000	HTWOS	Corbin et al. 2005
241-T-104	Sluicing	360 ft^3	None	HTWOS	None
241-T-105	Sluicing	360 ft^3	None	HTWOS	None
241-T-106	Mobile retrieval system	360 ft^3	115,000	HTWOS	Corbin et al. 2005
241-T-107 [c]	Mobile retrieval system	360 ft^3	NSI [c]	HTWOS	None
241-T-108	Mobile retrieval system	360 ft^3	1,000	HTWOS	Corbin et al. 2005
241-T-109	Mobile retrieval system	360 ft^3	1,000	HTWOS	Corbin et al. 2005
241-T-110	Sluicing	360 ft^3	None	HTWOS	None
241-T-111	Mobile retrieval system	360 ft^3	1,000	HTWOS	Corbin et al. 2005
241-T-112	Sluicing	360 ft^3	None	HTWOS	None
241-T-201	Vacuum	30 ft^3	None	HTWOS	None
241-T-202	Vacuum	30 ft^3	None	HTWOS	None
241-T-203	Vacuum	30 ft^3	None	HTWOS	None
241-T-204	Vacuum	30 ft^3	None	HTWOS	Corbin et al. 2005

Table 2-11. Reference Case Analysis of Waste Management Area T (2 pages)

Inventory and Source Terms					
Sources	**Assumed Retrieval Method**	**Residual Volume**	**Volume Associated with Past Release [a] gal**	**Basis for Contaminant Inventory Estimate**	
				Residual Waste [b]	**Past Release**
241-T-301B catch tank [d]	TBD [d]	19.6 ft^3	None	Average	None
241-T tank farm pipelines [e]	TBD	0	None	Lambert 2005	NA

[a] Past leak volumes listed in Field and Jones (2005).

[b] Residual inventories from HTWOS model output (Kirkbride et al. 2005).

[c] NSI = not sufficient information. Tank T-107 is identified as a "confirmed or suspected" leaker in Hanlon (2005) but both Hanlon (2005) and Field and Jones (2005) state there is insufficient information for developing a leak volume at this time. As information becomes available, a leak volume will be developed.

[d] TBD = to be determined. Final disposition of MUSTs not yet determined; however, MUSTs were carried forward in the assessment assuming MUSTs will be retrieved to at least the HFFACO goal (Ecology et al. 1989, Milestone M-45-00) equivalent to the 200-Series tanks. The residual volume is calculated by ratio of the total volume of the MUST to the 200-Series tanks (e.g., the retrieval goal for the 55,000-gal 200-Series tanks is 30 ft^3; thus, a MUST that is ⅔ the size of the 200-Series tank would have a residual volume of 20 ft^3). Inventory was calculated based on average waste per ft^3 within the WMA calculated from the HTWOS model (Kirkbride et al. 2005).

[e] Final disposition of pipelines is not yet determined; however, pipelines were carried forward in the assessment. Pipeline residual volumes shown represent the volume of waste in plugged or blocked pipelines as determined by Lambert (2005).

NA = not applicable

Table 2-12. Reference Case Inventory Estimates for Waste Management Area T

Source Type	Dominant Contaminants for Groundwater Pathway Impacts [a]							Dominant Contaminants for Inadvertent Intruder Impacts [a]						
	C-14 Ci	Tc-99 Ci	I-129 Ci	Cr(VI) kg	NO_3 kg	NO_2 kg	U kg	Sr-90 Ci	Tc-99 Ci	Sn-126 Ci	Cs-137 Ci	Pu-239 Ci	Pu-240 Ci	Am-241 Ci
Past releases [b]	1.15E+00	3.90E+01	2.60E-02	5.36E+02	3.37E+04	1.53E+04	1.34E+01	6.17E+03	3.90E+01	5.02E-01	1.27E+04	2.22E+00	5.11E-01	7.98E+00
Tank residuals	3.63E-02	1.49E+00	4.20E-04	2.46E+02	4.96E+03	8.30E+02	1.02E+03	4.33E+03	1.49E+00	1.24E-02	8.13E+02	4.19E+01	5.63E+00	9.37E+00
Ancillary equipment residuals [c]	1.60E-04	6.58E-03	1.85E-06	1.08E+00	2.19E+01	3.67E+00	4.52E+00	NA	NA	NA	NA	NA	NA	NA

[a] The reference case analysis included all BBI contaminants. As described in Bowen (2004), the standard analyte list tracked in the BBI contains **25 chemicals** including:

- aluminum
- bismuth
- calcium
- chlorine
- chromium
- fluorine
- total inorganic carbon as carbonate
- iron
- mercury
- potassium
- lanthanum
- manganese
- sodium
- nickel
- nitrite
- nitrate
- oxalate
- lead
- phosphate
- silicon
- sulfate
- strontium
- uranium total
- zirconium
- total organic carbon

and **46 radionuclides** including:

- tritium
- carbon-14
- nickel-59
- cobalt-60
- nickel-63
- selenium-79
- strontium-90
- yttrium-90
- zirconium-93
- niobium-93m
- technetium-99
- ruthenium-106
- cadmium-113m
- antimony-125
- tin-126
- iodine-129
- cesium-134
- cesium-137
- barium 137m
- samarium-151
- europium-152
- europium-154
- europium-155
- radium-226
- actinium-227
- radium-228
- thorium-229
- protactinium-131
- thorium-232
- uranium-232
- uranium-233
- uranium-234
- uranium-235
- uranium-236
- neptunium-237
- plutonium-238
- uranium-238
- plutonium-239
- plutonium-240
- americium-241
- plutonium-241
- curium 242
- plutonium-242
- americium-243
- curium-243
- curium-244

[b] Inventories shown are the combined inventories from SST past releases and ancillary equipment past releases. Both release types were considered for the groundwater pathway analysis; however, only the SST past releases were included in the inadvertent intruder analysis (along with SST residuals).

[c] NA indicates insufficient information is available to make estimates of intruder impacts into ancillary equipment (e.g., pipelines, diversion boxes).

2.8 DESCRIPTION OF WASTE MANAGEMENT AREA TX-TY

This section provides site-specific information for WMA TX-TY. It is a summary from numerous documents that describe present conditions (Hanlon 2005), geology and hydrology (Reidel et al. 2006), subsurface contamination (Wood et al. 2001), and source terms (Kirkbride et al. 2005; Field and Jones 2005; Lambert 2005; Corbin et al. 2005).

2.8.1 Background

WMA TX-TY is located in the north-central portion of the 200 West Area (Figure 2-50) and encompasses the TX and TY tank farms. The TY tank farm is located adjacent to the northern boundary of the TX tank farm and is separated by the T Evaporator along their eastern fenceline. In general, the WMA TX-TY boundary is represented by the north fenceline of the TY tank farm on the north, roughly following the eastern fenceline of each tank farm on the east, the south fenceline of the TX tank farm on the south, and roughly following the western fenceline of each tank farm on the west.

The TX tank farm consists of eighteen 100-Series SSTs constructed between 1947 and 1949. The tanks are arranged in three rows of four and two rows of three tanks. The farm was originally built to provide supplemental tank space for the bismuth phosphate process (Wood et al. 2001). The TX farm received waste beginning in August 1949. Later, the TX tank farm was used as part of the uranium recovery process.

The TY tank farm contains six 100-Series SSTs constructed between 1951 and 1952. The tanks are arranged in three rows of two tanks each with cascade lines providing overflow. The TY tank farm was built to provide supplemental tank space for the uranium recovery process (Wood et al. 2001). The farm first received waste in the second quarter of 1953. Currently, the pumpable liquid wastes have been removed from the tanks in WMA TX-TY and all tanks have been interim stabilized (Hanlon 2005). Table 2-13 lists the estimated volume of waste stored in the WMA TX-TY tanks as of November 30, 2004.

The current understanding of contaminant occurrences and environmental conditions at WMA TX-TY is described in Wood et al. (2001). Detailed discussion of TX and TY tank farm construction and historical information on soil surface and vadose zone contamination in WMA TX-TY is provided in Williams (2000).

Vadose zone field characterization activities were initiated at WMA TX-TY during fiscal year 2003 in support of RCRA Corrective Action process requirements. The investigative approach for this work is described in Crumpler (2001). Myers (2005) documents the results of these investigations.

Figure 2-50. Location Map of TX and TY Tank Farms and Surrounding Facilities [a]

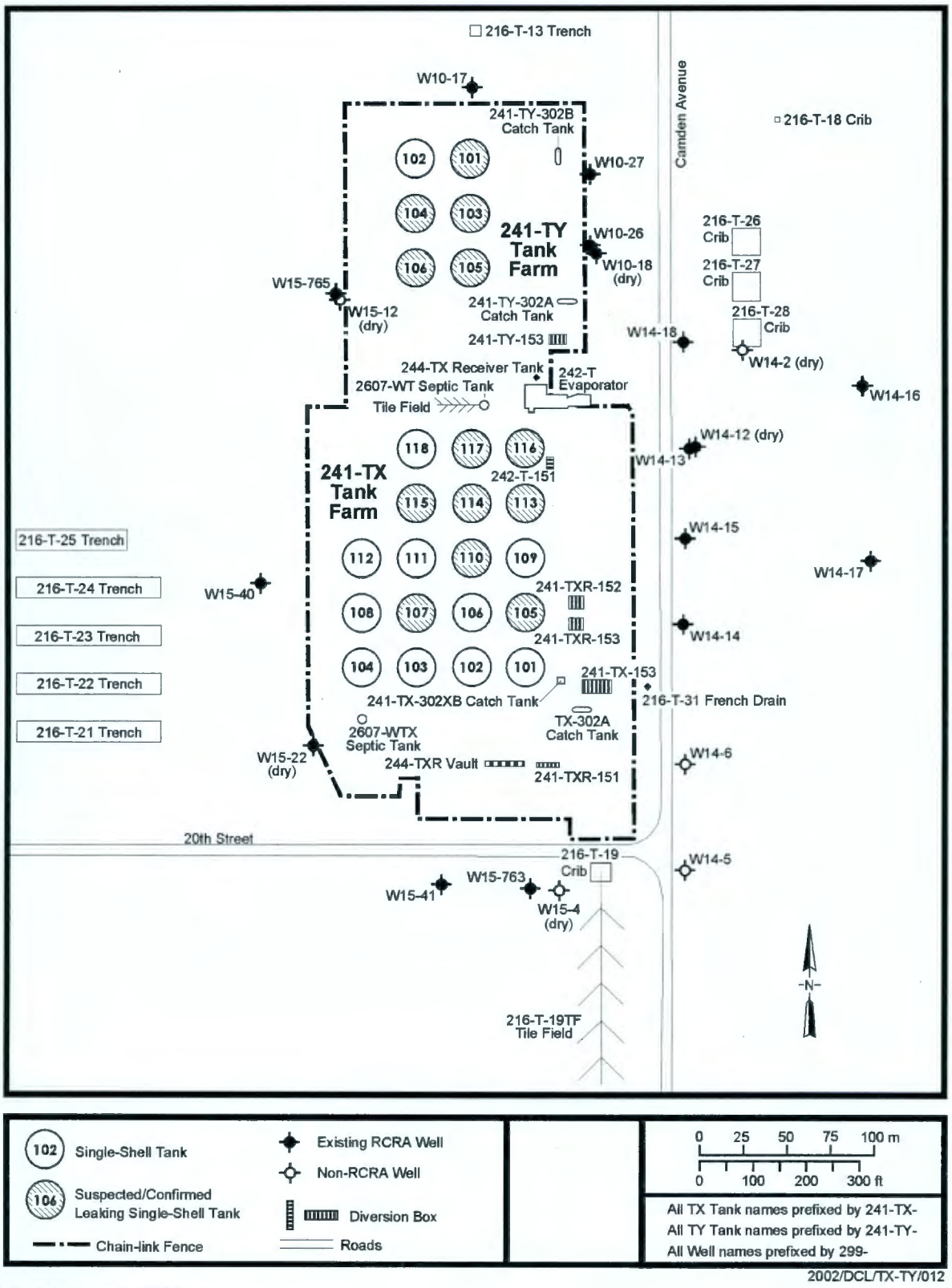

[a] *Reidel et al. (2006)*

Table 2-13. Waste Volume Estimates as of November 30, 2004, in Waste Management Area TX-TY Single-Shell Tanks [a]

Tank	Total Waste gal × 1,000	Supernate gal × 1,000	Sludge gal × 1,000	Saltcake gal × 1,000
TX Tank Farm				
241-TX-101	91	0	74	17
241-TX-102	217	0	2	215
241-TX-103	145	0	0	145
241-TX-104	69	2	34	33
241-TX-105	576	0	8	568
241-TX-106	348	0	5	343
241-TX-107	29	0	0	29
241-TX-108	127	0	6	121
241-TX-109	363	0	363	0
241-TX-110	467	0	37	430
241-TX-111	364	0	43	321
241-TX-112	634	0	0	634
241-TX-113	638	0	93	545
241-TX-114	532	0	4	528
241-TX-115	553	0	8	545
241-TX-116	599	0	66	533
241-TX-117	480	0	29	451
241-TX-118	247	0	0	247
TY Tank Farm				
241-TY-101	119	0	72	47
241-TY-102	69	0	0	69
241-TY-103	154	0	103	51
241-TY-104	44	1	43	0
241-TY-105	231	0	231	0
241-TY-106	16	0	16	0

[a] Hanlon (2005).

2.8.2 Infrastructure

This section describes the WMA TX-TY infrastructure components that were included in the SST PA. Those components are listed in Table 2-14. Reference case inventory development for those components is described in Section 2.8.7. Refer to Section 2.4 for generic infrastructure component descriptions and Section 2.5 for a summary of infrastructure inventory development methods.

Table 2-14. Operating Period and Capacities for Waste Management Area TX-TY Facilities Included in the Performance Assessment [a] (2 pages)

Facility	Removed From Service	Constructed	Operating Capacity gal
Single-Shell Tanks			
241-TX-101	1980	1947 to 1948	758,000
241-TX-102	1977		
241-TX-103	1980		
241-TX-104	1977		
241-TX-105	1977		
241-TX-106	1977		
241-TX-107	1977		
241-TX-108	1977		
241-TX-109	1977		
241-TX-110	1977		
241-TX-111	1977		
241-TX-112	1974		
241-TX-113	1971		
241-TX-114	1971		
241-TX-115	1977		
241-TX-116	1969		
241-TX-117	1969		
241-TX-118	1980		
241-TY-101	1973	1949 to 1952	758,000
241-TY-102	1979		
241-TY-103	1973		
241-TY-104	1974		
241-TY-105	1980		
241-TY-106	1959		
Miscellaneous Underground Storage Tanks			
241-TX-302A catch tank	1982	1949	17,700
241-TX-302XB catch tank	1985	1950	14,300
241-TY-302A catch tank	1981	1953	17,700
241-TY-302B catch tank	1981	1953	14,300

Table 2-14. Operating Period and Capacities for Waste Management Area TX-TY Facilities Included in the Performance Assessment [a] (2 pages)

Facility	Removed From Service	Constructed	Operating Capacity gal
241-TX DCRT	1981	Active	31,000
241-TXR-001 vault tank	1956 (244-TXR vault)	1951	50,000
241-TXR-002 vault tank		1951	15,000
241-TXR-003 vault tank		1951	15,000
Underground Waste Transfer Lines			
241-TX tank farm pipelines	NA	1947 to 1948	26,300 (+/-5,000)
241-TY tank farm pipelines	NA	1949 to 1952	1,700 (+/-1,000)

[a] Data on the facilities are from DOE-RL (2005) and Field (2003a).
DCRT = double-contained receiver tank
NA = not applicable

2.8.2.1 Single-Shell Tanks

The 100-Series tanks in the TX and TY tank farms are 75 ft in diameter and 32 ft tall. The TX and TY tanks have a 23-ft operating depth and an operating capacity of 758,000 gal. Typical tank configuration and dimensions are shown in Figure 2-51. The tanks sit belowgrade with at least 7 ft of soil cover to provide shielding from radiation exposure to operating personnel. Tank pits are located on top of the tanks and provide access to the tank, pumps, and monitoring equipment.

The TX farm tanks were constructed with cascade overflow lines in two 3-tank and three 4-tank series that allowed gravity flow of decanted liquid between tanks, while the TY farm tanks were constructed in three 2-tank cascade series (Wood et al. 2001).

2.8.2.2 Ancillary Equipment

A complete listing of the WMA TX-TY ancillary equipment currently identified for inclusion in the SST system closure is provided in Lee (2004). As discussed in Section 2.5.4, the ancillary components included in the SST PA consists of the underground waste transfer lines and MUSTs located inside each WMA boundary. For WMA TX-TY, the ancillary components analyzed consist of the TX and TY tank farms waste transfer piping and eight MUSTs. The MUSTs consist of four catch tanks (241-TX-302A, 241-TX-302XB, 241-TY-302A, 241-TY-302B), one double-contained receiver tank (244-TX DCRT), and three tanks in the 244-TXR vault (244-TXR-001, 244-TXR-002, 244-TXR-003).

Multiple levels of piping were installed over time in WMA TX-TY. A time line of piping installations is described in Williams (2000). It is estimated that there are approximately 13.6 mi (+/- 2.6 mi) of waste transfer piping in the TX tank farm and 0.9 mi (+/- 0.5 mi) in the TY tank farm (Field 2003a).

Figure 2-51. Typical Configuration and Dimensions of Single-Shell Tanks in Waste Management Areas T and TX-TY

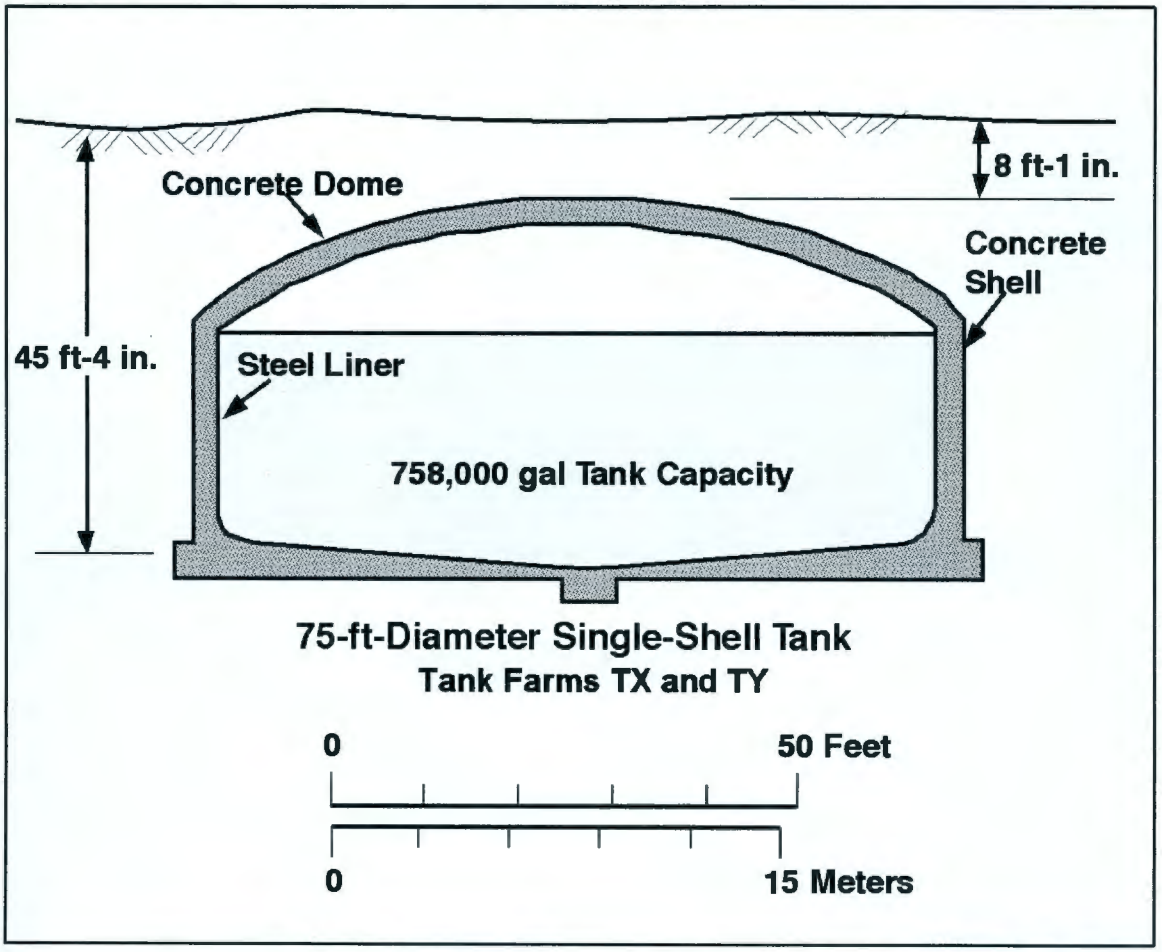

2.8.3 Geology

Following is an overview of the geology of WMA TX-TY summarized from the information provided in Reidel et al. (2006). Because WMAs T and TX-TY are in close proximity and have similar geologic conditions, they are discussed together in Reidel et al. (2006) and will be discussed together here. A generalized cross-section through WMA TX-TY is shown in Figure 2-52. Maps and cross-sections presented in Reidel et al. (2006) illustrate the distribution and thicknesses of these units in additional detail.

Figure 2-52. Fence Diagram Showing Cross-Sections through Waste Management Areas T and TX-TY [a]

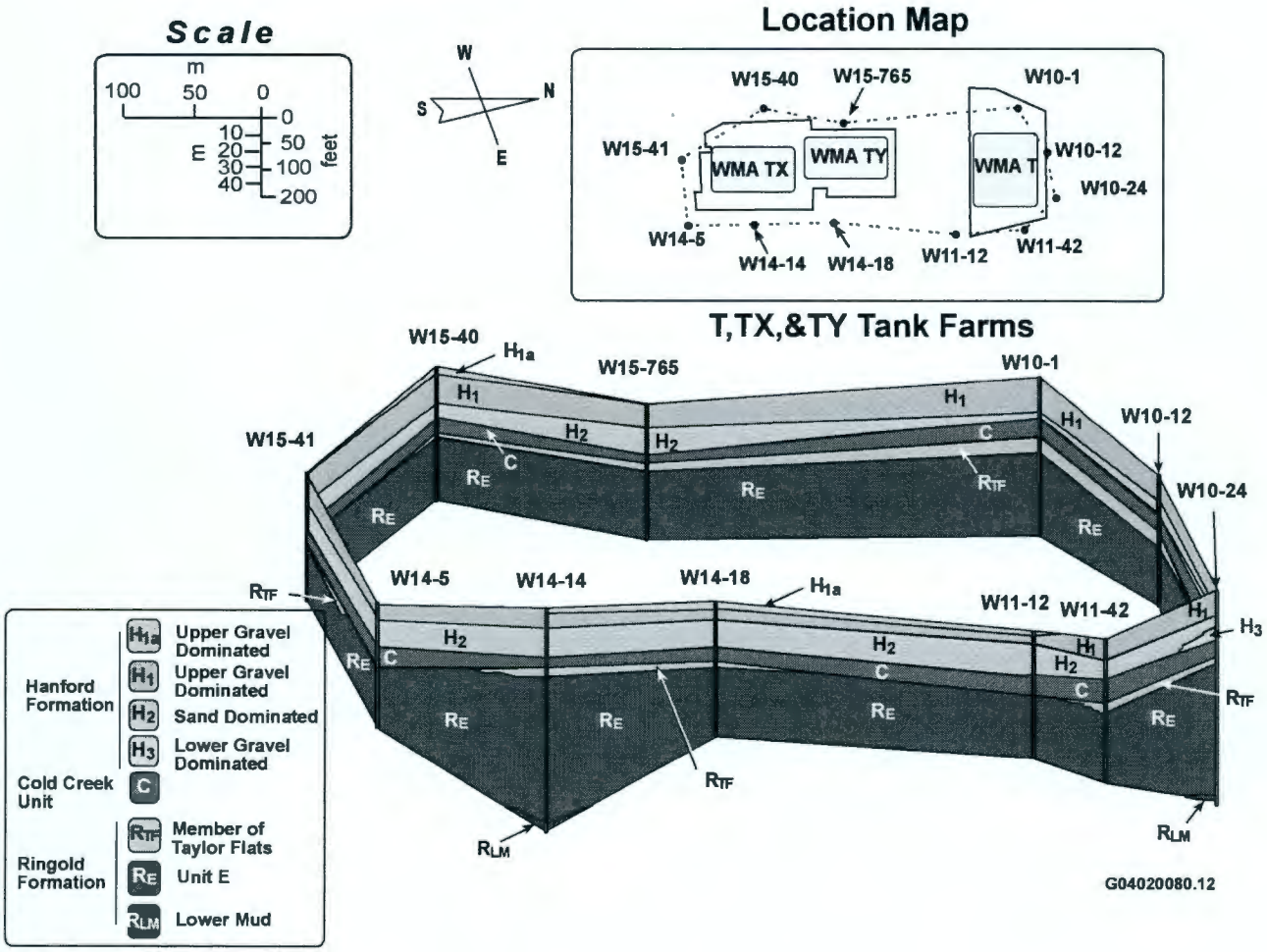

This document was to large to provide as a single document for download. It has been divided into smaller sections for easier download

Section 4 of 6

Document Information			
Document #	DOE/ORP-2005-01	Revision	0
Title	INITIAL SINGLE-SHELL TANK SYSTEM PERFORMANCE ASSESSMENT FOR THE HANFORD SITE		
DATE	04/18/2005		
Originator	CONNELLY MP	Originator Co.	CH2M
Recipient			
References			
Keywords			
Projects			
Other Information			

3.0 ANALYSIS OF PERFORMANCE

CONTENTS

3.1 INTRODUCTION 3-1

3.2 PERFORMANCE ASSESSMENT METHODOLOGY 3-2
- 3.2.1 Overview 3-3
- 3.2.2 Groundwater Pathway 3-6
- 3.2.3 Air Pathway 3-35
- 3.2.4 Intruder Pathway 3-37

3.3 NUMERICAL IMPLEMENTATION 3-39
- 3.3.1 Code Selection and Verification 3-39
- 3.3.2 Subsurface Transport Over Multiple Phases 3-40
- 3.3.3 Decision Management Tool 3-40

3.4 VALUES AND ASSUMPTIONS 3-41
- 3.4.1 Inventory 3-41
- 3.4.2 Surface Barrier and Pre- and Post-Barrier Recharge Rates 3-52
- 3.4.3 Grouted Tanks and Ancillary Equipment 3-56
- 3.4.4 Vadose Zone 3-58
- 3.4.5 Unconfined Aquifer 3-67
- 3.4.6 Exposure Parameters 3-68
- 3.4.7 Reference Case 3-68

3.5 SENSITIVITY CASES 3-69
- 3.5.1 Overview 3-69
- 3.5.2 Sensitivity Analysis Methodology for the Groundwater Pathway 3-70
- 3.5.3 Estimated Ranges for Selected Parameters in Groundwater Pathway Sensitivity Cases 3-74
- 3.5.4 Estimated Ranges for Selected Parameters in Groundwater Pathway "What if …?" Cases 3-81
- 3.5.5 Intruder Dose – Sensitivity to Parameter Assumptions 3-92
- 3.5.6 Air Pathway Risk – Sensitivity to Parameter Assumptions 3-95

3.6 REFERENCES 3-95

FIGURES

Figure 3-1. (a) General Performance Assessment Conceptual Model and (b) Numerical Groundwater Conceptual Model 3-4

Figure 3-2. Overall Modeling Approach for Performance Assessment for the Groundwater Pathway 3-7

Figure 3-3. Northwest-Southeast Cross-Section through Waste Management Area C 3-19

Figure 3-4. West-East Cross-Section through Waste Management Area S-SX 3-20

Figure 3-5. Infilled Sediments within Clastic Dikes 3-25

Figure 3-6. Conceptual Model of Fracture Flow under Unsaturated Conditions 3-26

Figure 3-7. Moisture Content Profiles for the Field Injection Experiment in the 200 East Area 3-29

Figure 3-8. Pre- and Post-Injection Moisture Plumes for the Field Injection Experiment in the 200 East Area 3-30

Figure 3-9. Technetium-99 Profile in Borehole 299-W10-196 from 241-T-106 Tank Leak 3-31

Figure 3-10. Results on Co-mingling of Plumes Based on Three-Dimensional Simulations 3-34

Figure 3-11. Process for Determination of Inventories from Past Leaks 3-44

Figure 3-12. Process for Determination of Inventories from Tank Residuals 3-45

Figure 3-13. Modeling Approach for Evaluating Closure System Variability Effects on Estimated Future Groundwater Contamination Levels Relative to Reference Case Results 3-72

TABLES

Table 3-1. Inventories for Selected Rows within Waste Management Areas C and S-SX 3-46

Table 3-2. Tank Farm Infiltration (Recharge) Estimates for Pre-Construction Period, Current Conditions, and Following Emplacement of Closure Barrier 3-55

Table 3-3. Composite van Genuchten-Mualem Parameters for Various Strata at Waste Management Areas C and S-SX 3-60

Table 3-4. Macroscopic Anisotropy Parameters for Various Strata at Waste Management Areas C and S-SX Based on Polmann (1990) Model 3-61

Table 3-5. Effective Bulk Density (g/cm^3) Estimates at Waste Management Areas C and S-SX 3-62

Table 3-6. Nonreactive Macrodispersivity Estimates for Various Strata at Waste Management Areas C and S-SX 3-63

Table 3-7. Contaminant Distribution Coefficients (mL/g) for Analytes that are Part of the Single-Shell Tank System Inventory 3-64

Table 3-8. Contaminant Distribution Coefficients (mL/g) for Non-Impacted Soils 3-67

Table 3-9. Reference Case Unconfined Aquifer Properties for Waste Management Areas C and S-SX 3-68

Table 3-10. Estimates of Ranges for Past Releases Within Waste Management Area C 3-76

Table 3-11. Estimates of Ranges for Past Releases Within Waste Management Area S-SX 3-77

Table 3-12. Unconfined Aquifer Properties for Waste Management Area C 3-78

Table 3-13. Unconfined Aquifer Properties for Waste Management Area S-SX 3-79

Table 3-14. Groundwater Pathway – Summary of Reference Case Parameters and Expected Ranges 3-80

Table 3-15. Alternatives to the Reference Case or "What if" Conditions for the Examination of the Level of Protectiveness Provided by the Reference Case for the Protection of Groundwater 3-82

Table 3-16. Potential Retrieval Leak Inventories for Hanford Waste Tanks within Waste Management Areas C and S-SX 3-88

Table 3-17. Intruder Pathway – Summary of Reference Case Parameters and Expected Ranges 3-93

3.0 ANALYSIS OF PERFORMANCE

3.1 INTRODUCTION

The SST PA provides an assessment of the long-term human health impacts associated with the proposed closure of the WMAs in the 200 Areas of the Hanford Site. As part of that assessment, the postulated events (scenarios) that can lead to adverse human health impacts and the pathways by which contaminants within the final closed system can potentially reach humans in the future must be identified. This chapter provides the methodology developed to assess the scenarios and pathways that were discussed in Chapter 1.0, and describes the approach used to estimate the impacts from the proposed closure action.

Specifically, this chapter describes the models, computer codes, and input data used to analyze the long-term performance of WMAs in the 200 East and 200 West Areas following their closure. For the analyses, the information discussed in Chapter 2.0 was translated into conceptual physical models that incorporate each feature of the natural and engineered barrier systems that impact the system performance. These conceptual models were then translated into numerical models to estimate the risk for each pathway. The best available data were used in the numerical models to estimate the long-term system performance. Where data were not available or were uncertain, assumptions were made and sensitivity cases identified to explore the functionality and capability of each feature of the natural and engineered barrier system.

The strategy for this SST PA was to define and analyze both a reference case and a suite of sensitivity cases. The reference case was developed using the best available information for the physical system and the WMA facilities, and the closure plans for each WMA. Sensitivity cases were defined to explore the relative impact of uncertainties in the models and data, and the assumptions on the estimated health impacts. For example, any potential leaks that may occur during retrieval of tank wastes are not included as part of the reference case, but were considered as part of the sensitivity analyses.

The following topics are discussed in this chapter:

- **Performance Assessment Methodology:** Section 3.2 describes the conceptual models developed for this SST PA, the translation of these conceptual models to numerical models, and the integration of the overall methodology used in the analyses.
- **Numerical Implementation:** Section 3.3 describes the software codes used to calculate the contaminant concentrations associated with different pathways at different locations and the translation of these concentrations as risk estimates to human health.
- **Values and Assumptions:** Section 3.4 describes the values and assumptions used in the numerical calculations to estimate the impacts. This section provides the estimate for the anticipated inventories in the WMAs at closure. This section also describes the values and assumptions associated with a reference case that are developed from the Hanford Site data.
- **Sensitivity Cases:** Section 3.5 describes sensitivity cases that reflect the variability in the system performance or data selected for the reference case.

In an effort to establish credibility and confidence in the data, assumptions, and methods used in the analysis, the following aspects were recognized and addressed:

- Nearly all data, including those for contaminant inventory, geology, hydrology, and geochemistry, were based on site characterization, sampling, measurements, and supplemented by modeling.
- Field-scale processes that are characteristic of highly heterogeneous Hanford Site sediments (e.g., lateral flow and migration) were simulated in vadose zone flow and transport models.
- Independent scientific and technical peer reviews were conducted.
- All computer codes used were benchmarked and verified.
- Sensitivity analyses were conducted to provide insight into the variability and robustness in the estimated impacts to selected assumptions and data choices made with respect to the calculations.

Results using the models and values are presented in Chapter 4.0 for the groundwater pathway scenario, in Chapter 5.0 for intruder scenarios, and in Section 6.5 for the air pathway scenario. Chapter 6.0 also presents the comparison to performance objectives.

An important aspect of the SST PA analysis is the conceptual model for vadose zone flow and transport, and its basis for use in the SST PA. As discussed in Section 3.2.2.4 (vadose zone conceptual model), each heterogeneous geologic unit within the vadose zone is replaced by its homogeneous equivalent. Each geologic unit is assigned its upscaled or effective hydraulic properties. As part of testing of the vadose zone conceptual model, the moisture content data that were collected at the Vadose Zone Test Facility (also known as the Sisson and Lu site) in the 200 East Area were analyzed as part of a separate task. The results of the analyses are presented in "Stochastic analysis of moisture plume dynamics of a field injection experiment" (Ye et al. 2005). A comparison of the observed moisture plume and the simulated moisture plume using an effective unsaturated hydraulic conductivity tensor for the Sisson and Lu site is described in "Estimation of effective unsaturated hydraulic conductivity tensor using spatial moments of observed moisture plume" (Yeh et al. 2005). The upscaled or effective hydraulic conductivities compare well with the laboratory-measured unsaturated hydraulic conductivity data based on small core samples at the site. As discussed in Yeh et al. (2005), the simulated moisture plume does reproduce the general behavior of the observed moisture plume at the field site. Spatial moments of the simulated plume based on the effective hydraulic conductivities are in reasonably good agreement with those for the observed plume (Figure 3 in Yeh et al. 2005), thereby providing an evaluation of the upscaling or effective parameter approach used in the modeling.

3.2 PERFORMANCE ASSESSMENT METHODOLOGY

The SST PA methodology uses conceptual models that are based on the physical system and expected contaminant migration pathways. The conceptual models were then translated into numerical models that are then used to estimate the risk for each pathway.

3.2.1 Overview

Figure 3-1a provides a schematic representation of both the tank system as it will exist at closure and the contaminant migration pathways evaluated in this SST PA. The manmade components of the system that influence contaminant migration include a surface barrier, the tanks and tank infrastructure, the tank fill, and the distribution of waste in the subsurface. The natural components of the system that influence contaminant migration are a number of mostly horizontal stratigraphic layers within the vadose zone and an underlying stratigraphic layer that is part of the unconfined aquifer. Figure 3-1b shows the translation of the conceptual model for the groundwater path to the implementation of the numerical models to calculate the impacts at the WMA fenceline.

The major pathways for contamination entering the environment are the groundwater pathway, the air pathway, and an intruder pathway. Under the groundwater pathway, it is assumed that water from rain and snowfall enters the subsurface, contacts waste, and carries dissolved contaminants to the unconfined aquifer. Under the air pathway, contaminant gases diffuse from the contaminant sources and into the atmosphere through the Modified RCRA Subtitle C Barrier. Finally, under the intruder pathway, a well is drilled through the contamination located within the tanks or ancillary equipment or in the vicinity of past releases within the vadose zone; the contamination is then brought to the surface where it comes into contact with humans.

Based on the conceptual models for these different pathways, numerical models were developed to estimate the contaminant concentrations within water, air, or soil as a function of time for various scenarios discussed in Chapter 1.0. Functional numerical models cannot be devised to precisely calculate contaminant migration processes in a natural system; simplifying assumptions are required to approximate ubiquitous heterogeneities of the natural system. Also, some aspects of future closure decisions that may affect contaminant migration estimates have not been finalized. Therefore, the numerical modeling approach must be sufficiently flexible to accommodate these uncertainties and to evaluate the effects of different closure decisions on contaminant migration estimates. Finally, contaminant concentration information is used to calculate estimated impacts with respect to the different exposure scenarios discussed in Chapter 1.0.

The SST PA methodology provides deterministic calculations of the estimated impacts from the proposed closure action. The risk impacts are calculated with the numerical models and a set of input values and assumptions that are most representative of the disposal system. This case is referred to as the reference case. The reference case provides the "expected" estimate for how the system may perform given the information available. As more information concerning the waste form, the disposal facility design, and disposal site location is gathered, the definition of the reference case is expected to evolve. The approach used in the reference case is not all inclusive; however, it does provide a reasonable estimate of the expected performance. Selected sensitivity cases have also been used to provide an indication of the sensitivity of the reference case results to assumptions and uncertainty in key parameters.

Figure 3-1. (a) General Performance Assessment Conceptual Model and (b) Numerical Groundwater Conceptual Model

(a)

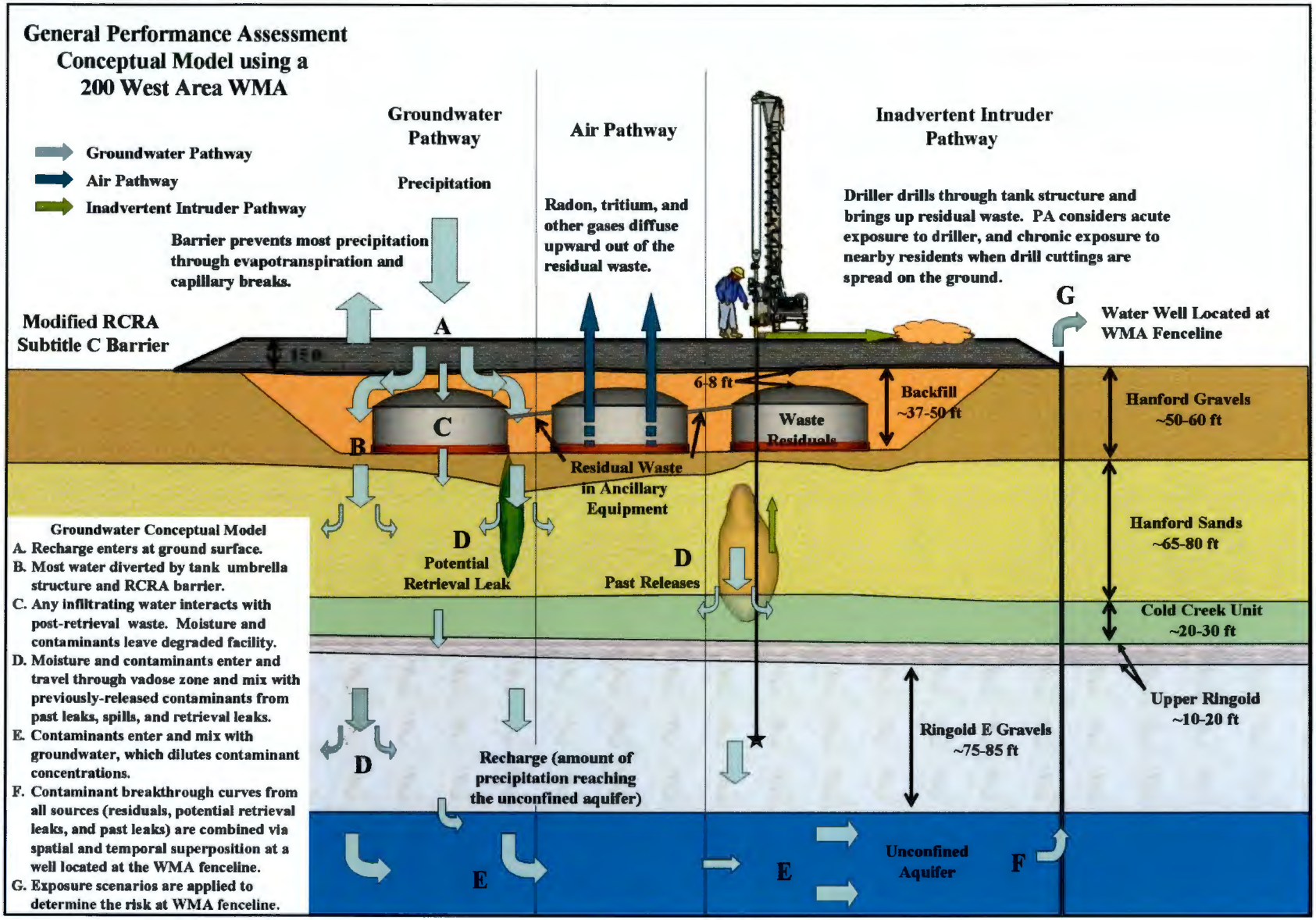

The geology shown in the figure is specific to the 200 West Area.

Figure 3-1. (a) General Performance Assessment Conceptual Model and (b) Numerical Groundwater Conceptual Model

(b)

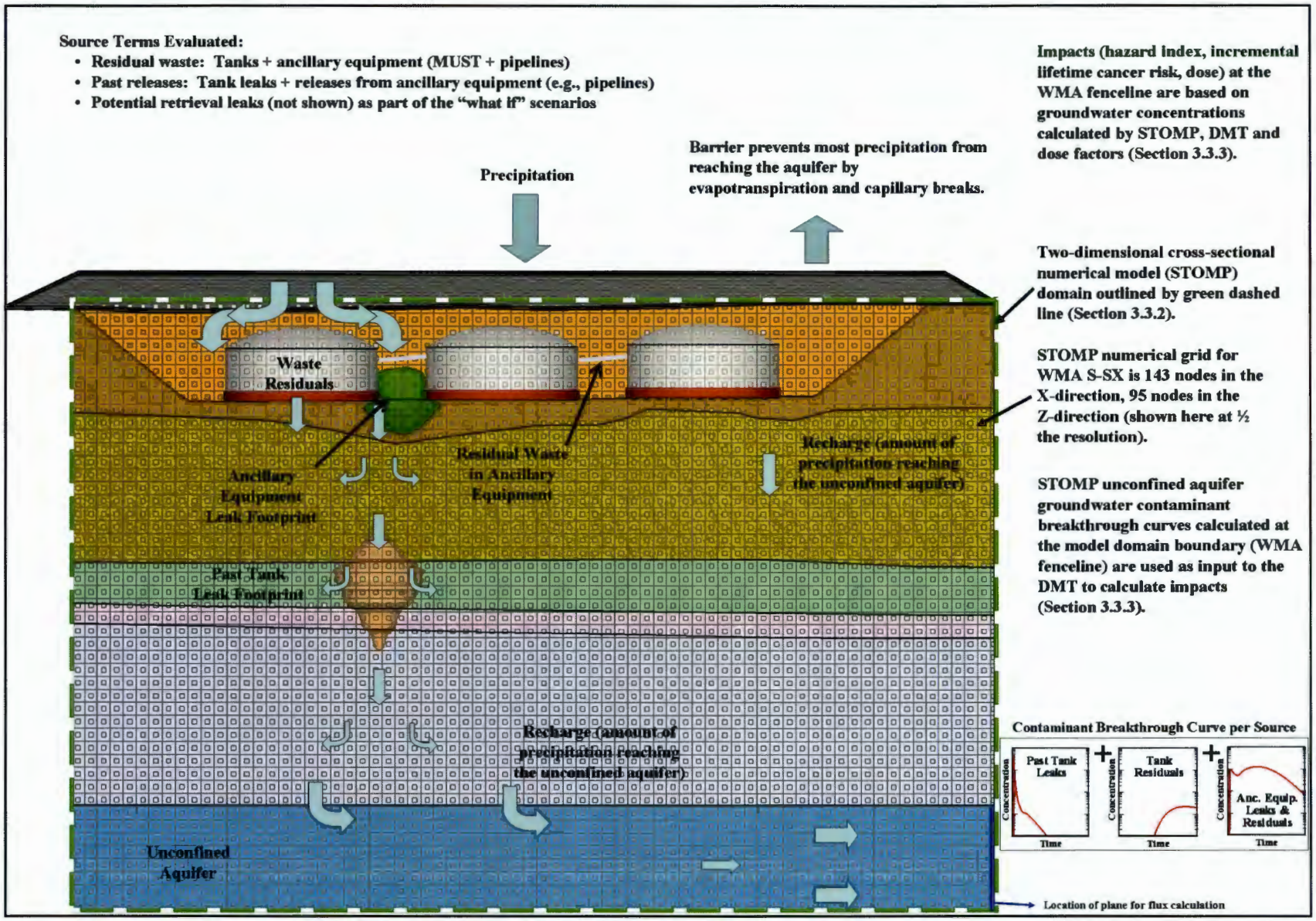

The geology shown in the figure is specific to the 200 West Area.

3.2.2 Groundwater Pathway

This section describes the SST PA methodology and the overall modeling approach for estimating the long-term impact and contaminant concentrations in the groundwater. Section 3.2.2.1 presents the overall modeling approach. Section 3.2.2.2 presents details on recharge (infiltration) estimates for various time periods. Section 3.2.2.3 discusses the contaminant release models for various source terms. Section 3.2.2.4 presents an extended discussion on the vadose zone flow and transport model. Section 3.2.2.5 discusses how the groundwater concentration estimates are converted into risk estimates.

3.2.2.1 Overall Modeling Approach

The overall modeling approach for the groundwater pathway is illustrated in Figure 3-2. As part of the closure, an assessment was conducted to evaluate impacts on groundwater resources (the concentration of contaminants in groundwater) and long-term human health risk (associated with groundwater use). The evaluations considered the extent of contamination from the following sources and processes:

- Residual waste in tanks
- Tank ancillary equipment (i.e., pipelines and MUSTs)
- Past releases (i.e., tank leaks and unplanned releases [UPR] or spills)
- Contaminant movement through the vadose zone to the saturated zone (groundwater)
- Contaminant movement in the groundwater to various calculation points
- Assumed human receptor activities at the WMA fenceline.

Contaminant sources modeled include:

- Residual waste in tanks
- Residual waste in tank ancillary equipment (i.e., pipelines and MUSTs)
- Past releases (i.e., tank leaks and UPRs) or leaks from ancillary equipment).

As indicated in Figure 3-2, the model assumed that infiltration of moisture from precipitation eventually enters the WMA (step 1), but most of the water is diverted around the tank structure during operations or around the surface barrier during closure (step 2). During the tank farm operational period, contaminants released within the vadose zone from past releases are driven by the infiltrating moisture (step 3a). Following closure, contaminants are released into the vadose zone from the degraded tank structure and ancillary equipment by contact with recharge water (steps 3b and 3c). The infiltrating water, along with contaminants from past releases and residual wastes from steps 2 and 3, travels through the vadose zone (step 4). The contaminants from all sources travel through the vadose zone until they reach the water table and the unconfined aquifer (step 5). The contaminant breakthrough curves (BTC) from residual wastes and past releases are combined via a spatial and temporal superposition (step 6). In the final step of the model, the exposure scenario risk factors are applied to estimated groundwater concentrations to determine risk (step 7).

Simplifying assumptions were made with respect to contaminant release, recharge, and flow and transport for the vadose zone and unconfined aquifer.

Figure 3-2. Overall Modeling Approach for Performance Assessment for the Groundwater Pathway

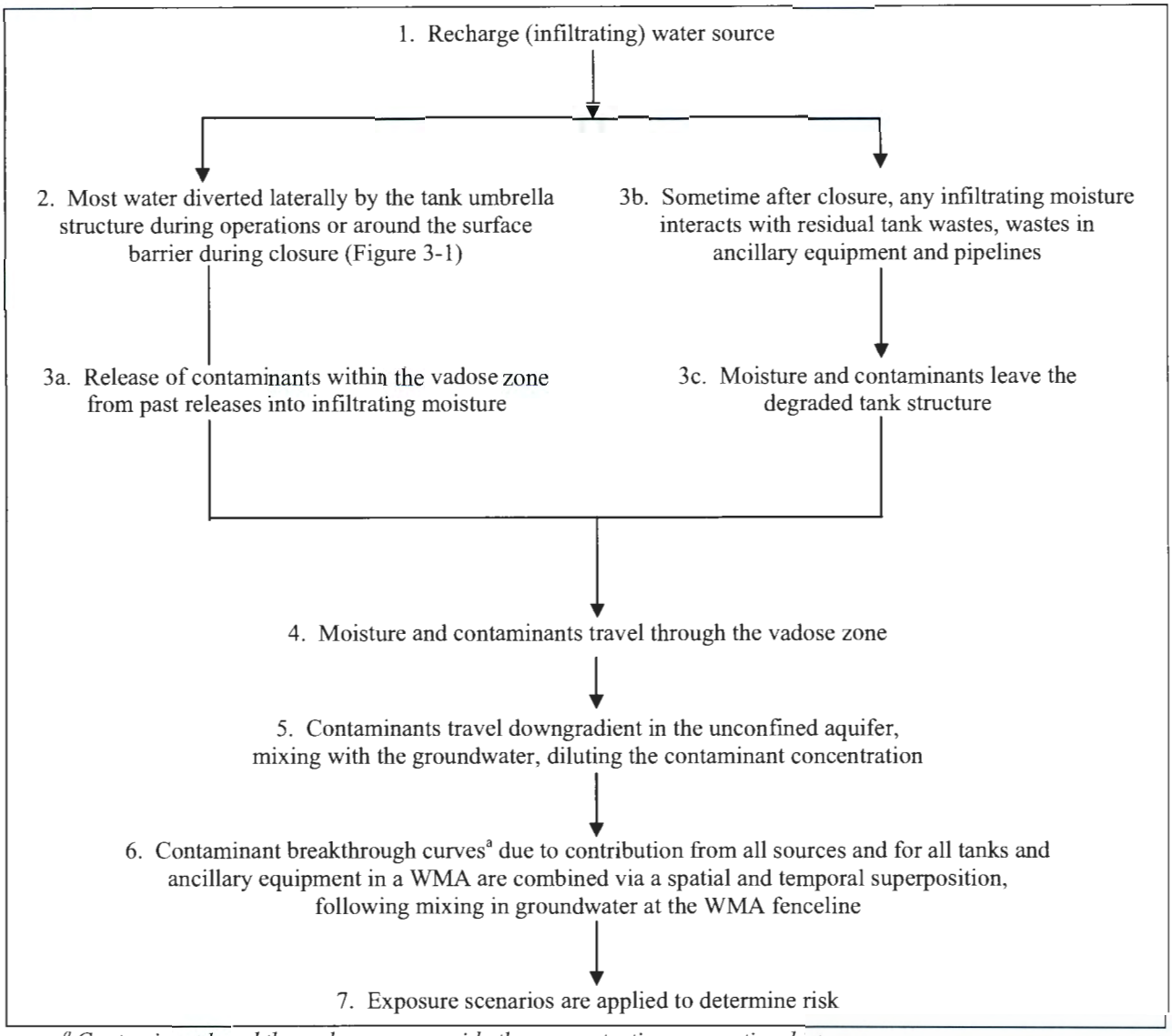

[a] *Contaminant breakthrough curves provide the concentration versus time history.*

Key Assumptions. Although much information exists concerning the Hanford Site, much less information exists that is specific to each WMA. The key assumptions were as follows:

- The closure barrier (i.e., Modified RCRA Subtitle C Barrier) for tanks and facilities in a WMA limits infiltration through the waste for a time period that is determined by the time of emplacement of the barrier and the time-dependent barrier performance.
- The fill material in the tanks is cementitious grout. The grout hydraulic properties are not varied during the simulation time.
- The reference case for this assessment assumes that the contaminant release from tank residual wastes is typical of a grouted waste (Section 3.2.2.3.2).

- Calculations are performed for unit curie (Ci) or unit mass (kg) as a source term for each of the three sources (i.e., tank residuals, tank ancillary equipment, and past releases). The contaminant BTC calculations assume proportionality between contaminant source inventory and estimated groundwater contaminant levels.
- Each of the three primary contaminant sources (past releases, tank residuals, and ancillary equipment residuals) can be modeled independently. Release and migration from one source does not alter similar processes occurring with the other sources (see discussion of superposition in Section 3.2.2.4.7).
- For each contaminant source in a WMA, the principle of spatial and temporal superposition is used to obtain a composite contaminant BTC at the WMA fenceline for all sources (Section 3.2.2.4.7).
- Past releases and their contaminant inventories are based on the best available information. In modeling past releases, vadose zone contaminant distributions are used as the initial condition, and the analysis begins in the year 2000.
- Inventories for residual waste in tanks and residual waste in the infrastructure for most cases are the best available estimates at this time.
- The vadose zone is modeled as an aqueous-gas porous media system where flow and transport through the gas phase are neglected (Section 3.2.2.4.7).
- Each heterogeneous geologic unit within the vadose zone is replaced by its homogeneous equivalent (see Figure 3-3 for WMA C and Figure 3-4 for WMA S-SX). Each geologic unit is assigned its upscaled or effective hydraulic properties. A range of K_d values is used to represent sediment-contaminant chemical interaction (Section 3.2.2.4.7).
- Results based on closure risk assessments for WMA C and WMA S-SX are used as the respective templates for analyses for the 200 East and 200 West Area WMAs. Future revisions to this SST PA will have separate analyses for other WMAs.
- Post-closure groundwater flow beneath WMA C was assumed to be parallel to tank row C-103, C-106, C-109 and C-112; similarly, post-closure groundwater flow beneath WMA S-SX was assumed to be parallel to tank row S-101, S-102, and S-103.
- All known contaminants in each WMA were modeled. A number of K_d bins are used to represent the range of sediment-contaminant chemical interaction for the variety of contaminants in various WMAs (Section 3.2.2.4.7).

The timeline for human actions used in this assessment is based on the best estimates available at the time of this writing.

For the groundwater pathway (Figure 3-2), the following models were developed to estimate the risk:

- Numerical models for contaminant release from the contaminant sources associated with the disposal action (step 3 in Figure 3-2) (Section 3.2.2.3)

- Numerical flow and transport model that calculates the flow and contaminant transport through the vadose zone and the unconfined aquifer up to the fenceline (steps 4 through 6 in Figure 3-2) (Section 3.2.2.4)
- Numerical calculation of the estimated risks associated with the public use of the groundwater (step 7 in Figure 3-2) (Section 3.2.2.5).

For this initial PA for the SSTs, detailed conceptual models and corresponding numerical models have been developed for WMA C and WMA S-SX. The results from these numerical calculations have provided estimated contaminant concentrations in the groundwater at the fenceline for each WMA and source term based on a unit curie (Ci) basis. The results are then scaled according to the appropriate inventory estimate. The results from the WMA C calculations are extrapolated to other WMAs in the 200 East Area (WMAs A-AX and B-BX-BY) (Section 3.2.2.4.8). Similarly, the results from the WMA S-SX calculations have been extrapolated to other WMAs in the 200 West Area (WMAs T, TX-TY, and U). A discussion of the justification for such an approach is provided in Section 3.2.2.4.8. Future revisions to this SST PA will include site-specific model calculations, as they are completed, for the contaminant transport to the fenceline for other WMAs.

3.2.2.2 Recharge

The term recharge (infiltration) is used to denote the moisture flux flowing past the evapotranspiration zone (i.e., the plant root zone) that percolates as deep drainage flux to the water table. Recharge is a major driver for contaminant transport from various waste sources to groundwater and to an eventual receptor. Long-term recharge estimates are needed for four different time periods:

- Before construction of tank farms
- During operation of tank farms
- The period during which a fully functional surface barrier is in place
- The period during which the surface barrier is degraded.

Recharge for conditions prior to construction of tank farms is primarily a function of soil type and infiltration characteristics of the native soils. During the operational period, a tank farm ground surface is covered with gravel to prevent growth of vegetation and provide radiation shielding for site workers. Bare gravel surfaces, however, enhance net infiltration of meteoric water, compared to undisturbed naturally vegetated surfaces. Infiltration is further enhanced in tank farms by the effect of percolating water being diverted by the impermeable sloping surface of the tank domes. This umbrella effect is created by the 75-ft (23-m) inside diameter of buried tank domes. Water, shed from the tank domes, then flows down the tank walls into the underlying sediments.

A Modified RCRA Subtitle C Barrier, which significantly reduces the meteoric recharge, is assumed to be in place over the tank farms by year 2032 and to function at its design specification for 500 years. Potential long-term barrier degradation mechanisms include periodic fires that temporarily remove vegetation and transpiration capability. Subsidence or animal burrowing (i.e., biointrusion) can also potentially create localized regions of enhanced moisture via infiltration. Critical components of the near-surface engineered systems include:

1) the vegetative cover to remove water by evapotranspiration, 2) the storage capacity of the surficial sediments to hold water in the shallow zone where it can be readily evapotranspired, and 3) biointrusion barriers to limit human, animal, and plant intrusion into the waste.

3.2.2.2.1 Simplifying Assumptions and Justifications. Recharge potential is enhanced for episodic events during the winter months when the precipitation is at its maximum and the evapotranspiration potential is at its minimum. Vadose zone flow and transport numerical modeling assumes that, for the long-term simulations over tens of thousands of years, the infiltration rates can be averaged on a yearly basis and the discrete nature of the precipitation events can be ignored. The effect of episodic precipitation events on vadose zone flow was investigated as part of a separate task. The results of simulation for a 20-year period of temporally varying precipitation for a surface barrier and a clean graveled surface are included in *Simulations of Infiltration of Meteoric Water and Contaminant Plume Movement in the Vadose Zone at Single-Shell Tank 241-T-106 at the Hanford Site* (Smoot et al. 1989, pp. 18-21). The results show that the temporal variation in drainage can effectively be ignored and an average value can be used with little loss of accuracy. Infiltration with depth through the thick, heterogeneous vadose zone in the 200 Areas dampens the effect of discrete events; therefore, episodic precipitation events can be replaced by an average annual recharge rate. Any potential unfavorable impacts from above-average, short-term infiltration events are not sustained over an extended depth within the thick, heterogeneous vadose zone that is characteristic of the 200 Areas.

Loss of vegetation through fire is temporary (i.e., 1 to 2 years) (Fayer and Szecsody 2004). Also, any potential subsidence is expected to be minimal because of the nature of the underlying material (grouted tanks). Burrowing animals do not create large-volume flow paths under unsaturated conditions (Fayer and Szecsody 2004).

The details of the surface barrier are not explicitly modeled in the numerical model. Instead, an average recharge rate is assumed at the bottom of the Modified RCRA Subtitle C Barrier shown in the conceptual model in Figure 3-1. Average recharge rates (pre- and post-barrier) that are input parameters to flow and transport models are described in Section 3.4.2.

3.2.2.3 Contaminant Release Model

The distribution of residual waste contaminants within the SSTs and ancillary equipment is not known. Contaminants within the tank farm pipelines (residual waste) are assumed to be readily available for transport with the infiltrating water. Residual wastes within the tanks are assumed to be surrounded by grout during the closure process. Release of residual wastes from MUSTs is modeled similarly to release of tank residual wastes.

Upon closure of a WMA, contaminants will be located either in the soils surrounding or beneath the tank farm structures, or within these structures. The contaminants currently residing within the vadose zone soils are from past releases (i.e., tank leaks and UPRs) during tank farm operations. Wastes currently residing within the vadose zone are therefore distributed over varying dimensions and depths. Two types of contaminant releases are considered: 1) instantaneous release (e.g., from past releases) and 2) releases occurring over an extended period (e.g., from residual waste). In the first case, the entire inventory is available for

contaminant transport immediately. In the second, the contaminants are available for transport only slowly, and the complete inventory may be released over thousands of years.

First, Section 3.2.2.3.1 describes modeling for release of contaminants from past releases. Section 3.2.2.3.2 presents a similar discussion for release of contaminants from residual tank waste. Section 3.2.2.3.3 describes modeling for release of contaminants from ancillary equipment. Simplifying assumptions made, as well as their justification for use in modeling contaminant release, are presented within each of the three following sections.

3.2.2.3.1 Past Releases. For past release contaminants within the vadose zone, release rates are dependent on contaminant-specific sorption and solubility reactions. In some locations, the dominant reactions affecting contaminant release have changed over time primarily because tank waste chemistry differed from that of ambient soil water and temporarily overwhelmed ambient equilibrium soil water conditions. These chemical perturbations were most significant at the time of the leak event and shortly thereafter, and at locations closest to the leak origin. However, the chemical buffering capacity of soil eventually eliminates tank chemistry influence, and releases are controlled by the ambient geochemical environment.

Each of the three primary contaminant sources (i.e., past releases, tank residuals, and ancillary equipment residuals) can be modeled independently. Release and migration from one source does not alter similar processes occurring with the other sources (see discussion of superposition in Section 3.2.2.4.7).

Chemical reactions that may retard contaminant release are assumed to be those controlled for the most part by the ambient environment. Even though enhanced mobility for several constituents has obviously occurred (e.g., cesium at tank SX-108 [Knepp 2002a], europium in numerous locations such as near tanks T-106 and TX-107 [Myers 2005]), field data suggest that contaminants within the deeper vadose zone behave chemically according to prevailing ambient conditions. Specifically, desorption experiments and solids characterization data from recent characterization borehole sediments (e.g., Knepp 2002a) show that cesium-137, strontium-90, and uranium are now largely immobile in vadose zone soil (i.e., consistent with the ambient geochemical environment).

The past releases including tank leaks and UPRs are listed in Corbin et al. (2005). The list is assumed to capture all major contaminant releases to the soil. Site characterization data are available (Knepp 2002a, 2002b) for the distribution and depth for the contaminant plumes in the vadose zone for various past releases.

Simplifying Assumptions and Justifications for Past Releases. For past releases, the following simplifying assumptions were made:

- One homogeneous contaminant distribution over one waste volume size and depth interval (based on field data from recently drilled boreholes) is assumed for all past releases within each WMA.
- The entire leaked inventory is readily available for transport with the infiltrating water where transport is only limited by the chemical adsorption to the soils.

Actual waste distribution can only be approximated because of limited field data. The use of one contaminant distribution to represent all tank leaks within a given WMA is justified based on the results of previous analyses (e.g., Knepp 2002a, 2002b). These analyses show that an assumed distribution has little effect on mass flux estimates because all contaminant inventories are contacted and migrate to groundwater at about the same rate. The depth locations for the contaminant distribution were selected to be representative of currently measured depths in the 200 East and 200 West Areas. Depending on K_d and timing of barrier placement, the depth location of the past tank leak within the vadose zone, for a given recharge rate, may impact the timing for the contaminant to reach the unconfined aquifer.

One homogeneous contaminant distribution over a single waste volume size and depth interval (based on field data from recently drilled boreholes) is assumed for all past releases within each WMA. The entire leaked inventory is readily available for transport with the infiltrating water.

The explicit methodology for estimating the contaminant release from each past release is based on the contaminant distributions and depths discussed in Section 3.4.3.1.1, and the use of the WMA C and WMA S-SX results as templates for the remaining WMAs in the 200 East and 200 West Areas, respectively (Section 3.2.2.4.8). More site-specific distributions will be used in later revisions of the SST PA.

3.2.2.3.2 Release of Contaminants from Residual Tank Wastes. The final tank residual waste configuration and inventories will be dependent on actual retrieval practices that remain to be applied to the tank waste. However, as discussed in Chapter 1.0 regarding defense in depth as applied to tank farm closure, the engineered barrier consists of a surface barrier and the grouted tank structure.

Simplifying Assumptions and Justifications for Residual Tank Wastes. The following simplifying assumptions were made for the contaminant release of residual tank wastes:

- Contaminant release from residual wastes in the tanks is dominated by diffusional processes.
- An analytical model for diffusion was used for residual waste contaminants released from tank bottom as a planar source (neglecting tank structure details and any future cracking that may occur within the grouted tank).
- Contaminant specific sorption and solubility were not modeled.
- The source location for the contaminant release from tanks was assumed to be directly beneath the tank.

Tank residual waste is largely encapsulated by low permeability materials and, therefore, is unlikely to be exposed to large amounts of recharge water for significant times beyond the closure date. Therefore, diffusion is assumed to be the dominant mechanism for contaminants to be released from the tanks into the surrounding soils. A simple analytical model (described below) has been selected to represent the contaminant release of residual waste from the closed tank system. Tank waste residuals reside in a grouted block consisting of the tank shell and

grouted interior. A mixing zone with a corresponding mixing length of contaminated grout was assumed for purposes of calculating diffusional flux from a contaminated zone. Diffusional flux at the grout soil barrier is a boundary condition in the vadose zone flow and transport model. Diffusion through the steel liner was not explicitly analyzed; cracks in the grout, steel liner, and outer concrete shell were not simulated. These factors were not simulated because too little characterization data are available to simulate the actual conditions. The simulation results were bounded by a sensitivity case, i.e., a release model where the grout was assumed to have the hydraulic properties of backfill material (i.e., sand and gravel) and the tank residuals were assumed to be readily dissolved in the infiltrating moisture (Section 3.5.4.3).

Contaminant release from residual wastes in the tanks is dominated by diffusional processes. An analytical model for diffusion was used for residual waste contaminants released from tank bottom as a planar source. This assumption neglects tank structure details and any impacts from future cracking that may occur within the grouted tank.

No chemical reactions between contaminants and grout were explicitly modeled in the analysis. For several contaminants (e.g., uranium), chemical reactions that reduce release rates do occur. By ignoring these effects, a release rate that was larger than expected was calculated.

The contaminant release rate from the ancillary equipment pipelines was assumed to be equivalent to the normalized release rates estimated for past tank leaks. A better estimate for the actual release rate must await additional characterization of the waste quantities and their locations within the ancillary equipment, and a better understanding of the planned final closure conditions. For this initial SST PA, on the basis of available information, the inventory associated with all pipeline waste was assumed to be located at a depth of 9 m (30 ft) bgs and uniformly distributed over a horizontal width of 7 m (25 ft). For MUSTs, the release of residual wastes was assumed to be equivalent to the contaminant release of tank residual wastes (Section 3.2.2.3.3).

As stated earlier, a diffusion-dominated release model was used to simulate the release of contaminants from stabilized (e.g., grouted tank) wastes for the reference case. In the absence of little or no advection through the tank waste, the release can be modeled as a diffusion-limited process. The diffusion from cylindrical containers leads to an expression for flux that contains infinite series (Crank 1975; Kozak et al. 1990). The analytical solution used is for one-dimensional diffusion through the tank bottom for a semi-infinite medium with the concentration C_0 throughout, initially, and with zero surface concentration, as follows:

$$C = C_0 \, erf \frac{x}{2\sqrt{(D_e t)}} \qquad \textbf{Eq. 3.1}$$

where:

C = estimated concentration
C_0 = initial concentration
x = distance
erf = standard error function
D_e = effective diffusion coefficient of the contaminants in the waste form
t = time.

The rate of loss of diffusing substance per unit area from the semi-infinite medium when the surface concentration is zero is given by Equation 3.2:

$$(D_e \frac{\partial C}{\partial x})_{x=0} = C_0 \sqrt{\frac{D_e}{\pi t}} \qquad \textbf{Eq. 3.2}$$

Equation 3.2 has the form of diffusional mass transfer based on leaching theory. The simplified release model leads to the following form:

$$q = A\, C_0 \sqrt{\frac{D_e}{\pi t}} \qquad \textbf{Eq. 3.3}$$

where:
q = release rate from a single waste cell (Ci/yr)
A = effective surface area of a single cell
C_0 = concentration in a cell.

The residual waste is likely contained in various cells with differing sizes and shapes. For the release model used herein, the cells were assumed to be of the same size and shape so that the diffusive release rate, Q, from all residual wastes in a tank can be based on Equation 3.4:

$$Q = C_0 \sqrt{\frac{D_e}{\pi t}} \sum_{i=1}^{n} A_i$$

$$= C_0 A_t \sqrt{\frac{D_e}{\pi t}} \qquad \textbf{Eq. 3.4}$$

where:
n = the number of cells
A_i = the surface area of individual cells
A_t = the total surface area.

Assuming that the cells are of constant size:

$$I = C_0 \sum_{i=1}^{n} V_i = C_0 V_t \qquad \textbf{Eq. 3.5}$$

where:
I = the total inventory
V_i = the volume of i-th cell
V_t = the total volume of all cells.

Combining the preceding equations:

$$Q = I \frac{A_t}{V_t} \sqrt{\frac{D_e}{\pi t}} \qquad \textbf{Eq. 3.6}$$

Recall that the real system consists of grout-filled tanks that have residual tank waste located predominantly on surfaces within these structures. Equation 3.6 is a reasonable approximation as long as the diffusional release time is much greater than the vadose zone travel time. See Section 3.4.3.1.2 for details on selection of A_t/V_t values.

3.2.2.3.3 Release of Contaminants from Ancillary Equipment. The final tank residual waste configuration and inventories within the ancillary equipment will be dependent on actual retrieval practices that remain to be applied to the ancillary equipment.

Simplifying Assumptions and Justifications. The tank ancillary equipment is broadly separated into pipelines and MUSTs. The following simplifying assumptions were made for the contaminant release of residual wastes from the ancillary equipment:

- The contaminants within the tank farm ancillary equipment (residual waste) pipelines were assumed to be readily available for transport with the infiltrating water.
- Details on the distribution of tank farm pipelines within the WMA are ignored. For pipelines, the location of inventory in the numerical simulations was assumed to be represented by a homogeneous distribution at a depth of approximately 9 m (approximately 30 ft) and extending horizontally for approximately 7 m (approximately 25 ft). The contaminant release from other ancillary equipment (e.g., MUSTs) was assumed to be equivalent to release of tank residual wastes, as discussed in Section 3.2.2.3.2.

Again, the use of one contaminant distribution to represent all pipeline inventory sources within a given WMA is justified based on the results of previous analyses (e.g., Knepp 2002a). These analyses show that an assumed distribution has little effect on mass flux estimates because all contaminant inventories are contacted and migrate to groundwater at about the same rate. The use of a depth of 9 m (30 ft) to represent the inventories for pipelines is justified because nearly all such ancillary equipment is located just beneath the surface. The assumption that contaminants within pipelines are readily available for transport with the infiltrating water is expected to result in higher than expected concentrations in the groundwater. Also, the barrier that the piping currently provides to infiltrating water is neglected in the SST PA analysis.

The contaminants within the tank farm ancillary equipment (residual waste) pipelines were assumed to be readily available for transport with the infiltrating water. The release of contaminants within the MUSTs (residual waste) is modeled as a diffusional release.

While final closure plans have not been identified, plans for grouting of some ancillary equipment (MUSTs) are being discussed. The use of the residual tank waste model to represent the release of residual tank waste from MUSTs is believed to be representative of the MUST contaminant release. Differences between MUSTs and SSTs include: 1) the location of the available inventory in MUSTs is not as deep as the tank waste residuals inventory, 2) the footprint for each MUST is typically less than a tank footprint resulting in different shadow effects for recharge, and 3) the contaminant release from the MUSTs may have different values for A_t/V_t when compared to the waste tanks (Section 3.2.2.3.2).

3.2.2.4 Vadose Zone Moisture Flow and Contaminant Transport Considerations

As discussed in Chapter 1.0 with respect to defense in depth, the vadose zone beneath a WMA is considered a natural barrier. Once contaminants enter the vadose zone, the low recharge (infiltration rate) controlled by the surface cover, the thickness of the vadose zone between tank bottom and the unconfined aquifer, and the soil-contaminant interaction prevent all but the least reactive contaminants from reaching the unconfined aquifer for thousands of years.

3.2.2.4.1 Overview. This section provides an overview of major features that affect flow and transport within the vadose zone underlying a WMA. The transport of contaminants from their locations within the closed system to the groundwater is a complicated process that depends on data and assumptions made for the following physical systems:

- WMA structures
- Vadose zone beneath a WMA.

First, this section describes the WMA facility structures (Section 3.2.2.4.2) important to the SST PA methodology. This is followed by a description of vadose zone stratigraphy (Section 3.2.2.4.3), hydraulic properties (Section 3.2.2.4.4), and geochemical effects (Section 3.2.2.4.5) that impact contaminant transport. Next, an overview is presented of the vadose zone flow and transport numerical model used in the SST PA (Section 3.2.2.4.6). Finally, a detailed justification is provided of important assumptions and simplifications of the vadose zone flow and transport model (Section 3.2.2.4.7).

3.2.2.4.2 Waste Management Area Structures. Section 2.4 provides a description of the engineered systems and barriers common to the WMA. The physical system includes the closure barrier and the complex structures that make up the closed WMA. These structures include the tank structures and the ancillary equipment that includes piping, diversions boxes, and other systems that support tank farm operations. These complex structures impact not only the release of contaminants but also the flow of moisture through the system. Moisture is one of the major transport mechanisms for moving contaminants from the closed system to the groundwater. Within the shallow subsurface, moisture fluxes are non-uniform because grout-filled tanks divert moisture flow between the tanks and increase flow rates in these regions. The varying moisture fluxes, however, even out within the deep subsurface below the tanks.

For the conceptual model, the following simplifying assumptions were made:

- The impact of the closure barrier on moisture flow was approximated by an assumed recharge rate into the facility (Section 3.2.2.2).
- The impact of the tanks on moisture flow was handled by assuming that the tanks are impermeable structures that divert flow.
- Details associated with all ancillary equipment on moisture flow were neglected.

The justification for using an estimated recharge rate is provided in Section 3.2.2.2. Also, the justification for neglecting the structural impacts on contaminant release is discussed in Section 3.2.2.3.2. The long-term performance of the tank structures as hydraulic barriers to the flow of moisture within the closed system is not known. It can be hypothesized that eventually cracks will form in the concrete and the steel will degrade at some point in the future.

The tanks are modeled as impermeable structures that divert infiltrating water around the structure.

3.2.2.4.3 Vadose Zone Stratigraphy beneath Waste Management Areas. The vadose zone underlying tank farms consists of several heterogeneous layers of sedimentary units. The layers vary in thickness at different locations (Chapter 2.0). Also, the depth to the water table varies with location. The 200 West Area WMAs are distinguished from the 200 East Area WMAs primarily by the presence of a well-developed calcium carbonate-rich caliche layer (Plio-Pleistocene unit) that has been a relatively effective barrier to contaminant transport from past tank leaks in the vertical direction. Also, clastic dikes (anomalous, subvertical linear features composed of layers of differing particle size distributions) occur that extend up to tens of meters in length and can cross cut the major layers. These features are generally less than 1 m wide.

The geologic cross-section used in WMA C modeling is shown in Figure 3-3. The sedimentary sequences overlying the basalt beneath the WMA C are, from top to bottom:

- Backfill (sandy gravel)
- Hanford formation – upper gravelly sequence (H1 unit, gravelly sand)
- Hanford formation – sand sequence (H2 unit, sand)
- Hanford formation – lower gravelly sequence (H3 unit, gravelly sand)
- Undifferentiated Plio-Pleistocene unit gravel (PPlg) and/or Ringold Formation Unit A [PPlg/(R) unit].

The geologic cross-section used in WMA S-SX modeling is shown in Figure 3-4; the numbers noted with each geologic unit in Figure 3-4 are the material type numbers used for modeling purposes. The sedimentary sequences, from top to bottom, are:

- Backfill (sandy gravel)
- Hanford formation – upper gravelly sequence (H1 unit, gravelly sand)
- Hanford formation – sand sequence (H2 unit, sand)
- Plio-Pleistocene unit – silty very fine sand to sandy silt
- Upper Ringold Formation – sand-dominated facies consisting of slightly silty coarse to medium sand
- Ringold Unit E – Ringold Formation comprising the vadose zone and upper part of the unconfined aquifer consists of slightly silty coarse- to medium-grained sandy gravel with intercalated gravelly sand.

3.2.2.4.4 Hydraulic Properties. Even though no site-specific data are available on soil moisture characteristics for tank farm sediments, data catalogs are available for 200 Areas soils. For this work, data on laboratory measurements for moisture retention, particle-size distribution, saturated and unsaturated hydraulic conductivity, and bulk density for individual stratum were based on data for similar soils in the 200 East and 200 West Areas. Details on vadose zone flow and transport properties are provided in various data package reports (*Modeling Data Package for an Initial Assessment of Closure of the C Tank Farm* [Khaleel et al. 2006a] and

Modeling Data Package for an Initial Assessment of Closure of the S and SX Tank Farms [Khaleel et al. 2006b]). For each stratum defined by the stratigraphic cross-sectional model, the small-scale laboratory measurements were upscaled to obtain equivalent horizontal and vertical unsaturated hydraulic conductivities as a function of mean tension (Khaleel et al. 2002). In addition, to reflect field conditions, the laboratory-measured moisture retention data were corrected for the presence of any gravel fraction in the sediment samples (Khaleel and Relyea 1997). As with flow modeling, each stratum was modeled with different transport parameters (i.e., bulk density, diffusivity, and dispersivity). See Section 3.4.4 for additional details on the equations for hydraulic properties and parameters used for the flow and contaminant transport calculations.

3.2.2.4.5 Geochemical Effects. Contaminant migration rates are element-specific because of the varying degrees of their chemical reactivity with soils (Krupka et al. 2004). Some contaminants are largely non-sorbing (i.e., technetium) and migrate with recharge water. Others are highly reactive and migrate very slowly (i.e., cesium).

Chemical reactions that occur when contaminants interact with soil solid phases and retard contaminant migration relative to water flow through the vadose zone are represented by single sorption (K_d) values (Section 3.2.2.4.7). Different K_d values are considered for particular contaminants, but only over a limited range (0 to 5 mL/g). The K_d value is the ratio of contaminant mass attached to soil solids versus mass dissolved in solution. The advantage of this approach is that K_d values can be easily incorporated in modeling transport. The disadvantage is that K_d values are entirely empirical and are used to represent many different kinds of chemical reactions that are dependent on the contaminant of interest, the soil solid phases present in the vadose zone, and the soil water chemistry. The effects of physical variables (moisture content and gravel fraction) and reactions (colloid formation and migration) are also incorporated in the K_d concept.

Figure 3-3. Northwest-Southeast Cross-Section through Waste Management Area C

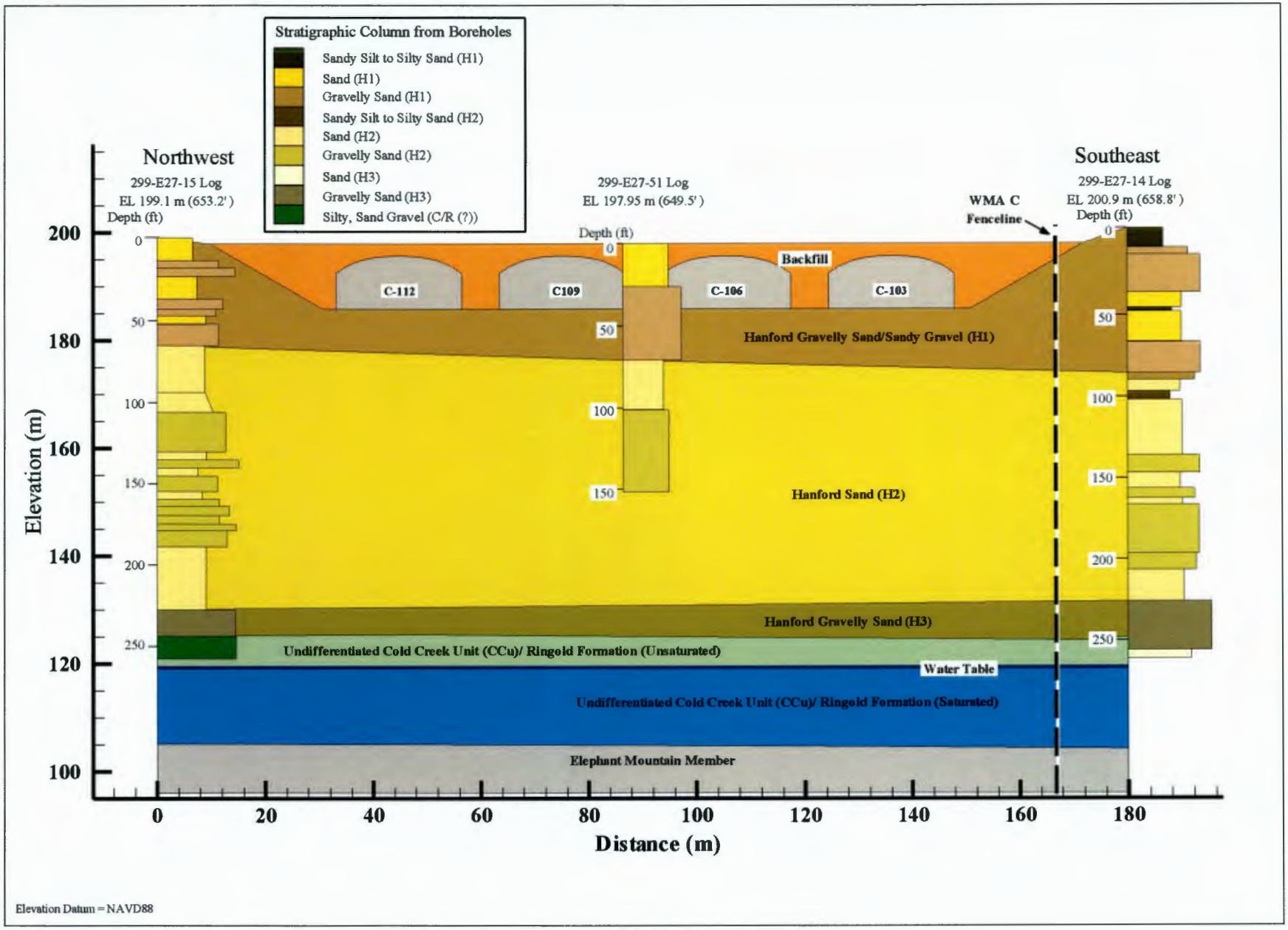

Figure 3-4. West-East Cross-Section through Waste Management Area S-SX

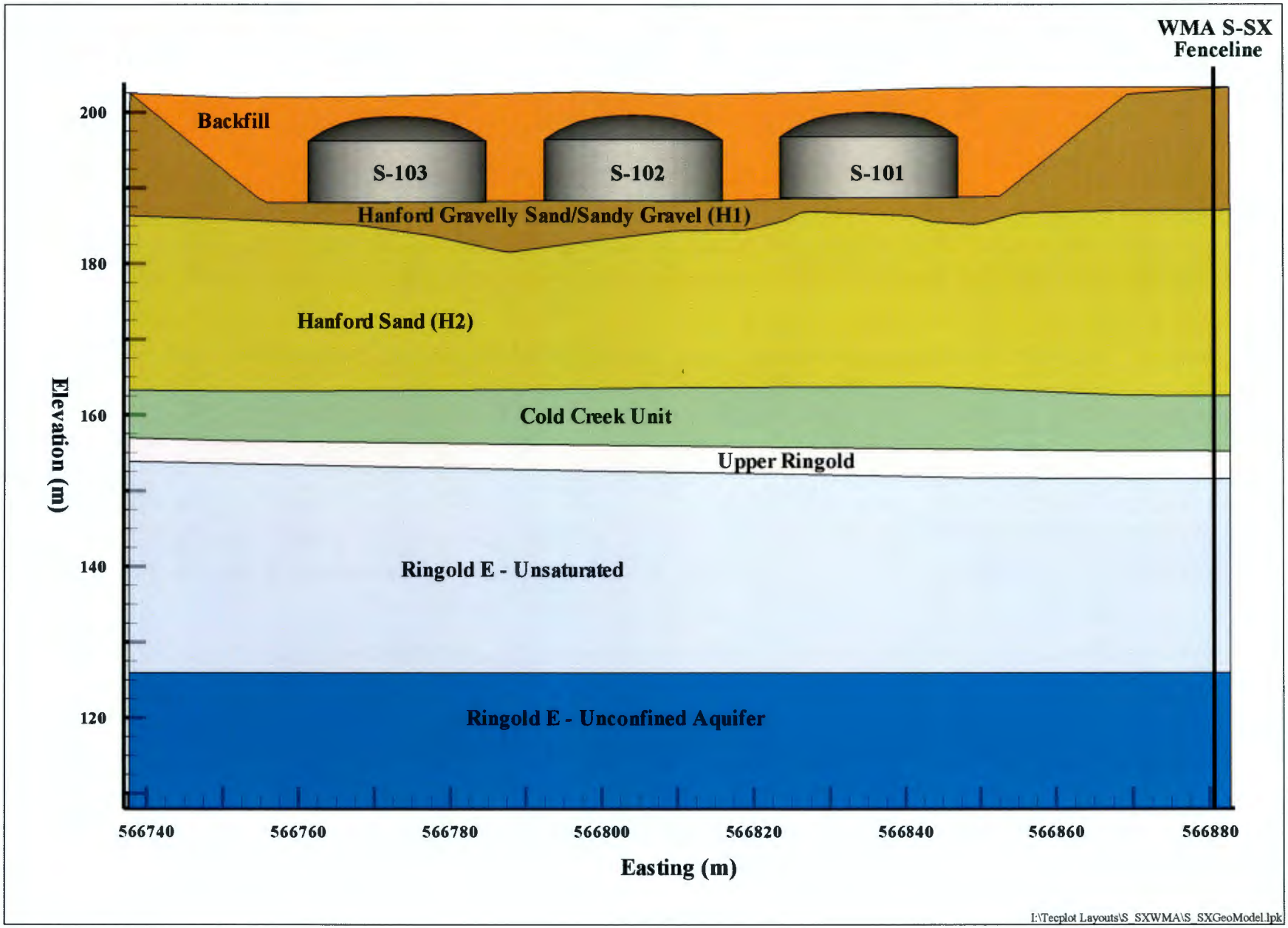

Despite its limitations, the empirical approach is considered adequate for several reasons. A range of K_d values can be derived for any contaminant discharged into the subsurface underlying the WMAs because contaminant reactivity with the subsurface system is dependent on the chemical nature of the contaminant and the ambient geochemical environment. If the geochemical environment remains fairly stable and can be simulated in the laboratory, a reproducible database can be developed to measure a range of K_d values that is reliable, regardless of the exact chemical reactions controlling observed behavior. Numerous analyses of undisturbed vadose zone soils and water chemistry at many locations in and around the WMAs have defined a consistent geochemical environment (Section 3.2.2.4.7). A long history of experimental work (Section 3.4.4.1.3) has provided an extensive database that has measured the reactivity of numerous contaminants under site-specific geochemical conditions characteristic of the ambient vadose zone. From this database, bounding ranges of K_d values have been developed for many contaminants of interest (Section 3.4.4.1.3).

Finally, for past releases and potential future leaks, the contaminant migration is assumed to be controlled by the current ambient geochemical environment. For past releases, the contaminant distribution in the soils was driven by the addition of tank waste into the vadose zone with chemical properties quite different from ambient soil water. Tank fluid properties (e.g., high salt content, high heat) influenced water and contaminant migration in the vadose zone near the source of release temporarily (Appendix D of Knepp 2002a). At the SX tank farm, for example, tank leaks containing hot, caustic, saline solution (8 to 10 molar sodium at 350°F or more) occurred. Cesium-137 mobility was thus greatly enhanced because high sodium content in the tank fluid pre-empted sorption sites causing cesium to migrate deeper than usual within the vadose zone (Appendix D of Knepp 2002a). Recent field characterization studies show that while these contaminants were mobilized shortly after the tank leak, their current state of mobility is consistent for ambient conditions. For example, desorption experiments and solids characterization data from recent characterization borehole sediments (e.g., Knepp 2002a) show that cesium-137, strontium-90, and uranium are now largely immobile in vadose zone soil. The potential for enhanced mobility for contaminants associated with past releases has been considered in these analyses through the use of effective K_d values associated with chemically impacted soils (pore water chemistry having high pH). See Section 3.4.4 for additional details on the geochemical model and parameters used for the flow and contaminant transport calculations.

3.2.2.4.6 Vadose Zone Flow and Transport Numerical Model. A two-dimensional flow and transport numerical model along a row of tanks was used for the integrated vadose zone-unconfined aquifer vertical cross-section. To account for three-dimensional aspects, the tank centerline mass flux and BTCs were transformed to average values across the tank farm fenceline on the basis of comparison of three- and two-dimensional results; the comparison evaluated the peak to peak comparison of contaminant concentrations for a long-lived mobile radionuclide (Zhang et al. 2004). See Section 3.2.2.4.9 for additional details.

The two-dimensional numerical model for WMA C assumes that the groundwater flow beneath the WMA is parallel to tank row C-103, C-106, C-109, and C-112. This flow direction is assumed to be consistent with the post-Hanford unconfined aquifer hydraulic gradient. Similarly, the two-dimensional numerical model for WMA C assumes that the groundwater flow

beneath the WMA is parallel to tank row S-101, S-102, and S-103. This flow direction is assumed to be consistent with the post-Hanford unconfined aquifer hydraulic gradient.

As discussed earlier, for past releases, the vadose zone flow and transport model does not model the release event itself but uses the contaminant footprint as an initial condition for modeling past releases. A further discussion on the use of contaminant footprint in modeling is presented in Section 3.2.2.4.7.

The vadose zone simulations were composed of steady-flow and transient components, where flow fields developed from the steady-flow component were used to initialize the transient simulation. Steady-state initial conditions (that represent pre-Hanford Site operations) were developed by simulating from a unit hydraulic gradient condition to a steady-state condition, dictated by the initial meteoric recharge at the surface, water table elevation, water table gradient, no flux vertical boundaries, distribution of hydrologic properties, and location of impermeable tanks.

Simulations already completed in support of WMAs C and S-SX closure risk assessments are used as templates for other WMAs in the 200 East and 200 West Areas, respectively. That is, the relatively slight differences in geology between tank farms in a given part of the 200 East Area or 200 West Area are ignored. Also, this approach assumes that the post-closure groundwater flow direction for the other WMAs is predominately from west to east and parallel to the tank rows oriented in that direction. See Section 3.2.2.4.8 for a discussion on the justification for this approach. Future versions of this SST PA will perform vadose zone calculations based on site-specific data for other WMAs.

The steady-flow simulation, representing flow conditions for the year when a tank farm construction is completed (e.g., 1945 for C tank farm and 1952 for S tank farm), was used as the initial condition for all subsequent flow and transport simulations.

Transient conditions were conducted for the period from the time of tank farm construction to the year 2000, followed by a 10,000-year closure period (i.e., years 2032 to 12032) that involved changes in the flow fields in response to current conditions, placement of closure barrier, and effects of a degraded barrier. The infiltration (recharge) estimates for various times are described in Section 3.4.2.

An equivalent porous continuum model (Section 3.2.2.4.7) is assumed; fluid flow within the vadose zone is described by Richards' equation (Jury et al. 1991). The contaminant transport is described by the conventional advective-dispersive transport equation with an equilibrium linear sorption coefficient (K_d) formulation. A further justification for using a linear isotherm model is presented in Section 3.2.2.4.7. A series of mobile to moderately retarded contaminant species (K_d = 0, 0.02, 0.1, 0.2, 0.6, 1.0, 2.0, and 5.0 mL/g) were calculated for each run. The use of a suite of distribution coefficients allows for application of simulated results to a wide range of contaminants of concern (CoC). No temperature effects are considered for the vadose zone model (i.e., the model used is isothermal) (Section 3.2.2.4.7).

The vadose zone model considers the ubiquitous lateral flow in 200 Areas. As is evident from a large number of field observations in the 200 Areas: 1) lateral movement of water and

contaminants is usually significant if the medium is stratified (as in the 200 Areas), 2) the initial moisture content is low, 3) the size of the application area is small relative to the size of the unsaturated zone, and 4) the application rate is small (Gelhar et al. 1985). Further details are provided in Section 3.2.2.4.7.

A key assumption in the modeling is that each of the three contaminant sources can be modeled separately and that temporal and spatial superposition can be used to estimate the cumulative impacts from different contaminant sources for each WMA. Detailed justification for superposition as well as for other assumptions used in modeling are presented in Section 3.2.2.4.7.

3.2.2.4.7 Justification for Flow and Transport Models Used. An understanding of the transport behavior of what has already leaked and how rapidly it is moving in vertical, as well as in lateral, directions within the vadose zone is useful in developing conceptual models for contaminant transport from all sources within a WMA. Based on extensive site characterization and field data, the vadose zone flow and transport model used in the SST PA incorporates a number of important characteristics. These include:

- Use of an equivalent porous continuum model
- Contaminant footprint as an initial condition for past releases
- Ubiquitous lateral flow
- Use of an isothermal model
- Use of a linear isotherm K_d model
- Use of superposition.

As discussed earlier, results from a separate task established a basis for the vadose zone conceptual model used in the SST PA. The results of this effort are described in Ye et al. (2005) and in Yeh et al. (2005). As discussed in Yeh et al. (2005), the simulated moisture plume does reproduce the general behavior of the observed moisture plume at the field site. Spatial moments of the simulated plume based on the effective hydraulic conductivities are in reasonably good agreement with those for the observed plume (Figure 3 of Yeh et al. 2005).

Use of an Equivalent Porous Continuum Model. To describe the bulk (or mean) flow behavior, each heterogeneous formation (e.g., gravelly sand unit in Figure 3-3) was replaced by its homogeneous equivalent, and effective or upscaled flow parameters were used to represent the homogeneous equivalent. Each formation unit was assigned different hydraulic properties. The laboratory-measured hydraulic properties were upscaled. Upscaling accounts for the fact that the numerical modeling applies to a scale that is much larger than the core scale at which laboratory measurements are available. As will be explained in Section 3.4.4.1.2, saturation-dependent anisotropy relationships (Polmann 1990) were invoked in recognition of field data from controlled and uncontrolled experiments that clearly show the dominant effect of lateral flow for the highly heterogeneous vadose sediments at the Hanford Site.

Each heterogeneous geologic unit within the vadose zone is replaced by its homogeneous equivalent (see Figure 3-3 for WMA C and Figure 3-4 for WMA S-SX). Each geologic unit is assigned its upscaled hydraulic properties.

The vadose zone flow and transport simulations were based on the porous continuum modeling assumption. Such an assumption is supported by field data on moisture and contaminant plumes at various controlled and uncontrolled experiment sites. The most likely "fast flow" path in Hanford sediments is due to presence of clastic dikes (Figure 3-5) that often cross cut sedimentary units, especially in the Hanford formation. The dikes are ubiquitous sedimentary structures observed in outcrops and trenches that expose the Hanford formation in the 200 Areas (Fecht et al. 1999). These are believed to represent dewatering structures that developed during compaction and settling of cataclysmic flood deposits during or soon after floodwaters drained from the Pasco Basin. The dikes are of particular interest because they occur as near-vertical tubular bodies filled with multiple layers of unconsolidated sediments. There is very little evidence, however, to indicate that they extend all the way from near the ground surface to the water table.

In general, the hydraulic properties of clastic dikes can be considered essentially as a subset of the porous matrix properties for the Hanford sediments. This is based on laboratory measurements of clastic dike samples. In general, clastic dike sediments represent properties of fine sediments such as fine sand, silt, and clay, and can therefore represent regions of high moisture content (Murray et al. 2003). Under unsaturated flow conditions, however, the dikes can act as a barrier to flow rather than as fast flow channels. For example, if the clastic dikes were filled with gravelly sediments (with large pore sizes), it is *not* feasible, for the following reasons, to have a scenario under unsaturated conditions where the bulk of the flow is through the dikes.

- The porous matrix has a much smaller average pore size than the gravelly media within the clastic dike.
- For the moisture regime under low recharge conditions, the gravelly sediments with a larger pore size than the surrounding porous matrix will have a limited ability to hold moisture, and the fluid will be attracted primarily to the porous matrix. The conceptual model schematic in Figure 3-6, where the bulk of the flow bypasses the media with large pore sizes under unsaturated conditions, illustrates this scenario.

Figure 3-5. Infilled Sediments within Clastic Dikes [a]

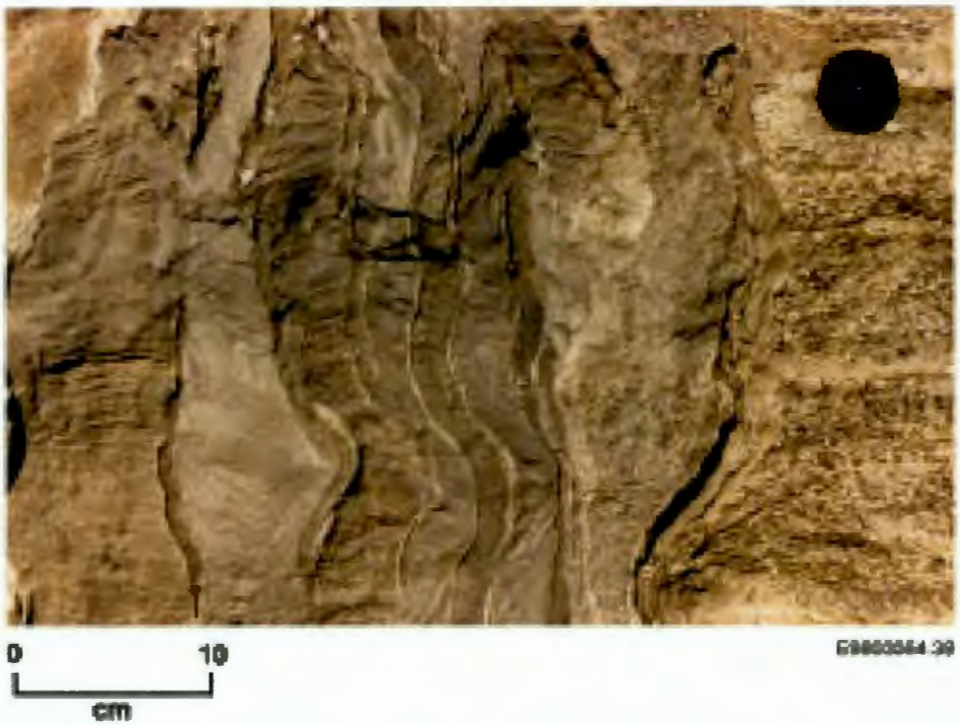

[a] *After (Fecht et al. 1999)*

The middle portion of the two figures above show the infilled sediments within a dike; the host sediments are shown on the left and right edges of the two figures.

Figure 3-6. Conceptual Model of Fracture Flow under Unsaturated Conditions [a]

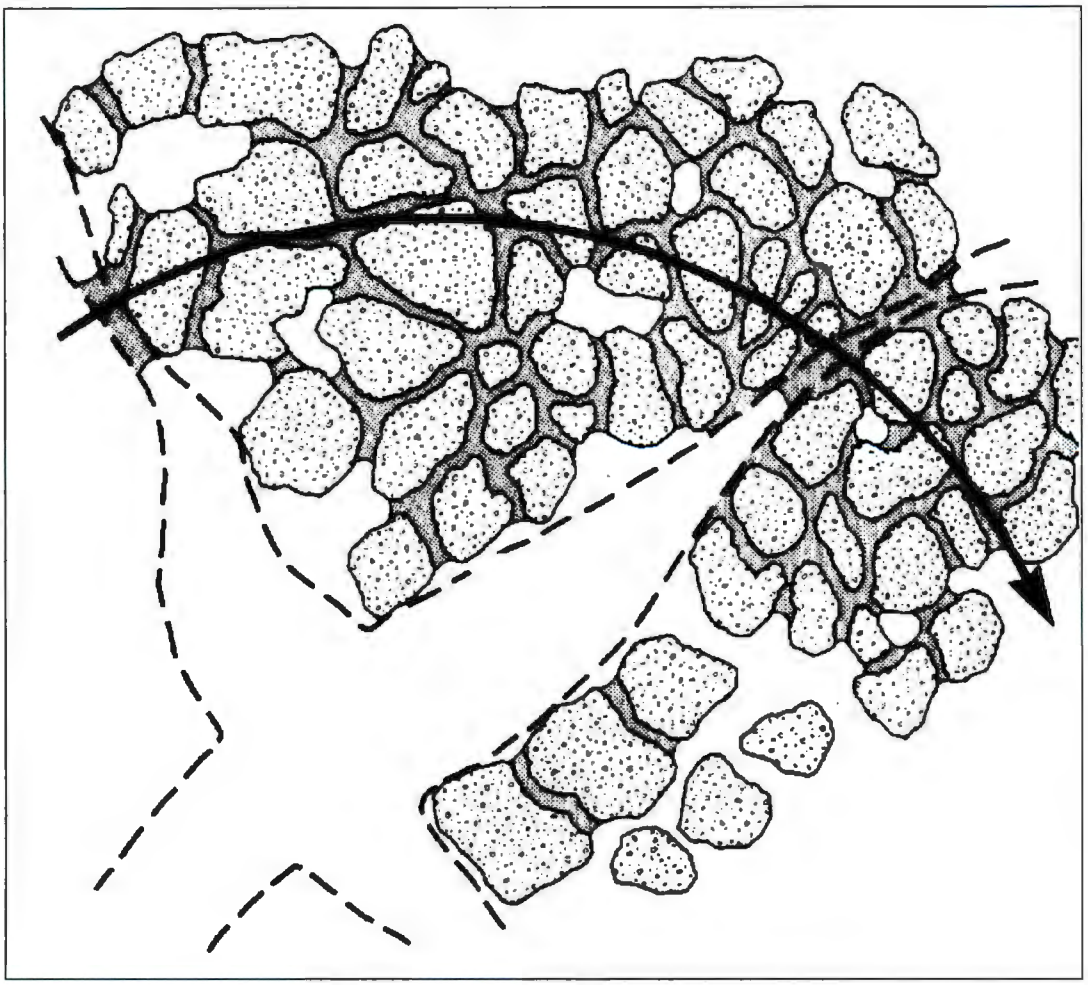

[a] *After Wang and Narasimhan (1985)*

The expanded vertical slice illustrates the fact that under unsaturated conditions and low recharge, the bulk flow bypasses the pathway formed by larger pore sizes and essentially follows the pathway formed by smaller pore size network. The large, open spaces in the figure mimic large pores such as those in a gravelly medium.

Thus, while clastic dikes do exist, it is less likely to intersect large segments of leaked wastes, and, when it does, the cross-sectional area of the intersection is small. Therefore, the presence of clastic dikes in unsaturated media appears unlikely to contribute much to the transport of the bulk quantity of leaked wastes and to long-term risk relative to higher peak concentrations for long-lived mobile radionuclides in groundwater. This is supported by the WMA S-SX FIR simulation results (Knepp 2002a).

The numerical results are also supported by studies reported elsewhere. These studies suggest that although preferential flow has been recognized and widely studied under saturated or near-saturated flow conditions (Nkedi-Kizza et al. 1983; De Smedt and Wierenga 1984), there is little evidence of it in arid and semiarid climates or under low water fluxes, particularly where soils are coarse-grained, such as those under the tank farms. Thus, under natural recharge

conditions, precipitation at arid sites is usually too low (in relation to saturated hydraulic conductivity) to invoke preferential flow; much of the water in the dry soils is simply adsorbed onto the grain surfaces and cannot move along preferred pathways.

Contaminant Footprint as an Initial Condition for Past Releases. For past releases, a leak itself is not modeled; rather, a representative footprint of the vadose zone contamination was used as the initial condition for modeling liquid flow. At the SX tank farm, for example, tank leaks occurred that contained hot, caustic, saline solution of 8 to 10 molar sodium at 350°F or more. As discussed earlier, such chemical perturbations were most significant at the time of the leak event and shortly thereafter and at locations closest to the leak origin. However, the chemical buffering capacity of soil eventually overcomes tank chemistry influence, and releases are controlled by the ambient geochemical environment. The current far-field physical, thermal, and chemical behavior of the contamination footprint is considerably different from the near-field physical, thermal, and chemical behavior in the vicinity at the time of a tank leak and approaches conditions closer to the deeper, undisturbed vadose zone. The use of the contaminant footprint as an initial condition therefore provides an attractive alternative to long-term modeling of actual tank leak events in a WMA. Further details on use of such a modeling approach are presented in Section 3.2.2.4.5.

Ubiquitous Lateral Flow. The highly heterogeneous nature of Hanford sediments is indeed very effective in smearing out the effects of large natural or manmade applications. This is best illustrated by the moisture content profiles (Ye et al. 2005; Yeh et al. 2005) at the controlled field injection experiment (the Sisson and Lu site) in the 200 East Area in the vicinity of WMA C. The site was used for an infiltration test in the year 2000 (Gee and Ward 2001). Water content distribution was measured on May 5, 2000, at the 32 radially arranged cased boreholes. Injections began on June 1 and 4,000 L of water were metered into an injection point (point source) 5 m below the land surface over a 6-hour period. Similarly, 4,000 L of water were injected in each subsequent injection on June 8, June 15, June 22, and June 28. During the injection period, neutron logging in 32 wells took place within a day following each of the first four injections. A wildfire burned close to the test site and prevented immediate logging of the moisture content distribution for the fifth injection on June 28. Three additional readings of the 32 wells were subsequently completed on July 7, July 17, and July 31. During each neutron logging, water contents were monitored at 0.305-m (12-in.) depth intervals starting from a depth of 3.97 m and continuing to a depth of 16.78 m, resulting in a total of 1,344 measurements for the eight observation times over a 2-month period. The moisture content profiles, as shown in Figure 3-7, clearly illustrate significant lateral spreading. As indicated in Figure 3-8, the pre- and post-injection moisture plumes are essentially confined within three layers (i.e., two fine-textured layers and a coarse-textured layer that is sandwiched in between the two fine-textured layers). Such behavior of the moisture plume is related to the moisture-dependent anisotropy phenomenon (Ye et al. 2005; Yeh et al. 2005). Such field-scale processes are included in the modeling.

The preponderance of lateral migration is also evident elsewhere. The 241-T-106 tank leak (115,000 gal) is the largest known tank leak at the Hanford Site. The leak occurred in 1973 at a corner of the tank. Figure 3-9 shows the 1993 technetium-99 profile in borehole 299-W10-196 in the vicinity of the tank leak (Freeman-Pollard et al. 1994). The vadose zone profile clearly shows that even after 20 years of migration, the contaminant peak concentration for the

long-lived mobile radionuclide is contained primarily within the fine-textured horizons at a depth of 35 to 40 m bgs and well above the water table. These field data suggest that the natural heterogeneity of the Hanford sediments plays an important role on flow and transport, and the significant lateral transport, which is in fact induced by media heterogeneities, is highly effective in containing plumes within the vadose zone for an extended period. A further corroboration of this phenomenon is evident at the 216-B-26 trench site in the 200 East Area. The BC cribs and trenches received nearly 30 Mgal of scavenged tank waste with possibly the largest inventory of technetium-99 ever disposed to soil at the Hanford Site. There is no evidence of groundwater contamination yet. In fact, field measurements suggest that, because of significant macroscopic anisotropy that is induced by media heterogeneities, the bulk of the technetium plume is concentrated within the fine-textured sediments at a depth of 30 to 35 m bgs almost 50 years after the high-volume discharge (Rucker and Sweeney 2004).

Thermal Effects and Use of an Isothermal Model. It should be noted that since the tanks contained large volumes of radioactive material, the heat generated by the decay of those radioactive materials heat the surrounding soil (Appendix D of Knepp 2002a). All simulations, nonetheless, were run using an isothermal model. The isothermal assumption is supported by a comparison of simulation results for non-isothermal and isothermal runs that appeared in Appendix D of Knepp (2002a).

Non-isothermal model simulations indicate that during periods of high-heat loads in the 1950s and 1960s, the thermal load from the boiling waste tanks altered flow patterns and caused large-scale redistribution of moisture. As a result, fluid and vapor flow near the high-heat tanks was dominated by vapor-liquid counterflow. Therefore, to understand the historical behavior, it is important to consider the strong coupling between the thermal and hydrologic environments. However, for impact assessment on the basis of the current thermal conditions in tank farms, long-term simulations on migration of long-lived mobile radionuclides were not significantly different for isothermal and non-isothermal conditions (Knepp 2002a).

Use of a Linear Isotherm K_d Model. As discussed earlier, no thermodynamically based conceptual or numerical models are presently available that are robust enough to accurately predict the degree of contaminant adsorption by undisturbed and disturbed sediments. The vadose zone conceptual model uses an empirical distribution coefficient, K_d, (or linear isotherm) to represent contaminant adsorption for relatively immobile contaminants (e.g., uranium). An inherent drawback of the K_d approach, of course, is its empirical nature. However, a considerable database of Hanford-specific K_d measurements is available (Krupka et al. 2004) for a variety of geochemical conditions and contaminants. For the expected concentrations of contaminants in the far field away from the near-field region of a tank leak, sorption can be considered to be independent of contaminant concentration and, therefore, K_d is assumed to be a constant for a given sediment-contaminant combination (Krupka et al. 2004). Therefore, given the extensive "empirical" database of site-specific conditions, the use of the K_d approach is considered to be a useful and valid approach for modeling contaminant adsorption for long-term risk assessments such as the SST PA. This approach has been used extensively in other risk assessments (Wood et al. 1995a, 1996; Mann et al. 2001; Knepp 2002a, 2002b).

Figure 3-7. Moisture Content Profiles for the Field Injection Experiment in the 200 East Area [a]

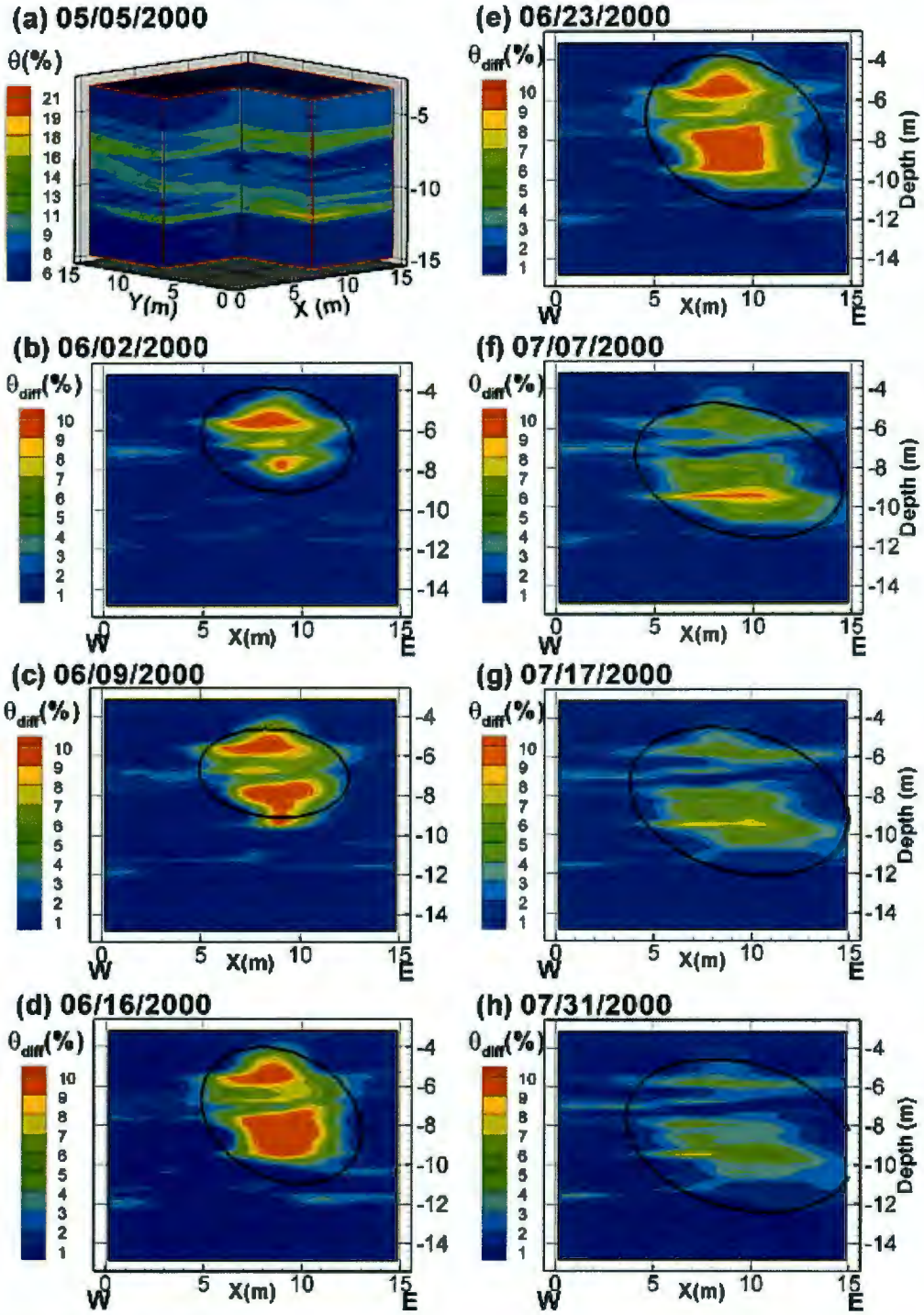

[a] *After Ye et al. (2005)*

(a) Initial moisture content on May 5, 2000, and (b) through (h) are east-west trending cross-sectional views of moisture content (θ) differences (measured θ – initial θ) along the plane passing through the injection well. The solid curves are the fitted ellipsoids.

Figure 3-8. Pre- and Post-Injection Moisture Plumes for the Field Injection Experiment in the 200 East Area [a]

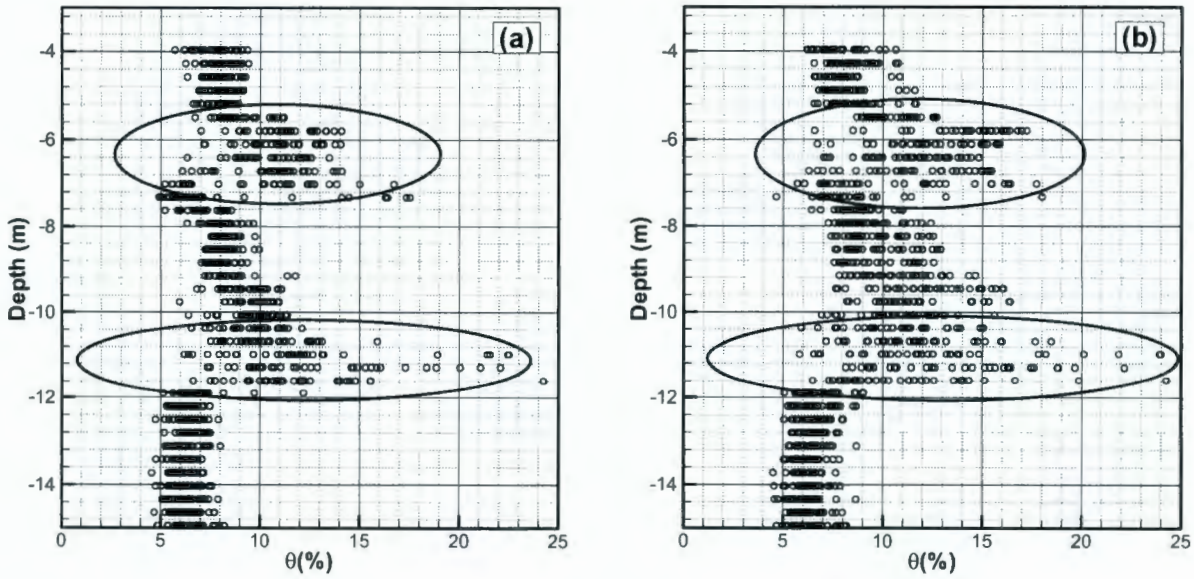

[a] *After Ye et al. (2005)*

Profiles of moisture content (%) measured on (a) May 5, 2000, and (b) July 31, 2000. The figures illustrate the fact that, in the absence of manmade injections, moisture contents at the field site are in equilibrium with natural recharge at the site.

Figure 3-9. Technetium-99 Profile in Borehole 299-W10-196 from 241-T-106 Tank Leak [a]

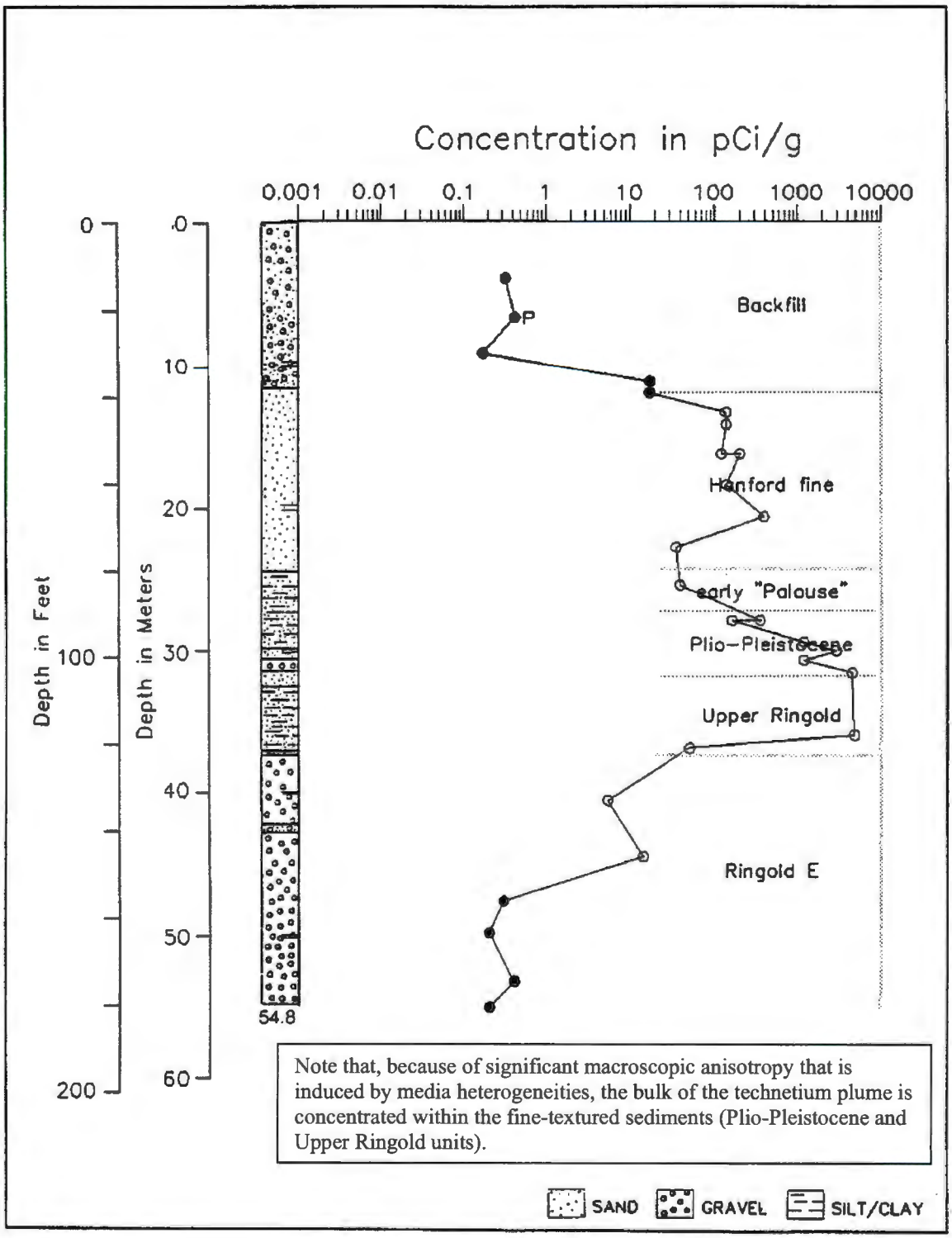

[a] *After Freeman-Pollard et al. (1994)*

Use of Superposition. A key assumption for the SST PA calculations is that each of the three contaminant sources can be modeled separately, and that temporal and spatial superposition can be used to estimate the cumulative impacts from different contaminant sources for each WMA. The assumption that different sources can be modeled separately implies that the contaminant release and transport for each source is independent from one another. This assumption is plausible because the past releases are modeled at locations beneath the tank and ancillary equipment waste residuals; the release models for these releases assume that the contaminants are available for transport with the infiltrating moisture. This assumption also assumes that the chemical adsorption of contaminants from one source is not impacted by another contaminant source within the WMA. This second assumption has not been substantiated. Geochemistry studies have indicated that high pH in the pore water can impact the K_d associated with contaminant transport through the vadose zone (Krupka et al. 2004). This potential impact needs to be addressed in future revisions to the SST PA. As a first approximation, the magnitude of this effect has been investigated in the sensitivity cases that look at minimum and maximum K_d values for CoCs (Section 3.5.3.4)

For each contaminant source in a WMA, the principle of spatial and temporal superposition is used to obtain a composite contaminant breakthrough curves at the WMA fenceline for all sources (Section 3.2.2.4.7).

3.2.2.4.8 Extrapolation of WMA C and WMA S-SX Results to Other WMAs.

As indicated earlier, the numerical simulations were not performed for all tank farm WMAs. Detailed simulations were conducted for all three source terms for WMA C and WMA S-SX in the 200 East and 200 West Areas, respectively. Results based on numerical simulations performed for WMA C were used as a template for other 200 East Area farms, and results from WMA S-SX were used as a template for results for other farms in 200 West Area. Specifically, the BTCs for WMA C and WMA S-SX provided inventory normalized concentrations in the groundwater at the WMA fenceline for each contaminant source (i.e., past releases, tank residuals, and ancillary equipment residuals). To estimate the concentrations for each tank row in any WMA, the appropriate inventories associated with the contaminant sources for that tank row were multiplied by the appropriate BTC for that WMA (200 East or 200 West Area) and source term to obtain the contaminant concentration for that source term and tank row.

This approach for estimating the impacts from other tank rows in other WMAs is considered reasonable at this time for the following reasons:

- The general stratigraphy in the 200 West Area is similar for other WMAs in that area. The general stratigraphy in the 200 East Area is similar for other WMAs in that area as depicted by the fence diagram for each WMA in Chapter 2.0. (A major impact on simulation is the lateral migration of the contaminant plume within the vadose zone.)
- The distance to the groundwater for each WMA in the 200 West Area is approximately the same; similarly, the distance to the groundwater for each WMA in the 200 East Area is approximately the same. (A major impact on simulation is transport time for contaminant plume to the aquifer.)

- The sediment-contaminant distribution coefficients (K_d) for soils on the 200 Area plateau appear to be independent of location. (A major impact is retardation of transport times for contaminants with non-zero K_d values.)
- The hydraulic properties of the 200 West Area aquifer are similar beneath each WMA in that area; similarly, the hydraulic properties of the 200 East Area aquifer are similar beneath each WMA in that area. (A major impact is dilution of the contaminant flux at downgradient locations.)

A major impact neglected in extrapolation of WMAs C and S-SX results to other WMAs is the orientation of the groundwater flow with respect to the conceptual models for different WMAs.

3.2.2.4.9 Accounting for the Third Dimension. The model used to describe flow and transport up to the fenceline is an integrated two-dimensional, saturated-unsaturated, vertical cross-section along a row of tanks. Although the simulations in this analysis are two-dimensional, in reality, flow and transport from any source type will occur in three dimensions. Because of the long simulation times, simulating three-dimensional processes is not insignificant. Although two-dimensional (x-z; with x = horizontal dimension and z = vertical dimension) simulations have shorter run times, the absence of flow and transport in the third (y) dimension translates into higher concentration predictions. Therefore, results from two-dimensional simulations need to be translated into equivalent values for a three-dimensional domain to better predict contaminant concentrations in the groundwater; such a relation is not known a priori.

To evaluate the impact of the third dimension, an identical two-dimensional case was simulated in three dimensions (Zhang et al. 2004). This case scenario involved a hypothetical leak of 4,000 gal at the lower-right corner of tank S-103 that began on the first day of the year 2000. The leak was set to last for 14 days (Khaleel et al. 2006b) and contained a unit release of technetium-99 and uranium-238. The main difference between the two-dimensional and three-dimensional simulations was the thickness of the simulation domain in the horizontal direction (y direction) perpendicular to the flow direction. In the two-dimensional simulation, a unit width (1 m) was used. In three-dimensional simulations, the width was 153 m discretized into 3-m units. Hence, water and contaminant migration occurred in the y direction for the three-dimensional simulation, whereas it was absent in the two-dimensional simulation.

To examine the relationship between the concentrations for the two simulations, the fenceline aqueous concentrations of technetium-99 and uranium-238 with K_d = 0.03 mL/g were evaluated along the y direction for the three-dimensional simulation when the peak concentrations occurred (Zhang et al. 2004). Figure 3-10 shows that the highest concentrations occurred at the centerline of tanks S-101, S-102, and S-103 (y = 125 m), and as the distance from the tank centerline increased, the concentrations decreased. The concentration along the y direction was nearly symmetrical along the centerline of the tank. Approximately 99.4% of technetium-99 and 98.3% of uranium-238 were within 20 m of the centerline of the tank (from 105 to 145 m). Therefore, co-mingling of plumes (Figure 3-10) between rows is assumed to be negligible because the results of the three-dimensional simulation indicated that 99% of the contaminants remained within 20 m of the plume centerline.

Figure 3-10. Results on Co-mingling of Plumes Based on Three-Dimensional Simulations [a]

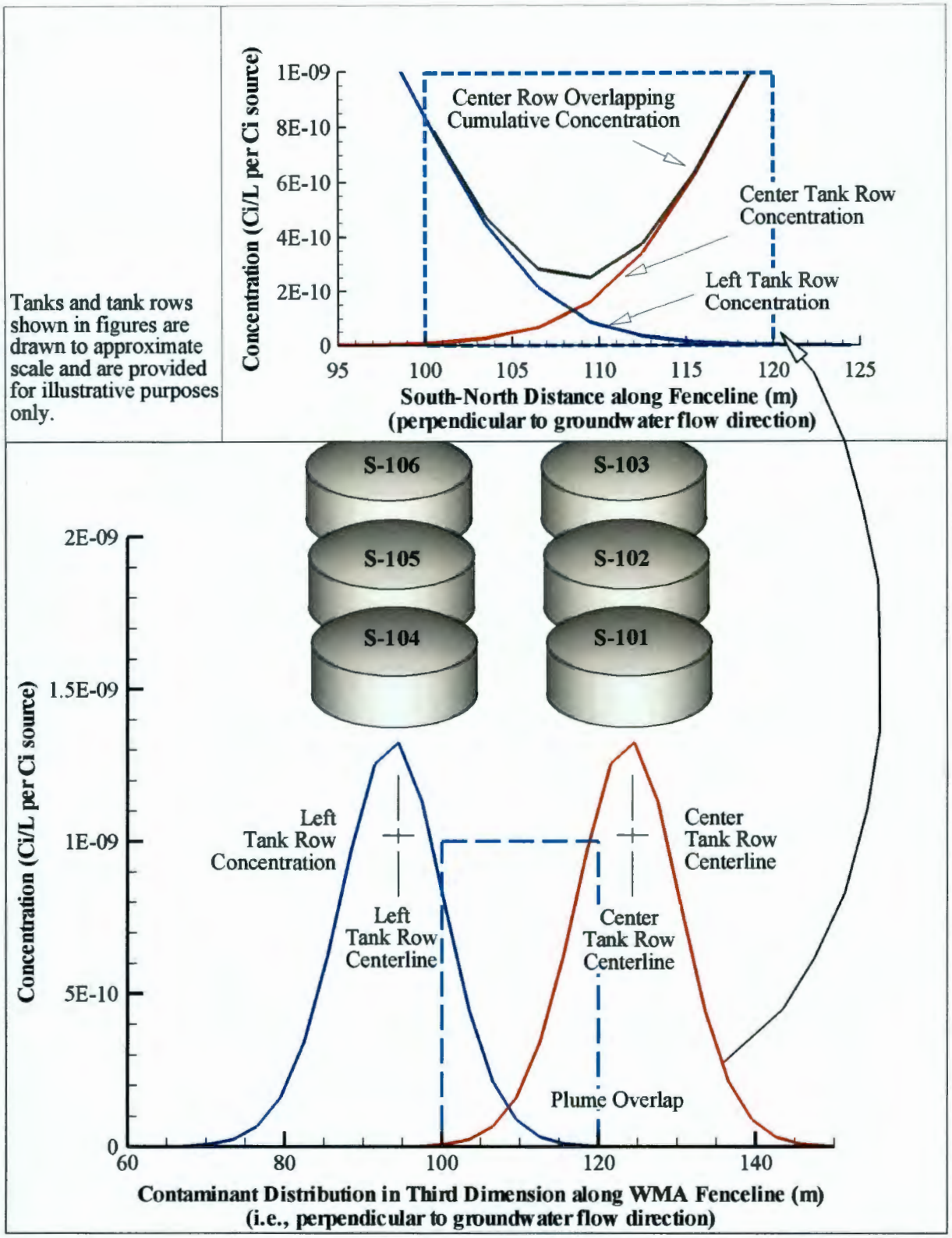

[a] *After Zhang et al. (2004)*

For both technetium-99 and uranium-238, the shape of the BTCs from the two-dimensional simulations was very similar to those from the three-dimensional simulations (Zhang et al. 2004). The ratio of the two-dimensional (C_{2d}) and three-dimensional (C_{3d}) peak technetium-99 concentrations was 41.1. The C_{2d}/C_{3d} ratio for uranium-238 with K_d = 0.03 mL/g was 36.6. The arrival time of the of the technetium-99 peak concentration from the two-dimensional simulation was 14 years earlier than that from the three-dimensional simulation. For uranium-238 with K_d = 0.03 mL/g, the arrival times of the first and second peak concentrations from the two-dimensional simulation were respectively 36 and 342 years earlier than those from the three-dimensional simulation.

Based on the preceding results on a minimum co-mingling of BTCs for adjacent row of tanks and the presence of an adequate separation distance for BTCs from neighboring tank rows, no summation of BTCs at the WMA fenceline for all tank rows was necessary to obtain the composite curve. This is because the BTCs for individual rows tracked different flow lines. The fenceline BTC that produced the maximum concentration among all tank rows was thus used as the composite BTC for a given WMA at its fenceline.

3.2.2.5 Estimated Human Health Risks

Unit health effects factors provided in Rittmann (2004) were used to convert the predicted groundwater contaminant concentrations into the estimated impacts of interest for this analysis. A unit health effects factor is a scenario- and contaminant-specific factor that provides the health effects per unit contaminant concentration in groundwater (e.g., all-pathways farmer dose and ILCR per pCi/L for radionuclides, ILCR and HI per mg/L for non-carcinogenic chemicals). Formulas and data used in calculating the factors are presented in Rittmann (2004). The beta and photon emitter dose from groundwater was calculated using unit dose factors based on an exposure of 4 mrem/yr to the maximally impacted organ. These unit dose factors were derived by dividing the 4 mrem/yr dose by MCLs provided in EPA guidance (EPA 2000a). Values for each metric were calculated by first multiplying the predicted groundwater contaminant concentrations by the appropriate unit health effects factor and then summing the contributions from all contaminants that contribute to a particular metric. The calculations were performed with the use of an integrated computational software platform (DMT). A general description of the software platform is provided in Section 3.3.3. A detailed description is provided in *Tank Closure Project Decision Management Tool Systems Requirements Specification* (Watson 2005b).

3.2.3 Air Pathway

Gases and vapors could travel upward from the closed WMA facility through the soil to the ground surface. As downward water flow also drives gases and vapors down, the air pathway is maximized with minimum downward water movement. Thus, no water flow is considered in the calculations for the protection of air resources. The air emissions following closure are estimated using a simple model that provides an upper bound on the possible doses from tritium and carbon-14, and the possible emission rate of radon-222 at the ground surface above the waste.

The principal mechanism by which nuclides migrate from the waste to the ground surface is gaseous diffusion. The analysis in Appendix E of *Exposure Scenarios and Unit Factors for the*

Hanford Tank Waste Performance Assessment (Rittmann 2004) shows that convection mechanisms such as atmospheric pressure and temperature variations, wind, and rainfall have negligible secondary effects on the release of contaminants to the air.

The diffusion of radioactive gases such as tritium (hydrogen-3 as water vapor), carbon-14 (as carbon dioxide), and radon-222 (an inert gas) can be represented using Fick's Law of diffusion with a loss term for radioactive decay (Jury et al. 1991). The amount available for diffusion (i.e., the source concentration) changes with time due to the release mechanism for the contaminants from the waste form and radioactive decay. Two cases (one for tritium and carbon-14, the other for radon-222) must be considered because the performance objectives differ.

Because the estimated WMA closure inventories for tritium and carbon-14 are small, a bounding approach was used to estimate the air release doses for this risk assessment. Specifically, half the entire tritium and carbon-14 inventories for each WMA are released over a 1-year period, the first year after closure. The other half diffuses downward. This approach ignores diffusion from the waste that has been occurring during the past decades. A bounding approach avoids the task of defining release mechanisms and rates of progress through the overlying soils. The air pathway doses are calculated by multiplying the total inventories at WMA closure for tritium and carbon-14 by their corresponding unit release dose factors from Rittmann (2004), and summing the effective dose equivalent (EDE) from these two contaminants.

The radon-222 emanation rate from the ground surface is estimated using the diffusion equation derived in Appendix E of Rittmann (2004). This rate depends on the thickness of the waste, the depth of the soil cover, the assumed diffusivity of radon gas through the waste and soil cover, and the concentration of radium-226 in the waste. The radium-226 produces radon-222 by radioactive decay. The radium-226 is produced by the radioactive decay of curium-242, plutonium-238, uranium-238, uranium-234, and thorium-230. Because the radium-226 accumulates slowly with time, with most of it coming from the uranium-238 and uranium-234, the radium-226 concentration reaches its maximum value at times greater than 100,000 years after closure.

Because the estimated WMA closure inventories for the precursors of radon-222 are small, a bounding approach was used to estimate the air release rate for this SST PA. Specifically, the maximum concentration of radium-226 in the waste was used in the diffusion calculation. It was assumed that the uranium has not migrated appreciably from its initial location in the waste. Both the residual tank waste and the soil contamination plumes from tank leaks and other UPRs were assumed to be located 15 ft bgs. Note that such a depth is considerably shallower than what actually exists. In effect, the layer of grout and the tank dome are ignored. This approach certainly exaggerates the rate at which radon-222 escapes from the waste matrix and diffuses to the ground surface. The equation used to calculate the radon emanation rate at the ground surface is shown below:

$$J_{Rn}(z_0) = C_{0,Rn}\, U_{Rn}$$

$$\text{where,}\quad U_{Rn} = \frac{2\,\mu_{Rn} D}{1 - e^{-2 z_0 \mu_{Rn}}} \quad \text{and} \quad \mu_{Rn} = \sqrt{\frac{\lambda_{Rn}}{D}} \qquad \textbf{Eq. 3.7}$$

$$C_{0,Rn} = \frac{Q_{T,Ra}\,\lambda_{Rn}}{\lambda_{Rn} V + 2 A \mu_{Rn} D \Omega} \quad \text{and} \quad \Omega = \frac{1 + e^{-2 z_0 \mu_{Rn}}}{1 - e^{-2 z_0 \mu_{Rn}}}$$

where:

A	= surface area footprint of the waste disposal site, in m^2
$C_{0,Rn}$	= average concentration of radon-222 in the waste pore space available for diffusion, in Ci per m^3 of waste
D	= diffusion coefficient for radon moving through air trapped in the waste and soil, 0.01 cm^2/s = 31.56 m^2/yr
$J_{Rn}(z_0)$	= upward diffusion flux of radon-222 at elevation z_0 above the waste, in Ci/m^2 per second
$Q_{T,Ra}$	= the total quantity of radium-226 in the waste at a given time after closure, in Ci; it is assumed that the radium-226 and its ancestors are stationary in the waste
U_{Rn}	= effective vertical diffusion speed of the radon-222 at the ground surface, in m/s
V	= total volume of waste, in m^3
z_0	= thickness of the soil above the waste, in m
λ_{Rn}	= radioactive decay constant for radon-222, 66.21 per year
μ_{Rn}	= inverse length parameter characteristic of radon-222 diffusing in the soil above the waste, 1.449 m^{-1}.

The radon diffusivity through the soil is taken to be 0.01 cm^2/s. This is based on the approximate binary diffusivity of radon in air (0.1 cm^2/s) scaled by a tortuosity factor of 0.1 to account for diffusion in the soil pore space.

The estimated impacts for these air releases are also discussed in Section 6.5.

3.2.4 Intruder Pathway

Two general cases of intruder exposures were evaluated. The first considers the radiation dose to an individual who excavates or drills a well into the closed WMA and brings some of the waste to the surface receiving an acute dose (contact with the waste for a relatively short period of time) (Section 5.3). The second considers the radiation dose to an individual who lives near the completed well receiving a chronic dose (exposed over a number of years) (Section 5.3).

Two acute cases were evaluated. The first involved excavating for a basement or building foundation or highway. The other acute case involved drilling a well through the buried waste. Because the WMA will be covered with at least a 15-ft soil surface barrier, the proposed excavations would not extend far enough below the ground surface to uncover any waste. The excavation scenario gives no radiation dose and is not evaluated any further. The construction of water wells in the 200 Areas is plausible due to the distance between the WMA and the nearest surface water (greater than 10 mi).

Three chronic cases were evaluated: 1) the rural farmer with a dairy cow, 2) the suburban resident with a garden, and 3) the commercial farmer. The chronic scenarios differ by what is done with the material taken from the well (well cuttings). The rural pasture scenario considers the well cuttings being scattered in a cow pasture. The suburban garden scenario considers a family planting a garden in the well cuttings. The commercial farm considers the well cuttings being present in an area that is planted with dry-land wheat, hay, or some other crop that is harvested and sold for profit. The owner of the commercial farm does not consume any of the crops himself. His only exposure to the exhumed waste occurs during the production of the crop.

The intruder analyses do not consider the effect of contaminated groundwater on the intruder by design (DOE 1999d). A complete evaluation of the exposure to the intruder would take into account the presence of mobile, long-lived radionuclides in the groundwater. However, because the time period of interest is 500 years after closure, it can be assumed that the waste contaminants have not migrated appreciably.

Groundwater pathway results are presented in Chapter 4.0. Thus, following current regulatory practices, the intruder analysis only evaluates the effect on the intruder from inadvertent contact with the exhumed waste and does not include exposure to groundwater.

The methodology used to assess the inadvertent intruder contaminant exposure for a closed SST WMA is based on the amount of contaminants and drilling spoils brought up during the drilling process and the assumptions associated with what is done with the material taken from the well. The amount of material taken from the well is directly proportional to the diameter of the well and the depth of the well (assumed to extend 6.1 m into the unconfined aquifer). Depending on location, a well could intercept only the residual tank waste or only the leak plume, or it could intercept both. Thus, three cases were considered for each of the significant contaminant sources for a given WMA:

- Tank residual only
- Tank leak only
- Tank residual and tank leak combined.

Leaks into the soil from other UPRs begin a short distance below the original ground surface and extend downward. Leaks into the soil during tank waste retrieval have not been included in the present analysis.

The fraction of the tank waste or soil contamination plume that is brought to the surface depends on the geometry of the waste. A cylindrical shape is assumed to represent the average waste distribution. For the underground tanks, the contaminated area is the entire tank bottom. The average waste thickness is about 1 in. and is assumed uniform across the tank bottom. The fraction of waste brought to the surface is calculated as the borehole cross-sectional area divided by the cross-sectional area for the tank.

For past releases, the geometric shape was assumed to be a cylinder with a vertical axis. The diameter and height of the cylinder are assumed to be equal to provide an average intruder case. The volume of the cylinder area was estimated from the volume of liquid leaked and an average soil filling fraction. The volumes of liquid were estimated from available historical records. The soil filling fraction was assumed to be 10%. Thus, about 10% of the soil volume is

occupied by the aqueous waste that leaked. The fraction of waste brought to the surface was calculated as the borehole cross-sectional area divided by the cross-sectional area for the contaminated soil. Appendix E contains a more detailed discussion of the waste geometry models and gives the waste fraction brought to the surface for each waste form and intruder scenario.

In the scenario, not all of the waste material taken from the borehole is available for inhalation or ingestion by the various intruders. The particle size distribution of the cuttings typically includes larger pieces that cannot be inhaled or ingested. The large particles are consequences of drilling technology that breaks rocks only as much as needed to facilitate removal from the hole. This minimizes wear on the drill bit. In addition, the waste may be in a chemical form that resists uptake by plants or dissolution in lung fluid.

The wastes located in the UPRs are part of the soil. Therefore, 100% of the exhumed soil contamination is available for inhalation and ingestion by the intruders. However, the wastes located inside the tanks are attached to interior (iron) surfaces of the underground tank. The majority of this waste is located on the bottom of the tank, with grout on top of the waste. The chemical form of the residual tank waste is uncertain. It could be very hard and insoluble, and thus have reduced availability for inhalation and ingestion. After 500 years, the waste could also crumble readily during drilling and prove to be accessible for uptake into garden plants or pasture grass. The fraction available would be nearly 100% if the waste is in this form. In the present analysis, the fraction of the exhumed tank waste that is available for inhalation and ingestion is assumed to be 100%.

3.3 NUMERICAL IMPLEMENTATION

Numerical modeling was used to derive quantitative impacts from the proposed disposal action. The conceptual models discussed in the previous section were translated into numerical models. The numerical models were then implemented using computer simulations.

This section contains a description of the strategy used for the computer simulation and provides a summary of the selection criteria used for the computer code. A description of the codes and the criteria used in their selection, as well as the process of translating the disposal facility concepts and the natural system into computer models, is presented. The parameters used in the computer simulations are discussed in Section 3.4.

3.3.1 Code Selection and Verification

This section discusses the computer codes used for this SST PA and justifies their technical adequacy. Two major codes were used:

- Subsurface Transport Over Multiple Phases (STOMP)[1]
- Decision Management Tool (DMT).

Other codes were also used for simple data manipulation (Microsoft Excel[2] spreadsheets) and figure generation after processing of STOMP and DMT results (Tecplot[3]).

[1] Subsurface Transport Over Multiple Phases (STOMP) is copyrighted by Battelle Memorial Institute, 1996.

3.3.2 Subsurface Transport Over Multiple Phases

The computer code STOMP was chosen to model flow and transport through the vadose zone and groundwater out to the WMA fenceline. STOMP meets the requirements of *Computer Code Selection Criteria for Flow and Transport Code(s) To Be Used in Vadose Zone Calculations for Environmental Analyses in the Hanford Site's Central Plateau* (Mann et al. 1999) and has been used for a number of risk assessments on the Hanford Site (e.g., Knepp 2002a, 2002b). Verification of STOMP is documented in *CH2M HILL_STOMP Quality Assurance Test Report* (McMahon 2005a).

3.3.3 Decision Management Tool

The DMT software (*Tank Closure Project Decision Management Tool Functional Design Requirements* [Watson 2005a]) was used to calculate groundwater concentration of selected constituents from user-defined tank closure scenarios, predict risk associated with contaminant concentration, and compare predicted risk to regulatory criteria. Although the concentration and risk calculations used are not complex, the sheer volume of inventory and of fate and transport data used in these analyses makes hand calculations or spreadsheet use time- and cost-prohibitive. The DMT performs the defined risk assessment calculations in a more efficient manner and allows for greater sensitivity analysis to be performed than previously possible using spreadsheet calculations. The attributes of the DMT that make this possible include the following:

- Object-oriented data structures created from user-chosen input data in text files in the user's file system during program startup. In addition to maximizing calculation efficiency and minimizing computer resource usage, this also allows rapid response to new or altered input data, while giving the user the flexibility to add or remove input data without any programming knowledge.
- All necessary calculations are centralized in the source code and require no setup time on the part of the user.
- An intuitive user interface allows the user to create tank closure scenarios and calculate any of a number of provided risk metrics. The results can be examined numerically and graphically for each time step during the simulation both by analyte and cumulative risk.

Additionally, the DMT is a platform providing a means to distribute risk assessment data and results to multiple end users with better confidence in the accuracy of the results, while supplying complete traceability of input data and assumptions. Verification of the DMT is documented in *Tank Closure Project Decision Management Tool Software Test Report* (Watson 2005c).

---

[2] Microsoft and Excel are registered trademarks or trademarks of Microsoft Corporation in the United States and/or other countries.

[3] Tecplot is a registered trademark or trademark of Tecplot, Inc.

3.4 VALUES AND ASSUMPTIONS

This section describes and justifies the key data and assumptions used to estimate human health impacts associated with the tank closure system. This section also describes the selection criteria and key assumptions for the data used in the numerical models described in Section 3.2 for the barriers and key features impacting contaminant migration for different pathways.

The performance analysis examined three contaminant pathways: groundwater, air, and the inadvertent intruder. Controlling parameters associated with the operating features and processes are identified in Section 1.4.3. The barriers and key features impacting contaminant transport for the groundwater pathway are the surface cover, the grouted tank structure and ancillary equipment, the vadose zone, and the unconfined aquifer. Only the surface barrier and grouted tank structure and ancillary equipment are the barriers and key features impacting contaminant transport for the air and inadvertent intruder pathways.

Finally, this section defines the selection of the parameters associated with the reference case. (The definition of sensitivity cases and their associated parameter selection are discussed in Section 3.5.) This section has been organized into the following subsections:

- Inventory (Section 3.4.1)
- Surface cover and pre- and post-barrier recharge rates (Section 3.4.2)
- Grouted tank and ancillary equipment (Section 3.4.3)
- Vadose zone (Section 3.4.4)
- Unconfined aquifer (Section 3.4.5)
- Exposure scenarios (Section 3.4.6)
- Reference case (Section 3.4.7).

3.4.1 Inventory

Inventory remaining within the WMA subsurface at the time of closure is a key parameter for PAs because the estimated human health risks are proportional to the inventory of key contaminants associated with a closure site. This section provides an overview of the approaches used to derive the various inventory estimates and enabling assumptions. Detailed discussions of the methodologies used to develop the inventory estimates are available in cited references; inventory data are summarized in Appendix C.

3.4.1.1 Overview

Three sources of contaminants were considered in this SST PA:

- Past SST leaks and discharges of tank waste inside the tank farms
- Residual waste remaining in tanks after retrieval
- Residual waste in tank farm infrastructure (e.g., waste pipelines and catch tanks).

Inventory estimates for past tank leaks, discharges of waste to the soil column, and waste inventories associated with ancillary equipment were developed following the general methodology used to estimate current tank waste inventory estimates (Kupfer et al. 1998). That is, best estimates of waste volumes are coupled with projected waste compositions to develop inventory estimates. Inventory estimates associated with future activities such as waste

residuals remaining in the tank after retrieval were developed using the HTWOS (Kirkbride et al. 2005). The HTWOS model combines current estimates of tank waste compositions from the BBI with projected retrieval methodologies to project waste residual compositions expected to remain in the Hanford Site waste tanks at the end of the retrieval process. The model includes experimental based wash and caustic leach factors to estimate the sluicing efficiency in removing sludge from the tanks. The model also provides composition estimates of fluids being removed from the tanks. Inventories from potential waste loss events during waste retrieval activities were developed by multiplying projected retrieval fluid compositions by the estimated leak volumes for each tank.

Inventory estimates used in this SST PA were taken from three primary documents. The latest assessment of SST leak volumes and waste loss volumes within the tank farms is documented in Field and Jones (2005). Inventory estimates for these leaks and waste loss events were reported by Corbin et al. (2005). Waste residuals remaining in the tanks after completion of retrieval activities were documented in Kirkbride et al. (2005). The inventory estimates for ancillary equipment (e.g., pipelines and MUSTs) within the tank farms are documented in Appendix C.

Inventory estimates in Appendix C include 25 chemicals, 46 radionuclides, and supplemental analytes as provided by HTWOS. However, previous risk assessment analyses have led to the conclusion that long-term risks are driven by a small subset of chemicals and radionuclides. For brevity, the data and discussions presented in this section focus on this major contaminant subset. All contaminants listed in Appendix C were included in the modeling analysis.

3.4.1.2 Past Leaks

Human health impacts of leaks from SSTs or other waste loss events within the SST farms are closely linked to both the type of waste and the volumes of waste lost to the soil column. Inventory estimates for chemicals and radionuclides lost to the vadose zone were developed by integrating information from historical tank farm records with recent field investigations data. Historical tank farm records include compilations of waste transfer records (Anderson 1990; Agnew 1997), extensive documentation of process wastes being transferred to the SSTs (see process chemistry discussion in Appendix B), and analysis of the historical gross gamma logging data. Field data include recent spectral gamma logging of all drywells in all SST farms (Field and Jones 2005), as well as results from selected drilling and sampling projects (Knepp 2002a, 2002b). The general approach used to develop SST leak inventories is outlined schematically in Figure 3-11 and is documented in *Inventory Estimates for Single-Shell Tank Leaks in S and SX Tank Farms* (Jones et al. 2000b). The time and volumes of SST leaks were developed based on an analysis of historical records and field characterization data (Field and Jones 2005). The development of leak inventory estimates is documented in Corbin et al. (2005). Inventory data were developed for each waste loss event that has been identified within each tank farm (Corbin et al. 2005) and are available in the cited report. The complete suite of inventory estimates for past leaks is documented in Appendix C of this SST PA.

Inventory estimates associated with past leaks from tanks, UPRs, tank residuals, and ancillary equipment within WMAs C and S-SX are provided in Table 3-1 for selected radionuclides and chemicals. Contaminants listed in Table 3-1 for the groundwater pathway will be among the first

to arrive in the unconfined aquifer beneath each WMA and, as shown by past analyses (Mann et al. 2001; Lee 2004), will dominate the post-closure groundwater pathway impacts. Contaminants listed for inadvertent intruder impacts are the contaminants shown by past analyses (Mann et al. 2001; Mann and Connelly 2003) to be the major contaminants contributing to the intruder doses. Complete inventories for all past tank leaks, UPRs, tank residuals, and releases from ancillary equipment for these two WMAs and other WMAs are provided in Appendix C.

3.4.1.3 Tank Residual Wastes

Estimates for the residual waste inventory in each SST were developed as part of the HTWOS model run (Kirkbride et al. 2005). The general approach used to develop tank residual waste inventory estimates is outlined schematically in Figure 3-12. Further discussion of the HTWOS model is provided in Sections 2.5.1.1 and 2.5.3. As discussed in Section 2.5.3, the HTWOS model assumed 360 $ft^3$of waste remained in the 100-Series SSTs and 30 ft^3 remained in the 200-Series SSTs. The composition of the residual waste in the 100-Series SSTs was estimated as 35 wt% water washed solids with one-half concentration of bulk as-retrieved supernate (except tank C-106, which uses current BBI since it has been retrieved). Values for the wash and caustic leach factors are based on experimental data (reported in the BBI).

Table 3-1 summarizes the inventory for residual waste in each SST for WMAs C and S-SX. Complete inventories for all contaminants within the residual waste for each tank are provided in Appendix C.

A complete list of contaminant inventory for each WMA and for all contaminants is presented in Appendix C. Inventory estimates for tank waste residuals as well as those for ancillary equipment residuals are based on HTWOS. Inventory estimates for past tank leaks as well as UPRs are based on SIM.

Figure 3-11. Process for Determination of Inventories from Past Leaks

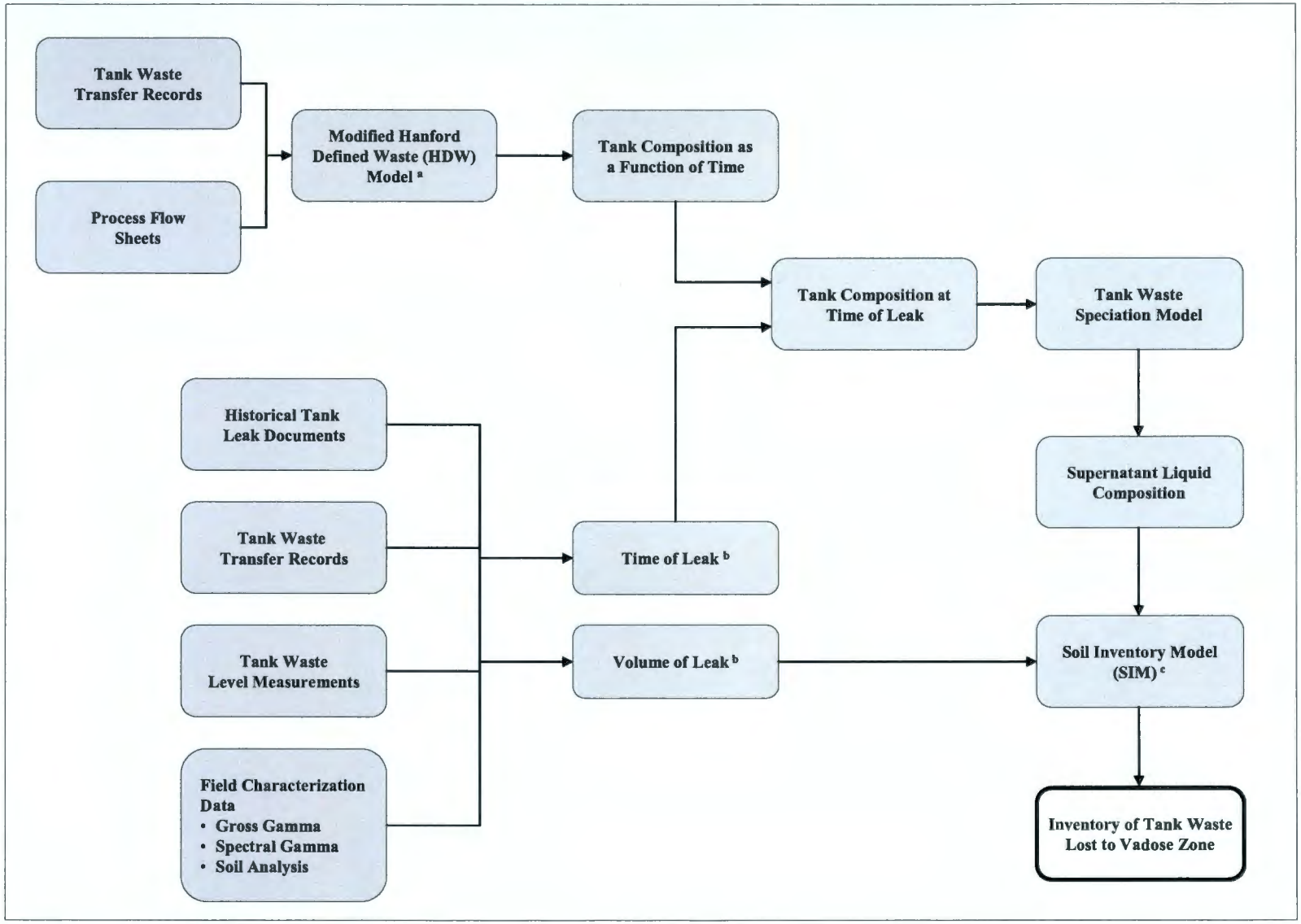

[a] *Higley and Place (2004)*
[b] *Field and Jones (2005)*
[c] *Corbin et al. (2005)*

Figure 3-12. Process for Determination of Inventories from Tank Residuals

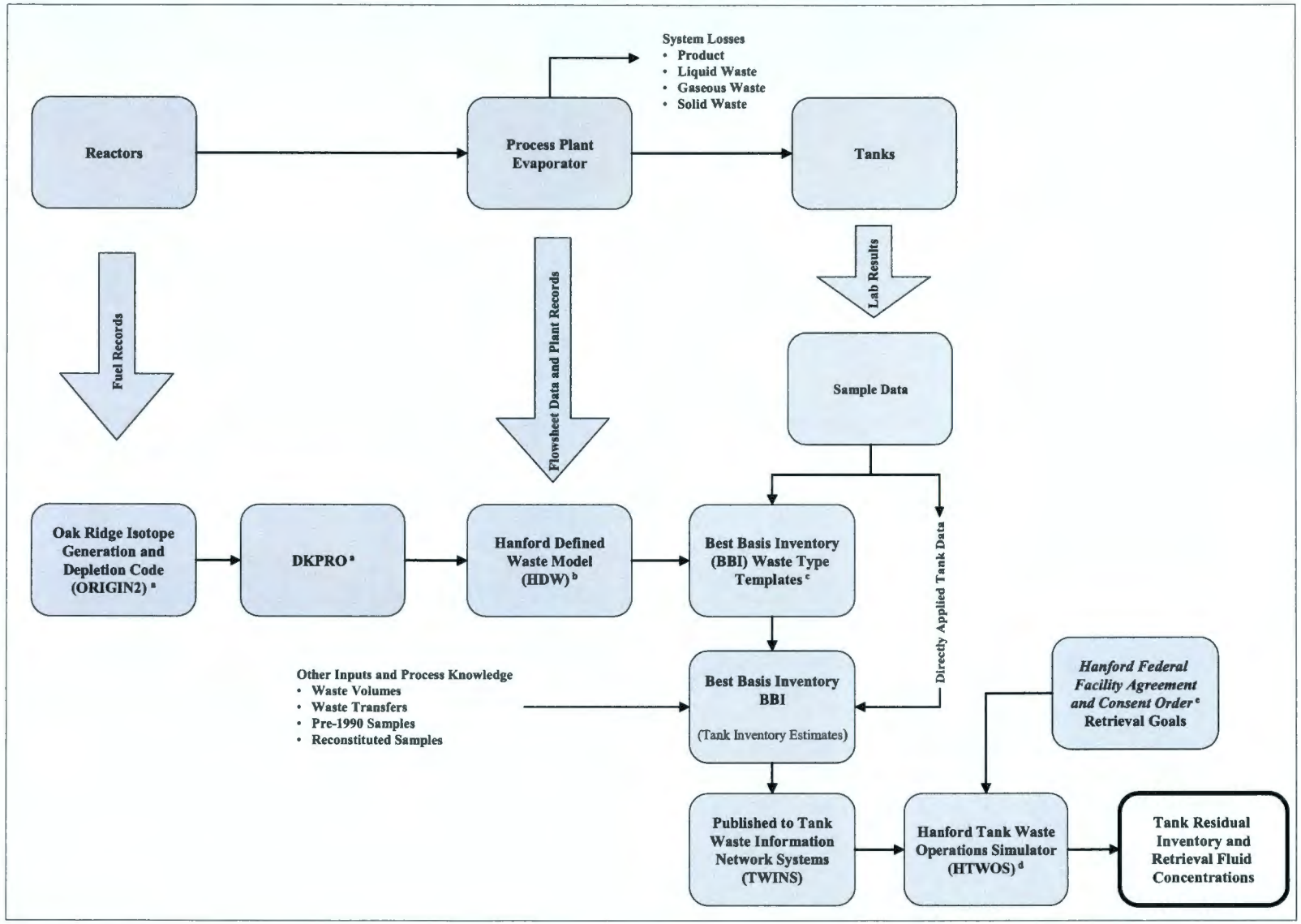

[a] *Watrous (2002)*
[b] *Higley and Place (2004)*
[c] *Place et al. (2005)*
[d] *Kirkbride et al. (2005)*
[e] *Ecology et al. (1989)*

Table 3-1. Inventories for Selected Rows within Waste Management Areas C and S-SX (6 pages)

Source [c]	Contaminants for Groundwater Pathway Impacts [a]					Contaminants for Inadvertent Intruder Impacts [b]						
	Tc-99 Ci [d]	I-129 C [d]	Cr kg [d]	NO_3^- kg [d]	NO_2^- kg [d]	Sr-90 Ci [d]	Tc-99 Ci [d]	Sn-126 Ci [d]	Cs-137 Ci [d]	Pu-239 Ci [d]	Pu-240 Ci [d]	Am-241 Ci [d]
Waste Management Area C												
Tank Row 241-CR Vault												
Past Releases												
UPR-200-E-81	2.74E-02	2.38E-02	2.17E+01	5.81E+03	1.78E+03	7.34E+01	2.74E-02	2.72E-04	8.60E+01	6.88E-01	1.62E-01	7.59E-01
UPR-200-E-82	1.42E+00	8.39E-04	1.62E+01	7.64E+02	3.93E+02	2.44E+01	1.42E+00	1.84E-02	1.48E+02	4.96E-02	1.15E-02	6.62E-02
UPR-200-E-86	4.92E+00	2.61E-03	6.04E+01	1.27E+03	1.49E+03	1.68E+02	4.92E+00	6.51E-02	1.98E+04	3.44E-01	7.49E-02	4.57E-01
Other Residuals												
241-CR vault	4.60E-02	2.18E-04	1.68E+00	4.42E+01	1.76E+01	2.88E+03	4.60E-02	9.01E-03	3.40E+02	3.38E+00	7.26E-01	3.88E+00
Ancillary Equipment (pipelines)												
Plugged and blocked pipelines	3.58E-05	3.03E-07	1.05E-02	3.13E+00	7.13E-02	7.78E-08	3.58E-05	1.36E-07	1.58E-10	6.03E-06	2.03E-06	5.92E-04
Tank Row C-101/C-104/C-107/C-110												
Past Releases												
C-101	2.25E-01	1.21E-04	1.51E+00	5.03E+01	4.07E+01	7.75E+00	2.25E-01	2.96E-03	8.52E+02	1.90E-02	3.87E-03	2.10E-02
C-104	0.00E+00	0.00E+00	0.00E+00	0.00E+00	0.00E+00	0.00E+00	0.00E+00	0.00E+00	0.00E+00	0.00E+00	0.00E+00	0.00E+00
C-107	0.00E+00	0.00E+00	0.00E+00	0.00E+00	0.00E+00	0.00E+00	0.00E+00	0.00E+00	0.00E+00	0.00E+00	0.00E+00	0.00E+00
C-110	2.43E-02	3.11E-05	1.47E+00	1.30E+03	5.08E+01	1.63E+01	2.43E-02	2.70E-04	7.45E+01	2.50E-02	2.46E-03	1.07E-02
UPR-200-E-107	7.07E-05	9.06E-08	3.14E-03	3.44E+00	1.39E-01	4.69E-02	7.07E-05	7.65E-07	2.17E-01	5.60E-05	6.04E-06	3.10E-05
Tank Residuals												
C-101	2.79E-03	1.68E-03	4.18E+00	3.37E+02	3.84E+01	6.41E+02	2.79E-03	7.80E-05	2.44E+02	8.07E+00	1.43E+00	1.43E+00
C-104	2.35E-01	4.23E-03	9.75E+00	7.40E+01	1.38E+02	3.12E+03	2.35E-01	5.33E-04	4.62E+02	3.63E+01	9.33E+00	4.44E+01
C-107	2.13E-01	2.72E-03	6.25E+00	3.34E+02	1.34E+02	1.76E+04	2.13E-01	5.28E-01	3.98E+02	1.85E+01	3.00E+00	5.68E+01
C-110	1.67E-01	1.18E-06	7.83E+00	5.62E+02	3.39E+01	9.08E+01	1.67E-01	1.13E-04	2.07E+02	1.99E+00	2.17E-01	1.20E+00

Table 3-1. Inventories for Selected Rows within Waste Management Areas C and S-SX (6 pages)

Source [c]	Contaminants for Groundwater Pathway Impacts [a]					Contaminants for Inadvertent Intruder Impacts [b]						
	Tc-99 Ci [d]	I-129 C [d]	Cr kg [d]	NO_3^- kg [d]	NO_2^- kg [d]	Sr-90 Ci [d]	Tc-99 Ci [d]	Sn-126 Ci [d]	Cs-137 Ci [d]	Pu-239 Ci [d]	Pu-240 Ci [d]	Am-241 Ci [d]
Tank Row C-102/C-105/C-108/C-111												
Past Releases												
C-102	0.00E+00	0.00E+00	0.00E+00	0.00E+00	0.00E+00	0.00E+00	0.00E+00	0.00E+00	0.00E+00	0.00E+00	0.00E+00	0.00E+00
C-105	2.26E-01	8.85E-05	1.42E+00	1.14E+02	3.77E+01	8.99E+00	2.26E-01	3.04E-03	6.21E+02	1.60E-02	4.25E-03	1.88E-02
C-108	0.00E+00	0.00E+00	0.00E+00	0.00E+00	0.00E+00	0.00E+00	0.00E+00	0.00E+00	0.00E+00	0.00E+00	0.00E+00	0.00E+00
C-111	5.38E-02	2.64E-03	5.27E+00	1.07E+03	4.66E+02	8.42E+02	5.38E-02	6.95E-04	1.95E+02	1.00E-01	2.11E-02	2.49E+00
Tank Residuals												
C-102	3.20E-03	1.58E-03	5.83E+00	1.99E+02	5.78E+01	2.52E+02	3.20E-03	8.70E-05	1.21E+02	3.26E+01	7.81E+00	9.55E+00
C-105	5.57E-01	5.99E-04	2.56E+00	5.24E+01	4.34E+01	3.34E+03	5.57E-01	2.05E-05	5.71E+02	1.50E+01	2.96E+00	8.01E+00
C-108	4.05E-02	7.03E-06	5.92E+00	1.16E+02	6.43E+01	3.54E+02	4.05E-02	2.82E-04	3.51E+03	1.43E-01	1.55E-02	4.60E-01
C-111	1.58E-02	2.00E-04	2.19E+00	1.27E+02	6.58E+01	2.80E+04	1.58E-02	3.20E-04	1.22E+02	5.16E+00	1.00E+00	5.88E+00
Tank Row C-103/C-106/C-109/C-112												
Tank Residuals												
C-103	7.17E-02	4.63E-04	6.02E+00	5.81E+00	5.94E+01	2.48E+04	7.17E-02	2.06E-03	6.53E+02	4.26E+01	8.92E+00	1.94E+01
C-106 [e]	1.65E-01	6.30E-04	3.78E+00	3.48E+01	4.14E+01	6.61E+04	1.65E-01	1.62E+00	1.45E+03	1.67E+01	3.57E+00	6.52E+01
C-109	4.96E-01	4.28E-04	1.68E+00	1.61E+02	1.03E+02	8.45E+03	4.96E-01	4.44E-04	5.74E+03	2.17E+00	3.72E-01	1.67E+00
C-112	7.23E-01	3.41E-04	1.84E+00	2.45E+02	1.74E+02	1.72E+04	7.23E-01	4.72E-04	6.57E+03	2.39E+00	3.01E-01	1.34E+01
Other Residuals (Ancillary Equipment)												
C-301	1.25E-02	5.92E-05	4.57E-01	1.20E+01	4.77E+00	7.83E+02	1.25E-02	2.45E-03	9.22E+01	9.18E-01	1.97E-01	1.05E+00
Tank Row C-201/C-202/C-203/C-204												
Past Releases												
C-201	1.07E-02	6.42E-07	7.80E-01	9.69E+01	2.63E+01	1.91E+02	1.07E-02	1.42E-04	4.30E+01	1.17E-02	2.53E-03	5.56E-01
C-202	8.77E-03	5.25E-07	6.37E-01	7.92E+01	2.15E+01	1.56E+02	8.77E-03	1.16E-04	3.52E+01	9.56E-03	2.06E-03	4.55E-01
C-203	8.29E-03	4.96E-07	6.03E-01	7.49E+01	2.03E+01	1.48E+02	8.29E-03	1.10E-04	3.32E+01	9.04E-03	1.95E-03	4.30E-01
C-204	7.04E-03	4.21E-07	5.12E-01	6.36E+01	1.72E+01	1.26E+02	7.04E-03	9.33E-05	2.82E+01	7.68E-03	1.66E-03	3.65E-01

Table 3-1. Inventories for Selected Rows within Waste Management Areas C and S-SX (6 pages)

Source [c]	Contaminants for Groundwater Pathway Impacts [a]					Contaminants for Inadvertent Intruder Impacts [b]						
	Tc-99 Ci [d]	I-129 C [d]	Cr kg [d]	NO_3^- kg [d]	NO_2^- kg [d]	Sr-90 Ci [d]	Tc-99 Ci [d]	Sn-126 Ci [d]	Cs-137 Ci [d]	Pu-239 Ci [d]	Pu-240 Ci [d]	Am-241 Ci [d]
Tank Residuals												
C-201	1.21E-02	6.88E-07	8.66E+00	8.60E+01	3.04E+01	1.08E+02	1.21E-02	1.53E-04	1.26E+01	8.95E+00	1.93E+00	1.42E+00
C-202	1.13E-02	6.66E-07	6.32E+00	7.77E+01	2.54E+01	2.04E+02	1.13E-02	1.48E-04	1.08E+01	7.90E+00	1.71E+00	6.67E-01
C-203	1.88E-03	6.61E-07	1.69E+01	1.60E+02	7.96E+00	2.78E+01	1.88E-03	1.47E-04	2.02E+00	1.55E+00	3.34E-01	7.88E-02
C-204	6.02E-03	5.31E-07	9.86E+00	3.13E+01	2.17E+01	1.52E+01	6.02E-03	1.18E-04	6.62E+00	7.99E-03	1.73E-03	1.95E-03
Waste Management Area S-SX												
Tank Row S-101/S-102/ S-103												
Tank Residuals												
S-101	6.77E-02	8.41E-04	6.19E+01	1.20E+02	4.14E+01	3.23E+03	6.77E-02	7.63E-03	1.43E+02	2.42E+00	4.75E-01	1.63E+00
S-102	5.87E-01	1.84E-04	5.90E+02	4.74E+02	9.52E+01	1.05E+04	5.87E-01	2.88E-01	6.13E+03	1.11E+01	2.38E+00	2.08E+01
S-103	7.10E-01	1.42E-04	7.07E+02	3.16E+02	7.22E+01	5.73E+03	7.10E-01	2.09E-01	1.70E+02	1.37E+01	2.86E+00	1.98E+01
Tank Row S-104/S-105/S-106												
Past Releases												
S-104	3.95E-02	5.57E-05	1.45E+01	4.99E+03	1.20E+03	1.02E+02	3.95E-02	3.68E-04	1.18E+02	4.61E-01	1.01E-01	6.11E-01
S-105	0.00E+00	0.00E+00	0.00E+00	0.00E+00	0.00E+00	0.00E+00	0.00E+00	0.00E+00	0.00E+00	0.00E+00	0.00E+00	0.00E+00
S-106	0.00E+00	0.00E+00	0.00E+00	0.00E+00	0.00E+00	0.00E+00	0.00E+00	0.00E+00	0.00E+00	0.00E+00	0.00E+00	0.00E+00
Tank Residuals												
S-104	2.80E-02	2.84E-04	7.54E+00	1.38E+02	1.48E+01	2.78E+03	2.80E-02	3.28E-03	8.21E+01	2.45E+00	5.00E-01	1.42E+00
S-105	2.15E+00	1.71E-04	3.26E+02	7.08E+02	1.50E+01	3.45E+02	2.15E+00	7.26E-01	1.29E+03	1.70E+00	3.41E-01	1.37E+00
S-106	7.27E-01	2.20E-04	7.26E+02	9.09E+02	6.69E+01	1.85E+03	7.27E-01	1.90E-01	7.59E+02	1.02E+00	2.23E-01	3.30E+00
Tank Row S-107/S-108 /S-109												
Tank Residuals												
S-107	9.77E-03	8.97E-05	2.26E+01	2.92E+01	1.54E+01	1.24E+03	9.77E-03	1.23E-03	1.83E+02	5.08E+00	1.06E+00	3.13E+00
S-108	7.00E-01	2.12E-04	6.66E+02	7.91E+02	1.05E+02	3.13E+03	7.00E-01	1.94E-01	7.88E+02	4.50E+00	9.63E-01	1.25E+01
S-109	1.21E+00	2.00E-04	4.12E+02	1.63E+03	2.01E+01	4.93E+03	1.21E+00	4.15E-01	3.06E+01	4.99E+00	9.82E-01	4.07E+00

Table 3-1. Inventories for Selected Rows within Waste Management Areas C and S-SX (6 pages)

Source [c]	Contaminants for Groundwater Pathway Impacts [a]					Contaminants for Inadvertent Intruder Impacts [b]						
	Tc-99 Ci [d]	I-129 C [d]	Cr kg [d]	NO_3^- kg [d]	NO_2^- kg [d]	Sr-90 Ci [d]	Tc-99 Ci [d]	Sn-126 Ci [d]	Cs-137 Ci [d]	Pu-239 Ci [d]	Pu-240 Ci [d]	Am-241 Ci [d]
Tank Row S-110/S-111/ S-112												
Tank Residuals												
S-110	2.11E-01	1.59E-04	9.69E+01	6.52E+02	3.83E+01	2.96E+03	2.11E-01	3.42E-02	1.24E+02	4.00E+00	7.90E-01	3.91E+00
S-111	3.28E-01	2.22E-04	1.60E+02	5.97E+02	8.37E+01	7.87E+03	3.28E-01	4.02E-02	2.06E+03	2.84E-01	5.90E-02	6.24E-01
S-112	4.84E-03	1.05E-03	1.82E+01	1.34E+01	3.54E+00	1.76E+04	4.84E-03	7.36E-01	2.45E+01	8.87E+00	1.57E+00	1.46E+01
Tank Row SX-101/SX-102/SX-103												
Tank Residuals												
SX-101	1.93E-01	1.86E-04	1.18E+03	9.32E+02	7.67E+01	1.93E+04	1.93E-01	1.14E-01	1.20E+03	2.86E+01	5.83E+00	3.14E+01
SX-102	9.80E-01	2.22E-04	6.35E+02	6.44E+02	2.04E+02	1.18E+04	9.80E-01	1.29E-01	3.79E+02	8.15E+00	1.71E+00	1.82E+01
SX-103	2.09E-01	1.88E-04	1.79E+02	6.93E+02	1.24E+02	6.32E+03	2.09E-01	3.94E-02	2.79E+02	3.12E+00	6.38E-01	8.96E+00
Other Residuals (Ancillary Equipment)												
SX-302	5.40E-03	5.87E-06	5.99E+00	1.10E+01	1.85E+00	6.13E+02	5.40E-03	1.09E-03	1.41E+01	7.24E-01	1.59E-01	6.41E-01
Tank Row SX-104/SX-105/SX-106												
Past Releases												
SX-104	4.51E+00	4.39E-03	6.17E+01	4.65E+03	2.46E+03	5.76E+01	4.51E+00	5.65E-02	5.93E+03	1.09E-01	2.38E-02	1.49E-01
SX-105	0.00E+00	0.00E+00	0.00E+00	0.00E+00	0.00E+00	0.00E+00	0.00E+00	0.00E+00	0.00E+00	0.00E+00	0.00E+00	0.00E+00
SX-106	0.00E+00	0.00E+00	0.00E+00	0.00E+00	0.00E+00	0.00E+00	0.00E+00	0.00E+00	0.00E+00	0.00E+00	0.00E+00	0.00E+00
Tank Residuals												
SX-104	1.36E-01	9.23E-05	6.69E+01	3.30E+02	5.13E+01	3.42E+03	1.36E-01	1.85E-02	1.80E+02	4.23E+00	8.31E-01	3.07E+00
SX-105	4.27E-01	2.15E-04	2.76E+02	5.95E+02	1.90E+02	8.84E+03	4.27E-01	9.40E-02	5.49E+02	3.59E+01	7.01E+00	2.24E+01
SX-106	7.33E-01	2.89E-04	5.60E+02	6.99E+02	2.22E+02	1.65E+03	7.33E-01	1.78E-01	2.05E+03	1.24E+01	2.67E+00	2.21E+01

Table 3-1. Inventories for Selected Rows within Waste Management Areas C and S-SX (6 pages)

Source [c]	Contaminants for Groundwater Pathway Impacts [a]					Contaminants for Inadvertent Intruder Impacts [b]						
	Tc-99 Ci [d]	I-129 C [d]	Cr kg [d]	NO_3^- kg [d]	NO_2^- kg [d]	Sr-90 Ci [d]	Tc-99 Ci [d]	Sn-126 Ci [d]	Cs-137 Ci [d]	Pu-239 Ci [d]	Pu-240 Ci [d]	Am-241 Ci [d]
Tank Row SX-107/SX-108/SX-109												
Past Releases												
SX-107	6.01E+00	9.28E-03	1.63E+02	1.23E+04	5.93E+03	1.41E+02	6.01E+00	6.57E-02	1.79E+04	2.88E-01	6.13E-02	3.82E-01
SX-108	1.40E+01	2.17E-02	3.81E+02	2.87E+04	1.38E+04	3.29E+02	1.40E+01	1.53E-01	4.18E+04	6.73E-01	1.43E-01	8.92E-01
SX-109	8.01E-01	1.24E-03	2.18E+01	1.64E+03	7.90E+02	1.88E+01	8.01E-01	8.76E-03	2.39E+03	3.84E-02	8.17E-03	5.10E-02
Tank Residuals												
SX-107	1.52E-02	1.65E-04	8.33E+00	6.96E+01	1.42E+01	3.13E+03	1.52E-02	1.73E-03	1.68E+02	3.89E+00	7.56E-01	1.94E+00
SX-108	7.16E-02	5.08E-04	8.78E+01	1.21E+03	5.07E+01	7.47E+04	7.16E-02	5.04E-03	2.11E+03	5.56E+01	1.08E+01	2.81E+01
SX-109	6.01E-02	6.88E-04	1.78E+01	2.82E+02	1.69E+01	1.77E+03	6.01E-02	7.51E-03	3.32E+02	2.42E+00	4.80E-01	1.65E+00
Tank Row SX-110/SX-111/SX-112												
Past Releases												
SX-110	3.35E-01	2.59E-04	4.43E+00	2.86E+02	1.17E+02	1.82E+01	3.35E-01	4.34E-03	1.42E+02	1.38E-02	3.14E-03	2.91E-02
SX-111	2.28E-01	1.56E-04	2.82E+00	1.44E+02	7.05E+01	7.86E+00	2.28E-01	2.95E-03	5.26E+01	9.01E-03	2.11E-03	1.52E-02
SX-112	4.01E-01	6.19E-04	1.09E+01	8.21E+02	3.95E+02	9.39E+00	4.01E-01	4.38E-03	1.19E+03	1.92E-02	4.09E-03	2.55E-02
Tank Residuals												
SX-110	4.70E-02	4.96E-05	1.58E+01	2.42E+02	2.27E+01	3.08E+03	4.70E-02	5.28E-03	6.32E+01	3.87E+00	7.57E-01	2.24E+00
SX-111	2.58E-02	2.70E-05	1.11E+01	1.18E+02	1.82E+01	3.29E+03	2.58E-02	3.14E-03	4.49E+01	4.12E+00	8.03E-01	2.21E+00
SX-112	2.10E-02	2.14E-05	1.01E+01	9.55E+01	1.68E+01	3.37E+03	2.10E-02	2.54E-03	3.93E+01	4.20E+00	8.17E-01	2.21E+00

Table 3-1. Inventories for Selected Rows within Waste Management Areas C and S-SX (6 pages)

Source [c]	Contaminants for Groundwater Pathway Impacts [a]					Contaminants for Inadvertent Intruder Impacts [b]						
	Tc-99 Ci [d]	I-129 C [d]	Cr kg [d]	NO_3^- kg [d]	NO_2^- kg [d]	Sr-90 Ci [d]	Tc-99 Ci [d]	Sn-126 Ci [d]	Cs-137 Ci [d]	Pu-239 Ci [d]	Pu-240 Ci [d]	Am-241 Ci [d]
Tank Row SX-113/SX-114/SX-115												
Past Releases												
SX-113	1.50E+00	2.39E-03	1.62E+02	7.87E+03	1.99E+03	1.40E+02	1.50E+00	1.59E-02	4.23E+03	2.88E-01	5.59E-02	3.80E-01
SX-114	0.00E+00	0.00E+00	0.00E+00	0.00E+00	0.00E+00	0.00E+00	0.00E+00	0.00E+00	0.00E+00	0.00E+00	0.00E+00	0.00E+00
SX-115	4.53E+00	7.04E-03	2.37E+02	1.43E+04	6.04E+03	3.11E+02	4.53E+00	4.88E-02	1.49E+04	9.56E-01	2.08E-01	1.27E+00
Tank Residuals												
SX-113	7.52E-04	7.70E-07	4.38E-01	3.90E+00	1.10E+00	1.27E+02	7.52E-04	5.12E-06	1.43E+02	3.55E-01	6.89E-02	2.27E-01
SX-114	5.87E-02	5.92E-04	1.64E+01	2.57E+02	2.49E+01	2.05E+03	5.87E-02	6.40E-03	3.22E+02	2.74E+00	5.39E-01	1.72E+00
SX-115	4.25E-02	4.21E-05	2.92E+02	2.71E-08	1.71E+00	2.00E+05	4.25E-02	5.25E-03	1.68E+01	2.35E+02	5.51E+01	2.12E+02
Ancillary Equipment (Pipelines)												
Plugged and blocked pipelines	1.77E-02	1.65E-05	2.23E-01	1.71E+01	8.46E+00	2.09E-01	1.77E-02	3.18E-04	2.11E+01	3.92E-04	7.60E-05	6.37E-04

[a] Major contaminants for groundwater impacts based on estimated chemical distribution coefficients ≤ 0.2 mL/g (Section 3.4.4.1.3).

[b] Major contaminants for inadvertent intruder impacts based on major contaminants contributing to the intruder doses in previous analysis (Mann et al. 2001; Mann and Connelly 2003).

[c] Tank residuals inventories from Kirkbride et al. (2005), inventories for tank leaks and unplanned releases from Corbin et al. (2005), pipeline inventories from Lambert (2005).

[d] Radionuclide inventories in Ci decayed to January 1 2004; chemical inventories in kg.

[e] Tank inventory for C-106 from best basis inventory (TWINS 2005).

3.4.1.4 Other Residual Wastes

The development of waste inventory estimates for ancillary equipment and transfer piping systems in the SST farms is still in its infancy. As discussed in Section 2.5.4, the scope of ancillary equipment included in this SST PA includes inactive MUSTs, vaults, and blocked and plugged waste transfer pipelines.

A complete list of ancillary equipment associated with each WMA is provided in Section 2.4.3.

Transfer lines associated with the SST system are believed to be about 154 km (96 mi) in total length (Field 2003b). This includes approximately 1,400 different lines ranging in size from 2 to 6 in. in diameter. The average diameter is about 3 in. These transfer lines were directly contaminated with waste. Contaminant concentrations for the waste in the blocked and plugged pipelines were assumed to be that of the average contaminant concentration currently in the particular tank farm. To obtain the contaminant inventory, the presumed volume was multiplied by the estimated contaminant concentration (Lambert 2005).

3.4.1.5 Data Structure

As discussed in the conceptual model defined in Section 3.2.2.1, the SST PA analysis used the inventory data, among other inputs, to generate a contaminant BTC at the WMA fenceline. For example, in the C tank farm, the vadose zone contamination sources associated with the tank row containing tanks C-103, C-106, C-109, and C-112 were used to compute the BTCs based on the STOMP calculations, the DMT tool, and the superposition principle to estimate the contaminant concentrations in the groundwater at the WMA fenceline. This process was followed throughout the seven WMAs.

3.4.2 Surface Barrier and Pre- and Post-Barrier Recharge Rates

The primary feature of the surface barrier with respect to the groundwater pathway is to limit moisture infiltration into each closed WMA system. Long-term estimates are needed for the moisture flux through a fully functional surface barrier as well as for the degraded barrier. These estimates were derived from lysimeter and tracer measurements combined with a modeling analysis.

Results from more than three decades of work are available on meteoric recharge estimates at the Hanford Site. Infiltration (recharge) can vary greatly depending on factors such as climate, vegetation, surface condition, and soil texture. Studies conducted over the last decade at the Hanford Site (Gee et al. 1992, 1996; Wing and Gee 1994; Fayer and Walters 1995; Fayer et al. 1996, 1999; Ward et al. 1997) suggest that recharge rates can vary from less than 0.1 mm/yr (0.004 in./yr) on a variety of soil and vegetative combinations to greater than 130 mm/yr (5.1 in./yr) on bare basalt outcrops or bare, gravel-covered waste sites (Gee et al. 1992). Detailed experimental work has also been performed on infiltration rates through surface barriers (Fayer and Szecsody 2004).

For the SST PA analyses, recharge estimates were needed for four different time periods: 1) prior to construction of the tanks, 2) current operations (from now until the placement of a

surface barrier), 3) surface barrier performance (during its design life), and 4) surface barrier performance for the degraded surface barrier (after its design life). The numerical simulations for the SST PA were run starting in the year tank farms were constructed, and continue for 10,000 years after closure. Recharge estimates for the period prior to the tank construction were needed to estimate the steady-state moisture conditions within the vadose zone prior to the start of simulations. Recharge estimates corresponding to current operations and corresponding to surface barrier performance are key inputs into the transport calculations discussed in Section 3.2.2.4.

3.4.2.1 Recharge Estimates for Pre-Development Conditions

Recharge estimates for the conditions prior to tank construction are based on correlations of soil types and infiltration characteristics of the native soils. Data supporting these recharge estimates for the 200 East and 200 West Areas soils are documented in Last et al. (2004b). Within the 200 East Area, recharge estimates range between 0.9 and 3.0 mm/yr for soils with established shrub-steppe vegetation. Similarly, within the 200 West Area, recharge estimates range between 3 and 4 mm/yr for soils with established shrub-steppe vegetation.

For the numerical simulations, the initial moisture contents (and the initial matric suctions) for the flow domain are established by allowing the vadose zone model to equilibrate with an infiltration rate representative of natural infiltration for tank farm location. For both WMAs C and S-SX, the representative infiltration rate was assumed to be 3.5 mm/yr (0.14 in./yr).

3.4.2.2 Recharge During Tank Farm Operations

Currently, each tank farm ground surface is covered with gravel to prevent vegetation growth and provide radiation shielding for site workers. Bare gravel surfaces, however, enhance net infiltration of meteoric water, compared to undisturbed naturally vegetated surfaces. Infiltration is further enhanced in tank farms by the effect of percolating water being diverted by the impermeable, sloping surface of the tank domes. This umbrella effect is created by the 75-ft (23-m) inside diameter of buried tank domes. Water, shed from the tank domes, then flows down the tank walls into the underlying sediments. Sediments adjacent to the tanks, while remaining unsaturated, can attain elevated moisture contents (Kline and Khaleel 1995). Enhanced infiltration from a gravel-covered tank dome can provide potential for faster transport of contaminants to the water table. Although site-specific infiltration data are being collected in BX, S, and T tank farms, insufficient data are available for site-specific estimates of natural infiltration at each farm.

For purposes of this SST PA, a reference case infiltration estimate of 100 mm/yr (3.93 in./yr) is used prior to barrier emplacement (Table 3-2). Data from experimental sites such as the Field Lysimeter Test Facility and the prototype Hanford barrier, both in the 200 Areas, suggest that recharge through gravels can vary from 15 to 70% of precipitation, with the lower amount occurring under vegetated conditions (Gee et al. 1996; Fayer and Walters 1995; Fayer et al. 1996).

3.4.2.3 Recharge beneath a Functioning Surface Barrier

Current plans are to use a Modified RCRA Subtitle C Barrier over the surface of each WMA as part of its closure (Section 1.7.3). The current pre-conceptual design for the Modified RCRA Subtitle C Barrier is based on DOE-RL (1996) and includes cover vegetation, silt loam layer(s), gravel layer(s), and an asphalt layer over the grading fill layer. The silt loam layer provides for moisture storage and allows evapotranspiration to occur before deep percolation can occur. The silt loam, along with the underlying gravel layer, forms a capillary break and impedes moisture flow across the interface. The design also includes an asphalt layer that provides biointrusion control and hinders human intrusion.

Extensive laboratory and modeling work and limited field testing of surface barriers have been performed; results are summarized in Fayer and Szecsody (2004). Lysimeter testing has been performed for different surface barrier concepts including a Modified RCRA Subtitle C Barrier with silt loam layers having depths between 1 and 2 m. Lysimeter data from the prototype Hanford barrier (Wing and Gee 1994) have also been collected and analyzed. Finally, modeling has been performed to address potential climate change impacts and no vegetation impacts on surface barrier performance.

The lysimeter drainage data that has been collected since 1989 suggests that the recharge rate beneath surface barriers having at least 1 m of silt loam is zero under ambient precipitation conditions. Most of these lysimeters did not contain an asphalt layer. Simulation results reported in Fayer and Szecsody (2004) investigated the sensitivity of the lysimeter data to climate change, silt loam hydraulic properties, vegetation changes, erosion, and dune formation above the surface barrier. Results indicated that the performance of these surface barriers was robust in that the estimated recharge rates remained below 0.1 mm/yr. For the cases investigated, only in the case of dune formation and no vegetation on the surface barrier were the simulated recharge rates above 0.1 mm/yr.

Based upon a review of the results, Fayer and Szecsody (2004) recommend an expected recharge performance for surface barrier with at least a 1 m of silt loam above a gravel layer to be on the order of 0.1 mm/yr for the life of the barrier. This estimate did not take any credit for the asphalt layer that is currently part of the Modified RCRA Subtitle C Barrier design.

The final design for the surface barrier has not been developed; however, based on the extensive testing reported in Fayer and Szecsody (2004), surface barriers that will limit recharge rates are achievable. For PA simulations involving tank farms with a functioning surface barrier, a reference case recharge rate of 0.5 mm/yr (0.02 in./yr) is assumed.

3.4.2.4 Recharge beneath a Degraded Surface Barrier

For a degraded surface barrier, a range of potential recharge rates can be envisioned. Fayer and Szecsody (2004) investigated the possibility of the most likely natural failure mechanisms (i.e., bioturbation of the silt loam layer, wind erosion, and accretion of wind blown sand). With appropriate design considerations, Fayer and Szecsody (2004) argue that the failure possibility of these natural systems is quite low, and the emplaced silt-loam soils will continue to perform for as long as they remain in place. Based on these arguments, Fayer and Szecsody (2004) concluded that the long-term effectiveness of the surface barrier would continue to limit recharge rates to less than 0.1 mm/yr for thousands of years.

Since the final design for the surface barrier has not been developed and it is difficult to defend the continued performance of a surface barrier for long periods of time, the SST PA has assumed the surface barriers will maintain the recharge rate at or below 0.5 mm/yr for 500 years. At the end of 500 years, the surface barrier performance is assumed to degrade to permit an infiltration rate of 1.0 mm/yr and maintain that infiltration rate for the remainder of the simulation for the reference case.

3.4.2.5 Reference Case Recharge Estimates

Table 3-2 summarizes the timeline estimates for barrier emplacement in tank farms and the corresponding reference case recharge estimates.

Table 3-2. Tank Farm Infiltration (Recharge) Estimates for Pre-Construction Period, Current Conditions, and Following Emplacement of Closure Barrier

Condition Simulated	Recharge Estimate mm/yr (in./yr)	Duration	Comment
Before construction of tank farms	3.5 (0.14) [a]	Until steady-state moisture conditions are achieved for the year, tank farm construction is completed	Vadose zone flow simulated at the recharge rate of 3.5 mm/yr to develop initial moisture conditions for subsequent simulations.
Current conditions	100 (3.93)	Construction completion year to year 2032	Recharge is assumed to increase from the pre-construction period estimate of 3.5 mm/yr to the current value of 100 mm/yr. During this period, the ground cover is gravel with no vegetation. A Modified RCRA Subtitle C Barrier is assumed to be in place by year 2032.
Transition to conditions of restricted recharge due to Modified RCRA Subtitle C Barrier	0.5 (0.02)	Years 2032 to 2532	Recharge is assumed to decrease from a current estimate of 100 mm/yr to the barrier design value of 0.5 mm/yr. The barrier is assumed to function to its design estimate of 500 years.
Degraded barrier condition	1.0 (0.14)	Years 2532 to 12032	The barrier is degraded and recharge increases from 0.5 mm/yr to 1.0 mm/yr until the end of simulation at year 12032.

[a] Based on 8-year lysimeter data for graveled surface (Fayer et al. 1999).

3.4.3 Grouted Tanks and Ancillary Equipment

The grouted tanks and ancillary equipment form one of the engineered barriers within the WMA closure system. The corresponding values and assumptions for the performance of this barrier are the parameters that were chosen to represent the contaminant source term releases from each of the contaminant sources and assumptions associated with its role in diverting moisture from the contaminant sources. This section describes the data used to select parameters used in the numerical simulations for the contaminant release from different waste forms, and the assumptions made concerning the role of the engineered barrier in diverting moisture from the contaminant sources.

3.4.3.1 Contaminant Source Term Releases

3.4.3.1.1 Past Releases. The contaminant sources associated with past releases were assumed to be readily available for transport with the infiltrating moisture; any chemical retardation is modeled by the linear isotherm K_d model discussed in Section 3.2.2.4. The estimates for the inventories for each identified release event are described in Section 3.4.1.2 for WMA C and WMA S-SX for selected contaminants and provided in Appendix C for all contaminants and other WMAs.

The distribution for each past tank leak in each WMA in the 200 West Area was modeled as a 25-ft (7-m) diameter source at a depth of approximately 130 ft (39.6 m) bgs located between tanks S-102 and S-103 for WMA S-SX. Section 2.7.5.2 provides a detailed discussion on the contamination that has been characterized in WMA S-SX. Gamma readings in the southern part of the SX tank farm are significant to a depth of 40 m bgs. This depth has been assumed to represent the depth for all known tank leaks in the 200 West Area because no contamination has been measured at a greater depth in the vadose zone, except for readings from one borehole in WMA TX-TY where contamination was observed at a depth of 150 ft bgs (see discussions for each WMA in the "Vadose Zone Conditions" subsections in Sections 2.6 through 2.12). By selecting a maximum depth for all past tank leaks, the timing of the BTCs for past leaks is shortened and the peak contaminant concentration in the groundwater is maximized. The selection of a 25-ft diameter of the source term was based on numerical simulations performed for the S-SX FIR (Knepp 2002a); calculations were performed for differing horizontal distributions for the past leak contaminants for WMA S-SX. These calculations showed the contaminant concentrations in the groundwater to be relatively insensitive to the assumed horizontal distribution of the contaminants from past leaks in the vadose zone. Based on these results, a contaminant inventory footprint diameter of 25 ft (7 m) was assumed for past leaks.

The distribution for each past tank leak in each WMA in the 200 East Area was modeled as a 25-ft (7-m) diameter source at a depth of 150 ft (45.7 m) bgs located between tanks C-112 and C-109 for WMA C. The depth of 150 ft (45.7 m) was assumed for each leak. The "Vadose Zone Conditions" subsections in Sections 2.10 through 2.12 summarize the current understanding based on characterization of vadose zone contamination for WMAs C, B-BX-BY, and A-AX. The deepest indications for vadose zone contamination are seen at 70 m bgs for WMA B-BX-BY, and 26 m bgs for WMA A-AX; no significant past leak contamination was reported for WMA C.

3.4.3.1.2 Tank Residual Wastes. The anticipated situation at the end of the retrieval process is as follows: a non-uniform distribution of tank residual waste within the tank with potentially higher accumulations distributed on strengthening rings on the side walls and equipment left in the tanks, and at selected regions on the tank bottom that are difficult to reach (due to the retrieval process utilized on the tank). The retrieval process is assumed to be successful in meeting HFFACO volume requirements (Ecology et al. 1989). For the reference case, the SST PA assumes that the tank as well as MUST wastes has been stabilized by filling them with cementitious grout. This assumption is consistent with closure planning. Residual wastes in pipelines within a WMA are assumed to represent unstabilized wastes.

Residual Waste Volume. For this SST PA, the volume of waste left in the tanks is assumed to meet HFFACO requirements of 360 ft^3 (10.2 kL) for 100-Series tanks and 30 ft^3 (850 L) in 200-Series tanks (Ecology et al. 1989). Given the dimensions of the tanks and the above assumptions, the average thickness of the residual waste in a 100-Series tank would be 1.0 in. (2.54 cm), while that for the 200-Series tanks would be 1.4 in. (3.6 cm).

Residual Waste Release Model. A diffusion-dominated release model was used to model release of contaminants from tank residual wastes for the reference case. The key parameters in this model are the effective diffusion coefficient for each contaminant in the waste and the mixing thickness. For the reference case, a diffusion coefficient of 1×10^{-9} cm^2/sec was used based on the Savannah River Site work on Hanford Site tank wastes (Harbour et al. 2004).

In Equation 3.6, the surface area to volume ratio, A_t/V_t, can be interpreted as the mixing length for the diffusional release from the tank bottom. The mixing length value used in the diffusion-dominated release model, however, is much larger than the uniform thickness of the residual wastes in the tanks. The mixing length accounts for the heterogeneous distribution of residual wastes within a tank, as well as the thick concrete structure for the diffusional release of contaminants from the tank. First, the residual wastes are not expected to be homogeneously distributed to a uniform thickness of 1 in. Following pouring of grout in the tank, the release from the tank occurs over a time period that exceeds thousands of years. During this long time period, contaminants within the residual wastes are transported by downward diffusion into the underlying concrete structure as well as by upward diffusion into "clean" grout.

For the concrete structure, Goetz (2003) states for the 100-Series tanks:

> "Each SST shell has an approximate 1-ft thick concrete base slab, dome and cylindrical wall that rests on a circular footing integral with the tank and base slab."

The upward diffusive length (L) is estimated to be about 18 in. Thus, for release calculations, the residual waste, prior to release, resides within the tank bottom thickness of 18 in. This plus the "average" 12-in. thickness plus other tank structural components (such as 2 in. of grout within the tank, 3/8 in. of mastic material [an asphalt liner], and 3/8-in. steel liner) accounts for the 0.825 m of mixing length used in this SST PA.

Other process-based release models are described later as part of sensitivity analyses (Section 3.5.4.3).

The numerical model calculation for the contaminant release from the tank residuals assumed a unit curie (Ci) source uniformly distributed at the bottom of each tank with the diffusional release starting on January 1, 2032.

3.4.3.1.3 Residual Ancillary Equipment Wastes. As defined in Section 2.5, other residual wastes include ancillary equipment such as pipelines and MUSTs within each WMA. For the reference case simulations, the residual waste inventory from pipelines was assumed to be homogeneously distributed. The release from pipeline residuals was modeled as a uniform inventory distributed over an approximately 7-m (approximately 25-ft) diameter at approximately 9 m (approximately 30 ft) bgs with the start of release occurring on January 1, 2000. The pipeline residual waste is assumed to be unstabilized and readily available for transport with the infiltrating water. The release from residual wastes in MUSTs is treated similar to release of residual waste from a tank, with the start of release occurring on January 1, 2032.

3.4.4 Vadose Zone

3.4.4.1 Moisture Flow and Contaminant Transport Data

With the exception of the surface barrier (Section 3.4.2), the operational period between years 2000 and 2032, and the consideration for the concrete structure in the contaminant release model for tank residual wastes (Section 3.4.3.1.2), facility structures are basically ignored in the moisture flow and contaminant transport simulations. The effect of the surface barrier is accounted for by changing the infiltration rate (Section 3.4.2.3). Other facility structures (e.g., the structural integrity of tank and ancillary equipment) are assumed to disappear after year 2032. This assumption was made to simplify the simulations and was chosen because it results in higher than expected contaminant concentrations in the unconfined aquifer. Thus, during the near term, the tanks act like umbrellas diverting moisture flow. In later years, the tanks were assumed to be filled with grout for the reference case; the grout properties impact the moisture flow. These grout properties were assumed to remain unchanged over the simulation period of 10,000 years. Moisture flow and contaminant transport data are provided for the near field, the vadose zone, and the unconfined aquifer beneath the WMA. The near field is defined as the region above the bottom of the tanks as shown in Figures 3-3 and 3-4. The vadose zone begins just below the horizontal line corresponding to the bottom of the tanks in the models.

3.4.4.1.1 Near Field Flow and Transport Properties. The recharge into the near field is described in Section 3.4.2. For the reference case, the tank structure was assumed to function as an impermeable barrier. The contaminant release as a function of time from the grouted residual tank waste is introduced into the numerical calculation at the bottom of each tank. No chemical retardation of the release was assumed.

3.4.4.1.2 Vadose Zone Flow and Transport Parameters. Details on vadose zone flow and transport parameters are provided in various data packages (Khaleel et al. 2006a, 2006b). The following sections summarize the methods and data used for the reference case.

Moisture Retention and Unsaturated Hydraulic Conductivity. The moisture retention data are described using an empirical relationship (van Genuchten 1980):

$$\theta(h) = \theta_r + (\theta_s - \theta_r)\left\{1 + [\alpha h]^n\right\}^{-m} \qquad \textbf{Eq. 3.8}$$

where:

θ = volumetric moisture content [dimensionless]
h = matric potential or pressure head, which, for notational convenience, is considered as being positive (i.e., tension [cm])
θ_r = residual moisture content [dimensionless]
θ_s = saturated moisture content [dimensionless]
α = a fitting parameter (cm^{-1})
n = a fitting parameter [dimensionless]
m = 1 - 1/n.

Combining the van Genuchten model with Mualem's (1976) model for unsaturated conductivity:

$$K(h) = \frac{K_s\left\{1 - (\alpha h)^{mn}\left[1 + (\alpha h)^n\right]^{-m}\right\}^2}{\left[1 + (\alpha h)^n\right]^{m\ell}} \qquad \textbf{Eq. 3.9}$$

where:

$K(h)$ = unsaturated hydraulic conductivity [cm/s]
K_s = saturated hydraulic conductivity [cm/s]
ℓ = pore-connectivity parameter [dimensionless], estimated by Mualem to be about 0.5 for many soils.

It is well recognized that the estimated unsaturated conductivities, based on saturated conductivity and the van Genuchten retention model, can differ by up to several orders of magnitude with measured conductivities at the dry end (e.g., Khaleel et al. 1995). A simultaneous fit of both laboratory-measured moisture retention and unsaturated conductivity data was used in this work, and all five unknown parameters θ_r, θ_s, α, n, and K_s, with m=1-1/n (van Genuchten 1980) were fitted to the data via a code named RETention Curve (RETC) (van Genuchten et al. 1991). Thus, in order to obtain a better agreement with experimental data for the region of interest (i.e., relatively dry moisture regime), K_s is treated as a fitted parameter during the curve-fitting process. The pore size distribution factor, ℓ (Mualem 1976) was kept fixed at 0.5 during the simultaneous fitting.

Table 3-3 lists the composite-fitted van Genuchten-Mualem (van Genuchten 1980; van Genuchten et al. 1991) parameters for various strata at WMAs C and S-SX. Estimates for the equivalent horizontal and vertical hydraulic conductivities are presented in the following section.

Table 3-3. Composite van Genuchten-Mualem Parameters for Various Strata at Waste Management Areas C and S-SX [a]

Strata	Number of Samples	θ_s	θ_r	α 1/cm	n	ℓ	Fitted K_s cm/s
Backfill	10	0.1380	0.0100	0.0210	1.374	0.5	5.60E-4
Sand H2	12	0.3819	0.0443	0.0117	1.6162	0.5	9.88E-5
Gravelly Sand H3	8	0.2688	0.0151	0.0197	1.4194	0.5	5.15E-4
Gravelly Sand H1	11	0.2126	0.0032	0.0141	1.3730	0.5	2.62E-4
Plio-Pleistocene	4	0.4349	0.0665	0.0085	1.8512	0.5	2.40E-4
Plio-Pleistocene/ Ringold Sandy Gravel	10	0.1380	0.0100	0.0210	1.374	0.5	5.60E-4

[a] Khaleel et al. (2006a; 2006b)

Moisture-Dependent Anisotropy. Vadose zone moisture-dependent anisotropy is used to account for the extensive lateral migration that is well documented for 200 East and West Areas sediments (Khaleel et al. 2006a; Ye et al. 2005; Yeh et al. 2005). For saturated media, an averaging of the heterogeneities in geologic media at a smaller scale leads to an effective hydraulic conductivity value at the larger (macroscopic) scale, with the lateral hydraulic conductivity being much larger than the vertical conductivity. For unsaturated media, theoretical and experimental analyses of field-scale unsaturated flow indicate that for stratified sediments such as those in the 200 Areas, the effective hydraulic conductivity tensor is anisotropic with a tension-dependent (or moisture-dependent) anisotropy. The anisotropy ratio of horizontal hydraulic conductivity to vertical hydraulic conductivity increases with increasing tension or decreasing moisture content. Because the soil hydraulic properties are based on small-scale laboratory measurements, upscaling methods are used to apply them to the large-scale, heterogeneous vadose zone (Khaleel et al. 2002). Tension-dependent anisotropy provides a framework for upscaling small-scale measurements to the effective (upscaled) properties for the large-scale vadose zone.

A stochastic model (Polmann 1990) was used to evaluate tension-dependent anisotropy for sediments at each WMA. Note that Polmann parameters (Table 3-4) were only used to assign anisotropy ratios for various strata within the vadose zone and are described by the following equation (Equation 3.10):

$$
\begin{aligned}
&< LnK > = < LnK_s > - A < h > - \sigma^2_{LnKs} \lambda [p - p^2 < h > - \zeta^2 < h >] / (1 + A\lambda) \\
&\sigma^2_{LnK} = \sigma^2_{LnKs} [(1 - p < h >)^2 + \zeta^2 < h >^2] / (1 + A\lambda) \\
&K_h^{eq} = \exp[< LnK > + (\sigma^2_{LnK} / 2)] \\
&K_v^{eq} = \exp[< LnK > - (\sigma^2_{LnK} / 2)]
\end{aligned}
\qquad \textbf{Eq. 3.10}
$$

where:

σ^2_{LnK} = variance of log unsaturated conductivity (which depends on mean tension)

$<h>$ = mean tension (positive) = $|\psi|$

ψ = matric potential (negative)

σ^2_{LnKs} = variance of lnK_s

$<LnK_s>$ = mean of lnK_s

p = slope of the β versus lnK_s regression line, where β is the slope of the unsaturated conductivity curve and approximated locally based on the Gardner's (1958) exponential model

ζ = $\sigma_\delta/\sigma_{lnKs}$

σ_δ = standard deviation of the residuals in the β versus lnK_s regression

A = mean slope, β, for lnK vs. h

λ = vertical correlation lengths for lnK_s (assumed to be same as that of β)

K_h^{eq} = equivalent unsaturated horizontal conductivity

K_v^{eq} = equivalent unsaturated vertical conductivity.

Table 3-4. Macroscopic Anisotropy Parameters for Various Strata at Waste Management Areas C and S-SX Based on Polmann (1990) Model [a]

Strata	Number of Samples	$<LnK_s>$	$\sigma^2_{LnK_s}$	p	ζ	λ cm	A
Backfill	10	-15.76	3.56	-1.1E-4	1.84E-4	30	0.00371
Sandy H2	12	-14.59	1.50	-7.2E-4	6.55E-4	50	0.00620
Gravelly Sand H3	8	-15.30	1.83	-5.6E-4	5.16E-4	50	0.00415
Gravelly Sand H1	11	-14.85	1.94	-2.6E-4	2.50E-4	30	0.00368
Plio-Pleistocene	4	-10.43	1.01	2.4E-3	9.34E-4	50	0.0104
Plio-Pleistocene/ Ringold Sandy Gravel	10	-15.76	3.56	-1.1E-4	1.84E-4	30	0.00371

[a] Khaleel et al. (2006a; 2006b)

Effective Transport Parameters. The reference case effective transport parameter (bulk density, diffusivity, and dispersivity) estimates are presented in this section. Because of natural variability, the transport parameters are all spatially variable. The purpose is similar to the flow parameters, to evaluate the effect of such variability on the large-scale transport process.

Bulk Density Estimates. Bulk density (ρ_b) estimates are needed to calculate retardation factors for different species. The average ρ_b, E[ρ_b] (Table 3-5) estimates for various strata are based on Khaleel et al. (2006a, 2006b).

Table 3-5. Effective Bulk Density (g/cm^3) Estimates at Waste Management Areas C and S-SX

Strata/Material Type	E[ρ_b]
Backfill	2.13
Sandy H2	1.76
Gravelly sand H3	1.94
Gravelly sand H1	2.07
Plio-Pleistocene silty sand	1.65
Plio-Pleistocene/Ringold gravels	2.13

[a] Khaleel et al. (2006a; 2006b)

Diffusivity. It was assumed that the effective, large-scale diffusion coefficients for all strata at a WMA are a function of volumetric moisture content, θ, and can be expressed using the Millington-Quirk (1961) empirical relation:

$$D_e(\theta) = D_0 \frac{\theta^{10/3}}{\theta_s^2} \qquad \textbf{Eq. 3.11}$$

where:

$D_e(\theta)$ = effective diffusion coefficient of an ionic species as a function of moisture content

D_0 = molecular diffusion coefficient for the same species in free water.

The molecular diffusion coefficient for all species in free water was assumed to be 2.5×10^{-5} cm^2/sec (Kincaid et al. 1995).

Macrodispersivity Estimates for Nonreactive Species. The Gelhar and Axness equation (Gelhar 1993) is used to estimate asymptotic values of macrodispersivity. To account for the effects of unsaturated flow, a modified version is used:

$$A_L(< h >) = \sigma_{LnK}^2 \lambda \qquad \textbf{Eq. 3.12}$$

where the longitudinal macrodispersivity depends on the mean tension $< h >$.

To apply Equation 3.12, an estimate of the vertical correlation scale for unsaturated conductivity is needed. A correlation length of the order of about 50 cm was obtained for saturated hydraulic conductivity for sediments near the C tank farm (Khaleel et al. 2006a). For unsaturated conditions, an increase in the variance of log unsaturated conductivity is expected to be compensated in part by a decrease in the correlation scale of log unsaturated conductivity. A correlation length of 30 cm is assumed for log unsaturated conductivity for all strata. Table 3-6 provides the log unsaturated conductivity variances and the estimated longitudinal (A_L) and transverse (A_T) macrodispersivities for various strata. The transverse dispersivities are estimated as one tenth of the longitudinal values (Gelhar et al. 1992).

Table 3-6. Nonreactive Macrodispersivity Estimates for Various Strata at Waste Management Areas C and S-SX

Strata	σ^2_{LnK}	Correlation length, λ cm	A_L cm	A_T cm
Backfill	4.54	30	~150	15
Sandy H2	4.60	30	~150	15
Gravelly Sand H3	4.95	30	~150	15
Gravelly Sand H1	3.19	30	~100	10
Plio-Pleistocene Sandy Silt	0.92	30	~50	5
Plio-Pleistocene/Ringold Sandy Gravel	4.54	30	~150	15

Heterogeneous Sorption Enhanced Macrodispersivities for the Reactive Species. The net effect of sorption is to retard the velocity at which the contaminant migrates through the porous media. Because sorption for specific contaminants may be a function of soil properties, as the soil properties experience spatial variability, the sorption also varies (Gelhar 1993; Talbott and Gelhar 1994). Stochastic analysis results for macrodispersivity enhancement for various strata in WMA C and S-SX are given in the modeling data package reports (Khaleel et al. 2006a, 2006b).

3.4.4.1.3 Contaminant Distribution Coefficients. Table 3-7 lists the contaminant distribution coefficient (K_d) bins used in this SST PA for various contaminants. Contaminant K_d values are adapted from:

- Section 4.3 of *Vadose Zone Hydrogeology Data Package for the 2004 Composite Analysis* (Last et al. 2004a)
- *Hanford Contaminant Distribution Coefficient Database and Users Guide* (Cantrell et al. 2002, 2003)
- *Soil Screening Guidance: Technical Background Document* (EPA 2000a)
- *Selection of K_d Values for INTEC Groundwater Modeling* (Jenkins 2001)
- *Engineering Design File – Fate and Transport Modeling Results and Summary Report* (INEEL 2004)
- *A Practical Guide to Groundwater and Solute Transport Modeling* (Spitz and Moreno 1996)
- *Risk Assessment Information System* (ORNL 2005).

A number of K_d bins are used to represent the range of sediment-contaminant chemical interaction for the variety of contaminants in various WMAs (Section 3.2.2.4.7).

Table 3-7. Contaminant Distribution Coefficients (mL/g) for Analytes that are Part of the Single-Shell Tank System Inventory (2 pages)

K_d = 0 mL/g			
Tritium	Tantalum	Oxalate	Neodymium
Carbon-14	Tellurium	Phosphate	N-nitroso-di-n-propylamine
Technetium-99	Tungsten	Benzyl alcohol	n-Nitrosomorpholine
Bismuth	Yttrium	Chloroethene	Phenol
Cerium	Acetate	Cyclohexanone	Pyridine
Chloride	Ammonia	Dichloromethane	Tetrahydrofuran
Chromium	Ammonium	Diethyl ether	Vanadium pentoxide
Praseodymium	Fluoride	Ethyl Acetate	2-Butanone(MEK)
Rhodium	Formate	Glycolate	2-Chlorophenol
Rubidium	Hydroxide	Isobutanol	2-Ethoxyethanol
Sodium	Nitrate	Lanthanum	2-Nitropropane
Sulfate	Nitrite	n-Butyl alcohol	2-Propanone
K_d = 0.02 mL/g			
Benzene	Nitrobenzene	1, 1, 1-Trichloroethane	1, 2-Dichloroethane
Carbon disulfide	Toluene	1, 1, 2, 2-Tetrachloroethane	4-Methyl-2-pentanone (MIBK)
Carbon tetrachloride	trans-1, 3-dichloropropene	1, 1, 2-Trichloroethane	
Chloroform	Trichlorofluoromethane	1, 1, 2-Trichloroethylene	
Ethylbenzene	Xylenes	1, 1-Dichloroethene	
K_d = 0.1 mL/g			
Cobalt-60	Cresylic acid	o-Nitrophenol	2, 4, 6-Trichlorophenol
Cobalt	m-Cresol	o-Xylene	2, 4-Dinitrotoluene
Chlorobenzene	o-Dichlorobenzene	Tetrachloroethylene	2-Methylphenol
K_d = 0.2 mL/g			
Iodine-129	Pentachlorophenol	1, 4-Dichlorobenzene	
p-Chloro-m-cresol	1, 1, 2-Trichloro-1, 2, 2-trifluoroethane	2, 4, 5-Trichlorophenol	
K_d = 0.6 mL/g			
Uranium-232	Uranium-235 + D	Uranium	1, 2, 4-Trichlorobenzene
Uranium-233	Uranium-236	Naphthalene	
Uranium-234	Uranium-238 + D	Tributyl phosphate	

Table 3-7. Contaminant Distribution Coefficients (mL/g) for Analytes that are Part of the Single-Shell Tank System Inventory (2 pages)

K_d = 1.0 mL/g			
Ruthenium-106	Europium-152	Aluminum	Ruthenium
Cadmium-113m	Europium-154	Antimony	Thorium
Antimony-125	Europium-155	Cadmium	Tin
Tin-126	Radium-226 + D	Europium	Acenaphthene
Samarium-151	Radium-228 + D	Manganese	Ruthenium
K_d = 2.0 mL/g			
Selenium-79	Neptunium-237 + D	Plutonium-241 + D	Curium-244
Thorium-228 + D	Plutonium-238	Curium-242	Silver
Thorium-229 + D	Plutonium-239	Plutonium-242	Boron
Thorium-230	Plutonium-240	Americium-243 + D	Di-n-butylphthalate
Thorium-232	Americium-241	Curium-243	
K_d = 5.0 mL/g			
Actinium-227 + D	Zirconium-93	Mercury	Zirconium
Cesium-134	Arsenic	Molybdenum	Cyanide
Cesium-137 + daughters	Barium	Nickel	Aroclor-1254
Molybdenum-93	Beryllium	Selenium	Butylbenzylphthalate
Nickel-59	Calcium	Silicon	Di-n-octylphthalate
Nickel-63	Copper	Strontium	Fluoranthene
Niobium-93m	Iron	Thallium	Hexachlorobutadiene
Niobium-94	Lead	Titanium	Hexachloroethane
Protactinium-231	Lithium	Vanadium	Pyrene
Strontium-90 + D	Magnesium	Zinc	

Contaminant K_d values for many of the organic chemicals were estimated using the organic carbon partition coefficients (K_{oc}) method described in *Understanding Variation in Partition Coefficient K_d Values* (EPA 1999), and an estimated fractional organic carbon content for Hanford Site sediments of 0.03% (Cantrell et al. 2003). Contaminants for which inventory estimates exist and that do not have an assigned K_d value are assumed to have a $K_d = 0$. A soil material description of low organic, low salt, with a near-neutral pH is assumed. Appendix D contains a complete listing of contaminants and K_d bins. A brief discussion of each major contaminant follows.

Uranium. Uranium mobility is one of the most difficult features of the analysis to estimate. Significant work on uranium speciation and mobility is documented in Knepp (2002b) and Myers (2005). Last et al. (2004b) recommends the best estimate K_d value for uranium selected

for most Hanford Site impact zones and source categories is 0.8 mL/g, with a range of 0.2 to 4. A reference case of 0.6 mL/g is selected for use in the reference case to represent a balance between possible conditions associated with tank wastes near the source and within the much larger vadose zone away from the source.

Technetium-99 (as Pertechnetate). The best estimates for the K_d values of pertechnetate are zero. The ranges were taken to be from zero to 0.1 mL/g for all source and impact zone categories (except gravel corrected). When comparing this range to values tabulated in Cantrell et al. (2002), the range may appear to be somewhat narrow; however, in most cases when higher K_d values were measured, the K_d values were not significantly greater than the standard deviation. As a result of this and the fact that it is known that pertechnetate is a very weak adsorbate, the narrow range for the K_d values was selected.

Iodine-129 (as Iodide). The value selected for the iodide K_d appropriate for most Hanford Site impact zones and source categories is 0.2 mL/g with a range of 0.1 to 2 mL/g. K_d values are assumed to be the same as those for groundwater.

Chromium. The geochemical behavior of chromium has been reviewed by Rai et al. (1988), Palmer and Wittbrodt (1991), Richard and Bourg (1991), and Palmer and Puls (1994). Ball and Nordstrom (1998) present a critical review of the thermodynamic properties for chromium metal and its aqueous ions, hydrolysis species, oxides, and hydroxides. A complete discussion on chromium geochemistry in the Hanford sediments can be found in Krupka et al. (2004).

Chromium(VI) as chromate (CrO_4^{2-}) is likely to be the dominant chromium species in the Hanford vadose zone and upper unconfined aquifer because its domain of predominance extends over a wide range of pH and Eh conditions that are appropriate for the vadose zone and upper unconfined aquifer. Chromium (III) complexes with dissolved ligands such as fluoride, ammonia, and cyanide (Baes and Mesmer 1976).

Limited studies infer that Cr(III), like other +3 cationic metals, is strongly and specifically absorbed by iron and manganese oxides present in soil (Korte et al. 1976). Cantrell et al. (2003) compiled in a single source, K_d values measured with Hanford sediment for radionuclides and CoCs that have potential human health effects in the vadose zone and groundwater at the Hanford Site. Cantrell et al. (2003, Table 10) list the K_d values determined for Cr(VI) for Hanford sediments; they found only a limited number of studies of Cr(VI) adsorption on Hanford sediments. The measured K_d values for Cr(VI) on Hanford sediments range from 0 to 1, with typical values being zero or close to zero, and based on these results, concluded that adsorption of Cr(VI) is very low to nonexistent under normal Hanford groundwater conditions unless conditions are acidic.

Nitrate and Nitrite. The behavior of nitrogen species, such as nitrate, in aqueous, soil, and geochemical systems has been discussed by Lindsay (1979), Lindsay et al. (1981), Stumm and Morgan (1981), Rai et al. (1987), Hem (1986), and others. A large number of studies have been completed related to the chemical and biological processes that transfer nitrogen between the atmosphere, lithosphere, hydrosphere, and biosphere. Nitrate (NO_3^-) is highly mobile and does not sorb or precipitate in sediment systems.

Nitrate is one of the most widespread contaminants associated with past Hanford Site operations. Nitrate does not readily adsorb on minerals under near-neutral and slightly alkaline pH conditions common in sediment systems, and is typically not included in most databases of K_d. Nitrate and nitrite (NO_2^-) are typically assigned K_d values of 0 mL/g. Cantrell et al. (2003) identified only one study in which nitrate adsorption was measured using Hanford sediments. The limited number of K_d values determined for nitrate from this study are listed in Table 12 of Cantrell et al. (2003). Based on these measurements, Cantrell et al. (2003) concluded that within experimental error, nitrate adsorption under Hanford Site relevant conditions is essentially zero (i.e., $K_d = 0$).

Table 3-8 summarizes the contaminant distribution coefficients used for the reference case and the measured ranges in these values for non-impacted soils.

Table 3-8. Contaminant Distribution Coefficients (mL/g) for Non-Impacted Soils [a, b]

Contaminant	Reference Case	Minimum	Maximum
Uranium	0.6	0.2	4
Iodine-129	0.2	0.1	2
Technetium-99	0	0	0.1
Nitrite	0	0	0
Nitrate	0	0	0
Chromium	0	0	0.3

[a] Refers to far-field modeling domain with ambient conditions, and unaffected by past releases and tank leak chemistry.

[b] Last et al. (2004b)

3.4.4.2 Use of Waste Management Areas C and S-SX Breakthrough Curves for Other Waste Management Areas

Detailed contaminant transport calculations using STOMP have only been performed for WMA C and WMA S-SX. Detailed calculations are planned for the other WMAs and will be incorporated into future revisions of the SST PA. To provide an estimate of the human health impacts anticipated from other WMAs that have not been explicitly modeled, the modeling results from WMA C calculations have been used to scale the estimated impacts for other WMAs in the 200 East Area. Similarly, the modeling results from the WMA S-SX calculations have been used to scale the estimated impacts from other WMAs in the 200 West Area. Section 3.2.2.4.8 provides a description of this approach and discusses the reasons why such an approach can provide reasonable estimates for the impacts for other WMAs.

3.4.5 Unconfined Aquifer

For the integrated, saturated-unsaturated, two-dimensional, cross-sectional model up to the WMA fenceline, the flow parameters needed for unconfined aquifer calculations are saturated hydraulic conductivity, effective porosity, hydraulic gradient, and depth to water table. These parameters for WMAs C and S-SX are given in Table 3-9. Estimates of hydraulic properties shown in Table 3-9 are taken from the work of Wurstner et al. (1995) that was used to

develop the Hanford Site groundwater model. Hydraulic gradients are based on the Hanford Site-wide groundwater model (Wurstner et al. 1995; Cole et al. 2001b) estimates of post-Hanford conditions.

Table 3-9. Reference Case Unconfined Aquifer Properties for Waste Management Areas C and S-SX

Property	WMA C	WMA S-SX
Saturated hydraulic conductivity (meters/day)	3,000	25
Effective porosity (unitless)	0.25 (Hanford gravel)	0.10 (Ringold)
Hydraulic gradient (unitless)	1×10^{-5}	5×10^{-4}
Depth to water table (m)	79	78

3.4.6 Exposure Parameters

The reference case analysis exposure scenario for the groundwater pathway is industrial use. For comparative purposes, the all-pathway farmer scenario and residential scenario for ILCR are also considered (Chapter 1.0). The reference case exposure scenarios for the intruder pathway are acute exposure to a well driller and post-intruder rural pasture. Other intruder scenarios considered in this SST PA include the suburban garden and commercial farmer. These exposure scenarios are discussed in Chapter 1.0. The dose parameters are based on Rittmann (2004).

3.4.7 Reference Case

The reference case incorporates the most reasonable and representative information currently available. As more information concerning the waste form, closure design, and closure site locations are gathered, the definition of the reference case is expected to evolve.

The details of the models and related data for the reference case are presented in this section. The major features of the reference case are as follows:

- The future land use of the 200 Areas is envisioned as being a protected area (i.e., with no artificial recharge from irrigated farming).
- The source terms for the risk assessment consist of three separate sources following closure: 1) past releases, 2) residual waste in the tanks following closure, and 3) residual waste in the ancillary equipment following closure (Section 3.4.3.1).
- The release mechanism for past releases is modeled as being transported with natural recharge (Section 3.4.3.1.1).
- The residual tank waste follows the HFFACO goal of 360 ft^3 (10.2 kL) for 100-Series tanks and 30 ft^2 (850 L) for 200-Series tanks or 1% residual waste volume for both 100- and 200-Series tanks (Ecology et al. 1989) (Section 3.4.3.1.2).
- The release mechanism for tank residual wastes is modeled as being diffusion-dominated with a diffusion coefficient of 1×10^{-9} cm^2/sec (Section 3.4.3.1.2).

- The recharge rates before construction of the tank farms, for the tank farm operation period up to year 2032, for the non-degraded barrier (years 2032 to 2532), and for the degraded barrier (years 2532 to 12032) are assumed to be the same for all WMAs in the 200 West Area (3.5, 100, 0.5, and 1 mm/yr, respectively). The recharge rates for the different time periods are assumed to be the same for all WMAs in the 200 East Area (3.5, 100, 0.5, and 1 mm/yr, respectively) (Section 3.4.2).
- The vadose zone flow and transport properties developed from field and laboratory measurements conducted in the 200 Areas were used in the vadose zone modeling to calculate BTCs for contaminants in the groundwater at the WMA C fenceline (Section 3.4.4.1.2).
- The vadose zone flow and transport properties developed from field and laboratory measurements conducted in the 200 Areas were used in the vadose zone modeling to calculate BTCs for contaminants in the groundwater at the WMA S-SX fenceline (Section 3.4.4.1.2).
- The unconfined flow and transport properties for WMAs in the 200 East Area are based on those for WMA C, whereas the properties for WMAs in the 200 West Area are based on those for WMA S-SX (Section 3.4.5).
- The BTCs developed for WMA C for each contaminant source term were used to estimate the BTCs for other WMAs in the 200 East Area (WMAs B-BX-BY and A-AX) (Section 3.4.4.2).
- The BTCs developed for WMA S-SX for each contaminant source term were used to estimate the BTCs for other WMAs in the 200 West Area (WMAs T, TX-TY, and U) (Section 3.4.4.2).

The following sections provide a rationale for the selection of the sensitivity analysis case values and assumptions.

3.5 SENSITIVITY CASES

3.5.1 Overview

This section describes the sensitivity analyses and the associated parameter estimates used to evaluate environmental contamination and human health impacts associated with the tank closure system. The sensitivity analysis provides information (Section 4.11 and Chapter 5.0) that addresses the following issues:

- How well can the performance of the closure system be estimated?
- How important are the "barriers" to the performance of the system?
- What is the value of additional information to reduce estimated uncertainty?

These issues arise largely because of inherent variability within the tank closure system. Heterogeneities in the natural system, long-term degradation of engineered barrier performance, and future human actions can affect future environmental contamination. Such variability generates uncertainty about real-time contaminant migration characteristics and limits the ability of the modeler to adequately portray system features and processes that affect future

environmental contamination levels (e.g., predictive uncertainty). Because tank closure system variability cannot be completely resolved (also referred to as irreducible variability), a range of future environmental impacts are estimated that account for effects of this variability and provide a qualitative measure of uncertainty. To complete these estimates, a suite of sensitivity cases has been formulated in which variability was quantified as ranges of modeling input parameter values that envelope reference case values. The resulting set of changes in estimated environmental (e.g., groundwater) contamination levels in combination with reference case results provided ranges of plausible future contamination levels caused by tank closure system variability effects.

Of the three major pathways (i.e., groundwater, air, and intruder), the most complicated analysis involves the groundwater pathway. Contaminant migration through the subsurface is influenced by all major components of the closure system. Therefore, the greatest amount of potentially significant parameter variability is associated with this pathway. As with the reference case analysis (Section 3.4), the bulk of this section is devoted to this pathway. Section 3.5.2 is a description of the sensitivity analysis methodology; Sections 3.5.3 and 3.5.4 describe selected cases and associated parameters and parameter values.

Sensitivity analyses for the intruder pathway were focused on a range of human activities (e.g., scenarios) that cause variable levels of exposure to contaminants. Four exposure scenarios, one acute and three chronic, are described in Chapter 5.0, and parameter changes affecting the assumed amounts of exhumed waste and degree of mixing with soil are summarized in Section 3.5.5. No sensitivity analyses were conducted for the air pathway. The air pathway analysis is a bounding analysis that provides an implausible maximum environmental impact that satisfies the regulatory criteria (Section 3.5.6). Consequently, a sensitivity analysis was considered unnecessary.

Groundwater pathway sensitivity analyses provided a plausible range of future groundwater contamination levels derived from closure system variability effects.

Sources of variability include natural system heterogeneities, long-term engineered barrier performance degradation, and future human actions.

Intruder pathway sensitivity analyses estimated human heath effects for various human activity exposure scenarios and exposure pathways.

3.5.2 Sensitivity Analysis Methodology for the Groundwater Pathway

The methodology for the groundwater pathway uses a deterministic approach to calculate a plausible range of future groundwater contamination levels at the WMA fenceline that is generated by site-specific closure system variability and encompasses the reference case result. This approach is deterministic because potential groundwater contamination levels are determined for discrete parameter values that define ranges in parameter (e.g., minimum, reference case, and maximum values). Collectively, the suite of analytical results defines a finite range of plausible future groundwater contamination levels. Although there is a qualitative expectation that the actual groundwater contamination levels should tend toward the reference case estimate (e.g., the purpose of the reference case assumptions is to provide the best estimate of actual closure system conditions), the analyses do not assign a likelihood of occurrence to a

particular outcome. These results contrast with those provided by a probabilistic/stochastic approach, in which a continuum of parameter values are often considered and their likelihood of occurrence is assumed. These assumptions are then propagated through the analysis to a set of realizations where the likelihood of a particular outcome occurring can be calculated.

The approach described herein was selected for the following reasons:

- Closure system performance is being compared with respect to numerous deterministic criteria (e.g., groundwater protection criteria and various human health effects). Comparison of deterministic criteria with deterministic analytical results provides a transparent indication of acceptable or unacceptable performance.
- The available database describes the major features and processes affecting contaminant transport in some detail (e.g., precipitation and infiltration rates, subsurface hydrogeologic characteristics, contaminant-specific geochemical behavior) and is amenable to the quantification of minimum and maximum values of critical parameters. The database, for the most part, is not considered adequate to assign probability distribution functions to various parameters.
- Manipulation of single and multiple changes in parameter values coupled with associated changes in future groundwater contamination levels provides insight into the relative importance of various features and processes affecting contaminant transport. These results also provide estimates of plausible variability in future groundwater contamination levels (e.g., uncertainty around the reference case outcome) and illustrate the estimated range of plausible outcomes due to irreducible system variability.
- This approach identifies additional important data needs. Importance is defined as data that are currently unavailable and are needed to better quantify a parameter value range that may generate relative large changes in projected groundwater contamination levels.

A flow chart of the sensitivity case methodology for the groundwater pathway is provided in Figure 3-13. In this methodology, sensitivity cases were derived to evaluate the effects of system variability, groundwater contamination analyses were completed for each case, and comparisons of sensitivity case results (estimated groundwater contamination levels at the WMA fenceline) to reference case results were made.

Initially, sensitivity cases were derived from the reference case modeling assumptions (Section 3.2-3.4) which defined the following:

- Site-specific closure system features and processes affecting contaminant migration
- Parameters that describe these features and processes
- Site-specific reference parameter values.

Figure 3-13. Modeling Approach for Evaluating Closure System Variability Effects on Estimated Future Groundwater Contamination Levels Relative to Reference Case Results

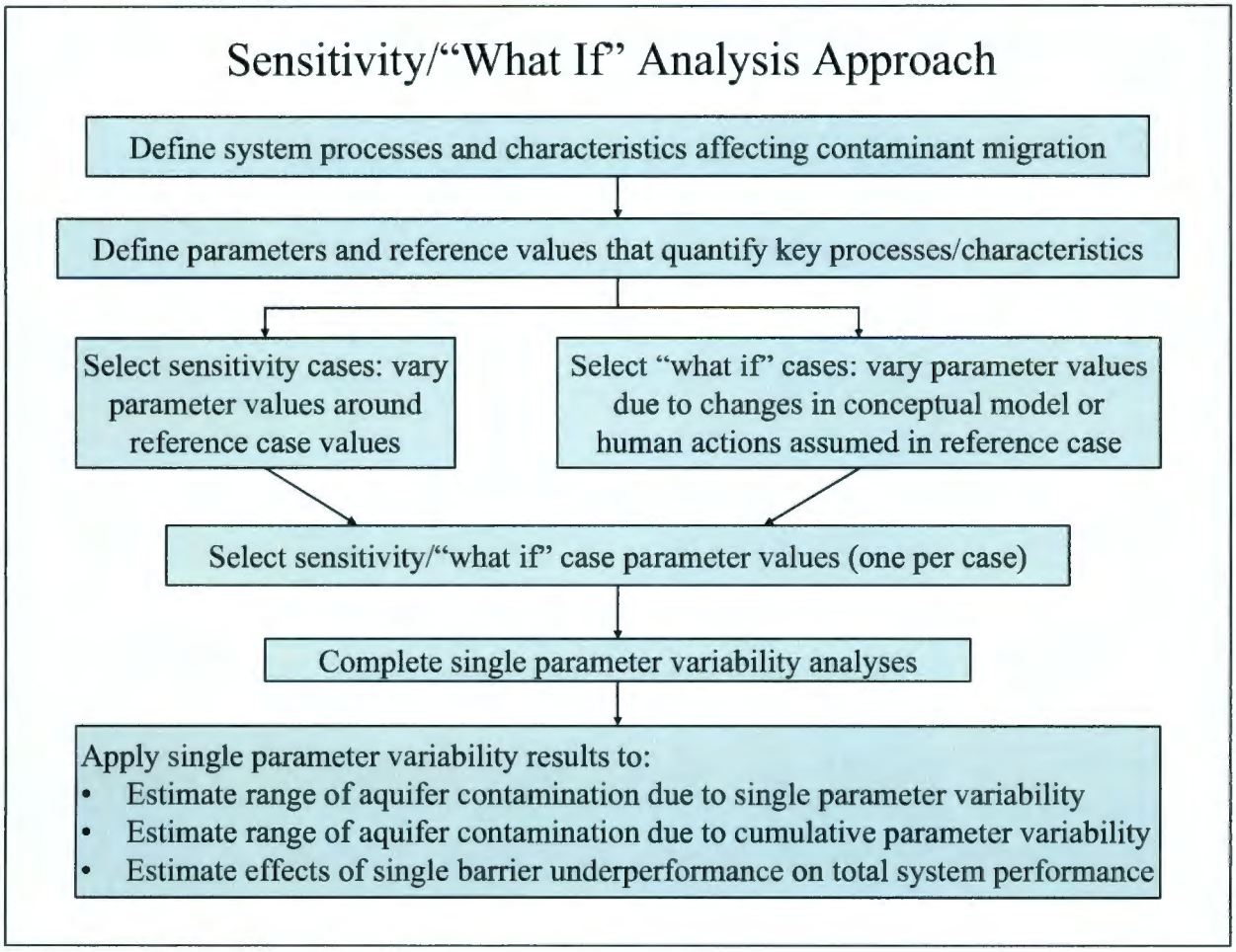

Critical features and processes included site-specific natural system characteristics such as low infiltration rates, a thick vadose zone, the current distribution of contaminants with the vadose zone, and engineered components including the surface barrier, and the grouted tank structure. Significant processes included unsaturated flow in the vadose zone, contaminant-specific geochemical reactivity with the subsurface sediments, and mixing of contaminated vadose zone water with clean unconfined aquifer water. Parameters describing these features and processes fell into three broad categories: recharge rates, waste characteristics (e.g., inventory and release mechanisms), and geohydrologic properties of the vadose zone and unconfined aquifer.

To proceed with the sensitivity analysis, two types of cases were distinguished, sensitivity cases and "what if" cases. The sensitivity cases (Section 3.5.3) assumed all primary reference case assumptions were unchanged and simply varied parameter values with respect to reference case values. In the "what if" cases (Section 3.5.4), alteration of postulated reference case assumptions affecting contaminant migration was assumed (e.g., different physical or chemical processes or human actions that altered system conditions). To represent these different assumptions,

different parameter estimates were considered. In these analyses, only contaminant migration to the WMA fenceline and only migration from waste sources in WMAs C and S-SX (representing 200 East and West Area geohydrology, respectively) were considered. Also, sensitivity analysis results were only generated for constituents that reached the unconfined aquifer in reference case analyses.

Each sensitivity and "what if" case usually assumed a change in one parameter value and, in some cases, the substitution or addition of a parameter relative to the reference case. By grouping cases that considered value changes to the same parameter for specific contaminants present in specific waste sources, a value range for a given parameter was generally defined by at least three values, a reference case value, a minimum value, and a maximum value. For example, the reference case operational period recharge rate was 100 mm/yr and two sensitivity cases were generated that assumed operational period recharge rates of 40 and 140 mm/yr to define the minimum and maximum values, respectively (Section 3.5.3.1). Then, by completing a contaminant migration analysis that estimated the groundwater impacts for each sensitivity/"what if" case and associated parameter value change within each parameter group, a range of groundwater contamination levels was generated in response to parameter value change.

Changes in groundwater contamination levels at the WMA fenceline in response to parameter value changes were calculated and, for ease of comparison, expressed as ratios of the peak groundwater contamination levels from the sensitivity case to peak levels estimated in the reference case (Sections 4.11.1 through 4.11.4). These ratios, referred to as peak ratios, indicated the sensitivity of contaminant migration to variability of a particular parameter because each ratio was associated with specific single parameter value changes (e.g., single parameter variability). Estimated increases or decreases in groundwater contamination levels were indicated by peak ratio values greater or less than unity, respectively. Relatively larger or smaller ratios for given parameter ranges indicated greater sensitivity of groundwater contaminant levels to variability of the feature or process represented by the parameter. These ratios also indicated uncertainty around the reference case estimate with respect to variability of a particular parameter. That is, the plausible range of estimated groundwater contamination levels was constrained by the plausible range of site-specific parameter values determined from site-specific data.

The results of the single parameter variability analyses were then used for two additional applications, a cumulative variability analysis (Section 4.11.4.5) and a barrier underperformance analysis (Section 4.11.5). The calculation processes for these two applications are provided in their respective sections. The cumulative variability analysis estimated the effects of multiple and simultaneous parameter value changes on groundwater contamination levels for given contaminant/waste type combinations. Because the effects of variability in all significant parameters were considered at once, a cumulative uncertainty in peak groundwater contamination levels with respect to the reference case estimates was provided.

The barrier underperformance analysis estimated the effects of single or multiple barrier underperformances (i.e., the surface barrier, the grouted tank structure, and/or the vadose zone) on total system performance with respect to reference case assumptions. In these analyses, parameters describing barrier functions and associated sensitivity/"what if" case results were

selected. Using peak ratios, underperformance factors were calculated to estimate the potential increases in groundwater contamination levels with respect to degradation of single or multiple barriers. Again, because estimated groundwater contamination increases were tied to plausible parameter value ranges, uncertainty in system performance was estimated.

3.5.3 Estimated Ranges for Selected Parameters in Groundwater Pathway Sensitivity Cases

Estimated ranges for recharge, contaminant release from residual waste and past releases, vadose zone parameters, contaminant distribution coefficients, and unconfined aquifer parameters are discussed in Sections 3.5.3.1 through 3.5.3.5.

3.5.3.1 Recharge

As discussed earlier, recharge is a major driver for contaminant transport from various waste forms to groundwater and to an eventual receptor. Recharge information is needed for four time periods associated with tank farm closure: 1) prior to construction of tank farms, 2) during tank farm operations, 3) the period when the emplaced surface barrier performs as designed, and 4) the period when the surface barrier performance is degraded. Although site-specific infiltration data are being collected in the BX, S, and T tank farms for the operation period, insufficient data are available for site-specific estimates of natural infiltration for a given WMA. Based on results of long-term lysimeter experiments, a reference value (100 mm/yr) is used in this assessment for the present-day, gravel-covered tank farms, before placement of the Modified RCRA Subtitle C Barrier. This value is based on 9 years of testing at the Field Lysimeter Test Facility for a surface treatment of "sandy gravel side slope" (Fayer and Szecsody 2004, p. A.20) and is rounded upward from the reported value of 99.8 mm/year (Fayer and Szecsody 2004, p. 7.8).

To examine the effect of expected ranges in this parameter, a lower value (40 mm/yr) and a higher value (140 mm/yr) were selected. The 140 mm/year is the result of an enhanced precipitation experiment on the "sandy gravel side slope" treatment. This treatment is referenced as "useful for characterizing deep drainage at the high-level waste tank farms at Hanford" (Fayer and Szecsody 2004, p. A.6). Enhanced precipitation represented three times the average precipitation. Approximately 140 mm of the precipitation was observed to have infiltrated.

The lower value is supported by the prototype barrier testing summary results from Wittreich et al. (2003). On the basis of 7 years of monitoring data, Wittreich et al. (2003) reported that the annual drainage rate of 21.5% of precipitation (37.8 mm/yr) through sparsely vegetated sandy gravel representing the "sandy gravel side slope" became recharge. Such a percentage (i.e., 21.5%) represents a lower value of approximately 40 mm/yr.

The surface barrier is an important engineered barrier for a WMA. Once it is emplaced, the surface barrier performance directly impacts the recharge into the WMA. The current pre-conceptual design of the Modified RCRA Subtitle C Barrier is based on DOE-RL (1996). The barrier is designed to provide containment and long-term hydrologic protection for a period of 500 years and consists of 8 layers. The design accounts for human and biointrusion control, and is based on a silt loam moisture storage unit and a capillary break. The thickness of the

surface cover over the WMAs is assumed to be at least 5 m. The barrier is assumed to be thick enough to ensure that the waste resides at a depth of at least 5 m below the barrier surface.

Recent work (Fayer and Szecsody 2004) recommends an expected performance for such a barrier to be on the order of 0.1 mm/yr for the life of the barrier. The report also concludes that, with appropriate design considerations, the possibility of the most likely natural failure mechanisms (i.e., biointrusion of the silt loam layer, wind erosion, and accretion of wind blown sand) to occur is quite low, and that the emplaced silt-loam soils will continue to perform as designed. Fayer and Szecsody work has not been extended to address the range of conditions that might be encountered leading to a decline in performance of surface barriers placed on tank farms. For this reason, and due to the lack of any detailed surface barrier design for tank farm closure, the reference case infiltration rate is set at 0.5 mm/yr for the first 500 years of the simulation. This value is the performance requirement used for the design of the Hanford barrier. A range of 0.1 to 1.0 mm/yr is selected to address the expected range in this parameter over the 500-year design life for the barrier. The reference infiltration rate is five times above the recommended reference value (Fayer and Szecsody 2004). The upper range of 1.0 is simply 10 times the expected performance estimate of 0.1 mm/yr, while the lower estimate is the expected performance recommendation (Fayer and Szecsody 2004). Given that the source of construction materials are identical for the tank farm barriers and for the Integrated Disposal Facility PA assumed in Fayer and Szecsody's work, a barrier design value of 0.5 mm/yr is considered easily attainable and will likely be improved as the tank farm closure project advances.

At the end of 500 years, the surface barrier infiltration rate is assumed to degrade to 1.0 mm/yr and maintain that infiltration rate for the remainder of the simulation. A range of 0.5 mm/yr to 3.5 mm/yr for the 200 East and 200 West Area is further assumed. The upper ranges are based on soil types and infiltration characteristics of the native soils as reported in *Geographic and Operational Site Parameters List (GOSPL) for the 2004 Composite Analysis* (Last et al. 2004b). The lower range represents a case whereby the surface barrier remaining intact. Currently, only the assumed performance of the barrier is simulated.

3.5.3.2 Contaminant Release from Tank Residual Wastes and Past Releases

The reference case assumes that the rate at which the grouted tank residual waste is made available for transport to groundwater is through the process of diffusion (Section 3.4.3.1.2). No allowance is made for other potential barriers (such as the tank structure) that would likely delay release.

The DOE Office of River Protection has identified three distinct functions for tank fill (Lee 2004). Grout formulations are designated to correspond to each of these three different functions:

- Stabilizing grout to eliminate residual liquid and stabilize contaminants in the tank residues
- Structural grout to provide structural support
- Capping grout to provide an intruder barrier.

Leaching tests (ANSI/ANS 16.1) of stabilizing grout formulations on simulated Hanford Site tank wastes led to the following recommendation (Harbour et al. 2004, p. 2):

> "Calculations of the effective diffusivities using measured Tc-99 values resulted in D_e of 1.9 E-09 to 2.1 E-10 cm^2/sec. The range using plus/minus 2 sigma (standard deviation) values for the Tc-99 concentrations gave an overall range from 1.3 E-09 to 1.1 E-14 cm^2/sec. These data can be used in support of PA calculations."

For this SST PA, a minimum D_e of 1 E-14 cm^2/sec and a maximum D_e of 1 E-8 cm^2/sec are used.

Past Releases. The estimate of past tank leaks and spills from tank farms into the vadose zone has undergone significant investigation in the past few years. Releases within a tank farm are highly variable with the largest leaks found in SX and T tank farms (Field and Jones 2005). The association of past releases with the specific operational history for each WMA requires an estimate of an expected range of release be developed on a WMA-specific basis. Tables 3-10 and 3-11 present such an evaluation for WMAs C and S-SX, respectively. All estimates are provided in gallons. Inventories of radiological and nonradiological contaminants will be linearly scaled based on the contaminant concentration estimates provided for the reference case and listed in Corbin et al. (2005).

The range in the maximum and minimum release volume estimates are conditioned on the available information for each event. Well-documented tank leaks and spills generally have low variability, while smaller tank leaks and spills have larger variability.

Table 3-10. Estimates of Ranges for Past Releases Within Waste Management Area C [a]

Tank/Spill	Reference Case Leak Volume gal	Minimum Leak Volume gal	Maximum Leak Volume gal	Comments
C-101	1,000	500	5,000	Liquid losses from this tank are adequately explained by evaporative cooling.
C-105	1,000	500	1,000	Vadose zone contamination most likely came from pipe leaks.
C-110	2,000	500	2,000	—
C-111	5,500	500	5,500	Historical data show that the liquid level decreases are associated with evaporative cooling.
C-201	550	550	1,000	Liquid losses are likely due to evaporation.
C-202	450	450	1,000	Liquid losses are likely due to evaporation.
C-203	400	400	1,000	Liquid losses are likely due to evaporation.
C-204	350	350	1,000	Liquid losses are likely due to evaporation.

[a] Unplanned releases and ancillary equipment releases are provided in Table 3-1.

Table 3-11. Estimates of Ranges for Past Releases Within Waste Management Area S-SX [a]

Tank/Spill	Reference Case Leak Volume gal	Minimum Leak Volume gal	Maximum Leak Volume gal	Comments
S-104	24,000	19,000	29,000	Well-documented leak volume. Assumed range is 20% of reference case.
SX-104	6,000	500	6,000	Liquid losses are likely due to evaporation.
SX-107	15,000	5,000	20,000	—
SX-108	35,000	15,000	50,000	—
SX-109	2,000	1,000	5,000	—
SX-110	1,000	500	1,000	—
SX-111	500	500	2,000	—
SX-112	1,000	500	5,000	—
SX-113	15,000	12,000	18,000	Well-documented leak volume. Assumed range is 20% of reference case.
SX-114	500	500	1,000	—
SX-115	50,000	40,000	60,000	Well-documented leak volume. Assumed range is 20% of reference case.

[a] Unplanned releases and ancillary equipment releases are provided in Table 3-1.

3.5.3.3 Vadose Zone Parameters

Sensitivity analysis associated with unsaturated flow parameters has been conducted in the past (DOE-RL 1999; Mann et al. 2001). Historical work (e.g., Mann et al. 2001) indicates this feature of the system is generally of secondary importance to others, such as recharge rates and inventory estimates of past releases. For the purpose of this SST PA, to account for sensitivity of unsaturated flow parameters, the saturated hydraulic conductivity is used as a scaling factor; the parameter variability is assumed to have a range of $\pm$ one order of magnitude from the reference case.

As discussed earlier (Section 3.2.2.4.7), the effect of discrete features such as clastic dikes on vadose zone flow and transport were investigated in Knepp (2002a). Specific simulations were run to evaluate the effects of clastic dikes on the peak groundwater concentration at the WMA fenceline in the S-SX FIR (Knepp 2002a). As discussed in Section 3.2, simulated groundwater peak concentrations for long-lived mobile radionuclides were not significantly different for simulation cases with or without dikes. However, as discussed later, a case is simulated where a retrieval leak of 8,000 gal is assumed to occur for a 100-Series tank in the vicinity of a postulated clastic dike.

3.5.3.4 Contaminant Distribution Coefficients

Table 3-8 presents a summary of the reference case, and maximum and minimum ranges of contaminant K_d values for contaminants affecting risk through the groundwater pathway. These K_d values have been used for contaminant transport calculations through the vadose zone and through the unconfined aquifer to the WMA fenceline.

3.5.3.5 Unconfined Aquifer Parameters

Two distinct hydrologic regimes must be considered when examining the potential range of unconfined aquifer properties. Groundwater within the western portion of the Central Plateau is contained within the Ringold Formation, while groundwater within the eastern portion of the Central Plateau is generally found in the Hanford formation. The Ringold Formation is a semi-indurated, intercalated, coarse-grained fluvial sequence. For the Ringold Formation, variability in aquifer properties is generally low in comparison to the Hanford formation. The Hanford formation is predominately fluvial sand and gravel, often composed of open framework gravels having extremely high transmissivities.

Saturated media variables that impact modeling results include horizontal hydraulic conductivity, effective porosity, and hydraulic gradient. Hydraulic properties have been measured over the past 50 years and are documented in a number of reports (DOE 1988; Thorne and Newcomer 1992; and more recently, Wurstner et al. 1995). The aquifer saturated hydraulic conductivity in the vicinity of WMA S-SX is generally quite low, increases to the north, and finally decreases toward the northern edge of the 200 West Area. Hydraulic conductivities in the 200 East Area are generally much higher and are highly dependent on the presence of fine or coarse aquifer materials. Ranges of hydraulic properties shown in Tables 3-12 and 3-13 are based on Wurstner et al. (1995) and were used to develop the Hanford Site groundwater model. Much less information is available on the variability in porosity for either formation. Effective porosities shown in Tables 3-12 and 3-13 are the values generally used for the respective formations (Khaleel et al. 2000, 2001). Hydraulic gradients are based on the Hanford Site-wide groundwater model (Wurstner et al. 1995; Cole et al. 2001b) estimation of post-Hanford conditions. Tables 3-12 and 3-13 provide estimates for WMAs C and S-SX, respectively, of the recommended ranges for aquifer properties for use in the sensitivity analysis.

Table 3-12. Unconfined Aquifer Properties for Waste Management Area C

Property	Reference Case	Minimum	Maximum
Hydraulic conductivity (m/day)	3,000	2,000	4,000
Effective porosity (unitless)	0.25 (Hanford gravel)	NC	NC
Hydraulic gradient (unitless)	0.00001	NC	NC
Depth to water table (m)	79	NC	NC

NC = not considered

Table 3-13. Unconfined Aquifer Properties for Waste Management Area S-SX

Property	Reference Case	Minimum	Maximum
Hydraulic conductivity (m/day)	25	7.5	50
Effective porosity (unitless)	0.1 (Ringold)	NC	NC
Hydraulic gradient (unitless)	0.0005	NC	NC
Depth to water table (m)	78	NC	NC

NC = not considered

Table 3-14 provides a summary of the parameters and their ranges for the natural and engineered barriers and features for the closed WMA. The minimum and maximum parameter ranges were used in the sensitivity analysis.

Table 3-14. Groundwater Pathway – Summary of Reference Case Parameters and Expected Ranges

Natural and Engineered Barriers/Features	Feature/Process	Reference Case	Parameter Range	
			Minimum	Maximum
Surface cover	P1: Infiltration	An infiltration rate of 100 mm/yr for the reference case during tank farm operation up to year 2032.	40 mm/yr	140 mm/yr
	P2: Infiltration	An infiltration rate of 0.5 mm/yr for the reference case for the barrier from years 2032 to 2532.	0.1 mm/yr	1.0 mm/yr
	P3: Infiltration	An infiltration rate of 1.0 mm/yr for the reference case for the barrier from years 2532 to 12032.	0.5 mm/yr	3.5 mm/yr
Grouted tank structure	P4: Residual release – Diffusion coefficient	Diffusion-dominated release for residual tank wastes with a diffusion coefficient of 1×10^{-9} cm^2/sec for the reference case.	1.0 E-14 cm^2/sec	1.0 E-8 cm^2/sec
	P5: Waste residual – Inventory	1 in. of waste	0.1 in. of waste residual	10 in. of waste residual
Vadose zone	P6: Past leaks depth – 200 East	150 ft bgs	130 ft bgs	170 ft bgs
	P7: Past leaks depth – 200 West	130 ft bgs	110 ft bgs	150 ft bgs
	P8: Past releases – Inventory	Reference case inventory	See discussion in Section 3.5.3.2	See discussion in Section 3.5.3.2
	P9: Unsaturated flow	Variation of unsaturated hydraulic conductivity via K_{sat} (defined for each vadose zone layer).	K_{sat} * 0.1 for each layer	K_{sat} * 10 for each layer
	P10: Uranium K_d	Reference case uranium of 0.6 mL/g	0.2 mL/g	4 mL/g
	P11: Iodine K_d	Reference case iodine of 0.2 mL/g	0.1 mL/g	2 mL/g
	P12: Technetium K_d	Reference case technetium of 0.0 mL/g	0 mL/g	0.1 mL/g
Unconfined aquifer – 200 East WMAs	P13: Hydraulic conductivity	3,000 m/day	2,000 m/day	4,000 m/day
	Effective porosity	0.25	NC	NC
	Hydraulic gradient	0.00001	NC	NC
	Depth to water table	79 m	NC	NC
Unconfined aquifer – 200 West WMAs	P14: Hydraulic conductivity	25 m/day	7.5 m/day	50 m/day
	Effective porosity	0.1	NC	NC
	Hydraulic gradient	0.0005	NC	NC
	Depth to water table	78 m	NC	NC

NC = not considered

* indicates multiply by the number.

3.5.4 Estimated Ranges for Selected Parameters in Groundwater Pathway "What if ...?" Cases

The reference case analysis represents the expected performance of the closed tank system. This section examines a number of postulated conditions or alternatives that, though considered less likely than the reference case, could potentially occur. The ability of the system to perform as expected even under these "unlikely" conditions is considered a measure of the robustness of the SST closure system. Should the results of these analyses show an unacceptable degradation of the WMA closure system performance, two options are available:

- The approach to retrieval and/or the design of the engineered system can be changed to provide an additional level of security, or
- Additional characterization of the system may be necessary to better determine the presence or absence of a problematic feature or to better characterize the natural feature leading to the unacceptable performance.

Table 3-15 summarizes the alternative or "what if" conditions examined. The likelihood of each set of scenarios is considered small but nonetheless presents an element under the philosophy of defense in depth that is considered important in investigating the level of protectiveness for the reference case (see defense in depth discussion in Section 1.6).

For the purposes of "what if" simulations, the condition stated in the alternative is addressed keeping all other features of the closure system unchanged. Unless stated otherwise, analyses are conducted on WMAs C and S-SX. The "what if" cases are grouped according to the key barriers and features identified in Section 1.7 as follows:

- Section 3.5.4.1 describes the "what if" conditions for the **surface barrier**
- Section 3.5.4.2 describes conditions for **potential retrieval leaks**
- Section 3.5.4.3 describes conditions for the **closed SSTs**
- Section 3.5.4.4 describes conditions for the **vadose zone**
- Section 3.5.4.5 describes "what if" conditions for the **exposure parameters**.

Table 3-15. Alternatives to the Reference Case or "What if" Conditions for the Examination of the Level of Protectiveness Provided by the Reference Case for the Protection of Groundwater (3 pages)

Barrier/Feature	Alternative	Condition	Description/Action
Surface Barrier	A1	What is impact of closing the farm before year 2032?	An earlier (year 2020) placement of the final closure interim barrier (as opposed to year 2032 for the reference case)/sensitivity case.
	A2	What is the impact of not closing the farms by year 2032?	A later (year 2050) placement of the final closure barrier will be examined/sensitivity case.
	A3	What is the impact of an interim barrier by year 2010 over major leaks?	An interim barrier will be placed over the large leaks in WMAs S-SX and C beginning in the year 2010/sensitivity case.
	A4	What is the impact of episodic infiltration?	The impacts of episodic infiltration are considered sufficiently analyzed in past work by Smoot et al. (1989). The results will be summarized, as appropriate.
	A5	What if the barrier subsides?	Degradation of the effectiveness of the barrier due to localized subsidence. It is believed that any useful analysis of this issue at this time requires a more advanced closure and barrier design conceptualization.
	A6	What if irrigated farming occurs after the loss of passive control (500 years)?	Based on information in Mann et al. (2001), an enhanced infiltration rate of 50 mm/yr is assumed to occur over the closed tank farm with the cover assumed removed. Enhanced infiltration would begin at the end of passive institutional controls/sensitivity case.
	A7	What if the barrier fails at the end of passive controls?	Assume that the barrier fails at the end of passive controls (500 years). Failure is assumed through loss of silt-loam mix and infiltration increases to background of 3.0 mm/yr in the 200 East Area and 4.0 mm/yr in the 200 West Area (Last et al. 2004b)/sensitivity case.
	A8	What if the barrier fails prior to the end of passive controls?	Assume that the barrier fails at the end of 300 years. Failure is assumed through loss of silt-loam mix and infiltration increases to background of 3.0 mm/yr in the 200 East Area and 4.0 mm/yr in the 200 West Area (Last et al. 2004b)/sensitivity case.

Table 3-15. Alternatives to the Reference Case or "What if" Conditions for the Examination of the Level of Protectiveness Provided by the Reference Case for the Protection of Groundwater (3 pages)

Barrier/Feature	Alternative	Condition	Description/Action
Grouted Tank/ Structure	A9a	What if the 100-Series tanks leak during retrieval?	9a: Simulate a retrieval leak loss of 8,000 gal per tank for a 100-Series tank that is assumed to be by the modified sluicing retrieval method/sensitivity case.
	A9b		9b: Simulate a retrieval leak loss of 20,000 gal per tank for a 100-Series tank that is assumed to be retrieved by the modified sluicing retrieval method/sensitivity case.
	A10	What if retrieval leaks occur at the 200-Series tanks, regardless of the use of dry retrieval methods?	Simulate the effects of a 400-gal leak for each 200-Series tank/sensitivity case.
	A11	What if the grout does not provide the level of encapsulation expected?	Conduct a bounding analysis of this situation based on the assumption of an advection-dominated release for residual tank wastes/sensitivity case.
	A12	What if more tank waste residual is left than expected?	This possibility is addressed in the sensitivity analysis of possible ranges of tank residue (Table 3-14).
	A13	What if a retrieval leak occurs over a past leak prior to tank stabilization?	Simulate an 8,000-gal retrieval leak occurring over a past leak.
	A14	What if the tanks behave like a "bathtub" and collect water, which then releases suddenly?	The void space left within the tank after grout fill is minimal that this is considered a highly unlikely scenario and is bounded by other analyses.

Table 3-15. Alternatives to the Reference Case or "What if" Conditions for the Examination of the Level of Protectiveness Provided by the Reference Case for the Protection of Groundwater (3 pages)

Barrier/Feature	Alternative	Condition	Description/Action
Vadose Zone	A15	What if potential preferential paths were missed during characterization?	Incorporate clastic dike effects for the retrieval leak simulation of 8,000 gal for a 100-Series tank that is assumed to be retrieved by the modified sluicing retrieval method.
	A16	What if the groundwater level does not decline as projected?	Simulate the effect by decreasing the vadose zone thickness by 2 m/sensitivity case.
	A17	What if the depths of past leaks were underestimated?	This contingency is addressed in the sensitivity analysis (Table 3-14).
	A18	What if past leak contamination were underestimated?	This contingency is addressed in the sensitivity analysis (Table 3-14).
	A19	What if remediation of up to 50% of past leaks were possible?	Simulate the removal or immobilization of 5%, 25%, and 50% of mobile contaminants from past leaks/sensitivity case.
	A20	What is the effect of assuming anisotropy for the vadose zone geologic units?	Simulate assuming isotropic saturated hydraulic conductivity for the individual geologic units within the vadose zone.

3.5.4.1 Surface Barrier

The first eight alternatives in Table 3-15 examine impacts to the reference case associated with the timing and performance of the surface barrier. Alternatives 1 and 2 address the timing of the placement of a barrier to infiltration. Currently, all WMAs are projected for closure by year 2032 per Milestone M-45-00 as found in the HFFACO (Ecology et al. 1989). The first two alternatives examine the importance of the timing of the final barrier over the entire farm, assuming an early closure in year 2020 and a late closure in year 2050.

The third alternative examines the importance of interim barriers over known past releases. An interim barrier is defined as a temporary barrier that would be installed to protect groundwater resources prior to complete retrieval and final closure of a tank farm. This alternative only postulates such a barrier over limited areas in deference to the potential impacts such a barrier might have on delaying final closure due to interference with field activities. The interim barrier is assumed to be installed over the largest tank leak or spill in WMAs S-SX and C starting in the year 2010.

The impacts of episodic infiltration (alternative 4) were addressed previously in Smoot et al. (1989). Smoot et al. (1989) addressed infiltration of meteoric water through sediments at the SST farms and the impact of this transient infiltration on contaminant plume movement for evaluating alternative remedial actions (i.e., interim barriers) for leaking SSTs at the Hanford Site. The results of this investigation are used to justify the use of temporally averaged infiltration rates for long-term simulations.

Subsidence of the barrier (alternative 5) is not expected to be a significant issue in the closure of tank farms. Large voids will be grouted and the surface cover will be designed to minimize the impacts of belowground subsidence should it unexpectedly occur and alter the performance of the surface barrier. An applicable and useful analysis of subsidence requires the development of a subsidence causing event and the propagation of the effects of such an event to the surface barrier. For such an analysis to have any value in the design process, the closure process including the barrier design needs to progress to a more complete state.

Alternatives 6 through 8 address the impacts to groundwater should the barrier effectively fail to provide the long-term reduced infiltration rates assumed for the closure system. This would require a significant breakdown in institutional controls. Alternatives 7 and 8 assume that such a breakdown occurs in 500 and 300 years, respectively, after closure. Infiltration is assumed to return to background conditions of 4 and 3 mm/yr for the 200 West and East Areas, respectively (GOSPL [Last et al. 2004b]).

Alternative 6 adds the extremely unlikely condition that after the barrier is removed, active farming occurs on the barrier site. Recharge associated with this alternative follows the approach outlined in the 2001 Hanford immobilized low-activity waste PA (Mann et al. 2001) and 200 East and 200 West Area solid waste burial ground PAs (Wood et al. 1995a, 1996). Recharge assumed from irrigated farming is assumed to average 50 mm/yr. This represents an overestimate of the irrigation volume available for infiltration. Historical estimated natural recharge rates range from 0.1 to 10 mm/yr depending on the crop and water management practices. Wine grapes would have the least recharge, while field crops would potentially have

the greatest deep percolation losses (recharge). This analysis assumed a 50 mm/yr rate of infiltration that is initiated at the end of passive controls.

3.5.4.2 Potential Retrieval Leaks

Alternatives 9a, 9b, 10, and 13 in Table 3-15 address alternatives to the reference case associated with the retrieval or processing of the tank waste. The reference case assumes that modified hydraulic sluicing will be used to retrieve waste from all 100-Series tanks considered sound. As alternative cases (9a, 9b, and 13), leaks of 8,000 gal, 20,000 gal, and 8,000 gal over a past leak, respectively, are analyzed for each of the 100-Series tanks assumed to be retrieved by modified sluicing methods. Each analysis is conducted separately to allow the impacts of the differing retrieval methods to be analyzed. Tanks in the 100-Series retrieved using the mobile retrieval system are not assumed to leak during retrieval. Alternative 10 considers a 400-gal leak for the 200-Series tanks.

Assumptions and Justifications for Retrieval Leaks. For retrieval leaks, the following simplifying assumptions were made:

- Hypothetical retrieval leaks of 8,000 gal (alternative 9a) and 20,000 gal (alternative 9b) were assumed from each 100-Series SST that is planned to be retrieved using the modified sluicing process. Known or suspected leakers are assumed to be retrieved using a process with limited water usage; therefore, retrieval leaks are not anticipated for these tanks.
- The retrieval leaks are modeled as starting on January 1, 2000, and leaking at a uniform rate for 14 days.
- All the leaked inventory is readily available for transport with the infiltrating water where transport is only limited by chemical adsorption to the soils.

By assuming that a leak occurs from every 100-Series tank planned to be retrieved using the modified sluicing process, it is possible that a maximum waste volume could infiltrate into the vadose zone. The difference between the actual and presently assumed lost waste volumes may be quite large as only a few tanks have given a clear indication of substantial loss of containment. Also, there was no evidence of a leak during the retrieval of C-106 tank waste (Lee 2004).

The simplifications for estimating the contribution to the BTCs for potential retrieval leaks are reasonable for the following reasons:

- The assumption of a lower leak volume (i.e., 8,000 gal) as a representative leak volume is based on estimates assigned to what leak volumes would be detectable during a sluicing retrieval process. Tank liquid level measurement accuracy is estimated to be approximately ± 1 in., which corresponds to approximately 3,000 gal. The 8,000-gal estimate was selected to represent detection under conditions where the tank is being sluiced. Such an estimate of 8,000 gal per tank has been used in earlier retrieval PAs (e.g., DOE-RL 1999).
- Assigning a date of January 1, 2000, for the leak is early and results in estimated concentrations from such leaks arriving at the unconfined aquifer earlier than would be estimated with actual leak dates.

- The 14-day leak duration assumed for the simulation is arbitrary; however, given the averaging that occurs in transport through the vadose zone, the resulting impact is relatively insensitive to this parameter.
- As an alternative case to an 8,000-gal leak, leaks of 20,000 gal are analyzed for each of the 100-Series tanks assumed to be retrieved by modified sluicing methods.

The contaminant sources associated with any potential retrieval leaks were assumed to be readily available for transport with the infiltrating moisture; any chemical retardation is modeled by the linear isotherm K_d model discussed in Section 3.2.2.4. The retrieval contaminant inventory is estimated by multiplying the leak volume (Section 3.5.3.2, Tables 3-10 and 3-11) by the estimated contaminant concentration in the transferring tank liquids for each tank. The source term was modeled with the leak starting on January 1, 2000, and the leak occurring at the bottom east corner of tank S-103 for the WMA S-SX calculations. For the WMA C calculations, the leak was assumed to occur at the bottom of tank C-112.

Inventories for Potential Retrieval Leaks. The composition of the fluid assumed to have been lost during the retrieval process was developed from the HTWOS run (Kirkbride et al. 2005). Inventory estimates were developed by multiplying the assumed leak volumes (i.e., 8,000 gal and 20,000 gal) by the projected fluid compositions for each tank retrieved using the modified sluicing technique. Tanks that are known or suspected to leak were assumed to be retrieved using an alternate retrieval process. For these tanks, no retrieval leaks were assumed.

Table 3-16 summarizes the inventory for potential tank retrieval leaks from SSTs in WMAs C and S-SX for selected radionuclides and chemicals. Complete inventories for all contaminants within the residual waste for each tank that was planned to be retrieved using the modified sluicing technique are provided in Appendix C.

Table 3-16. Potential Retrieval Leak Inventories for Hanford Waste Tanks within Waste Management Areas C and S-SX (2 pages)

Tank [c]	Contaminants for Groundwater Pathway Impacts [a]					Contaminants for Inadvertent Intruder Impacts [b]						
	Tc-99 Ci [d]	I-129 Ci [d]	Cr kg [d]	NO_3^- kg [d]	NO_2^- kg [d]	Sr-90 Ci [d]	Tc-99 Ci [d]	Sn-126 Ci [d]	Cs-137 Ci [d]	Pu-239 Ci [d]	Pu-240 Ci [d]	Am-241 Ci [d]
Waste Management Area S-SX												
S-101	2.98E-01	5.11E-05	1.33E+01	8.42E+02	2.91E+02	1.71E+01	2.98E-01	1.59E-03	6.46E+02	4.84E-06	1.05E-06	1.73E-05
S-102	1.02E+00	1.30E-03	1.96E+00	2.49E+03	5.18E+02	1.16E+01	1.02E+00	1.40E-02	1.25E+03	1.41E-02	3.01E-03	8.96E-03
S-103	1.02E+00	1.01E-03	5.19E+00	2.24E+03	5.12E+02	1.01E+01	1.02E+00	8.82E-03	1.21E+03	3.73E-03	7.79E-04	1.56E-03
S-105	1.24E+00	1.22E-03	2.47E+00	5.03E+03	1.06E+02	1.13E+01	1.24E+00	3.87E-03	2.92E+02	4.62E-04	9.37E-05	1.61E-03
S-106	1.61E+00	1.58E-03	2.14E+01	5.72E+03	4.51E+02	1.77E+01	1.61E+00	3.53E-03	1.52E+03	1.73E-03	3.77E-04	7.25E-03
S-107	4.34E-02	2.21E-05	5.51E+00	2.05E+02	1.08E+02	1.71E+01	4.34E-02	3.57E-05	1.83E+02	1.00E-03	2.10E-04	0.00E+00
S-108	1.55E+00	1.52E-03	1.59E+01	4.96E+03	7.04E+02	1.85E+01	1.55E+00	1.07E-03	1.52E+03	7.03E-03	1.50E-03	1.58E-02
S-109	1.46E+00	1.43E-03	6.96E+00	8.75E+03	1.04E+02	1.71E+01	1.46E+00	2.10E-03	2.00E+02	7.54E-03	1.48E-03	2.04E-03
S-110	1.15E+00	1.13E-03	2.89E+01	4.47E+03	2.68E+02	1.74E+01	1.15E+00	3.82E-03	8.82E+02	2.36E-02	4.67E-03	2.23E-02
S-111	1.61E+00	1.60E-03	2.60E+01	4.02E+03	5.71E+02	1.76E+01	1.61E+00	1.04E-02	1.17E+03	6.81E-03	1.42E-03	3.33E-03
S-112	1.00E-02	7.55E-03	4.22E-01	8.39E+01	2.37E+01	1.86E+01	1.00E-02	3.46E-04	4.55E+01	1.37E-02	2.43E-03	1.80E-02
SX-101	1.12E+00	1.35E-03	5.90E+01	5.32E+03	4.45E+02	1.82E+01	1.12E+00	2.22E-03	1.74E+03	2.05E-03	4.18E-04	1.61E-01
SX-102	1.56E+00	1.59E-03	2.36E+01	4.17E+03	1.40E+03	1.94E+01	1.56E+00	9.07E-03	2.72E+03	9.40E-03	1.98E-03	1.12E-02
SX-103	1.36E+00	1.34E-03	7.80E+00	4.78E+03	8.72E+02	1.88E+01	1.36E+00	3.45E-03	1.99E+03	1.88E-02	3.86E-03	1.99E-03
SX-105	1.57E+00	1.55E-03	1.37E+01	3.97E+03	1.32E+03	1.86E+01	1.57E+00	7.79E-03	1.71E+03	9.70E-02	1.89E-02	5.30E-02
SX-106	2.08E+00	2.08E-03	7.26E+00	4.54E+03	1.39E+03	1.93E+01	2.08E+00	7.63E-03	2.34E+03	9.16E-02	1.97E-02	3.26E-02

Table 3-16. Potential Retrieval Leak Inventories for Hanford Waste Tanks within Waste Management Areas C and S-SX (2 pages)

Tank [c]	Contaminants for Groundwater Pathway Impacts [a]					Contaminants for Inadvertent Intruder Impacts [b]						
	Tc-99 Ci [d]	I-129 Ci [d]	Cr kg [d]	NO_3^- kg [d]	NO_2^- kg [d]	Sr-90 Ci [d]	Tc-99 Ci [d]	Sn-126 Ci [d]	Cs-137 Ci [d]	Pu-239 Ci [d]	Pu-240 Ci [d]	Am-241 Ci [d]
Waste Management Area C												
C-102	1.75E-02	2.12E-03	1.11E+00	1.41E+03	4.10E+02	5.43E+01	1.75E-02	1.60E-05	4.20E+02	4.16E-02	9.96E-03	8.31E-01
C-103	5.04E-01	3.26E-03	5.92E-01	4.08E+01	4.18E+02	8.73E+01	5.04E-01	9.35E-05	4.74E+02	4.70E-02	9.90E-03	3.69E-01
C-104	1.42E+00	8.57E-03	3.53E+00	5.26E+02	9.82E+02	1.06E+02	1.42E+00	4.06E-04	1.34E+03	5.76E-02	1.48E-02	3.29E-01
C-107	6.15E-01	1.93E-02	9.21E+00	4.00E+02	9.45E+02	7.67E+01	6.15E-01	5.97E-02	5.87E+02	4.97E-01	8.07E-02	0.00E+00
C-108	2.86E-01	4.98E-05	6.00E+00	8.20E+02	4.55E+02	2.55E+01	2.86E-01	1.11E-05	1.59E+02	3.97E-03	4.31E-04	5.48E-02
C-109	1.37E+00	1.09E-03	5.10E+00	1.01E+03	6.91E+02	3.74E+01	1.37E+00	4.23E-06	8.83E+01	5.26E-02	9.04E-03	1.96E-02
C-112	1.92E+00	8.29E-04	4.00E+00	1.53E+03	1.16E+03	3.66E+01	1.92E+00	1.66E-06	1.98E+03	5.43E-02	6.83E-03	1.97E-01

[a] Major contaminants for groundwater impacts based on estimated chemical distribution coefficients $\leq$ 0.2 mL/g (Section 3.4.4.1.3).

[b] Major contaminants for inadvertent intruder impacts based on major contaminants contributing to the intruder doses in previous analysis (Mann et al. 2001; Mann and Connelly 2003).

[c] Potential tank retrieval leak inventories based on 8,000-gal leak estimate and average tank retrieval liquid concentration from Kirkbride et al. (2005).

[d] Radionuclide inventories in Ci decayed to January 1 2004; chemical inventories in kg.

3.5.4.3 Closed Tank Structure

The reference case assumes a diffusional release model for contaminants from tank residuals. This is a simplified model of tank release that assumes all the residual wastes is available for diffusion, and does not take into consideration the tank itself or chemical interactions of the residue with the waste form. The development of a refined release model and appropriate chemical/waste interaction database is needed to fully address this issue.

Alternative 11 in Table 3-15 addresses the unlikely possibility that the grout fill fails to encapsulate any of the waste and allows water to pass through the waste (i.e., via advective transport). The advection-dominated release model (mixing-cell cascade model) is used to simulate release from unstabilized wastes. For unstabilized wastes, the radionuclides exit the facility at a rate determined by the flow of water and the amount of dispersion (mixing) within the tank. The mixing-cell cascade model (Kozak et al. 1990) is based on the dispersion analysis of chemical reactors, and allows the analysis to incorporate the effects of dispersion within the tank in a simplified manner. In this model, the tank interior is considered to be composed of a cascade of N equal-sized, well-stirred cells in series. The total volume of the N cells is equal to the volume of the tank residual waste within the mixing zone.

The mixing-cell cascade model for N equal-sized cells is described by Equation 3.13:

$$Q(t) = qAC_0 \exp^{-\alpha N t} \sum_{n=1}^{N} \frac{(\alpha N t)^{n-1}}{(n-1)!} \qquad \textbf{Eq. 3.13}$$

where:

Q = release rate (Ci/yr)
t = time (yr)
q = vertical Darcy flux (m/yr)
A = horizontal (planar) area of the tank interior
α = $q/(\theta dR)$
θ = volumetric moisture content in the residual waste
d = vertical mixing depth (m)
R = retardation factor in the waste material (assumed R=1).

For advection-dominated release, backfill (sand and gravel) was used as the tank fill material. The spatially variable velocities, V, and moisture contents, θ, which are obtained via flow modeling within the tank, are used to determine C_0. A vertical mixing length, d, of 0.825 m (same as that for diffusion-dominated release) was assumed.

The initial concentration of contaminant in the interstitial water can be determined from Equation 3.14:

$$C_0 = \frac{m}{\theta V R} \qquad \textbf{Eq. 3.14}$$

where:

m = total facility inventory (assumed unity) of the radionuclides in the tank
V = equals total volume of the residual waste (i.e., 360 ft^3 [10.2 kL] for 100-Series tanks and 30 ft^3 [850 L] for 200-Series tanks or 1% residual following the HFFACO goal [Ecology et al. 1989]).

The mixing-cell cascade model provides results equivalent to that for a one-dimensional, convective-dispersion equation with varying values of the dispersion coefficient (Kozak et al. 1990). In the limit, as N approaches infinity, the model represents flow through a system with zero dispersion, whereas for N equal to one, the model represents flow with an infinite dispersion coefficient. A value of $N = 10$ will be used reflecting moderate dispersion.

Alternative 12 in Table 3-15 addresses the possibility that more tank residual wastes are left behind than the current baseline estimate of 360 ft^3 (approximately 1 in. of waste spread across the bottom of the tank). The impact of this alternative is addressed in the sensitivity analysis examining the range of tank residual wastes (Table 3-14).

Alternative 13 in Table 3-15 addresses the potential impacts should a pressurized water line break over a past release. It is assumed that, as part of good housekeeping, the issue of water line leaks from existing piping and infrastructure at the tank farms will be addressed and resolved. However, as part of the alternatives analysis, a water line leak could occur over a past leak prior to completion of retrieval. The impact of such an event would most likely be seen as earlier impacts on groundwater from the past leak. This analysis is reported in the WMA S-SX FIR (Knepp 2002a).

An alternative conceptualization that has been often proposed is the situation whereby a tank somehow behaves like a bathtub and fills its interstitial volume with water which is then presumed to be released all at once (alternative 14 in Table 3-15). This alternative is expected to release a small pulse of contaminants into the system instead of the more expected condition of release at a slower rate over a longer period. This alternative was posed when there was belief that the tank might be filled with a highly permeable and porous material such as sand. Current plans call for the tanks to be filled with grout, thus eliminating any possibility for a "bathtub" effect to occur. Also, the sensitivity case where the tank is assumed to be filled with backfill material (sand and gravel) and the tank residual waste contaminants are released with the infiltrating moisture provides a relative bounding case with respect to the bathtub effect. This alternative therefore will not be considered further.

3.5.4.4 Vadose Zone

An alternative characterization that potentially impacts the expected performance of the system is the potential unnoticed presence of clastic dikes (alternative 15 in Table 3-15). Clastic dikes are ubiquitous sedimentary structures observed in outcrops and trenches that expose the Hanford formation in the 200 Areas. The dikes are believed to represent dewatering structures that developed during compaction and settling of cataclysmic flood deposits during or soon after floodwaters drained from the Pasco Basin. The dikes are of particular interest because they occur as near-vertical tubular bodies filled with multiple layers of unconsolidated sediments. Simulations (alternative 15) were run to evaluate effects of clastic dikes on the peak concentration at the WMA fenceline.

The reference case assumed that the long-term, post-Hanford unconfined aquifer hydraulic head distribution is representative of the pre-Hanford Site operations condition. Alternative 16 in Table 3 15 (conceptualization) addresses the impacts if the aquifer were to drop by 2 m, thereby increasing the residence time of contaminants within the vadose zone.

Alternatives 17 and 18 in Table 3-15 examine differing conceptualizations regarding the size and location of past releases. This analysis is incorporated into the sensitivity analyses presented earlier. As discussed in Section 3.2, the simulated cases for past releases do not attempt to model a release event itself; instead, they model the potential risk posed by the existing vadose zone contamination footprint. Information on contamination footprints and their location within the vadose zone is based on spectral gamma data for drywells and recently-drilled borehole data in the vicinity of known releases. Modeling results contained in the FIRs (Knepp 2002a, 2002b) have shown that the peak concentrations for contaminant BTCs are influenced more by total inventory (Ci or Kg) than by spatial distribution of that inventory within the vadose zone. These results are also supported by past risk analysis (Jacobs 1998).

Alternative 19 in Table 3-15 is an examination of the impacts of an assumed immobilization of varying levels of mobile contaminants from past releases. No statement concerning the need to remediate is implied.

The individual geologic units within the vadose zone are known to be anisotropic with respect to saturated hydraulic conductivity. Alternative 20 in Table 3-15 is a postulated case that assumes arbitrarily that the vadose zone geologic units are not anisotropic.

3.5.4.5 Exposure Parameters

The reference case considers the estimated impacts to the all-pathway farmer for the groundwater pathway and the driller and post-intrusion rural pasture for the intruder scenario. Estimated impacts for other exposure scenarios are provided in Chapter 6.0 using the dose factors provided in Rittmann (2004).

3.5.5 Intruder Dose – Sensitivity to Parameter Assumptions

Intruder dose comes from inadvertent human intrusion into the waste disposal site after closure (Rittmann 2004). It is assumed that a well is drilled through the waste, bringing some of the waste to the surface where people can be exposed to it.[4] The risk metric for waste intrusion is the EDE from radionuclides in the waste. The projected dose depends first on the assumed exposure scenario because different exposure scenarios lead to different doses. The exposure scenarios are constructed from assumptions about which exposure pathways are applicable and which parameter values are appropriate. There are uncertainties associated with each of the parameters. The objective of this section is to quantify the likely range of each parameter.

The intruder dose depends on two quantities: 1) the soil contaminant concentration that the intruder is exposed to and 2) the exposure scenario dose factor. Parameters used to develop the scenario dose factors will not be discussed here; however, they do depend strongly on the waste composition. In addition, only the reference case intruder scenarios are discussed. The acute scenario is the well driller, while the reference case chronic scenario is the rural pasture with a cow.

For the acute scenario (well driller), the soil contaminant concentration used in the dose calculation is the average in the borehole cuttings. For the chronic scenarios (rural pasture),

[4] Intruder dose metrics are derived from 10 CFR 61 regulations and do not correspond with all-pathways exposure scenarios associated with groundwater.

the soil contaminant concentration used in the dose calculation is the average in the contaminated pasture. The soil contaminant concentration depends on the factors listed in Table 3-17. The waste composition is not listed because the relative amounts of various radionuclides can vary widely.

Table 3-17. Intruder Pathway – Summary of Reference Case Parameters and Expected Ranges

Parameter	Parameter Range		
	Minimum	Reference	Maximum
1. Waste concentration at closure	0.1 [a]	varies	10 [a]
2. Decay time at intrusion	100 yr	500 yr	1,000 yr
3. Waste thickness – tank residual	0.004 m	0.025 m	0.15 m
4. Waste thickness – unplanned releases	0.25 m*	varies	4 m*
5. Fraction available for internal dose (residual tank waste only)	0.01	0.1	1
6. Borehole depth – acute	70 m	80 m	90 m
7. Borehole diameter – chronic	8 in.	10 in.	12 in.
8. Spreading area – chronic	3,000 m^2	5,000 m^2	7,000 m^2
9. Tilling depth – chronic	0.1 m	0.15 m	0.20 m

[a] Fraction of reference case value representing minimum or maximum value for range.

* indicates multiply by the number.

Table 3-17, row 1, labeled "Waste concentration at closure" is the activity per unit volume or mass of the various radionuclides in a tank or UPR. The present inventory is the best estimate, but it may be larger or smaller by an order of magnitude. The inventory estimates err on the high side, so the largest concentration is unlikely to exceed a factor of 10 greater than the estimates used.

Row 2 labeled "Decay time at intrusion" is the time between site closure and intrusion. The range shown comes from DOE M 435-1.1 as the time period of interest for inadvertent intrusion.

Rows 3 and 4 address the assumed waste thickness. Two rows are needed because residual waste and the UPRs to soil have different uncertainties. The residual waste in the tanks has an average thickness of 1 in. or less. Due to the shape of the bottom of the tank and the difficulty in removing some attached solids, the waste thickness will vary. Based on the shape of the tank bottom, the amount of waste exhumed could be larger by a factor of 6 if the intruder's well passes through the center of the tank. The intruder dose varies linearly with the thickness of the residual tank waste.

The thickness of UPRs to the soil depends on the horizontal spread of the plume. As discussed earlier, releases can lead to significant horizontal spreading (Section 3.2.2). The reference case

assumes that the plume has a diameter equal to its height. The relative height and width of the plume could vary by a factor of 5, based on observed plumes near the underground tanks that have leaked in the past. Another consideration is the volume of the soil compared to the volume of liquid that entered the soil. The reference case assumes that the contaminated soil has a volume 10 times the volume of the liquid. The likely range for the soil-filling fraction is 5% to 15% based on soil porosity and residual moisture content. The combination of these ranges leads to a waste thickness that may vary by a factor of 4 from the reference case.

The fraction of the exhumed waste that is available to produce internal dose (row 5) is important because the external pathway may sometimes be a small contributor to the intruder dose. For these cases, the intruder dose is roughly proportional to the fraction available for internal dose. When the external pathway is important, there is a sublinear relationship between this fraction and the intruder dose. The fraction available is estimated to range from 1% up to a maximum of 100%. Since the fraction used in the intruder calculations is 10%, the fraction available could be larger or smaller by a factor of 10. The intruder doses will vary by nearly the same factor.

The borehole depth (row 6) is important for the well driller scenario (acute). The ratio of waste thickness to borehole depth determines the waste dilution. The uncertainty in this parameter is small. The depth to groundwater is known and unlikely to change significantly in the future.

The borehole diameter (row 7) is important for the rural pasture scenario (chronic). The volume of waste exhumed depends on the cross-sectional areas for the well. The uncertainty in this parameter is small. The well diameter is based on current drilling practices near the Hanford Site.

Rows 8 and 9 indicate the volume of soil into which the exhumed waste is diluted. The dilution volume is the product of the spreading area and the tilling depth. Note that the pasture area is much larger than the likely spreading area for the borehole cuttings. The cow forages over the well cuttings and elsewhere in the pasture until it obtains the amount of food it eats in a year. The milk concentration varies during the year, but the average is proportional to the average soil concentration in the pasture.

Note also that if the spreading area (row 8) changes appreciably, other exposure parameters must change also. Smaller spreading areas lead to reduced contact with the contaminants. They require less attention, so the individual spends less time in the contaminated area and therefore receives smaller external doses. The individual also inhales and ingests less contaminated dust. For the pasture scenario, the spreading area is driven by the caloric intake for the cow. Reducing the area of the pasture means higher concentrations in the pasture grass, but the cow eats less from the pasture and obtains food elsewhere. Hence, the spreading area is assumed to vary by no more than the range shown in Table 3-17.

The tilling depth (row 9) is also related to the thickness of soil from which grasses derive nutrients. If the tilling depth is much smaller, the soil concentration is larger, but the plants obtain a portion of their nutrients from uncontaminated depths of the soil. Hence, the tilling depth is assumed to vary by no more than the range shown in Table 3-17.

3.5.6 Air Pathway Risk – Sensitivity to Parameter Assumptions

The air pathway addresses volatile contaminants remaining in the closed disposal system and their migration through the grouted tank structure and surface cover. An examination of this pathway leads to the following observations supporting the use of a bounding analysis:

- Few contaminants in the waste are volatile.
- For the important volatile contaminants (tritium, carbon-14, and radon-222), estimations of remaining inventory indicate small quantities will remain in the tank waste at closure.
- Very low human exposure impacts are estimated under credible exposure scenarios.

The low human exposure impact considered possible through this pathway, even under an extreme set of bounding conditions (Section 3.2.3), does not warrant a more complicated analysis examining features and processes of the release mechanism for vapors.

3.6 REFERENCES

10 CFR 61, "Licensing Requirements for Land Disposal of Radioactive Waste," *Code of Federal Regulations*, Washington, D.C., as amended.

Agnew 1997. S.F. Agnew, 1997, *Hanford Tank Chemical and Radionuclide Inventories: HDW Model, Rev. 4*, LA-UR-96-3860, Los Alamos National Laboratory, Los Alamos, New Mexico.

Anderson 1990. J.D. Anderson, 1990, *A History of the 200 Area Tank Farms*, WHC-MR-0132, Westinghouse Hanford Company, Richland, Washington.

ANSI/ANS 16.1, 1986, "Measurements of the Leachability of Solidified Low-Level Radioactive Wastes by a Short-Term Test Procedure," prepared by the American Nuclear Society Standards Committee Working Group ANS-16.1, Approved by the American National Standards Institute, Inc., American Nuclear Society, La Grange Park, Illinois.

Baes and Mesmer 1976. C.F. Baes, Jr. and R.E. Mesmer, 1976, *The Hydrolysis of Cations*, John Wiley and Sons, New York, New York.

Ball and Nordstrom 1998. J.W. Ball and D.K. Nordstrom, 1998, "Critical evaluation and selection of standard state thermodynamic properties for chromium metal and its aqueous ions, hydrolysis species, oxides, and hydroxides," *J. Chem. Engineering Data*, Vol. 43(6), pp. 895-918.

Cantrell et al. 2002. K.J. Cantrell, R.J. Serne, and G.V. Last, 2002, *Hanford Contaminant Distribution Coefficient Database and Users Guide*, PNNL-13895, Rev. 0, Pacific Northwest National Laboratory, Richland, Washington.

Cantrell et al. 2003. K.J. Cantrell, R.J. Serne, and G.V. Last, 2003, *Hanford Contaminant Distribution Coefficient Database and Users Guide*, PNNL-13895, Rev. 1, Pacific Northwest National Laboratory, Richland, Washington.

Cole et al. 2001b. C.R. Cole, M.P. Bergeron, S.K. Wurstner, P.D. Thorne, S. Orr, and M.I. McKinley, 2001, *Transient Inverse Calibration of Hanford Site-Wide Groundwater Model to Hanford Operational Impacts – 1943 to 1996*, PNNL-13447, Pacific Northwest National Laboratory, Richland, Washington.

Corbin et al. 2005. R.A. Corbin, B.C. Simpson, M.A. Anderson, W. Danielson III, J.G. Field, T.E. Jones, M.D. Freshley, and C.T. Kincaid, 2005, *Hanford Soil Inventory Model, Rev. 1*, RPP-26744, Rev. 0, CH2M HILL Hanford Group, Inc., Richland, Washington.

Crank 1975. J. Crank, 1975, *The Mathematics of Diffusion*, Oxford University Press, Oxford, England.

De Smedt and Wierenga 1984. F. De Smedt and P.J. Wierenga, 1984, "Solute Transfer through Columns of Glass Beads," *Water Resources Res*. Vol. 20:225-232.

DOE 1988. *Consultation Draft: Site Characterization Plan, Reference Repository Location, Hanford Site, Washington*, DOE/RW-0164, U.S. Department of Energy, Washington, D.C.

DOE 1999d. *Format and Content Guide for U.S. Department of Energy Low-Level Waste Disposal Facility Performance Assessments and Composite Analysis,* U.S. Department of Energy, Washington, D.C.

DOE M 435.1-1, 2001. *Radioactive Waste Management Manual*, U.S. Department of Energy, Washington, D.C.

DOE-RL 1996. *Focused Feasibility Study of Engineered Barriers for Waste Management Units in the 200 Areas*. DOE/RL-93-033, Rev. 1, U.S. Department of Energy, Richland Operations Office, Richland, Washington.

DOE-RL 1999. *Retrieval Performance Evaluation Methodology for the AX Tank Farm*, DOE/RL-98-72, U.S. Department of Energy, Richland Operations Office, Richland, Washington.

Ecology et al. 1989. Ecology, EPA, and DOE, 1989, *Hanford Federal Facility Agreement and Consent Order*, as amended, Washington State Department of Ecology, Olympia, Washington, U.S. Environmental Protection Agency, and U.S. Department of Energy, Washington D.C.

EPA 1999. *Understanding Variation in Partition Coefficient K_d Values*, EPA/402/R-99/004A, Office of Air and Radiation, U.S. Environmental Protection Agency, Washington, D.C.

EPA 2000a. *Soil Screening Guidance for Radionuclides: Technical Background Document*, EPA/540/R-00-006, Office of Solid Waste and Emergency Response, U.S. Environmental Protection Agency, Washington, D.C.

Fayer and Szecsody 2004. M.J. Fayer and J.E. Szecsody, 2004, *Recharge Data Package for the 2005 Integrated Disposal Facility Performance Assessment*, PNNL-14744, Pacific Northwest National Laboratory, Richland, Washington.

Fayer and Walters 1995. M.J. Fayer and T.B. Walters, 1995, *Estimated Recharge Rates at the Hanford Site,* PNL-10285, Pacific Northwest Laboratory, Richland, Washington.

Fayer et al. 1996. M.J. Fayer, G.W. Gee, M.L. Rockhold, M.D. Freshley, and T.B. Walters, 1996, "Estimating Recharge Rates for a Groundwater Model using a GIS," *Journal of Environmental Quality*, Vol. 25, pp. 510-518.

Fayer et al. 1999. M.J. Fayer, E.M. Murphy, J.L. Downs, F.O. Khan, C.W. Lindenmeier, and B.N. Bjornstad, 1999, *Recharge Data Package for the Immobilized Low-Activity Waste 2001 Performance Assessment,* PNNL-13033, Pacific Northwest National Laboratory, Richland, Washington.

Fecht et al. 1999. K.R. Fecht, K.A. Lindsey, B.N. Bjornstad, D.G. Horton, G.V. Last, and S.P. Reidel, 1999, *Clastic Injection Dikes of the Pasco Basin and Vicinity – Geologic Atlas Series,* BHI-01103, Rev. 0, Bechtel Hanford, Inc., Richland, Washington.

Field 2003b. J.G. Field, 2003, *Best-Basis Inventory Process Requirements*, RPP-7625, Rev. 3, CH2M HILL Hanford, Group, Inc., Richland, Washington.

Field and Jones 2005. J.G. Field and T.E. Jones, 2005, *Tank Farm Vadose Zone Contamination Volume Estimates,* RPP-23405, Rev. 1, CH2M HILL Hanford Group, Inc, Richland, Washington.

Freeman-Pollard et al. 1994. J.R. Freeman-Pollard, J.A. Caggiano, and S.J. Trent, 1994, *Engineering Evaluation of the GAO-RCED-89-157, Tank 241-T-106 Vadose Zone Investigation*, BHI-00061, Rev. 00, Bechtel Hanford, Inc., Richland, Washington.

Gardner 1958. W.R. Gardner, 1958, "Some Steady-State Solutions of the Unsaturated Moisture Flow Equation with Applications to Evaporation from a Water Table," *Soil Sci.* Vol. 85, pp. 228-232.

Gee and Ward 2001. G.W. Gee and A.L. Ward, 2001, *Vadose Zone Transport Field Study: Status Report*, PNNL-13679, Pacific Northwest National Laboratory, Richland, Washington.

Gee et al. 1992. G.W. Gee, M.J. Fayer, M.L. Rockhold, and M.D. Campbell, 1992, "Variations in Recharge at the Hanford Site," *Northwest Sci.* Vol. 66, No. 4, pp. 237-250.

Gee et al. 1996. G.W. Gee, A.L. Ward, B.G. Gilmore, S.O. Link, G.W. Dennis, and T.K. O'Neil, 1996, *Hanford Prototype-Barrier Status Report: FY 1996,* PNNL-11367, Pacific Northwest National Laboratory, Richland, Washington.

Gelhar 1993. L.W. Gelhar, 1993, *Stochastic Subsurface Hydrology*, Prentice Hall, New York, New York.

Gelhar et al. 1985. L.W. Gelhar, A. Mantoglou, C. Welty, and K.R. Rehfeldt, 1985, *A review of field-scale physical solute transport processes in saturated and unsaturated porous media*, Rep. EA-4190, Electric Power Res. Inst., Palo Alto, California.

Gelhar et al. 1992. L.W. Gelhar, C. Welty, and K.R. Rehfeldt, 1992, "A Critical Review of Data on Field-Scale Dispersion in Aquifers," *Water Resources Research,* Vol. 28, pp. 1955-1974.

Goetz 2003. T.G. Goetz, 2003, *Tank Farms Documented Safety Analysis*, RPP-13033, Rev. 0, CH2M HILL Hanford Group, Inc., Richland, Washington.

Harbour et al. 2004. J.R. Harbour, T.B. Edwards, T.H. Lorier, and C.A. Langton, from Westinghouse Savannah River Company, and R.C. Moore, J.L. Krumhansl, K.C. Holt, F. Salas, and C.A. Sanchez, Sandia National Laboratory, 2004, *Stabilizing Grout Compatibility Study,* WSRC-TR-2004-00021, Rev. 0, Westinghouse Savannah River Company, Aiken, South Carolina.

Hem 1986. J.D. Hem, 1986, "Study and Interpretation of the Chemical Characteristics of Natural Water," United States Geological Survey Water-Supply Paper 2254, U.S. Geological Survey, Washington, D.C.

Higley and Place 2004. B.A. Higley and D.E. Place, 2004, *Hanford Defined Waste Model Revision 5.0*, RPP-19822, Rev. 0, CH2M HILL Hanford Group, Inc., Richland, Washington.

INEEL 2004. *Engineering Design File – Fate and Transport Modeling Results and Summary Report*, EDF-ER-275, Rev. 3, Idaho National Engineering and Environmental Laboratory, Idaho Falls, Idaho.

Jacobs 1998. *Final AX Tank Farm Vadose Zone Screening Analysis for the Retrieval Performance Evaluation Criteria Assessment*, prepared for U.S. Department of Energy, Richland Operations Office, by Jacobs Engineering Group, Inc., Richland, Washington.

Jenkins 2001. "Kd Values for INTEC Groundwater Modeling (EM-ER-01-115)," letter from T. Jenkins, U.S. Department of Energy, Idaho Operations Office, Idaho Falls, Idaho, to M. Doornbos, BBWI, Idaho Falls, Idaho, dated July 3.

Jones et al. 2000b. T.E. Jones, R.A. Watrous, and G.T. Maclean, 2000, *Inventory Estimates for Single-Shell Tank Leaks in S and SX Tank Farms*, RPP-6285, Rev. 0, CH2M HILL Hanford Group, Inc., Richland, Washington.

Jury et al. 1991. W.A. Jury, W.R. Gardner, and W.H. Gardner, 1991, *Soil Physics*, Wiley and Sons, Inc., New York, New York.

Khaleel and Relyea 1997. R. Khaleel and J.F. Relyea, 1997, "Correcting Laboratory-Measured Moisture Retention Data for Gravels," *Water Resources Research,* Vol. 33, No. 8, pp. 1875-1878.

Khaleel et al. 1995. R. Khaleel, J.F. Relyea, and J.L. Conca, 1995, "Evaluation of van Genuchten-Mualem Relationships to Estimate Unsaturated Conductivity at Low Water Contents," *Water Resources Research,* Vol. 31, No. 11, pp. 2659-2668.

Khaleel et al. 2000. R. Khaleel, T.E. Jones, A.J. Knepp, F.M. Mann, D.A. Myers, P.M. Rogers, R.J. Serne, and M.I. Wood, 2000, *Modeling Data Package for S-SX Field Investigation Report (FIR)*, RPP-6296, Rev. 0, CH2M HILL Hanford Group, Inc., Richland, Washington.

Khaleel et al. 2001. R. Khaleel, T.E. Jones, A.J. Knepp, F.M. Mann, D.A. Myers, and M.I. Wood, 2001, *Modeling Data Package for B-BX-BY Field Investigation Report (FIR)*, RPP-9223, Rev. 0, CH2M HILL Hanford Group, Inc., Richland, Washington.

Khaleel et al. 2002. R. Khaleel, T.-C.J. Yeh, and Z. Lu, 2002, "Upscaled Flow and Transport Properties for Heterogeneous Unsaturated Media," *Water Resources Research*, Vol. 38(5), p. 1053, doi:10.1029/2000WR000072.

Khaleel et al. 2006a. R. Khaleel, M.P. Connelly, and W.J. McMahon, 2006, *Modeling Data Package for an Initial Assessment of Closure of the C Tank Farm*, RPP-13310, Rev. 1, CH2M HILL Hanford Group, Inc., Richland, Washington.

Khaleel et al. 2006b. R. Khaleel, M.P. Connelly, and W.J. McMahon, 2006, *Modeling Data Package for an Initial Assessment of Closure of the S and SX Tank Farms*, RPP-17209, Rev. 1, CH2M HILL Hanford Group, Inc., Richland, Washington.

Kincaid et al. 1995. C.T. Kincaid, J.W. Shade, G.A. Whyatt, M.G. Piepho, K. Rhoads, J.A. Voogd, J.H. Westsik, Jr., M.D. Freshley, K.A. Blanchard, and B.G. Lauzon, 1995, *Performance Assessment of Grouted Double-Shell Tank Waste Disposal at Hanford*, WHC-SD-WM-EE-004, Rev. 1, Westinghouse Hanford Company, Richland, Washington.

Kirkbride et al. 2005. R.A. Kirkbride. P.J. Certa, T.M. Hohl, A.M. Johnson, and R.S. Wittman, 2005, *Hanford Tank Waste Operations Simulator Model Data Package for the Development Run for the Refined Target Case,* RPP-RPT-23412, Rev. 0A, CH2M HILL Hanford Group, Inc., Richland, Washington.

Kline and Khaleel 1995. N.W. Kline and R. Khaleel, 1995, *Effect of Moisture-Dependent Anisotropy and Enhanced Recharge Around Underground Storage Tanks*, WHC-SA-2680-FP, Westinghouse Hanford Company, Richland, Washington.

Knepp 2002a. A.J. Knepp, 2002, *Field Investigation Report for Waste Management Area S-SX*, RPP-7884, Rev. 0, CH2M HILL Hanford Group, Inc., Richland, Washington.

Knepp 2002b. A.J. Knepp, 2002, *Field Investigation Report for Waste Management Area B-BX-BY*, RPP-10098, Rev. 0, CH2M HILL Hanford Group, Inc., Richland, Washington.

Korte et al. 1976. N.E. Korte, J. Skopp, W.H. Fuller, E.E. Niebla, and B.A. Alesii, 1976, "Trace element movement in soils: Influence of soil physical and chemical properties," *Soil Sci. J.* 122:350-359.

Kozak et al. 1990. M.W. Kozak, M.S.Y. Chu, P.A. Mattingly, J.D. Johnson, and J.T. McCord, 1990, *Background Information for the Development of a Low-Level Waste Performance Assessment Methodology*, NUREG/CR-5453 [SAND89-2509], Volume 5, U.S. Nuclear Regulatory Commission, Washington, D.C.

Krupka et al. 2004. K.M. Krupka, R.J. Serne, and D.I. Kaplan, 2004, *Geochemical Data Package for the 2005 Hanford Integrated Disposal Facility Performance Assessment*, PNNL-13037, Rev. 2, Pacific Northwest National Laboratory, Richland, Washington.

Kupfer et al. 1998. M.J. Kupfer, A.L. Boldt, K.M. Hodgson, L.W. Shelton, B.C. Simpson, R.A. Watrous, M.D. LeClair, G.L. Borsheim, R.T. Winward, B.A. Higley, R.M. Orme, N.G. Colton, S.L. Lambert, D.E. Place, and W.W. Schulz, 1998, *Standard Inventories of Chemicals and Radionuclides in Hanford Site Tank Wastes*, HNF-SD-WM-TI-740, Rev. 0B, prepared by Lockheed Martin Hanford Corporation for Fluor Daniel Hanford, Inc., Richland, Washington.

Lambert 2005. S.L. Lambert, 2005, *Residual Waste Inventories in the Plugged and Abandoned Pipelines at the Hanford Site*, RPP-25113, Rev. 0, CH2M HILL Hanford Group, Inc., Richland, Washington.

Last et al. 2004a. G.V. Last, E.J. Freeman, K.J. Cantrell, M.J. Fayer, G.W. Gee, W.E. Nichols, B.N. Bjornstad, and D.G. Horton, 2004, *Vadose Zone Hydrogeology Data Package for the 2004 Composite Analysis*, PNNL-14702, Rev. 0, Pacific Northwest National Laboratory, Richland, Washington.

Last et al. 2004b. G.V. Last, W.E. Nichols, and C.T. Kincaid, 2004, *Geographic and Operational Site Parameters List (GOSPL) for the 2004 Composite Analysis*, PNNL-14725, Rev. 0, Pacific Northwest National Laboratory, Richland, Washington.

Lee 2004. T.A. Lee, 2004, *Single-Shell Tank System Closure Plan*, RPP-13774, Rev. 2, CH2M HILL Hanford Group, Inc., Richland, Washington.

Lindsay 1979. W.L. Lindsay, 1979, *Chemical Equilibria in Soils*, John Wiley and Sons, New York, New York.

Lindsay et al. 1981. W.L. Lindsay, M. Sadiq, and K.L. Porter, 1981, "Thermodynamics in inorganic nitrogen transformation," *Soil Sci. Soc. Am. J.* 45:61-66.

Mann et al. 1999. F.M. Mann, C.T. Kincaid, W.J. McMahon, and S.B. Yabusaki, 1999, *Computer Code Selection Criteria for Flow and Transport Code(s) to be Used in Vadose Zone Calculations for Environmental Analyses in the Hanford Site's Central Plateau*, HNF-5294, Rev. 0, CH2M HILL Hanford Group, Inc. Richland, Washington.

Mann et al. 2001. F.M. Mann, K.C. Burgard, W.R. Root, R.J. Puigh, S.H. Finfrock, R. Khaleel, D.H. Bacon, E.J. Freeman, B.P. McGrail, S.K. Wurstner, and P.E. LaMont, 2001, *Hanford Immobilized Low-Activity Tank Waste Performance Assessment: 2001 Version,* DOE/ORP-2000-24, Rev. 0, U.S. Department of Energy, Office of River Protection, Richland, Washington.

Mann and Connelly 2003. F.M. Mann and M.P. Connelly, 2003, *Preliminary Performance Assessment for Waste Management Area C at the Hanford Site, Washington*, DOE/ORP-2003-11, Rev. 0, U.S. Department of Energy, Office of River Protection, Richland, Washington.

McMahon 2005a. W.J. McMahon, 2005, *CH2M HILL_STOMP Quality Assurance Test Results*, RPP-25859, Rev. 0, CH2M HILL Hanford Group, Inc. Richland, Washington.

Millington and Quirk 1961. R.J. Millington and J.P. Quirk, 1961, "Permeability of Porous Solids," *Trans. Faraday Soc,* Vol. 57, pp. 1200-1207.

Mualem 1976. Y. Mualem, 1976, "A New Model for Predicting the Hydraulic Conductivity of Unsaturated Porous Media," *Water Resources Research,* Vol. 12, No. 3, pp. 513-522.

Murray et al. 2003. C.J. Murray, A.L. Ward, and J. Wilson, 2003, *Influence of Clastic Dikes on Vertical Migration of Contaminants in the Vadose Zone at Hanford*, PNNL-14224, Pacific Northwest National Laboratory, Richland, Washington.

Myers 2005. D.A. Myers, 2005, *Field Investigation Report for Waste Management Areas T and TX-TY*, RPP-23752, Rev. 0-A, CH2M HILL Hanford Group, Inc., Richland, Washington.

Nkedi-Kizza et al. 1983. P. Nkedi-Kizza, J.W. Biggar, M.T. van Genuchten, P.J. Wierenga, H.M. Selim, J.M. Davidson, and D.R. Nielsen, 1983, "Modeling Tritium and Chloride 36 Transport Through an Aggregated Oxisol," *Water Resources Res*. Vol. 19:691-700.

ORNL 2005. Risk Assessment Information System. Online at http://risk.lsd.ornl.gov/index.shtml

Palmer and Puls 1994. C.D. Palmer and R.W. Puls, 1994, "Natural Attenuation of Hexavalent Chromium in Groundwater and Soils," EPA/540/5-94/505, U.S. Environmental Protection Agency, Ada, Oklahoma.

Palmer and Wittbrodt 1991. C.D. Palmer and P.R. Wittbrodt, 1991, "Processes Affecting the Remediation of Chromium-Contaminated Sites," *Environ. Health Perspectives*, Vol. 92, pp. 25-40.

Place et al. 2005. D.E. Place, B.A. Higley, and, C.W. Burrup, 2005, *Best-Basis Inventory Template Compositions of Common Tank Waste Layers*, RPP-8847, Rev. 1A, CH2M HILL Hanford Group, Inc, Richland, Washington.

Polmann 1990. D.J. Polmann, 1990, *Application of Stochastic Methods to Transient Flow and Transport in Heterogeneous Unsaturated Soils,* Ph.D. Thesis, Massachusetts Institute of Technology, Cambridge, Massachusetts.

Rai et al. 1987. D. Rai, C.C. Ainsworth, L.E. Eary, and S.V. Mattigod, 1987, *Inorganic and Organic Constituents in Fossil Fuel Combustion Residues, Volume 1: A Critical Review*, EPRI EA-5176, prepared for the Electric Power Research Institute, Palo Alto, California by Pacific Northwest National Laboratory, Richland, Washington.

Rai et al. 1988. D. Rai, J.M. Zachara, L.E. Eary, C.C. Ainsworth, J.E. Amonette, C.E. Cowan, R.W. Szelmeczka, C.T. Resch, R.L. Schmidt, S.C. Smith, and D.C. Girvin, 1988, *Chromium Reactions in Geologic Materials*, EPRI EA-5741, Electric Power Research Institute, Palo Alto, California.

Resource Conservation and Recovery Act of 1976, 42 USC 6901 et seq.

Richard and Bourg 1991. F.C. Richard and A.C.M. Bourg, 1991, "Aqueous Geochemistry of Chromium: A Review," *Water Research*, 25:807-816.

Rittmann 2004. P.D. Rittmann, 2004, *Exposure Scenarios and Unit Factors for the Hanford Tank Waste Performance Assessment*, HNF-SD-WM-TI-707, Rev. 4, CH2M HILL Hanford Group, Inc., Richland, Washington.

Rucker and Sweeney 2004. D.F. Rucker and M.D. Sweeney, 2004, *Plume Delineation in the BC Cribs and Trenches Area*, PNNL-14948, Pacific Northwest National Laboratory, Richland, Washington.

Smoot et al. 1989. J.L. Smoot, J.E. Szecsody, B. Sagar, G.W. Gee, and C.T. Kincaid, 1989, *Simulations of Infiltration of Meteoric Water and Contaminant Plume Movement in the Vadose Zone at Single-Shell Tank 241-T-106 at the Hanford Site*, WHC-EP-0332, Westinghouse Hanford Company, Richland, Washington.

Spitz and Moreno 1996. K. Spitz and J. Moreno, *A Practical Guide to Groundwater and Solute Transport Modeling*, John Wiley and Sons, Inc., New York, New York.

Stumm and Morgan 1981. W. Stumm and J.J. Morgan, 1981, *Aquatic Chemistry: Chemical Equilibria Rates in Natural Waters*, John Wiley and Sons, Inc., New York, New York.

Talbott and Gelhar 1994. M.E. Talbott and L.W. Gelhar, 1994, *Performance Assessment of a Hypothetical Low-Level Waste Facility: Groundwater Flow and Transport Simulation,* NUREG/CR-6114, Vol. 3, U.S. Nuclear Regulatory Commission, Washington, D.C.

Thorne and Newcomer 1992. P.D. Thorne and D.R. Newcomer, 1992, *Summary and Evaluation of Available Hydraulic Property Data for the Hanford Site Unconfined Aquifer System*, PNL-8337, Pacific Northwest Laboratory, Richland, Washington.

TWINS 2005. *Tank Waste Information Network System (TWINS) 3.* Online at http://twins.pnl.gov/twins.htm (accessed April 21, 2005).

van Genuchten 1980. M.Th. van Genuchten, 1980, "A Closed-Form Equation for Predicting the Hydraulic Conductivity of Unsaturated Soils," *Soil Sci. Soc. Am. J,* Vol. 44, pp. 892-898.

van Genuchten et al. 1991. M.Th. van Genuchten, F.J. Leij, and S.R. Yates, 1991, *The RETC Code for Quantifying the Hydraulic Functions of Unsaturated Soils*, EPA/600/2-91/065, U.S. Environmental Protection Agency, Washington, D.C.

Wang and Narasimhan 1985. J.S. Wang and T.N. Narasimhan, 1985, "Hydrologic mechanisms governing fluid flow in saturated, fractured porous media," *Water Resources Research*, 21:1861-74.

Ward et al. 1997. A.L. Ward, G.W. Gee, and M.D. White, 1997, *A Comprehensive Analysis of Contaminant Transport in the Vadose Zone beneath Tank SX-109,* PNNL-11463, Pacific Northwest National Laboratory, Richland, Washington.

Watrous 2002. R.A. Watrous, 2002, *Activity of Fuel Batches Processed through Hanford Separations Plants 1944 thru 1989*, RPP-13489, Rev. 0, CH2M HILL Hanford Group, Inc., Richland, Washington.

Watson 2005a. D.J. Watson, 2005, *Tank Closure Project Decision Management Tool Functional Design Requirements*, RPP-24200, Rev. 0, CH2M HILL Hanford Group, Inc., Richland, Washington.

Watson 2005b. D.J. Watson, 2005, *Tank Closure Project Decision Management Tool Systems Requirements Specification*, RPP-24201, Rev. 0, CH2M HILL Hanford Group, Inc., Richland, Washington.

Watson 2005c. D.J. Watson, 2005, *Tank Closure Project Decision Management Tool Software Test Results*, RPP-25525, Rev. 0, CH2M HILL Hanford Group, Inc., Richland, Washington.

Wing and Gee 1994. N.R. Wing and G.W. Gee, 1994, "Quest for the Perfect Cap," *Civil Engineering* 64(10):38-41.

Wittreich et al. 2003. C.D. Wittreich, J.K. Linville, G.W. Gee, and A.L. Ward, 2003, *200-BP-1 Prototype Hanford Barrier Annual Monitoring Report for Fiscal Year 2002*, CP-14873, Rev. 0, Fluor Hanford, Inc., Richland, Washington.

Wood et al. 1995a. M.I. Wood, R. Khaleel, P.D. Rittmann, A.H. Lu, S.H. Finfrock, R.J. Serne, K.J. Cantrell, and T.H. DeLorenzo, 1995, *Performance Assessment for the Disposal of Low-Level Waste in the 200 West Area Burial Grounds*, WHC-EP-0645, Westinghouse Hanford Company, Richland, Washington.

Wood et al. 1996. M.I. Wood, R. Khaleel, P.D. Rittmann, S.H. Finfrock, T.H. DeLorenzo, and D.Y. Garbrick, 1996, *Performance Assessment for the Disposal of Low-Level Waste in the 200 East Area Burial Grounds*, WHC-SD-WM-TI-730, Rev. 0, Westinghouse Hanford Company, Richland, Washington.

Wurstner et al. 1995. S.K. Wurstner, P.D. Thorne, M.A. Chamness, M.D. Freshley, and M.D. Williams, 1995, *Development of a Three-Dimensional Ground-Water Model of the Hanford Site Unconfined Aquifer System: FY 1995 Status Report*, PNL-10886, Pacific Northwest National Laboratory, Richland, Washington.

Ye et al. 2005. M. Ye, R. Khaleel, and T.-C.J. Yeh, 2005, "Stochastic analysis of moisture plume dynamics of a field injection experiment," *Water Resour. Res.*, 41, W03013, doi: 10.1029/2004WR003735

Yeh et al. 2005. T.-C.J. Yeh, M. Ye, and R. Khaleel, 2005, "Estimation of effective unsaturated hydraulic conductivity tensor using spatial moments of observed moisture plume," *Water Resour. Res.*, Vol. 41, W03014, doi:10.1029/2004WR003736.

Zhang et al. 2004. Z.F. Zhang, V.L. Freedman, S.R. Waichler, and M.D. White, 2004, *2004 Initial Assessments of Closure for the S-SX Tank Farm: Numerical Simulations*, PNNL-14604, Pacific Northwest National Laboratory, Richland, Washington.

This document was to large to provide as a single document for download. It has been divided into smaller sections for easier download

Section 5 of 6

Document Information			
Document #	DOE/ORP-2005-01	Revision	0
Title	INITIAL SINGLE-SHELL TANK SYSTEM PERFORMANCE ASSESSMENT FOR THE HANFORD SITE		
DATE	04/18/2005		
Originator	CONNELLY MP	Originator Co.	CH2M
Recipient			
References			
Keywords			
Projects			
Other Information			

4.0 MODELING RESULTS FOR THE GROUNDWATER PATHWAY

CONTENTS

4.1 INTRODUCTION 4-1

4.2 GENERAL DESCRIPTION OF REFERENCE CASE ANALYTICAL RESULTS 4-2
- 4.2.1 Contaminants Presented 4-2
- 4.2.2 Mobile Contaminant Breakthrough Curve Features 4-3
- 4.2.3 Sorption Coefficient Effects on Breakthrough Curves 4-5

4.3 LONG-TERM CONTAMINANT CONCENTRATIONS FOR WASTE MANAGEMENT AREA S-SX 4-8
- 4.3.1 Previous Modeling Efforts for Waste Management Area S-SX 4-9
- 4.3.2 Waste Management Area S-SX Fenceline Results 4-9
- 4.3.3 Results for Waste Management Area S-SX Waste Components 4-11
- 4.3.4 Discussion of Results and Conclusions for Waste Management Area S-SX 4-15

4.4 LONG-TERM CONTAMINANT CONCENTRATIONS FOR WASTE MANAGEMENT AREA T 4-22
- 4.4.1 Previous Modeling Efforts for Waste Management Area T 4-22
- 4.4.2 Waste Management Area T Fenceline Results 4-23
- 4.4.3 Results for Waste Management Area T Waste Components 4-24
- 4.4.4 Discussion of Results and Conclusions for Waste Management Area T 4-27

4.5 LONG-TERM CONTAMINANT CONCENTRATIONS FOR WASTE MANAGEMENT AREA TX-TY 4-34
- 4.5.1 Previous Modeling Efforts for Waste Management Area TX-TY 4-34
- 4.5.2 Waste Management Area TX-TY Fenceline Results 4-35
- 4.5.3 Results for Waste Management Area TX-TY Waste Components 4-37
- 4.5.4 Discussion of Results and Conclusions for Waste Management Area TX-TY 4-40

4.6 LONG-TERM CONTAMINANT CONCENTRATIONS FOR WASTE MANAGEMENT AREA U 4-47
- 4.6.1 Previous Modeling Efforts for Waste Management Area U 4-47
- 4.6.2 Waste Management Area U Fenceline Results 4-47
- 4.6.3 Discussion of Results and Conclusions for Waste Management Area U 4-52

4.7 LONG-TERM CONTAMINANT CONCENTRATIONS FOR WASTE MANAGEMENT AREA C 4-59
- 4.7.1 Previous Modeling Efforts for Waste Management Area C 4-59
- 4.7.2 Waste Management Area C Fenceline Results 4-60
- 4.7.3 Results for Waste Management Area C Waste Components 4-63
- 4.7.4 Discussion of Results and Conclusions for Waste Management Area C 4-64

4.8 LONG-TERM CONTAMINANT CONCENTRATIONS FOR WASTE MANAGEMENT AREA B-BX-BY 4-73
4.8.1 Previous Modeling Efforts for Waste Management Area B-BX-BY 4-73
4.8.2 Waste Management Area B-BX-BY Fenceline Results 4-74
4.8.3 Results for Waste Management Area B-BX-BY Waste Components 4-74
4.8.4 Discussion of Results and Conclusions for Waste Management Area B-BX-BY 4-79

4.9 LONG-TERM CONTAMINANT CONCENTRATIONS FOR WASTE MANAGEMENT AREA A-AX 4-87
4.9.1 Previous Modeling Efforts for Waste Management Area A-AX 4-87
4.9.2 Waste Management Area A-AX Fenceline Results 4-87
4.9.3 Results for Waste Management Area A-AX Waste Components 4-88
4.9.4 Discussion of Results and Conclusions for Waste Management Area A-AX 4-92

4.10 SUMMARY OF GROUNDWATER IMPACTS FOR THE REFERENCE CASE 4-99

4.11 SUMMARY OF RESULTS OF SENSITIVITY AND "WHAT IF" ANALYSES 4-101
4.11.1 Recharge 4-105
4.11.2 Source Term Characteristics 4-122
4.11.3 Hydrology 4-137
4.11.4 Integration of Sensitivity and "What If" Analyses Effects on Groundwater Impacts at the Waste Management Area Fencelines 4-154
4.11.5 Impacts of Individual Barrier Underperformance on Total System (Multiple Barrier) Performance 4-172

4.12 REFERENCES 4-177

FIGURES

Figure 4-1. Idealized 200 West Area Waste Component Mobile Contaminant Breakthrough Curves and Contributing Factors 4-4

Figure 4-2. Idealized 200 West Area Early Release Contaminant Mobility Comparison 4-7

Figure 4-3. Representative 200 West Area Residual Release Contaminant Mobility Comparison 4-7

Figure 4-4. Waste Management Area S-SX Technetium-99 Breakthrough Curves by Waste Source Component 4-16

Figure 4-5. Waste Management Area S-SX Iodine-129 Breakthrough Curves by Waste Source Component 4-17

Figure 4-6. Waste Management Area S-SX Hexavalent Chromium Breakthrough Curves by Waste Source Component 4-18

Figure 4-7. Waste Management Area S-SX Nitrate Breakthrough Curves by Waste Source Component 4-19

Figure 4-8. Waste Management Area S-SX Nitrite Breakthrough Curves by Waste Source Component 4-20

Figure 4-9. Waste Management Area S-SX Uranium Breakthrough Curves by Waste Source Component 4-21

Figure 4-10. Waste Management Area T Technetium-99 Breakthrough Curves by Waste Source Component 4-28

Figure 4-11. Waste Management Area T Iodine-129 Breakthrough Curves by Waste Source Component 4-29

Figure 4-12. Waste Management Area T Hexavalent Chromium Breakthrough Curves by Waste Source Component 4-30

Figure 4-13. Waste Management Area T Nitrate Breakthrough Curves by Waste Source Component 4-31

Figure 4-14. Waste Management Area T Nitrite Breakthrough Curves by Waste Source Component 4-32

Figure 4-15. Waste Management Area T Uranium Breakthrough Curves by Waste Source Component 4-33

Figure 4-16. Waste Management Area TX-TY Technetium-99 Breakthrough Curves by Waste Source Component 4-41

Figure 4-17. Waste Management Area TX-TY Iodine-129 Breakthrough Curves by Waste Source Component 4-42

Figure 4-18. Waste Management Area TX-TY Hexavalent Chromium Breakthrough Curves by Waste Source Component 4-43

Figure 4-19. Waste Management Area TX-TY Nitrate Breakthrough Curves by Waste Source Component 4-44

Figure 4-20. Waste Management Area TX-TY Nitrite Breakthrough Curves by Waste Source Component 4-45

Figure 4-21. Waste Management Area TX-TY Uranium Breakthrough Curves by Waste Source Component 4-46

Figure 4-22. Waste Management Area U Technetium-99 Breakthrough Curves by Waste Source Component 4-53

Figure 4-23. Waste Management Area U Iodine-129 Breakthrough Curves by Waste Source Component 4-54

Figure 4-24. Waste Management Area U Hexavalent Chromium Breakthrough Curves by Waste Source Component 4-55

Figure 4-25. Waste Management Area U Nitrate Breakthrough Curves by Waste Source Component 4-56

Figure 4-26. Waste Management Area U Nitrite Breakthrough Curves by Waste Source Component 4-57

Figure 4-27. Waste Management Area U Uranium Breakthrough Curves by Waste Source Component 4-58

Figure 4-28. Waste Management Area C Technetium-99 Breakthrough Curves by Waste Source Component 4-67

Figure 4-29. Waste Management Area C Iodine-129 Breakthrough Curves by Waste Source Component 4-68

Figure 4-30. Waste Management Area C Hexavalent Chromium Breakthrough Curves by Waste Source Component 4-69

Figure 4-31. Waste Management Area C Nitrate Breakthrough Curves by Waste Source Component 4-70

Figure 4-32. Waste Management Area C Nitrite Breakthrough Curves by Waste Source Component 4-71

Figure 4-33. Waste Management Area C Uranium Breakthrough Curves by Waste Source Component 4-72

Figure 4-34. Waste Management Area B-BX-BY Technetium-99 Breakthrough Curves by Waste Source Component 4-81

Figure 4-35. Waste Management Area B-BX-BY Iodine-129 Breakthrough Curves by Waste Source Component 4-82

Figure 4-36. Waste Management Area B-BX-BY Hexavalent Chromium Breakthrough Curves by Waste Source Component 4-83

Figure 4-37. Waste Management Area B-BX-BY Nitrate Breakthrough Curves by Waste Source Component 4-84

Figure 4-38. Waste Management Area B-BX-BY Nitrite Breakthrough Curves by Waste Source Component 4-85

Figure 4-39. Waste Management Area B-BX-BY Uranium Breakthrough Curves by Waste Source Component 4-86

Figure 4-40. Waste Management Area A-AX Technetium-99 Breakthrough Curves by Waste Source Component 4-93

Figure 4-41. Waste Management Area A-AX Iodine-129 Breakthrough Curves by Waste Source Component 4-94

Figure 4-42. Waste Management Area A-AX Hexavalent Chromium Breakthrough Curves by Waste Source Component 4-95

Figure 4-43. Waste Management Area A-AX Nitrate Breakthrough Curves by Waste Source Component 4-96

Figure 4-44. Waste Management Area A-AX Nitrite Breakthrough Curves by Waste Source Component 4-97

Figure 4-45. Waste Management Area A-AX Uranium Breakthrough Curves by Waste Source Component 4-98

Figure 4-46. Cumulative Variability Analysis Approach 4-167

Figure 4-47. Barrier Underperformance Analysis Approach 4-173

TABLES

Table 4-1. Waste Management Area S-SX Tank Rows and Waste Components Included in Modeling 4-10

Table 4-2. Estimated Concentrations of Contaminants from All Waste Components Appearing at the Waste Management Area S-SX Fenceline 4-11

Table 4-3. Waste Management Area S-SX Tank Row Peak Radionuclide Concentrations 4-12

Table 4-4. Waste Management Area S-SX Tank Row Peak Nonradionuclide Concentrations 4-13

Table 4-5. Waste Management Area T Tank Rows and Waste Components Included in Modeling 4-23

Table 4-6. Estimated Concentrations of Contaminants from All Waste Components Appearing at the Waste Management Area T Fenceline 4-24

Table 4-7. Waste Management Area T Tank Row Peak Radionuclide Concentrations 4-26

Table 4-8. Waste Management Area T Tank Row Peak Nonradionuclide Concentrations 4-26

Table 4-9. Waste Management Area TX-TY Tank Rows and Waste Components Included in the Modeling 4-35

Table 4-10. Estimated Concentrations of Contaminants from All Waste Components Appearing at the Waste Management Area TX-TY Fenceline 4-36

Table 4-11. Waste Management Area TX-TY Tank Row Peak Radionuclide Concentrations 4-38

Table 4-12. Waste Management Area TX-TY Tank Row Peak Nonradionuclide Concentrations 4-39

Table 4-13. Waste Management Area U Tank Rows and Waste Components Included in Modeling 4-48

Table 4-14. Estimated Concentrations of Contaminants from All Waste Components Appearing at the Waste Management Area U Fenceline 4-49

Table 4-15. Waste Management Area U Tank Row Peak Radionuclide Concentrations 4-50

Table 4-16. Waste Management Area U Tank Row Peak Nonradionuclide Concentrations 4-51

Table 4-17. Waste Management Area C Tank Rows and Waste Components Included in Modeling 4-60

Table 4-18 Contaminants Unique to Tank C-106 Post-Retrieval Sample Results 4-61

Table 4-19. Estimated Concentrations of Contaminants from All Waste Components Appearing at the Waste Management Area C Fenceline 4-62

Table 4-20. Waste Management Area C Tank Row Peak Radionuclide Concentrations 4-65

Table 4-21. Waste Management Area C Tank Row Peak Nonradionuclide Concentrations 4-66

Table 4-22. Waste Management Area B-BX-BY Tank Rows and Waste Components Included in Modeling 4-75

Table 4-23. Estimated Concentrations of Contaminants from All Waste Components Appearing at the Waste Management Area B-BX-BY Fenceline 4-76

Table 4-24. Waste Management Area B-BX-BY Tank Row Peak Radionuclide Concentrations 4-77

Table 4-25. Waste Management Area B-BX-BY Tank Row Peak Nonradionuclide Concentrations 4-78

Table 4-26. Waste Management Area A-AX Tank Rows and Waste Components Included in Modeling 4-88

Table 4-27. Estimated Concentrations of Contaminants from All Waste Components Appearing at the Waste Management Area A-AX Fenceline 4-89

Table 4-28. Waste Management Area A-AX Tank Row Peak Radionuclide Concentrations 4-90

Table 4-29. Waste Management Area A-AX Tank Row Peak Nonradionuclide Concentrations 4-91

Table 4-30. Reference Case Peak Fenceline Concentrations for Selected Contaminants Within the Single-Shell Tank System 4-100

Table 4-31. Waste Management Area C Recharge Sensitivity and "What If" Cases for Tank Waste Residual Releases 4-107

Table 4-32. Waste Management Area C Recharge Sensitivity and "What If" Cases for Past Releases 4-111

Table 4-33. Waste Management Area S-SX Recharge Sensitivity and "What If" Cases for Tank Waste Residual Releases 4-114

Table 4-34. Waste Management Area S-SX Recharge Sensitivity and "What If" Cases for Past Releases 4-118

Table 4-35. Waste Management Area C Source Term Characteristics Sensitivity and "What If" Cases for Tank Waste Residual Releases 4-124

Table 4-36. Waste Management Area C Source Term Characteristics Sensitivity and "What If" Cases for Past Releases 4-127

Table 4-37. Waste Management Area S-SX Source Term Characteristics Sensitivity and "What If" Cases for Tank Waste Residual Releases 4-130

Table 4-38. Waste Management Area S-SX Source Term Characteristics Sensitivity and "What If" Cases for Past Releases 4-132

Table 4-39. Waste Management Area C Hydrology Sensitivity and "What If" Cases for Tank Waste Residual Releases 4-140

Table 4-40. Waste Management Area C Hydrology Sensitivity and "What If" Cases for Past Releases 4-144

Table 4-41. Waste Management Area S-SX Hydrology Sensitivity and "What If" Cases for Tank Waste Residual Releases 4-147

Table 4-42. Waste Management Area S-SX Hydrology Sensitivity and "What If" Cases for Past Releases 4-150

Table 4-43. Comparison (by Ratio) of Sensitivity and "What If" to Reference Case Peak Values for Technetium-99 Initially Present in Past Releases at Waste Management Area C 4-156

Table 4-44. Comparison (by Ratio) of Sensitivity and "What If" to Reference Case Peak Values for Technetium-99 Initially Present in Past Releases at Waste Management Area S-SX 4-157

Table 4-45. Comparison (by Ratio) of Sensitivity and "What If" to Reference Case Peak Values for Iodine-129 Initially Present in Past Releases at Waste Management Area C 4-159

Table 4-46. Comparison (by Ratio) of Sensitivity and "What If" to Reference Case Peak Values for Iodine-129 Initially Present in Past Releases at Waste Management Area S-SX 4-162

Table 4-47. Comparison (by Ratio) of Sensitivity and "What If" to Reference Case Peak Values for Technetium-99 Initially Present in Tank Waste Residuals at Waste Management Area C 4-163

Table 4-48. Comparison (by Ratio) of Sensitivity and "What If" to Reference Case Peak Values for Technetium-99 Initially Present in Tank Waste Residuals at Waste Management Area S-SX 4-164

Table 4-49. Summary of Groundwater Contamination Impacts from Increased Recharge Rate Cases for Iodine-129 and Uranium Migration from Tank Residual Waste and Uranium Migration from Past Releases 4-166

Table 4-50. Categorization of Sensitivity and "What If" Cases with Respect to Potential for Reduction in Variability Effects on Peak Groundwater Contamination Values 4-168

Table 4-51. Cumulative Variability Factors for Mobile and Semi-Mobile Radionuclides that Reach Peak/Maximum Values within the Modeled Time Period (12032) 4-171

Table 4-52. Impacts of Single or Multiple Barrier Degradation on Total System Performance for Mobile Contaminants Released from Tank Residual Waste at Waste Management Areas C and S-SX 4-175

Table 4-53. Impacts of Single Barrier Degradation on Total System Performance for Mobile and Semi-Mobile Contaminants in Past Releases at Waste Management Areas C and S-SX 4-176

4.0 MODELING RESULTS FOR THE GROUNDWATER PATHWAY

4.1 INTRODUCTION

This chapter presents estimated long-term contaminant transport modeling results for three contaminant source components (i.e., past releases, tank residual inventory, and ancillary equipment residual inventory). Both reference, sensitivity, and "what if" cases (described in Chapter 3.0) were analyzed. Reference cases were analyzed for all WMAs in the SST system. The reference cases assumed central tendency input parameter values of current and closure conditions at WMAs C and S-SX, except for the contaminant inventory estimates, which were WMA-specific. These analyses provided peak groundwater concentration estimates that were used in the performance evaluation discussed in Chapter 6.0. Chapter 6.0 provides human health impact estimates that assumed consumption and other uses of groundwater contaminated at these levels.

Vadose zone transport for 122 contaminants was modeled for each WMA. Three contaminant source components were modeled:

- Past releases
- Tank residual inventory
- Ancillary equipment residual inventory.

In general, the greatest impacts occur early in the simulation from tank past releases. Impacts from tank and ancillary equipment residuals are minor and occur at the end of the simulation.

Sensitivity and "what if" case analyses were analyzed for WMAs C and S-SX. The sensitivity and "what if" cases assume parameter values above and below the reference case values that reflect plausible value ranges of site-specific features and processes. These analyses provide ranges of maximum groundwater concentrations around the reference case values.

The combined results from the reference, sensitivity, and "what if" case analyses provided several major insights including:

- An understanding of features and processes that control the potential occurrence and level of tank waste contaminants in the unconfined aquifer
- A means of defining a plausible range of maximum future contamination levels around reference case estimates (e.g., an estimate of variability)
- An evaluation of the impacts of potential underperformance of the defense in depth barriers on total system performance.

Section 4.2 describes the general types of reference case results common to all of the WMA-specific analyses as is discussed in each of the succeeding WMA-specific sections (Sections 4.3 through 4.9). A comparison of the reference case contaminant transport modeling results among the WMAs is provided in Section 4.10. In Section 4.11, contaminant transport modeling results from the sensitivity and "what if" analyses are described and compared to the reference case results.

4.2 GENERAL DESCRIPTION OF REFERENCE CASE ANALYTICAL RESULTS

Each of the following WMA-specific sections (Sections 4.3 through 4.9) summarizes previous contaminant transport modeling efforts and describes reference case results at the WMA fenceline.

> Mobile contaminants from past releases arrive at the WMA fenceline early in the simulation, while mobile contaminants from tank residuals arrive thousands of years later in the simulation.

WMA fenceline results, organized by contaminant, identify the WMA tank row causing the highest level of groundwater contamination for each waste source. The results for selected contaminants (Section 4.2.1) are summarized in a figure (e.g., Figure 4-4) with six plots. Five plots show the estimated concentration distribution over time at the fenceline, also known as a breakthrough curve (BTC), and identifies the waste source and tank location from which the contaminant originated. General characteristics of BTCs are described more fully in Sections 4.2.2 and 4.2.3. The sixth BTC at the bottom of the figure superimposes the previous five to illustrate the maximum impact for the WMA. Each section also contains a summary table (e.g., Table 4-2), which identifies the waste source and tank row where the largest concentration was calculated for contaminants that reached the fenceline at non-negligible concentrations within the modeled time frame. Other summary tables (e.g., Tables 4-3 and 4-4) compare contaminant-specific peak concentrations among the tank rows modeled in the WMA for selected contaminants.

4.2.1 Contaminants Presented

Although the long-term contaminant transport modeling analysis for each WMA evaluated all the contaminants with their estimated inventories, only six contaminants were selected for the following discussion: technetium-99, hexavalent chromium, iodine-129, nitrate, nitrite, and uranium. These six were selected to illustrate a range of mobility within the vadose zone: technetium-99 and hexavalent chromium are highly mobile contaminants, iodine-129 is less mobile (referred to as semi-mobile), and uranium is the least mobile of these constituents within the vadose zone (referred to as less-mobile). These six contaminants were also selected because they represent general water quality indicators, have been measured in the unconfined aquifer, and their projected concentrations are measurable.[1] These six contaminants will be referred to as "indicator contaminants" for the remainder of the chapter.

An average of 41 contaminants appeared at the fenceline per WMA by the end of the 10,000-year simulation time frame. Contaminants with fenceline concentrations below the effective zero of the analysis either had no inventory in the contaminant source component being modeled, decayed to concentrations below the effective zero of the analysis, or did not reach the groundwater because of chemical interaction with soils.

---

[1] For the purposes of Chapter 4.0, concentrations below 1.0×10^{-2} pCi/L for radionuclide contaminants and 1.0×10^{-5} mg/L for nonradionuclide contaminants are treated as effectively zero.

An average of 41 contaminants appeared at the fenceline per WMA during the simulation.

Six indicator contaminants were selected to illustrate a range of mobility and because they are the primary risk drivers:

- Technetium-99
- Hexavalent chromium
- Iodine-129
- Nitrate
- Nitrite
- Uranium.

4.2.2 Mobile Contaminant Breakthrough Curve Features

Figure 4-1 provides typical waste component BTCs for a mobile contaminant (K_d = 0 mL/g). Generally, two major peaks occur over time from waste component releases: an early maximum peak from contamination at depth from past leaks and a later, significantly lower peak from post-closure tank residuals. Although Figure 4-1 is an example figure illustrating this point, it does not reflect any WMA-specific data. The relative contributions of ancillary equipment inventories to the other components are generally not as large as those portrayed in Figure 4-1, but for purposes of illustration, the BTC has been enlarged. The following general description of source-specific component contributions generally applies to all the WMAs in the SST system, and should facilitate an understanding of the results in the WMA–specific result sections.

4.2.2.1 Past Releases Component

The past releases (also referred to as past leaks) waste component is comprised of past tank leaks and UPRs. These past releases, as well as residuals from plugged and blocked pipelines, are considered early releases due to the immediate availability in the simulation of their inventories for transport starting in the year 2000. Past release component BTCs for mobile contaminants generally exhibit an early maximum peak, a rapid decline in concentration leading to a secondary inflection or peak, and then a gradual decline in concentration to effectively zero in the last half of the simulation period.

The initial peak concentration occurs relatively early when the mobile contaminant inventories are accessible to recharge water, and recharge rates are maximized because the surface barrier is not operational until the year 2032. The rapid decline in concentration after the initial peak reflects the reduced recharge rate due to emplacement of the Modified RCRA Subtitle C Barrier. The reduced recharge rate results in less moisture movement through the vadose zone and in a lower contaminant concentration at the fenceline. The secondary peak or inflection occurs when contaminants present in the vadose zone are influenced by the higher recharge rate caused by barrier degradation. The primary differences between the two past release component BTCs are that the past leak component has an early concentration peak and a subsequent inflection in the curve, while the UPR component has a lower magnitude initial peak followed by a secondary peak and a longer discharge to the aquifer than the past leak component. These differences are caused by the placement of the contamination in the vadose zone at the beginning of the simulation; past leaks are assumed to be closer to the aquifer (130 ft bgs in the 200 West Area and 150 bgs in the 200 East Area) than UPRs (30 ft bgs). Therefore, more past leak inventory than UPR inventory is discharged at the beginning of the simulation because the past leak component has a shorter travel distance to the unconfined aquifer.

Figure 4-1. Idealized 200 West Area Waste Component Mobile Contaminant Breakthrough Curves and Contributing Factors

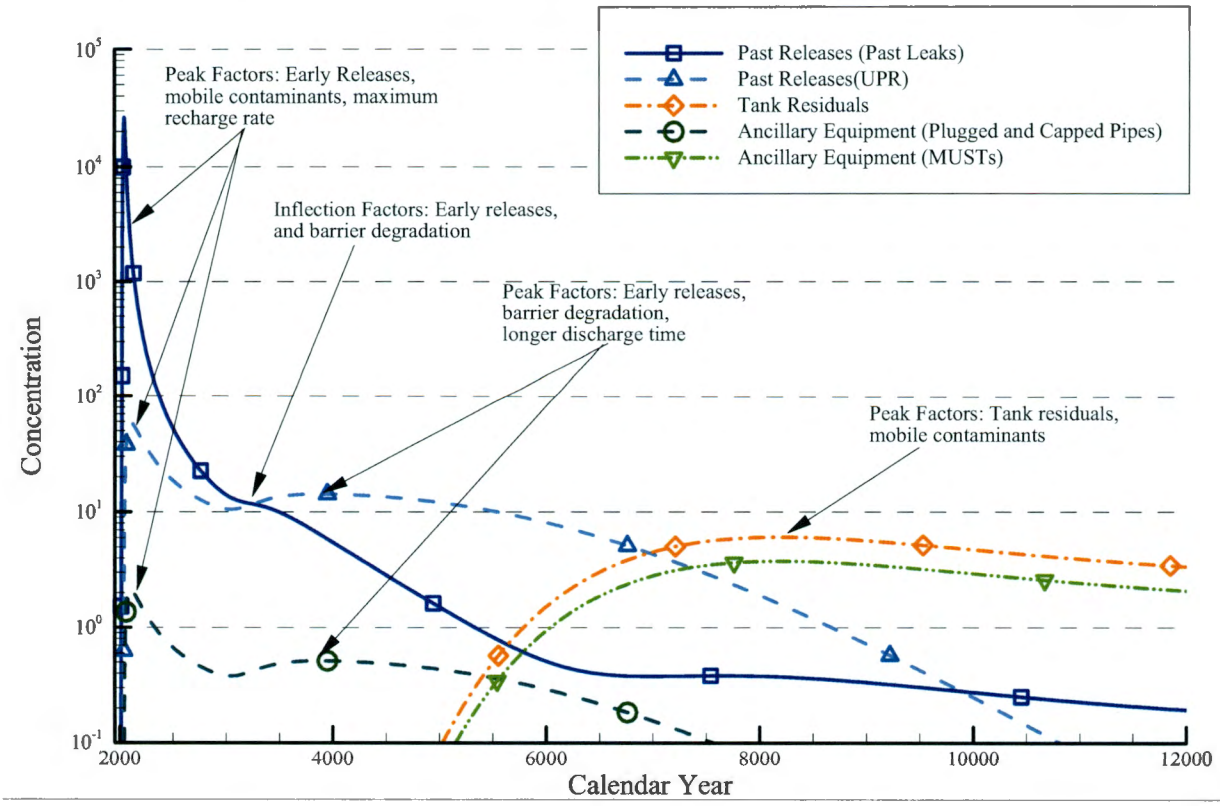

A majority of the past leak component inventory is discharged to the aquifer before the Modified RCRA Subtitle C Barrier is emplaced. The longer travel distance of the UPR component to the aquifer results in more UPR component inventory remaining in the vadose zone when the barrier is installed. The remaining UPR component inventory is then influenced by increased recharge rates from barrier degradation, resulting in the secondary peak seen in the UPR BTC. Past leaks were modeled at a depth of 130 ft (39.6 m) bgs in 200 West Area WMAs. Past leaks in 200 East Area WMAs were modeled at a depth of 150 ft (45.7 m). Past leaks in both areas were modeled with a simulated diameter of 25 ft (8 m) and were available for transport at the beginning of the simulation. UPRs were modeled at a depth of 30 ft (9.1 m) and were available for transport at the beginning of the simulation.

4.2.2.2 Ancillary Equipment Residuals Component

The ancillary equipment residuals component is comprised of plugged and blocked pipelines, vaults, and MUSTs. Mobile contaminants from the plugged and blocked pipeline residuals component, like past release contaminants, are assumed to be in contact with recharge water immediately. The estimated BTC has an early maximum peak, a rapid decline in concentration leading to a secondary inflection (or a secondary peak), and then exhibits a slow decline in concentration through the last half of the simulation period. Like the UPR waste component, the pipeline component was modeled as having an inventory with shallow placement in the vadose zone. The long travel distance from the pipeline inventory placement in the vadose zone to the aquifer results in an initial peak prior to barrier placement, followed by a smaller secondary peak

with a long discharge period. The rapid decline in fenceline concentration following the first peak reflects the reduced recharge rate caused by the barrier emplacement. The secondary peak or inflection is caused by the influence of increased recharge following barrier degradation.

The MUST residuals ancillary component, which is modeled as a tank residuals component, exhibits a curve with the same characteristics as the tank residuals component: concentrations of mobile contaminants projected to have concentrations greater than effective zero around year 4000 and peaking in the last half of the simulation period with a slow decline in concentration throughout the end of the simulation period. The ancillary equipment component (i.e., MUSTs) provides a negligible contribution to most WMA contaminant concentrations.

Plugged and blocked pipeline ancillary equipment component contamination was modeled as a uniformly distributed 25-ft diameter inventory at 25 ft bgs available for transport at the beginning of the simulation.

4.2.2.3 Tank Residuals Component

Mobile contaminant BTCs from tank residuals peak during the last half of the simulation period. Tank residual concentrations become greater than effective zero after barrier degradation as increased recharge carries mobile tank residual contaminants through the vadose zone. Tank residuals become the dominant component contributing to fenceline concentration about halfway through the simulation. Tank residual concentrations typically peak in the last third of the simulation period, and then exhibit a slow decline through the end of the simulation period. Contaminant release from the tank residuals component (i.e., SST residuals) was modeled as diffusional release from the base of the tanks beginning January 1, 2032. Of the three contaminant source components, residual contaminants discharge for the longest time period into the unconfined aquifer. The tank residuals and MUST residuals components are considered late releases because the contaminants are not available for transport until the year 2032 due to reduced recharge from existing barriers.

4.2.3 Sorption Coefficient Effects on Breakthrough Curves

Figure 4-2 contains idealized (non-WMA specific) BTCs for a mobile analyte (K_d of 0 mL/g, e.g., technetium-99), a semi-mobile analyte (K_d of 0.2 mL/g, e.g., iodine-129), and a less-mobile analyte (K_d of 0.6 mL/g, e.g., uranium) from early releases in 200 West Area vadose zone soils. Figure 4-2 illustrates how the mobility of a contaminant affects its BTC. Generally, BTCs for mobile contaminants (reproduced in a simplified form from Figure 4-1) exhibit an early maximum peak caused by high pre-barrier recharge rates and high past leak contaminant mobility resulting in rapid transport to the unconfined aquifer starting in the year 2000. Post-barrier recharge rates result in a rapid decline in concentrations until the year of barrier degradation (year 2532), when recharge rates increase. About a quarter of the way through the simulation period, there is either an inflection or secondary peak in the curve resulting from the past leak contaminants being transported by the increased recharge from barrier degradation. Concentrations then exhibit a slow decline for the remainder of the simulation period as the rest of the early release contaminant inventory is transported away from the point of comparison.

BTCs for semi-mobile contaminants (i.e., $K_d = 0.2$ mL/g), as illustrated in Figure 4-2, peak later in the simulation period than those for the mobile contaminants, indicating semi-mobile

contaminants reach groundwater after mobile contaminants. High pre-barrier recharge rates (prior to year 2032) rapidly transport semi-mobile contaminants within the vadose to the unconfined aquifer at the beginning of the simulation. Decreased post–barrier recharge rates cause the concentration increase rate to slow. Within about 500 years of barrier degradation, the resulting increased recharge rate begins to cause an increase in contaminant concentration. This increase continues throughout the rest of the simulation period, suggesting that the peak concentration was not reached in the simulation time frame. The relatively flat curve shape at the end of the simulation period suggests that concentrations are close to their peak at this time.

Less-mobile contaminants (i.e., K_d = 0.6 mL/g or greater) reach the aquifer after the semi-mobile contaminants. Although a maximum is reached at the end of the modeling period (year 12032), the increasing concentration at that time shows that the peak was not reached during the simulation. The scale for the less-mobile contaminant in Figure 4-2 is extended to less than effective zero to facilitate comparison of the behavior of less-mobile contaminants with the behavior of semi-mobile and mobile contaminants.

Figure 4-3 illustrates idealized BTCs for a mobile contaminant (K_d = 0 mL/g), a semi-mobile contaminant (K_d = 0.2 mL/g), and a less-mobile contaminant (K_d = 0.6 mL/g) from late releases (e.g., tank residuals) in 200 West Area vadose zone soils. In Figure 4-3, contaminants are released into the vadose by diffusion through stabilizing grout after projected tank integrity failure in year 2032. Once in the vadose zone, mobile contaminants are transported by the reduced recharge rate caused by the emplaced Modified RCRA Subtitle C Barrier. Contaminant transport rates increase with increased post–barrier recharge, peaking in the last half of the simulation period, and then exhibiting a slow decline for the remainder of the simulation period as the rest of the contaminant inventory is transported away from the point of comparison. Semi-mobile and less-mobile contaminant concentrations do not exceed the effective zero in the simulation time frame, indicating these contaminants have not been transported the entire distance from the tanks to the unconfined aquifer.

Figure 4-2. Idealized 200 West Area Early Release Contaminant Mobility Comparison

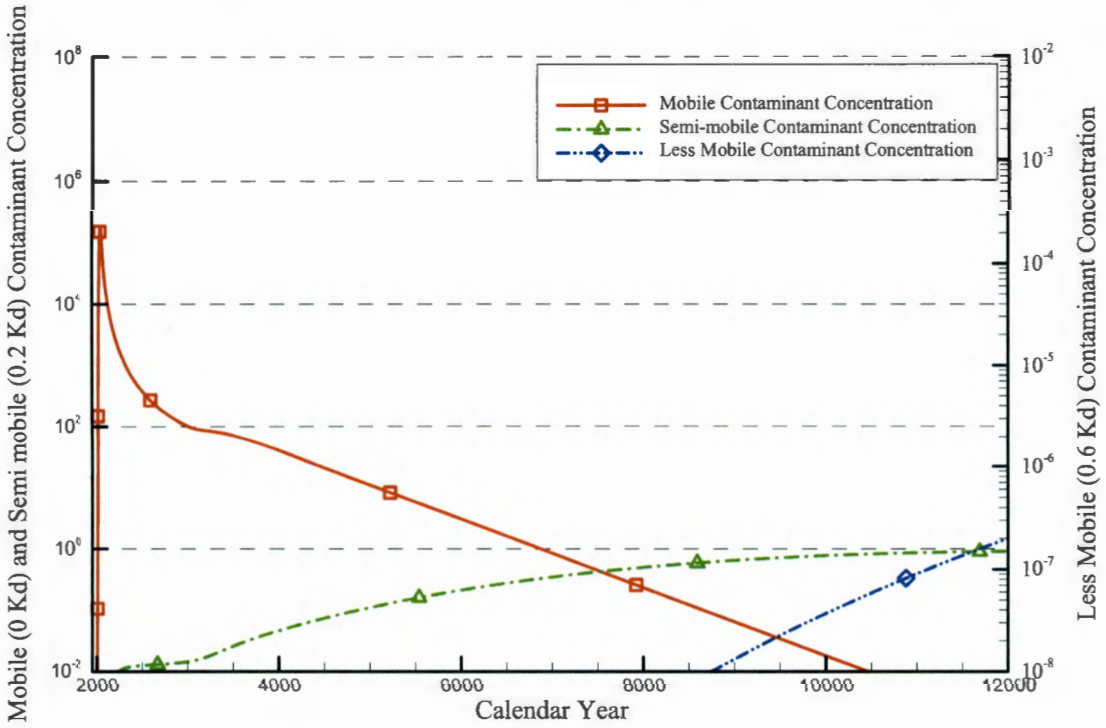

Figure 4-3. Representative 200 West Area Residual Release Contaminant Mobility Comparison

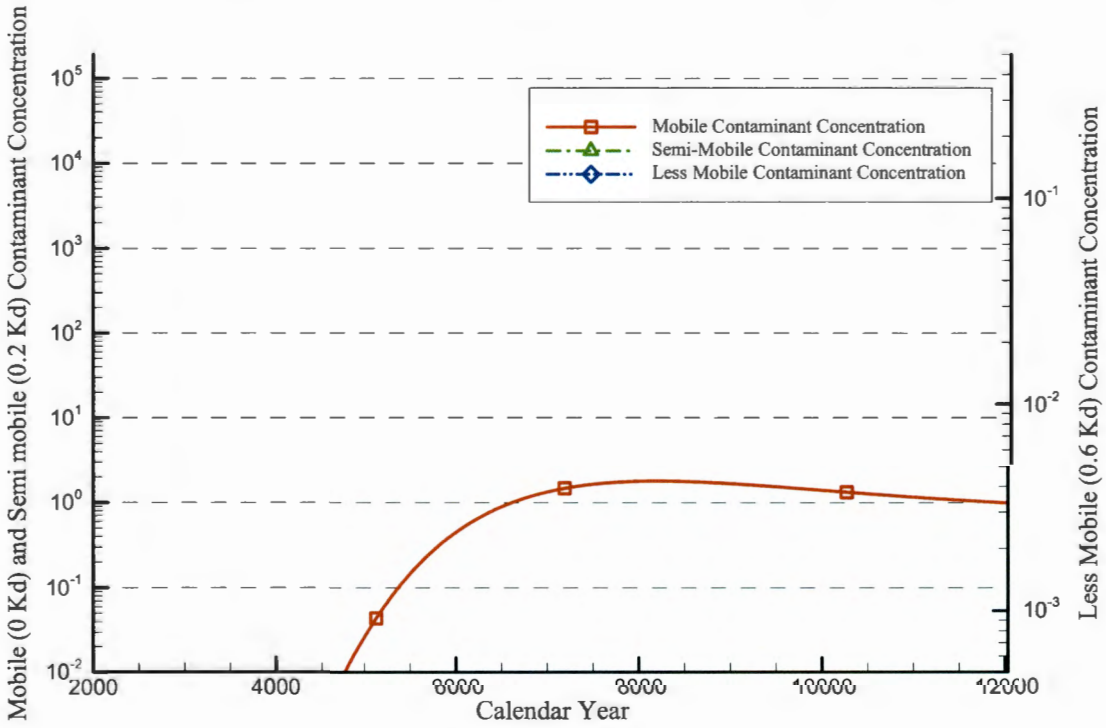

Understanding the WMA-specific results presented in the following sections requires familiarity with the transport behavior of the individual source components and sorption coefficient effects presented in this section. The following key conclusions will facilitate an understanding of WMA-specific contaminant transport discussions:

- Mobility of a contaminant is important: Mobile contaminants will reach groundwater sooner than semi-mobile and less-mobile contaminants from the same source component.
- Mobile contaminants from past release component arrive early in the simulation: Mobile contaminant inventories are accessible to recharge water and recharge rates are maximized because the surface barrier is not operational until the year 2032.
- Mobile contaminants from tank residuals arrive late in the simulation and have lower magnitude impacts compared to past releases: These contaminants are influenced by lower recharge rates resulting from barrier emplacement and by longer travel distance to the unconfined aquifer.
- Semi-mobile contaminants from past releases can reach the unconfined aquifer late in the simulation.
- Less-mobile contaminants from past releases can potentially reach the unconfined aquifer late in the simulation, but this is unlikely.
- Semi-mobile and less-mobile contaminants from tank residuals do not reach the unconfined aquifer during the 10,000-year simulation.

4.3 LONG-TERM CONTAMINANT CONCENTRATIONS FOR WASTE MANAGEMENT AREA S-SX

This section presents contaminant transport modeling results for the indicator contaminants selected for WMA S-SX. The numerical calculation point for this analysis is the WMA S-SX fenceline. Impacts of individual source components (past releases, tank residuals, and ancillary equipment residuals) to the system are presented.

Significant groundwater contamination driven by tank past leaks is predicted to reach the WMA S-SX fenceline.

Contamination from tank residuals has minor groundwater concentration impacts late in the simulation.

WMA S-SX has 27 tanks aligned in 9 rows that are effectively parallel with the groundwater flow (Figure 2-33). The S tank farm has twelve 100-Series tanks (758,000 gal) (Chapter 2.0) (Williams 2001a) and the SX tank farm has fifteen 100-Series tanks (1,000,000 gal). Reference case contaminant inventory estimates were developed for each row based on the information in Chapter 3.0. Impacts to groundwater from individual waste components were then evaluated on a row-by-row basis. This section presents the contaminant concentration estimates for the highest contributing row for each source component.

4.3.1 Previous Modeling Efforts for Waste Management Area S-SX

Risk Assessment for Waste Management Area S-SX Closure Plan (Connelly 2004) estimated long-term groundwater impact for a variety of contaminants. Peak concentrations for the contaminants presented in this chapter and Connelly (2004) differ, and are caused primarily by differences in assumptions. Compared to this analysis, differences in parameter inputs and modeling assumptions in Connelly (2004) include:

- Barrier emplacement and residual release start date in year 2050 rather than in year 2032
- A higher degraded barrier recharge rate
- Tank residual waste release start date that coincides with barrier emplacement
- A higher diffusion coefficient for tank residuals
- A slightly deeper emplacement of the residual ancillary equipment inventory within the vadose zone.

Prior to Connelly (2004), the S-SX FIR (Knepp 2002a) modeled long-term groundwater concentrations for technetium-99, chromium, and nitrate from past leaks in this WMA. The primary focus of the modeling was to characterize the effects of various closure strategies, particularly interim barriers, for the WMA. Peak concentrations for technetium-99 and nitrate presented in this chapter and in the S-SX FIR differ by about a factor of 3, while the estimated chromium concentrations are slightly lower in this chapter than in the FIR. The primary cause for this difference is the placement of the inventory within the vadose zone in the model. In the FIR, individual contaminant inventories were placed in the vadose zone model as layers. Contaminant layer depth was determined by observations of contaminant depth in borehole samples. Consequently, chromium had a greater travel distance to the water table in the FIR model and therefore resulted in lower concentrations relative to the SST PA. Other variations between modeling efforts include:

- Site-specific distribution of contaminants within the vadose zone was developed for the FIR, while the SST PA uses a more generic distribution of contaminants within the vadose zone.
- Closure barrier is placed over the site in year 2040 in the FIR, and in year 2032 in the SST PA.
- The FIR uses the inventory from Jones et al. (2000b), while the inventory used for the SST PA is from Corbin et al. (2005).
- The FIR modeled a lower barrier recharge rate and a higher post-barrier recharge rate than the SST PA.

4.3.2 Waste Management Area S-SX Fenceline Results

Twenty-one contaminants in WMA S-SX had fenceline concentrations above the effective zero within the 10,000-year simulation period. Table 4-1 defines the tank rows in WMA S-SX and summarizes waste sources included in each row. The designation for each tank row is the lowest numbered tank in the sequence (e.g., S-101 identifies the row consisting of tanks S-101, S-102, and S-103). These designations will be used throughout Section 4.3. The WMA S-SX plugged and blocked pipelines are not listed in Table 4-1 because they do not coincide with a single tank row and were therefore modeled as a separate source. Table 4-2 lists the contaminants with

fenceline concentrations above the effective zero indicating the dominant source term and the tank row providing the inventory responsible for the peak concentration estimate.

Table 4-1. Waste Management Area S-SX Tank Rows and Waste Components Included in Modeling

Tank Row	Residual Waste		Past Releases	
	Tanks	Ancillary Equipment	Tank Leaks	Past Shallow Releases
S-101	241-S-101 241-S-102 241-S-103	None	None	None
S-104	241-S-104 241-S-105 241-S-106	None	241-S-104 past leak	None
S-107	241-S-107 241-S-108 241-S-109	None	None	None
S-110	241-S-110 241-S-111 241-S-112	None	None	None
SX-101	241-SX-101 241-SX-102 241-SX-103	241-SX-302 catch tank	None	None
SX-104	241-SX-104 241-SX-105 241-SX-106	None	241-SX-104 past leak	None
SX-107	241-SX-107 241-SX-108 241-SX-109	None	241-SX-107 past leak 241-SX-108 past leak 241-SX-109 past leak	None
SX-110	241-SX-110 241-SX-111 241-SX-112	None	241-SX-110 past leak 241-SX-111 past leak 241-SX-112 past leak	None
SX-113	241-SX-113 241-SX-114 241-SX-115	None	241-SX-113 past leak 241-SX-115 past leak	None

Table 4-2. Estimated Concentrations of Contaminants from All Waste Components Appearing at the Waste Management Area S-SX Fenceline

Radionuclides [a]				
Analyte Name	**Peak Concentration pCi/L**	**Dominant Component**	**Peak Year**	**Row with Peak Concentration**
Tritium	3.80E+04	Past releases	2040	SX-113
Carbon-14	5.50E+03	Past releases	2043	SX-107
Cobalt-60	3.60E-02	Past releases	2054	SX-113
Technetium-99	1.92E+05	Past releases	2043	SX-107
Iodine-129	9.18E-01	Past releases	12032	SX-107
Nonradionuclides [b]				
Analyte Name	**Peak Concentration mg/L**	**Dominant Component**	**Peak Year**	**Row with Peak Concentration**
Ammonia	1.34E+00	Past releases	2043	SX-107
Bismuth	8.12E-03	Past releases	2043	SX-104
Cerium	2.87E-04	Tank residuals	8201	SX-101
Chloride	1.29E+01	Past releases	2043	SX-107
Chromium	5.22E+00	Past releases	2043	SX-107
Fluoride	3.33E-01	Past releases	2043	SX-104
Hydroxide	1.14E-01	Tank residuals	8201	SX-110
Lanthanum	2.83E-04	Tank residuals	8201	S-110
Neodymium	3.07E-04	Tank residuals	8201	SX-101
Nitrate	3.93E+02	Past releases	2043	SX-107
Nitrite	1.89E+02	Past releases	2043	SX-107
Oxalate	2.32E-02	Tank residuals	8201	S-101
Phosphate	1.02E+00	Past releases	2043	SX-104
Sodium	4.69E+02	Past releases	2043	SX-107
Sulfate	9.67E+00	Past releases	2043	SX-107
n-Butyl Alcohol	2.22E-01	Past releases	2043	SX-104

[a] The following radionuclides reached the fenceline during the modeling period, but had concentrations below the effective zero (1.0E-02 pCi/L): tin-126, radium-226 + D, uranium-233, uranium-234, uranium-235 + D, uranium-236, and uranium-238 + D.

[b] The following nonradionuclides reached the fenceline during the modeling period, but had concentrations below the effective zero (1.0E-05 mg/L): aluminum, cobalt, manganese, rhodium, uranium, and yttrium.

4.3.3 Results for Waste Management Area S-SX Waste Components

The past releases component is the primary contributing source component to fenceline concentrations in WMA S-SX for all of the indicator contaminants described in Section 4.2.1. The past releases component consists of both SST leaks and UPRs. Modeling of both source terms was the same except for the initial depth assignment (130 ft bgs for SST past leaks in the 200 East Area, 150 ft bgs for SST past leaks in the 200 West Area, and 30 ft bgs for UPRs). There are 10 total SST past leaks in the WMA. In S tank farm, there is only one tank row (tank row S-104) with a past tank leak. In SX tank farm, there is only one tank row

(tank row SX-101) without a past tank leak. There are no UPRs in WMA S-SX (Field and Jones 2005). Tank row SX-107 is projected to contribute the highest past releases component concentration for all the indicator contaminants considered for WMA S-SX, except uranium, which is not projected to occur at the fenceline above the effective zero concentration. Tank row SX-107 has past leaks from all three tanks in the row. Although tank row SX-110 also has past leaks from all three tanks in the row, the total inventory of the leaks from row SX-107 is greater than that from row SX-110.

For indicator contaminants considered in this section (Tables 4-3 and 4-4), tank retrieval to volume and inventories estimated by Kirkbride et al. (2005) results in different rows contributing the peak fenceline concentration from tank residuals. The tank residuals component consists of SST and ancillary equipment (i.e., MUST) residuals. The MUST residuals were incorporated into the tank residual calculations for each row because the SST and MUST residuals were modeled in the same manner (i.e., diffusion-limited release). The ancillary equipment residuals component in WMA S-SX consists of plugged and blocked pipelines in the S tank farm and the SX-302 catch tank, which resides in tank row SX-101. Both ancillary equipment sources provide negligible contributions to the overall concentrations for each of the indicator contaminants considered in this chapter.

Table 4-3 shows peak fenceline concentrations for radionuclides by tank row, and Table 4-4 shows peak fenceline concentrations for nonradionuclides by row. Both tables show concentrations from past releases and tank residuals source terms relative to the peak contributing tank row. The past releases component consists of past tank leaks and UPRs; however, no UPRs occur within WMA S-SX. Since MUST residuals are modeled as tank residuals, the tank residuals portion of the tables include MUSTs that reside within a tank row. Although the peak concentrations from different source components occur at different times, Tables 4-3 and 4-4 show that, for any given contaminant, the peak concentration estimate due to past leaks is between two and five orders of magnitude greater than the peak tank residual concentration for any given contaminant.

Table 4-3. Waste Management Area S-SX Tank Row Peak Radionuclide Concentrations [a] (2 pages)

Technetium-99				
	Past Releases Component, Peak Year: 2043		**Tank Residuals Component, Peak Year: 8191**	
Tank Row	**Peak Concentration pCi/L**	**Concentration Relative to Row SX-107**	**Peak Concentration pCi/L**	**Concentration Relative to Row S-104**
S-101	0.00E+00	0.00%	1.67E+01	47.04%
S-104	3.64E+02	0.19%	3.55E+01	100.00%
S-107	0.00E+00	0.00%	2.35E+01	66.20%
S-110	0.00E+00	0.00%	6.66E+00	18.76%
SX-101 [b]	0.00E+00	0.00%	1.70E+01	47.89%
SX-104	4.15E+04	22.00%	1.59E+01	44.79%
SX-107	1.92E+05	100.00%	1.80E+00	5.07%
SX-110	8.87E+03	5.00%	1.15E+00	3.24%
SX-113	5.55E+04	29.00%	1.25E+00	3.52%

Table 4-3. Waste Management Area S-SX Tank Row Peak Radionuclide Concentrations [a] (2 pages)

Iodine-129				
	Past Releases Component, Max. Year: 12032		**Tank Residuals Component**	
Tank Row	**Peak Concentration pCi/L**	**Concentration Relative to Row SX-107**	**Max. Concentration pCi/L [c]**	**Concentration Relative to Row with Peak Concentration**
S-101	0.00E+00	0.00%	0.00E+00	NA
S-104	0.00E+00	0.00%	0.00E+00	NA
S-107	0.00E+00	0.00%	0.00E+00	NA
S-110	0.00E+00	0.00%	0.00E+00	NA
SX-101	0.00E+00	0.00%	0.00E+00	NA
SX-104	1.25E-01	13.62%	0.00E+00	NA
SX-107	9.18E-01	100.00%	0.00E+00	NA
SX-110	2.95E-02	3.21%	0.00E+00	NA
SX-113	2.69E-01	29.30%	0.00E+00	NA

[a] Maximum values are shaded.

[b] Tank row SX-101 includes ancillary equipment residuals from SX-302 catch tank.

[c] Iodine-129 concentrations from the tank residuals component were not above effective zero (1.00E-02 pCi/L) for any row in the waste management area.

NA = not applicable

Table 4-4. Waste Management Area S-SX Tank Row Peak Nonradionuclide Concentrations [a] (2 pages)

Hexavalent Chromium				
	Past Releases Component, Peak Year: 2043		**Tank Residuals Component, Peak Year: 8201**	
Tank Row	**Peak Concentration mg/L**	**Concentration Relative to Row SX-107**	**Peak Concentration mg/L**	**Concentration Relative to Row SX-101**
S-101	0.00E+00	0.00%	1.70E-02	68.27%
S-104	1.33E-01	2.55%	1.32E-02	53.01%
S-107	0.00E+00	0.00%	1.38E-02	55.42%
S-110	0.00E+00	0.00%	3.44E-03	13.82%
SX-101[b]	0.00E+00	0.00%	2.49E-02	100.00%
SX-104	5.68E-01	10.88%	1.13E-02	45.38%
SX-107	5.22E+00	100.00%	1.42E-03	5.70%
SX-110	1.67E-01	3.20%	4.62E-04	1.86%
SX-113	3.68E+00	70.50%	3.86E-03	15.50%

Table 4-4. Waste Management Area S-SX Tank Row Peak Nonradionuclide Concentrations [a] (2 pages)

Nitrate				
	Past Releases Component, Peak Year: 2043		**Tank Residuals Component, Peak Year: 8201**	
Tank Row	**Peak Concentration mg/L**	**Concentration Relative to Row SX-107**	**Peak Concentration mg/L**	**Concentration Relative to Row S-107**
S-101	0.00E+00	0.00%	1.14E-02	37.25%
S-104	4.60E+01	11.70%	2.19E-02	71.57%
S-107	0.00E+00	0.00%	3.06E-02	100.00%
S-110	0.00E+00	0.00%	1.58E-02	51.63%
SX-101	0.00E+00	0.00%	2.85E-02	93.14%
SX-104	4.28E+01	10.89%	2.03E-02	66.34%
SX-107	3.93E+02	100.00%	1.95E-02	63.73%
SX-110	1.15E+01	2.93%	5.69E-03	18.59%
SX-113	2.04E+02	51.91%	3.25E-03	10.62%
Nitrite				
	Past Releases Component, Peak Year: 2043		**Tank Residuals Component, Peak Year: 8201**	
Tank Row	**Peak Concentration mg/L**	**Concentration Relative to Row SX-107**	**Peak Concentration mg/L**	**Concentration Relative to Row SX-104**
S-101	0.00E+00	0.00%	2.61E-03	45.16%
S-104	1.11E+01	5.87%	1.21E-03	20.93%
S-107	0.00E+00	0.00%	1.76E-03	30.45%
S-110	0.00E+00	0.00%	1.57E-03	27.16%
SX-101	0.00E+00	0.00%	5.09E-03	88.06%
SX-104	2.26E+01	11.96%	5.78E-03	100.00%
SX-107	1.89E+02	100.00%	1.02E-03	17.65%
SX-110	5.36E+00	2.84%	7.22E-04	12.49%
SX-113	7.40E+01	39.15%	3.47E-04	6.00%
Uranium				
Uranium concentrations from the past leak and tank residuals components were not above effective zero (1.00E-05 mg/L) for any row in the waste management area.				

[a] Maximum values are shaded.

[b] Tank row SX-101 includes ancillary equipment residuals from SX-302 catch tank.

Plugged and blocked pipelines do not fall within any one tank row and were evaluated separately. Plugged and blocked pipelines were modeled as a shallow release in the same manner as UPRs (i.e., initial depth of 30 ft bgs). Modeling results indicate that the plugged and blocked pipelines result in the following peak concentration estimates:

- Technetium-99: 5.48 pCi/L, peak year 2094
- Hexavalent chromium: 6.89×10^{-5} mg/L, peak year 2094
- Nitrate: 5.29×10^{-3} mg/L, peak year 2094
- Nitrite: 2.62×10^{-3} mg/L, peak year 2094.

Uranium concentrations from the plugged and blocked pipeline residual components in WMA S-SX are effectively zero.

Figures 4-4 through 4-9 provide the BTCs for each of the six indicator contaminants discussed in this section. Each of the first five plots in the figure is from a separate source component, with the bottom plot containing the previous five plots superimposed to illustrate the maximum impact. Blank plots indicate cases where the concentration for a source component does not exceed the effective zero for any tank row over the 10,000-year simulation period. In those cases, the tank row with the greatest inventory is indicated. The individual source component plots have a linear scale on the y-axis, but in order to show all the curves over the range of data, the maximum impact plot has a logarithmic scale y-axis. Each plot represents the BTC from the tank row contributing the peak concentration estimate for that source component. Also given in each of the plots is the time of the peak and the inventory for each of the like source terms in the row. The tank row containing the largest inventory is shown even though the peak concentration fell below the effective zero.

4.3.4 Discussion of Results and Conclusions for Waste Management Area S-SX

Estimated long-term groundwater impacts from three contaminant source components (i.e., past releases inventory, tank residuals inventory, and ancillary equipment residuals inventory) in WMA S-SX are modeled. Results of the analysis indicate that, for mobile contaminants, contamination at depth from SX-107, SX-108, and SX-109 tank leaks are the dominant contributors to fenceline concentration during the early part of the simulation period, and for the entire simulation period for less-mobile contaminants. Results also indicate that, regardless of contaminant mobility, the contaminant concentrations resulting from contamination at depth are orders of magnitude higher than the contaminant concentration resulting from the tank residuals component. For the tank residuals source component, each contaminant has a peak concentration from a different row. For the reference case, ancillary equipment has a negligible impact, with only four of the six indicator contaminants projected to have concentrations above effective zero.

The impact from tank residuals is two to five orders of magnitude below impacts from past releases, using HFFACO prescribed volume and retrieval estimates for WMA S-SX in Kirkbride et al. (2005). For the tank residuals and for all indicator contaminants only the row with the maximum impact is shown; the other tank rows are usually within a factor of 9 or lower of the row with the peak concentration, with a few rows being as much as a factor of 35 or lower (Tables 4-3 and 4-4).

Contaminants with high mobility (K_d less than 0.2 mL/g) exhibit concentration peaks that occur early in the simulation and prior to emplacement of the Modified RCRA Subtitle C Barrier. Contaminants with low mobility (K_d 0.2 mL/g or greater) exhibit increasing concentrations toward the end of the simulation period, dominated by the contamination at depth source component.

Figure 4-4. Waste Management Area S-SX Technetium-99 Breakthrough Curves by Waste Source Component

Technetium-99 K_d = 0.0 mL/g		
Past Releases	**Past Leaks from Tanks Tank Row SX-107 to SX-109** ^{99}Tc Inventory SX-107 = 6.00E+0 Ci SX-108 = 1.41E+1 Ci SX-109 = 8.00E-1 Ci Sum = 2.09E+1 Ci Peak = 1.92E+5 pCi/L Occurs in Year 2043	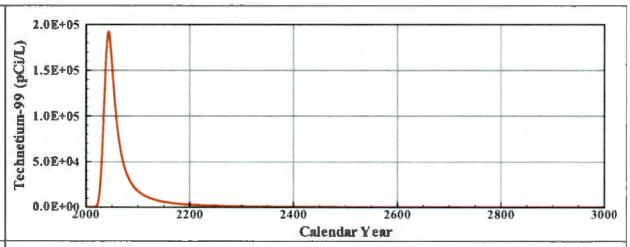
	No Shallow Releases within WMA S-SX	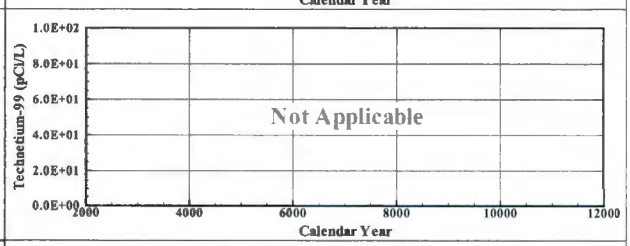
Residual Waste	**Tank Residuals SST Tank Row S-104 to S-106** ^{99}Tc Inventory S-104 = 3.00E-2 Ci S-105 = 2.15E+0 Ci S-106 = 7.30E-1 Ci Sum = 2.91E+0 Ci Peak = 35.5 pCi/L Occurs in Year 8191	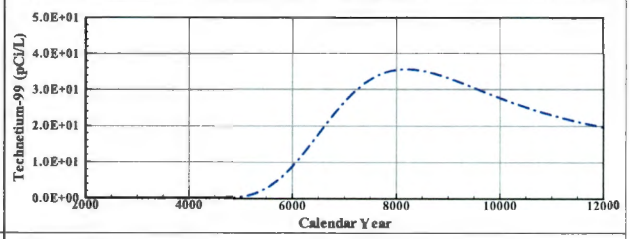
	Ancillary Equipment Pipeline Residuals ^{99}Tc Inventory S Farm =1.8E-2 Ci SX Farm = 0.0 Ci Peak = 5.48E+0 pCi/L Occurs in Year 2094	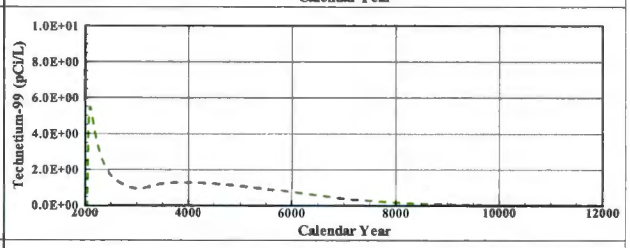
	Ancillary Equipment MUST ^{99}Tc Inventory SX-302 = 5.4E-3 Ci Peak = 6.6E-2 pCi/L Occurs in Year 8191	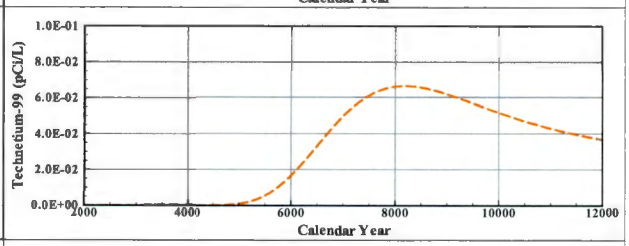
Maximum Impact Note: Shaded background indicates a change from a linear Y-Axis to a Log Y-Axis. This change in axis scale is necessary show all curves over the range of data in the same plot.		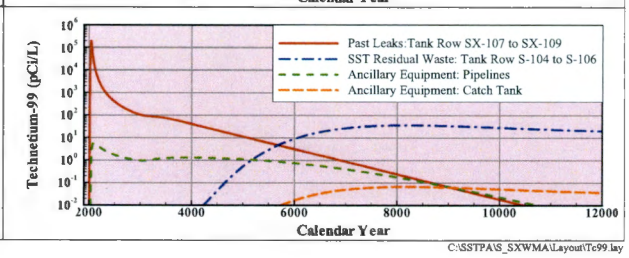

Figure 4-5. Waste Management Area S-SX Iodine-129 Breakthrough Curves by Waste Source Component

Iodine-129 K_d = 0.2 mL/g		
Past Releases	**Past Leaks from Tanks Tank Row SX-107 to SX-109** ^{129}I Inventory SX-107 = 9.28E-3 Ci SX-108 = 2.17E-2 Ci SX-109 = 1.24E-3 Ci Sum = 3.22E-2 Ci Maximum = 9.18E-1 pCi/L by End of Simulation	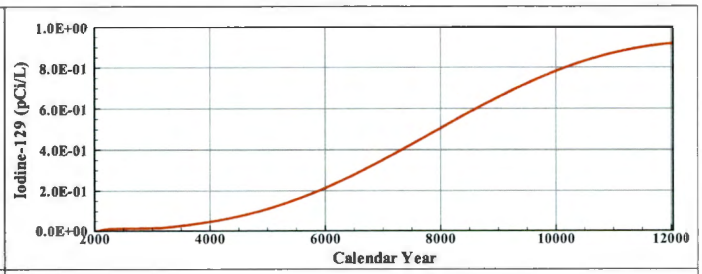
	No Shallow Releases within WMA S-SX	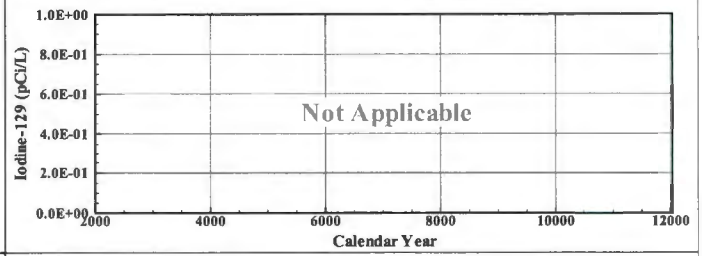
Residual Waste	**Tank Residuals SST Tank Row S-104 to S-106** ^{129}I Inventory S-104 = 2.84E-4 Ci S-105 = 1.71E-4 Ci S-106 = 2.20E-4 Ci Sum = 6.75E-4 Ci Maximum < 0.01 pCi/L by End of Simulation	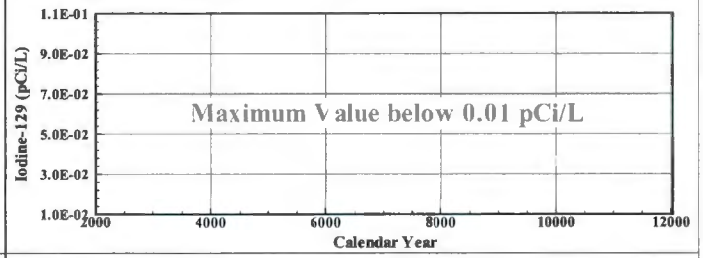
	Ancillary Equipment Pipeline Residuals ^{129}I Inventory S-Farm = 1.7E-5 Ci SX-Farm = 0.00 Ci Maximum < 0.01 pCi/L by End of Simulation	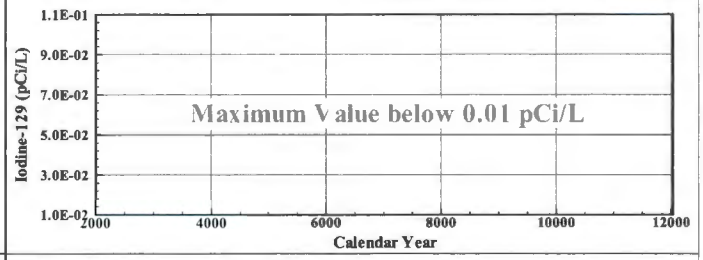
	Ancillary Equipment MUST ^{129}I Inventory SX-302 = 5.9E-6 Ci Maximum < 0.01 pCi/L by End of Simulation	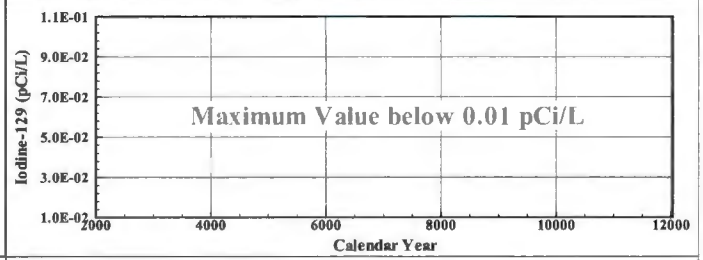
Maximum Impact Note: Shaded background indicates a change from a linear Y-Axis to a Log Y-Axis. This change in axis scale is necessary show all curves over the range of data in the same plot.		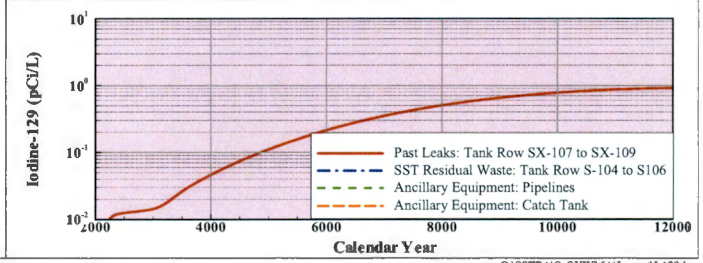

C:\SSTPA\S_SXWMA\Layout\I-129.lay

Figure 4-6. Waste Management Area S-SX Hexavalent Chromium Breakthrough Curves by Waste Source Component

Chromium K_d = 0.0 mL/g		
Past Releases	**Past Leaks from Tanks Tank Row SX-107 to SX-109** Chromium Inventory SX-107 = 1.64E+2 kg SX-108 = 3.82E+2 kg SX-109 = 2.18E+1 kg Sum = 5.67E+2 kg Peak = 5.2 mg/L Occurs in Year 2043	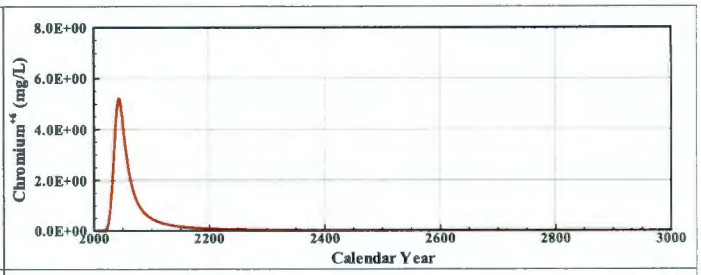
	No Shallow Releases within WMA S-SX	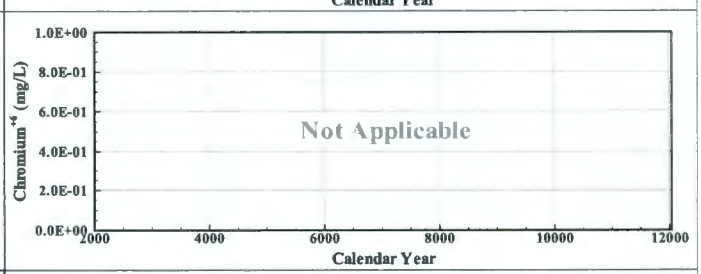
Residual Waste	**Tank Residuals SST Tank Row SX-101 to SX-103** Chromium Inventory SX-101 = 1.18E+3 kg SX-102 = 6.35E+2 kg SX-103 = 1.79E+2 kg Sum = 1.99E+3 kg Peak = 2.49E-2 mg/L Occurs in Year 8201	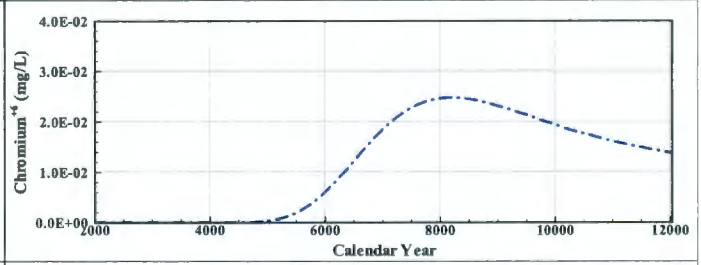
	Ancillary Equipment Pipeline Residuals Chromium Inventory S-Farm = 2.3E-1 kg SX-Farm = 0.0 kg Peak = 6.9E-5 mg/L Occurs in Year 2094	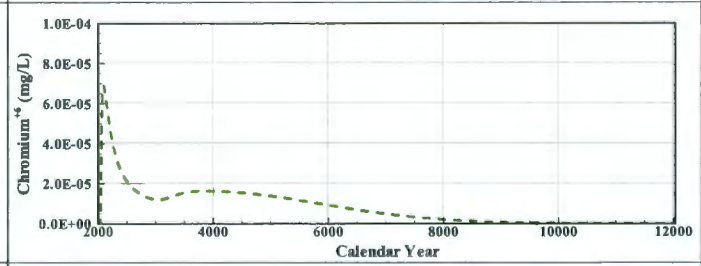
	Ancillary Equipment MUST Chromium Inventory SX-302 = 6.00E+0 kg Peak = 7.5E-5 mg/L Occurs in Year 8201	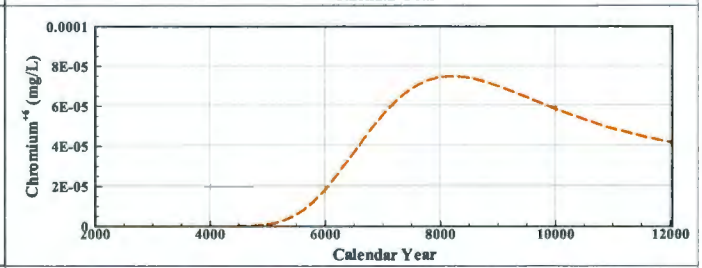
Maximum Impact Note: Shaded background indicates a change from a linear Y-Axis to a Log Y-Axis. This change in axis scale is necessary show all curves over the range of data in the same plot.		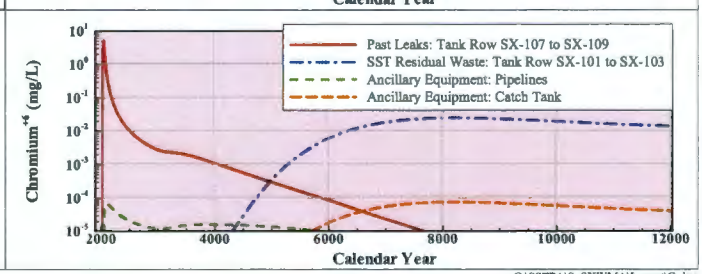

C:\SSTPA\S_SXWMA\Layout\Cr.lay

Figure 4-7. Waste Management Area S-SX Nitrate Breakthrough Curves by Waste Source Component

Nitrate
K_d = 0.0 mL/g

Past Releases

Past Leaks from Tanks Tank Row SX-107 to SX-109

Nitrate Inventory

SX-107 = 1.23E+4 kg
SX-108 = 2.87E+4 kg
SX-109 = 1.64E+3 kg
Sum = 4.27E+4 kg

Peak = 3.93E+2 mg/L
Occurs in Year 2043

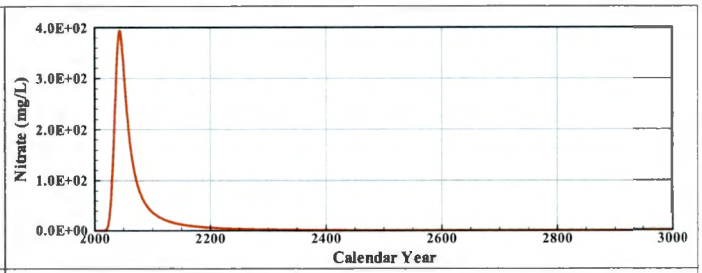

No Shallow Releases within WMA S-SX

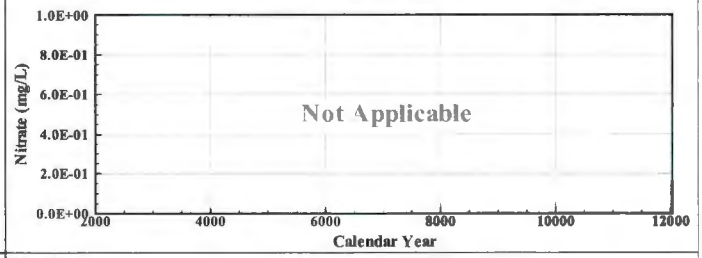

Residual Waste

Tank Residuals SST Tank Row S-107 to S-109

Nitrate Inventory

S-107 = 2.92E+1 kg
S-108 = 7.91E+2 kg
S-109 = 1.63E+3 kg
Sum = 2.45E+3 kg

Peak = 0.03 mg/L
Occurs in Year 8201

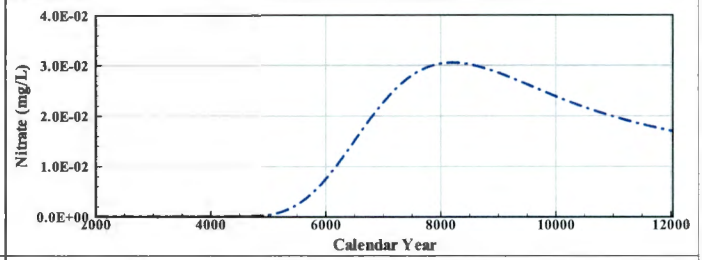

Ancillary Equipment Pipeline Residuals

Nitrate Inventory

S-Farm = 1.71E+1 kg
SX-Farm = 0.0 kg

Peak = 5.3E-3 mg/L
Occurs in Year 2094

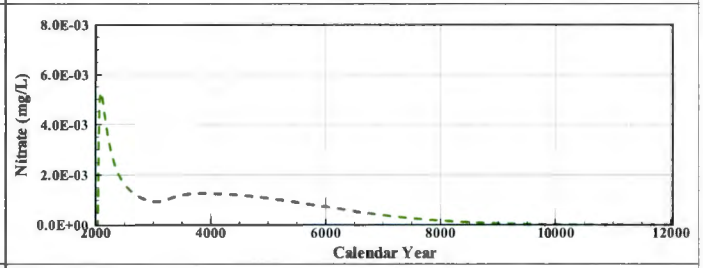

Ancillary Equipment MUST

Nitrate Inventory

SX-302 = 1.1E+1 kg

Peak = 1.4E-4 mg/L
Occurs in Year 8201

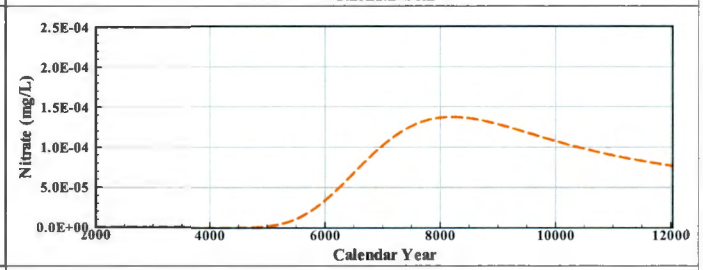

Maximum Impact

Note: Shaded background indicates a change from a linear Y-Axis to a Log Y-Axis. This change in axis scale is necessary show all curves over the range of data in the same plot.

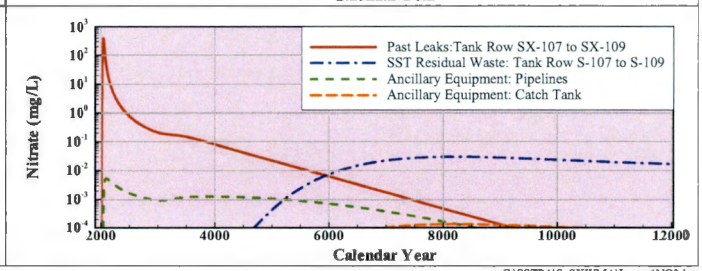

C:\SSTPA\S_SXWMA\Layout\NO3.lay

Figure 4-8. Waste Management Area S-SX Nitrite Breakthrough Curves by Waste Source Component

Nitrite K_d = 0.0 mL/g		
Past Releases	**Past Leaks from Tanks Tank Row SX-107 to SX-109** Nitrite Inventory SX-107 = 5.93E+3 kg SX-108 = 1.38E+4 kg SX-109 = 7.90E+2 kg Sum = 2.05E+4 kg Peak = 1.89E+2 mg/L Occurs in Year 2043	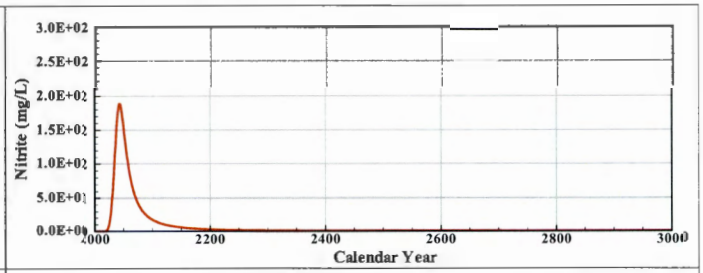
	No Shallow Releases within WMA S-SX	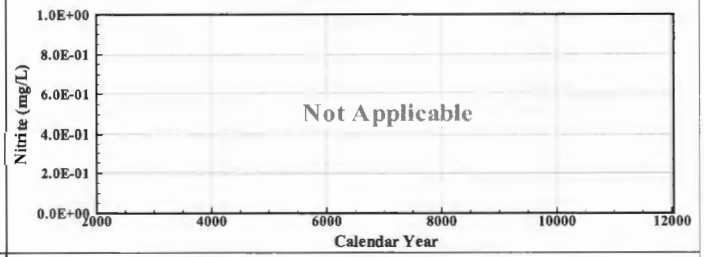
Residual Waste	**Tank Residuals SST Tank Row SX-104 to SX-106** Nitrite Inventory SX-104 = 51.3 kg SX-106 = 189.6 kg SX-107 = 222.1 kg Sum = 463.0 kg Peak = 5.78E-3 mg/L Occurs in Year 8201	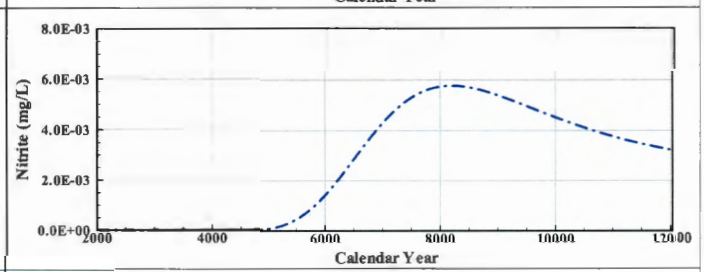
	Ancillary Equipment Pipeline Residuals Nitrite Inventory S-Farm = 8.50E+0 kg SX-Farm = 0.0 kg Peak = 2.6E-3 mg/L Occurs in Year 2094	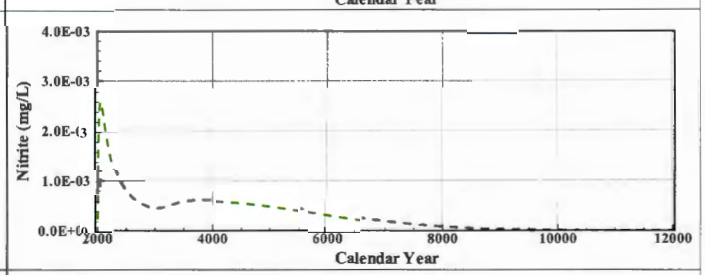
	Ancillary Equipment MUST Nitrate Inventory SX-302 = 1.9E+0 kg Peak = 2.3E-5 mg/L Occurs in Year 8201	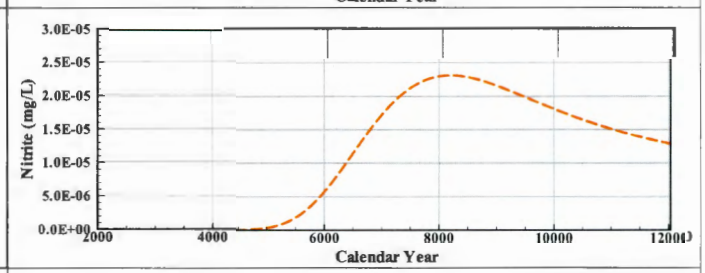
Maximum Impact Note: Shaded background indicates a change from a linear Y-Axis to a Log Y-Axis. This change in axis scale is necessary show all curves over the range of data in the same plot.		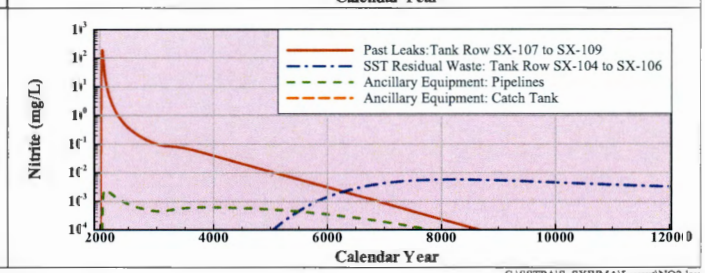

C:\SSTPA\S_SXWMA\Layout\NO2.lay

Figure 4-9. Waste Management Area S-SX Uranium Breakthrough Curves by Waste Source Component

Uranium K_d = 0.6 mL/g		
Past Releases	**Past Leaks from Tanks Tank Row SX-113 to SX-115** Uranium Inventory SX-113 = 1.8E+0 kg SX-114 = 0.0E+0 kg SX-115 = 5.8E+0 kg Sum = 7.6E+0 kg Maximum < 1E-5 mg/L by End of Simulation	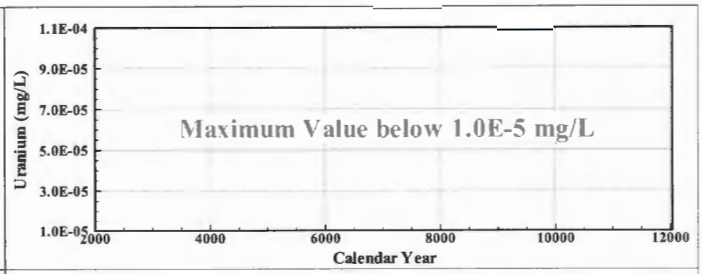
	No Shallow Releases within WMA S-SX	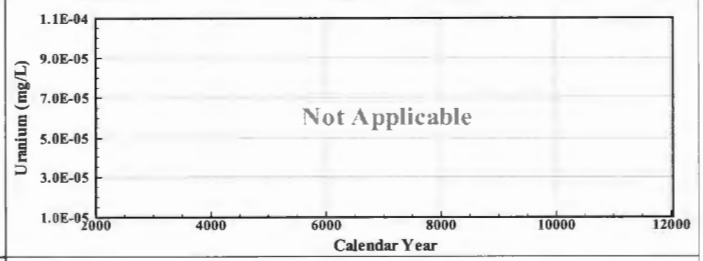
Residual Waste	**Tank Residuals SST Tank Row S-101 to S-103** Uranium S-101 = 7.34E+1 kg S-102 = 7.03E+2 kg S-103 = 1.14E+2 kg Sum = 8.91E+2 kg Maximum < 1E-5 mg/L by End of Simulation	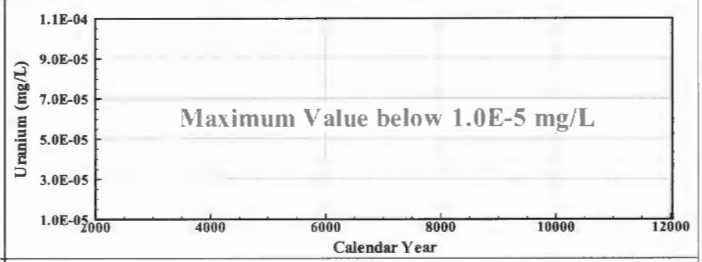
	Ancillary Equipment Pipeline Residuals Uranium Inventory S-Farm = 2.5E-3 kg SX-Farm = 0.00 kg Maximum < 1E-5 mg/L by End of Simulation	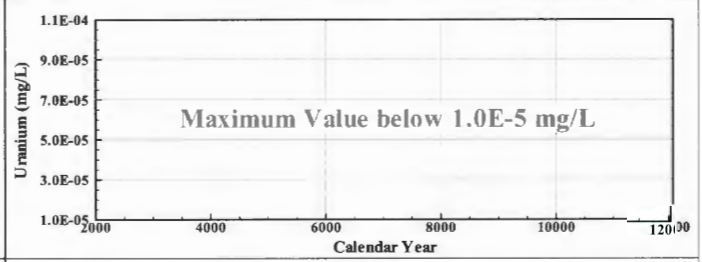
	Ancillary Equipment MUST Uranium SX-302 = 1.7E+0 kg Maximum < 1E-5 mg/L by End of Simulation	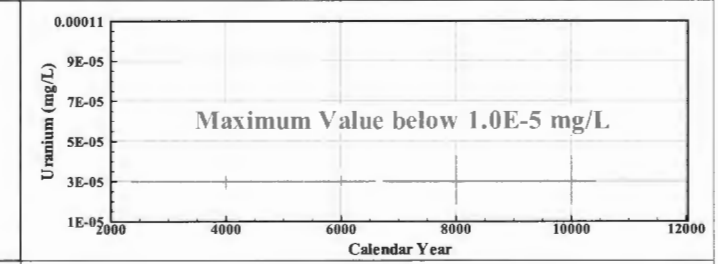
Maximum Impact Note: Shaded background indicates a change from a linear Y-Axis to a Log Y-Axis. This change in axis scale is necessary show all curves over the range of data in the same plot.		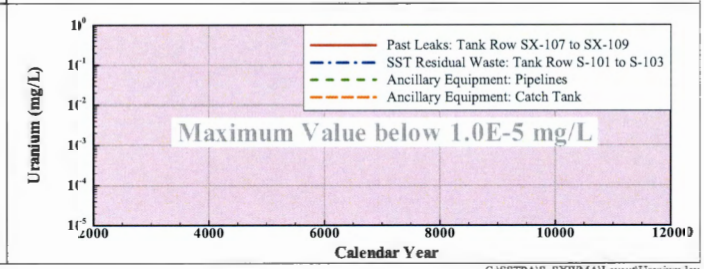

C:\SSTPA\S_SXWMA\Layout\Uranium.lay

4.4 LONG-TERM CONTAMINANT CONCENTRATIONS FOR WASTE MANAGEMENT AREA T

This section presents the contaminant transport modeling results for the indicator contaminants selected for WMA T. The numerical calculation point for this analysis is the WMA T fenceline. Impacts of individual source components (past releases, tank residuals, and ancillary equipment residuals) to the system are presented.

> Significant groundwater contamination driven by tank past leaks is predicted to reach the WMA T fenceline.
>
> Contamination from tank residuals has minor groundwater concentration impacts late in the simulation.
>
> The contaminant transport model developed for WMA S SX is used as a template for WMA T.

WMA T has twelve 100-Series tanks (530,000 gal) aligned in rows of three that are effectively parallel with the groundwater flow (Figure 2-44). In addition to the 100-Series tanks, there are four 200-Series tanks (55,000 gal) that are located approximately 100 ft to the west of the 100-Series SSTs. Tanks T-201 and T-202 are analyzed as part of the T-107 row, and tanks T-203 and T-204 are analyzed as part of the T-110 row. Reference case contaminant inventory estimates were developed for each row based on the information in Chapter 3.0. Impacts to groundwater from individual waste components were evaluated on a row-by-row basis. This section presents the contaminant concentration estimates for the highest contributing row for each source component.

As noted in Section 3.2.2.1, contaminant transport models were developed for WMA C and WMA S SX and are used as the templates for analyses for the 200 East Area and 200 West Area WMAs, respectively. The contaminant transport model designed for WMA S-SX was coupled with WMA T inventories to produce the results presented in this section. Subsequent versions of the SST PA will include WMA-specific contaminant transport models.

4.4.1 Previous Modeling Efforts for Waste Management Area T

The T and TX-TY FIR (Myers 2005) estimated long-term groundwater impact for past leaks in WMA T. The primary focus of the FIR modeling was to determine the effects of placing an interim surface barrier over the past leaks within the WMA. Peak concentrations estimate in the FIR for technetium-99, chromium, nitrate, and uranium-238 and those presented in this chapter differ by up to a factor of 4. The primary cause for this difference is the inventory estimate for the T-106 tank leak. The FIR uses the Jones et al. (2000a) inventory estimate, while the inventory used in this SST PA is from Corbin et al. (2005). If the differences in inventory are accounted for, the peak concentrations from the FIR are approximately twice those presented here. This variation can be accounted for by other differences between the two modeling activities, including:

- A closure barrier is emplaced in year 2040 in the FIR, and in year 2032 in the SST PA modeling.

- The FIR used a site-specific model developed to model past releases from WMA T, while the SST PA modeling uses a generic 200 West Area model developed to examine additional source terms within the WMA.
- Based on borehole data, the FIR uses site-specific distribution of contaminants within the vadose zone, while the SST PA modeling uses a more generic distribution of contaminants within the vadose zone.

4.4.2 Waste Management Area T Fenceline Results

For the 10,000-year simulation period, 21 contaminants had their estimated concentrations above the effective zero at the WMA TX-TY fenceline. Table 4-5 defines the tank rows in WMA T and summarizes waste sources included in each row. The designation for each tank row is the lowest numbered tank in the sequence (e.g., T-101 identifies the row consisting of tanks T-101, T-102, and T-103). Such a designation is used throughout Section 4.4. Table 4-6 lists the contaminants with fenceline concentrations above the effective zero indicating the dominant source term and the tank row providing the inventory responsible for the peak concentration.

Table 4-5. Waste Management Area T Tank Rows and Waste Components Included in Modeling

Tank Row	Residual Waste		Past Releases	
	Tanks	Ancillary Equipment	Tank Leaks	Past Shallow Releases
T-101	241-T-101 241-T-102 241-T-103	None	241-T-101 past leak 241-T-103 past leak	None
T-104	241-T-104 241-T-105 241-T-106	None	241-T-106 past leak	None
T-107	241-T-107 241-T-108 241-T-109 241-T-201 241-T-202	None	241-T-108 past leak 241-T-109 past leak	None
T-110	241-T-110 241-T-111 241-T-112 241-T-203 241-T-204	241-T-301B catch tank	241-T-111 past leak	None

Table 4-6. Estimated Concentrations of Contaminants from All Waste Components Appearing at the Waste Management Area T Fenceline

Radionuclides [a]				
Analyte Name	**Peak Concentration pCi/L**	**Dominant Source Term**	**Peak Year**	**Row with Peak Concentration**
Tritium	1.47E+04	Past releases	2040	T-104
Carbon-14	9.66E+03	Past releases	2043	T-104
Cobalt-60	7.71E-02	Past releases	2054	T-104
Technetium-99	3.44E+05	Past releases	2043	T-104
Iodine-129	7.02E-01	Past releases	12032	T-104
Nonradionuclides [b]				
Analyte Name	**Peak Concentration mg/L**	**Dominant Source Term**	**Peak Year**	**Row with Peak Concentration**
Ammonia	1.40E+00	Past releases	2043	T-104
Bismuth	3.18E-02	Tank residuals	8201	T-110
Cerium	6.88E-05	Tank residuals	8201	T-104
Chloride	8.93E+00	Past releases	2043	T-104
Chromium	4.64E+00	Past releases	2043	T-104
Fluoride	2.87E-01	Past releases	2043	T-104
Hydroxide	1.00E-01	Tank residuals	8201	T-101
Lanthanum	3.84E-03	Tank residuals	8201	T-110
n-Butyl alcohol	3.19E-02	Past releases	2043	T-104
Neodymium	3.28E-05	Tank residuals	8201	T-107
Nitrate	2.72E+02	Past releases	2043	T-104
Nitrite	1.23E+02	Past releases	2043	T-104
Oxalate	1.84E-03	Tank residuals	8201	T-110
Phosphate	2.22E+00	Past releases	2043	T-104
Sodium	3.42E+02	Past releases	2043	T-104
Sulfate	2.43E+01	Past releases	2043	T-104

[a] The following radionuclides reached the fenceline during the modeling period, but had concentrations below the effective zero (1.0E-02 pCi/L): tin-126, radium-226 + D, uranium-233, uranium-234, uranium-235 + D, uranium-236, and uranium-238 + D.

[b] The following nonradionuclides reached the fenceline during the modeling period, but had concentrations below the effective zero (1.0E-05 mg/L): aluminum, cobalt, manganese, and uranium.

4.4.3 Results for Waste Management Area T Waste Components

The past releases component is the primary contributing source component to fenceline concentrations in WMA T for all of the indicator contaminants described in Section 4.2.1. The past releases component consists of both SST past leaks and UPRs. Modeling of both source terms was the same except for the initial depth assignment (130 ft bgs for SST past leaks in the 200 East Area, 150 ft bgs for SST past leaks in the 200 West Area, and 30 ft bgs for UPRs). The past releases component consists only of past tank leaks, because no shallow UPRs

occur in WMA T (Field and Jones 2005). Tank row T-104 contains tank T-106, which had the largest release (115,000 gal) from any single-shell tank in the SST system, and is the row projected to contribute the highest past releases component concentration for all the indicator contaminants considered for WMA T.

Table 4-7 provides the peak fenceline concentrations for radionuclides by tank row, while Table 4-8 provides the same information for nonradionuclides. Both tables show concentrations from past releases and tank residuals source terms relative to the peak contributing tank row. The past releases component consists of past tank leaks and UPRs; however, no UPRs occur within WMA T. Since ancillary equipment (i.e., MUST) residuals are modeled as tank residuals, the tank residuals portion of the tables includes MUST that fall within a tank row. Although the peak concentrations from different source components occur at different times, Tables 4-7 and 4-8 show that the peak past leak concentration is up to five orders of magnitude greater than the peak tank residual concentration for any given contaminant.

For indicator contaminants considered in this section (Tables 4-7 and 4-8), tank retrieval to HFFACO prescribed volume and inventories estimated by Kirkbride et al. (2005) results in tank row T-104 contributing the peak technetium-99 fenceline concentration. However, unlike past leaks, where the magnitude of the leak at T-106 dominates, the amount of technetium-99 left in the remaining tank rows is approximately on the same order as that left in tank row T-104.

The ancillary equipment residuals component in WMA T consists of only the 241-T-301B catch tank. Since no inventory data exists for this tank, it was assumed that it would be retrieved to the volume given in Section 2.7.7 and the average inventory per cubic feet of waste would be assigned to that volume. The inventory of tank T-301B was summed with those from the tank residuals in tank row T-110. Lambert (2005), after an extensive literature search, found no documentation indicating a blocked or plugged pipeline within this WMA. Therefore, plugged and blocked pipelines were not considered in the analysis of WMA T impacts.

Figures 4-10 through 4-15 illustrate the BTCs for each of the six indicator contaminants described in Tables 4-7 and 4-8. Each plot in the figure represents a separate source component, with the bottom plot containing the previous five plots superimposed on each other to illustrate the maximum impact. Blank plots indicate cases where the concentration for a source component does not exceed the effective zero for any tank row over the 10,000-year simulation period. In those cases, the tank row with the greatest inventory is indicated. The individual source component plots have a linear scale on the y-axis, but in order to include the entire range of data, the maximum impact plot is shown on a logarithmic scale (y-axis). Each plot represents the BTC for the tank row contributing the peak concentration estimate for that source component. Also given in each of the plots are the time of the peak and the inventory for each of the like source terms in the row. The tank row containing the largest inventory is shown even though the peak concentration was below the effective zero. Additionally, tank row T-110 has the largest peak concentration for chromium, nitrate, and nitrite, and also contains the ancillary equipment (241-T-301B). To show the impacts for those chemicals in the ancillary equipment relative to the SST in tank row T-110, separate plots of the SST residuals and the MUST residuals are provided.

Table 4-7. Waste Management Area T Tank Row Peak Radionuclide Concentrations [a]

Technetium-99				
	Past Releases Component, Peak Year: 2043		**Tank Residuals Component, Peak Year: 8191**	
Tank Row	**Peak Concentration pCi/L**	**Concentration Relative to Row T-104**	**Peak Concentration pCi/L**	**Concentration Relative to Row T-104**
T-101	1.14E+04	3.31%	5.23E+00	69.00%
T-104	3.44E+05	100.00%	7.58E+00	100.00%
T-107	2.93E+03	0.85%	4.13E+00	54.49%
T-110 [b]	6.81E-02	0.00%	1.38E+00	18.21%
Iodine-129				
	Past Releases Component, Max. Year: 12032		**Tank Residuals Component**	
Tank Row	**Peak Concentration pCi/L**	**Concentration Relative to Row T-104**	**Max. Concentration pCi/L [c]**	**Concentration Relative to Max Row**
T-101	3.36E-02	4.79%	0.00E+00	NA
T-104	7.02E-01	100.00%	0.00E+00	NA
T-107	0.00E+00	0.00%	0.00E+00	NA
T-110	0.00E+00	0.00%	0.00E+00	NA

[a] Maximum values are shaded.

[b] Tank row T-110 includes ancillary equipment residuals from T-301B catch tank.

[c] Iodine-129 concentrations from the tank residuals component were not above effective zero (1.00E-02 pCi/L) for any row in the waste management area.

NA = not applicable

Table 4-8. Waste Management Area T Tank Row Peak Nonradionuclide Concentrations [a] (2 pages)

Hexavalent Chromium				
	Past Releases Component, Peak Year: 2043		**Tank Residuals Component, Peak Year: 8201**	
Tank Row	**Peak Concentration mg/L**	**Concentration Relative to Row T-104**	**Peak Concentration mg/L**	**Concentration Relative to Row T-110**
T-101	2.30E-01	4.96%	1.52E-04	7.31%
T-104	4.64E+00	100.00%	6.03E-04	28.99%
T-107	5.43E-02	1.17%	2.46E-04	11.83%
T-110 [b]	5.49E-03	0.12%	2.08E-03	100.00%
Nitrate				
	Past Releases Component, Peak Year: 2043		**Tank Residuals Component, Peak Year: 8201**	
Tank Row	**Peak Concentration mg/L**	**Concentration Relative to Row T-104**	**Peak Concentration mg/L**	**Concentration Relative to Row T-110**
T-101	2.65E+01	9.74%	1.19E-02	53.13%
T-104	2.72E+02	100.00%	9.23E-03	41.21%
T-107	1.08E+01	3.97%	1.88E-02	83.93%
T-110	1.10E+00	0.40%	2.24E-02	100.00%

Table 4-8. Waste Management Area T Tank Row Peak Nonradionuclide Concentrations [a] (2 pages)

Nitrite				
	Past Releases Component, Peak Year: 2043		**Tank Residuals Component, Peak Year: 8201**	
Tank Row	**Peak Concentration mg/L**	**Concentration Relative to Row T-104**	**Peak Concentration mg/L**	**Concentration Relative to Row T-110**
T-101	1.66E+01	13.50%	1.74E-03	28.62%
T-104	1.23E+02	100.00%	1.39E-03	22.86%
T-107	1.30E+00	1.06%	1.21E-03	19.90%
T-110	7.03E-05	0.00%	6.08E-03	100.00%
Uranium				
Uranium concentrations from the past leak and tank residuals components were not above effective zero (1.00E-05 mg/L) for any row in the waste management area.				

[a] Maximum values are shaded.

[b] Tank row T-110 includes ancillary equipment residuals from T-301B catch tank.

4.4.4 Discussion of Results and Conclusions for Waste Management Area T

Estimated long-term groundwater impacts from three contaminant source components (i.e., past releases inventory, tank residuals inventory, and ancillary equipment residuals inventory) in WMA T are modeled. Results of this analysis indicate that contamination at depth from past tank leaks occurring in tank row T-104 is estimated to contribute to the highest past releases component concentration for all the radionuclides and nonradionuclide contaminants. Furthermore, this row is also estimated to have the largest impact at the WMA fenceline from technetium-99 across all seven SST WMAs. The next highest impact due to technetium-99 comes from WMA S-SX tank row SX-107 at $1.92 \times 10^{+5}$ pCi/L, which is a little over half that found at WMA T ($3.44 \times 10^{+5}$ pCi/L).

If the tanks in WMA T are retrieved to HFFACO prescribed volume and inventories estimated by Kirkbride et al. (2005), the impact from the tank residuals is three to five orders of magnitude below that of past releases. For the residuals and for all indicator contaminants, only the row with the maximum impact is shown; the other tank rows are usually within a factor of 5 or less of the row with the peak concentration (Tables 4-7 and 4-8).

Due to existing vadose zone contamination and the maximum operational recharge occurring during that period, contaminants with high mobility (K_d less than 0.2 mL/g) exhibit concentration peaks that occur early in the simulation and prior to emplacement of the Modified RCRA Subtitle C Barrier. Contaminants with low mobility (K_d 0.2 mL/g or greater) exhibit increasing concentrations toward the end of the simulation period, dominated by the contamination at depth source component.

Figure 4-10. Waste Management Area T Technetium-99 Breakthrough Curves by Waste Source Component

Technetium-99 K_d = 0.0 mL/g		
Past Releases	**Past Leaks from Tanks Tank Row T-104 to T-106** ^{99}Tc Inventory T-104 = 0.00E+0 Ci T-105 = 0.00E+0 Ci T-106 = 3.74E+1 Ci Sum = 3.74E+1 Ci Peak = 3.44E+5 pCi/L Occurs in Year 2043	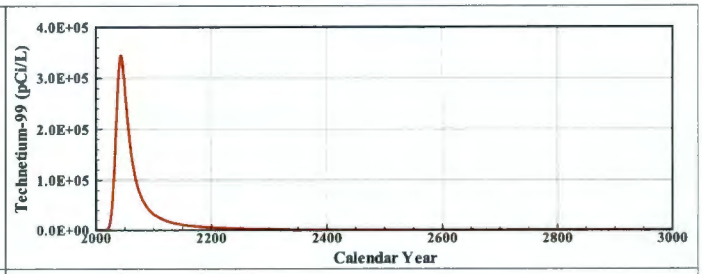
	No Shallow Releases within WMA T	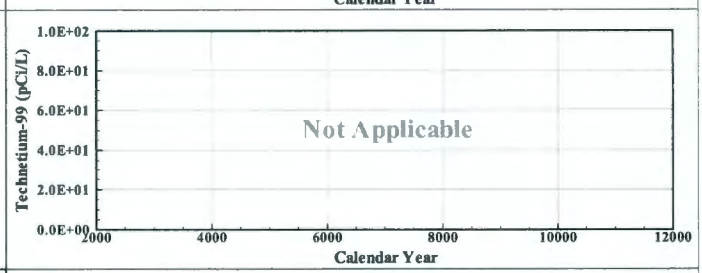
Residual Waste	**Tank Residuals SST Tank Row T-104 to T-106** ^{99}Tc Inventory T-104 = 3.00E-3 Ci T-105 = 5.50E-1 Ci T-106 = 6.70E-2 Ci Sum = 6.20E-1 Ci Peak = 7.58E+0 pCi/L Occurs in Year 8191	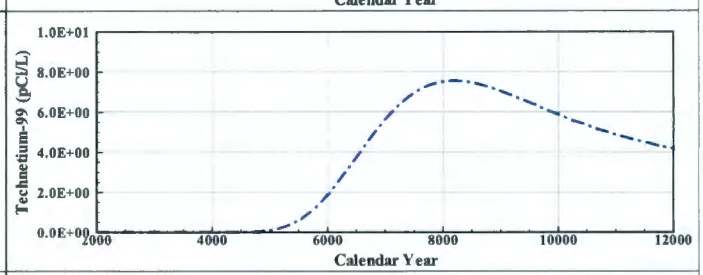
	Ancillary Equipment Pipeline Residuals No Blocked or Plugged Pipelines within WMA T	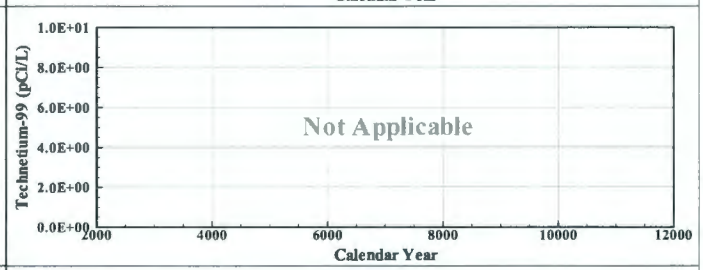
	Ancillary Equipment MUST ^{99}Tc Inventory T-301B = 6.6E-3 Ci Peak = 8.05E-2 pCi/L Occurs in Year 8191	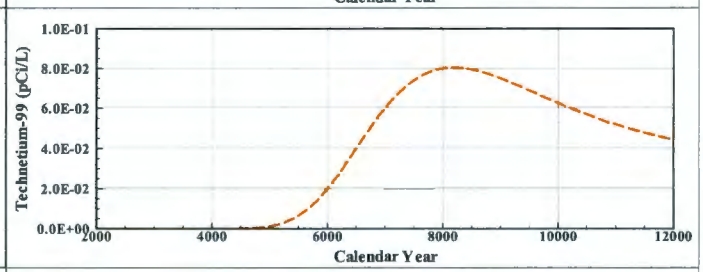
Maximum Impact Note: Shaded background indicates a change from a linear Y-Axis to a Log Y-Axis. This change in axis scale is necessary show all curves over the range of data in the same plot.		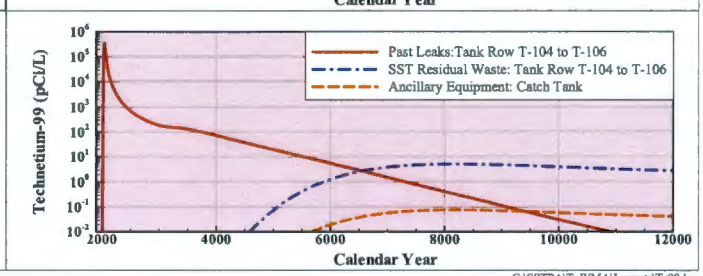

C:\SSTPA\T_WMA\Layouts\Tc99.lay

Figure 4-11. Waste Management Area T Iodine-129 Breakthrough Curves by Waste Source Component

Iodine-129 **K_d = 0.2 mL/g**		
Past Releases	**Past Leaks from Tanks Tank Row T-104 to T-106** ^{129}I Inventory T-104 = 0.00E+0 Ci T-105 = 0.00E+0 Ci T-106 = 2.50E-2 Ci Sum = 2.50E-2 Ci Maximum = 7.02E-1 pCi/L by End of Simulation	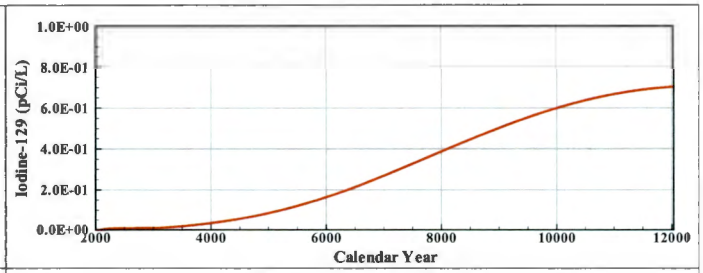
	No Shallow Releases within WMA T	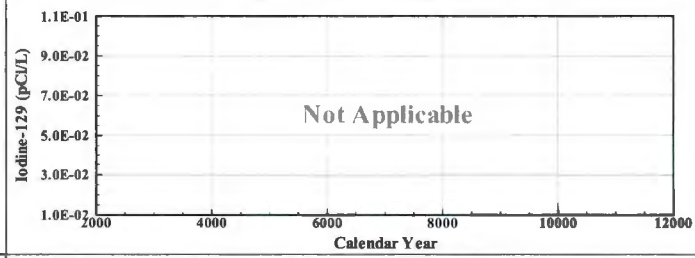
Residual Waste	**Tank Residuals SST Tank Row T-101 to T-103** ^{129}I Inventory T-101 = 1.50E-4 Ci T-102 = 1.20E-4 Ci T-103 = 0.85E-4 Ci Sum = 3.55E-4 Ci Maximum < 0.01 pCi/L by End of Simulation	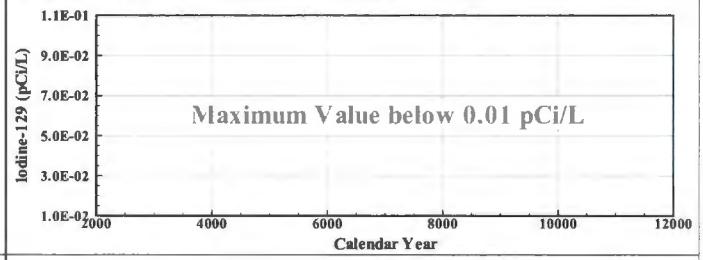
	Ancillary Equipment Pipeline Residuals No Blocked or Plugged Pipelines within WMA T	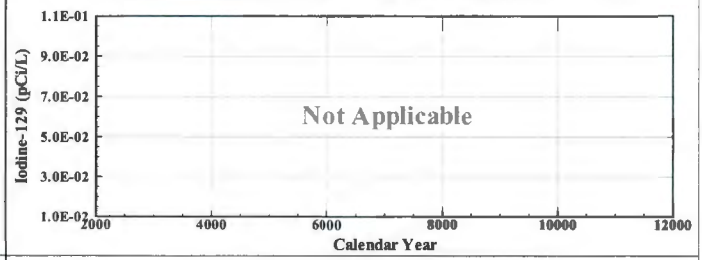
	Ancillary Equipment MUST ^{129}I Inventory T-301B = 1.9E-6 Ci Maximum < 0.01 pCi/L by End of Simulation	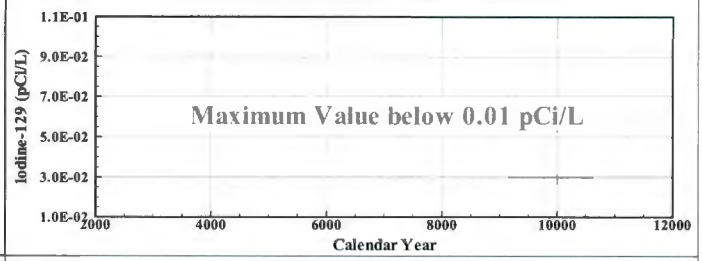
Maximum Impact Note: Shaded background indicates a change from a linear Y-Axis to a Log Y-Axis. This change in axis scale is necessary show all curves over the range of data in the same plot.		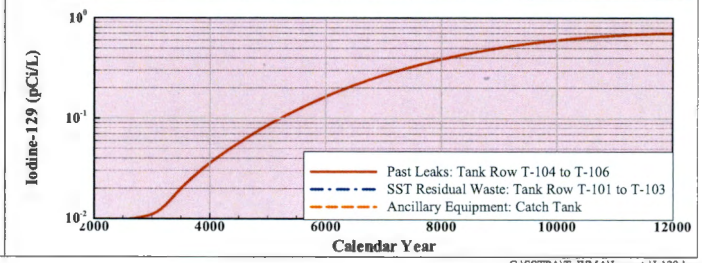

C:\SSTPA\T_WMA\Layouts\I-129.lay

Figure 4-12. Waste Management Area T Hexavalent Chromium Breakthrough Curves by Waste Source Component

Chromium **K_d = 0.0 mL/g**	**Past Leaks from Tanks** **Tank Row** **T-104 to T-106** Chromium Inventory T-104 = 0.00E+0 kg T-105 = 0.00E+0 kg T-106 = 5.04E+2 kg Sum = 5.04E+2 kg Peak = 4.64E+0 mg/L Occurs in Year 2043	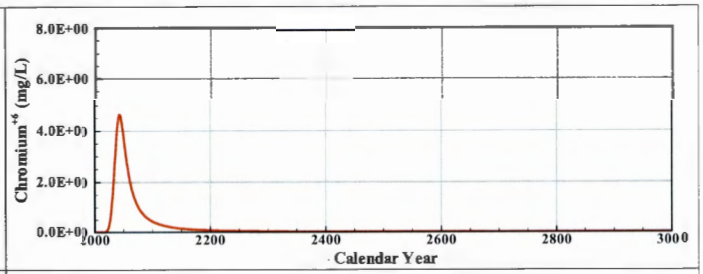
Past Releases	No Shallow Releases within WMA T	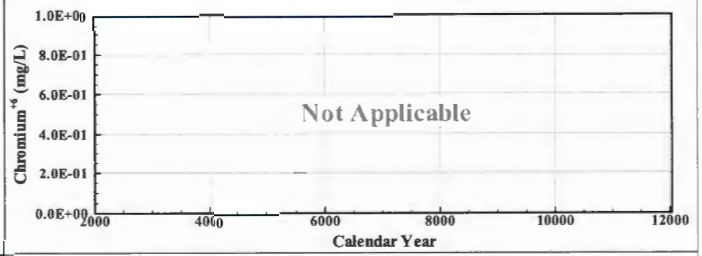
Residual Waste	**Tank Residuals** **SST Tank Row** **T-110 to T-112, T-203, T-204** Chromium Inventory T-110 = 4.99E+1 kg T-111 = 5.55E+1 kg T-112 = 5.16E+1 kg T-203 = 3.80E+0 kg T-204 = 4.90E+0 kg Sum = 1.66E+0 kg Peak = 2.07E-3 mg/L Occurs in Year 8201	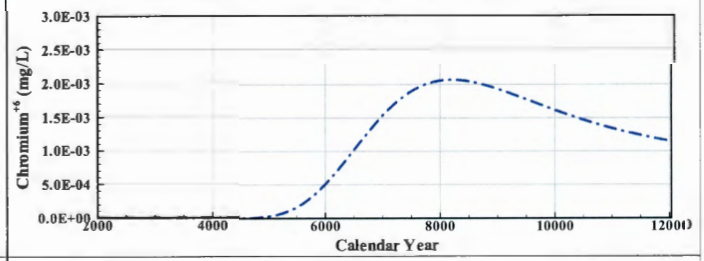
	Ancillary Equipment **Pipeline Residuals** No Blocked or Plugged Pipelines within WMA T	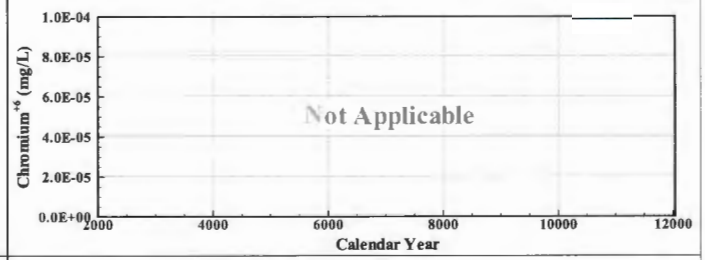
	Ancillary Equipment **MUST in Tank Row** **T-110 to T-112, T-203, T-204** Chromium Inventory T-301B = 1.10E+0 kg Peak = 1.4E-5 mg/L Occurs in Year 8201	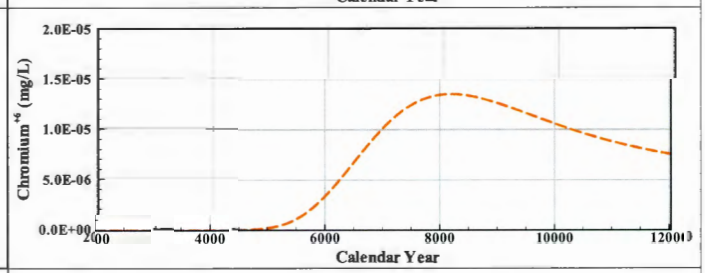
Maximum Impact Note: Shaded background indicates a change from a linear Y-Axis to a Log Y-Axis. This change in axis scale is necessary show all curves over the range of data in the same plot.		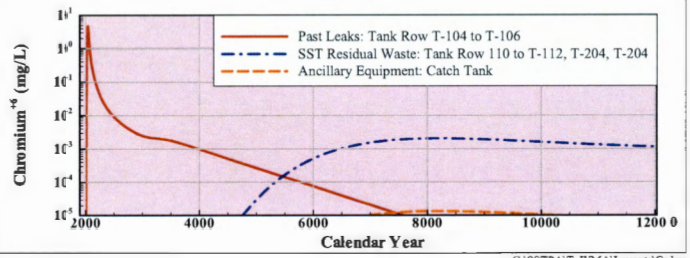

C:\SSTPA\T_WMA\Layouts\Cr.lay

Figure 4-13. Waste Management Area T Nitrate Breakthrough Curves by Waste Source Component

Nitrate **K_d = 0.0 mL/g**		
Past Releases	**Past Leaks from Tanks** **Tank Row** **T-104 to T-106** Nitrate Inventory T-104 = 0.00E+0 kg T-105 = 0.00E+0 kg T-106 = 2.95E+4 kg Sum = 2.95E+4 kg Peak = 2.72E+2 mg/L Occurs in Year 2043	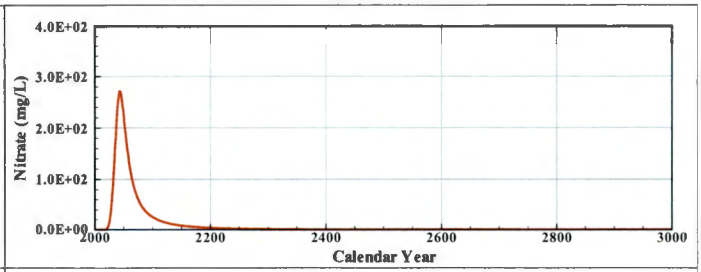
	No Shallow Releases within WMA T	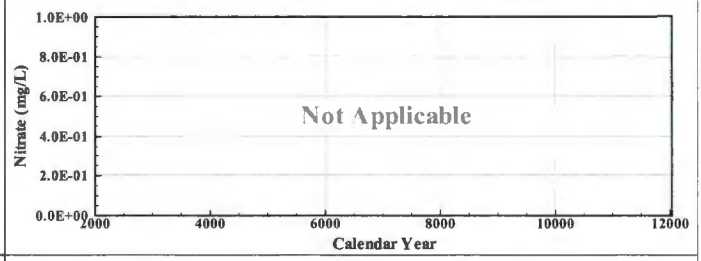
Residual Waste	**Tank Residuals** **SST Tank Row** **T-110 to T-112, T-203, T-204** Nitrate Inventory T-110 = 8.32E+0 kg T-111 = 6.90E+2 kg T-112 = 1.28E+2 kg T-203 = 6.30E+0 kg T-204 = 6.00E+0 kg Sum = 1.77E+3 kg Peak = 2.20E-2 mg/L Occurs in Year 8201	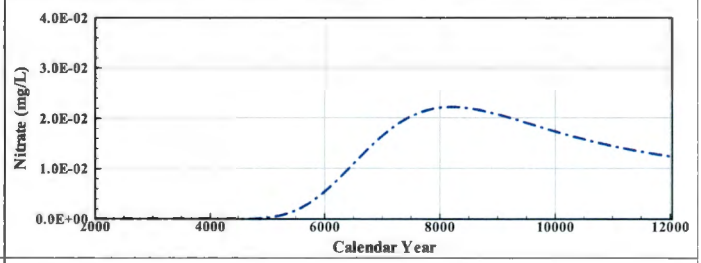
	Ancillary Equipment **Pipeline Residuals** No Blocked or Plugged Pipelines within WMA T	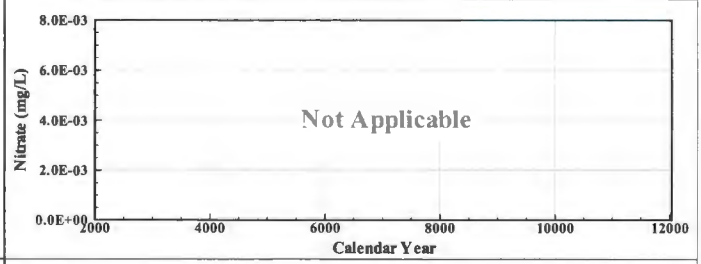
	Ancillary Equipment **MUST in Tank Row** **T-110 to T-112, T-203, T-204** Nitrate Inventory T-301B = 2.20E+0 kg Peak = 2.7E-4 mg/L Occurs in Year 8201	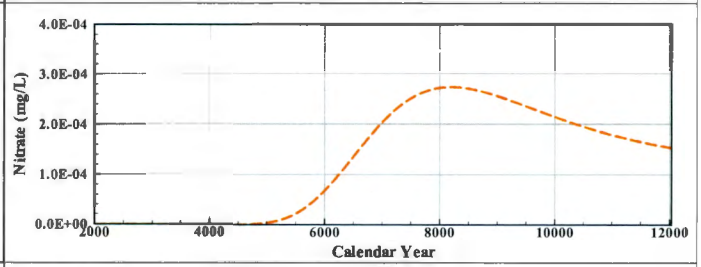
Maximum Impact Note: Shaded background indicates a change from a linear Y-Axis to a Log Y-Axis. This change in axis scale is necessary show all curves over the range of data in the same plot.		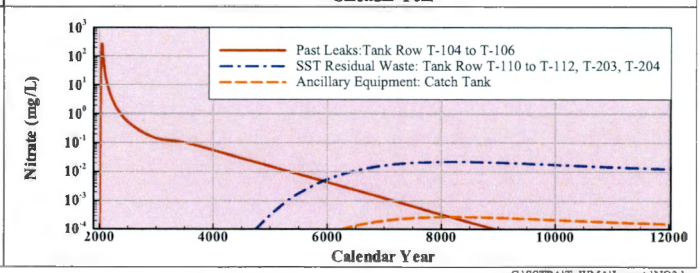

C:\SSTPA\T_WMA\Layouts\NO3.lay

Figure 4-14. Waste Management Area T Nitrite Breakthrough Curves by Waste Source Component

Nitrite **K_d = 0.0 mL/g**		
Past Releases	**Past Leaks from Tanks Tank Row T-104 to T-106** Nitrite Inventory T-104 = 0.00E+0 kg T-105 = 0.00E+0 kg T-106 = 1.33E+4 kg Sum = 1.33E+0 kg Peak = 1.23E+2 mg/L Occurs in Year 2043	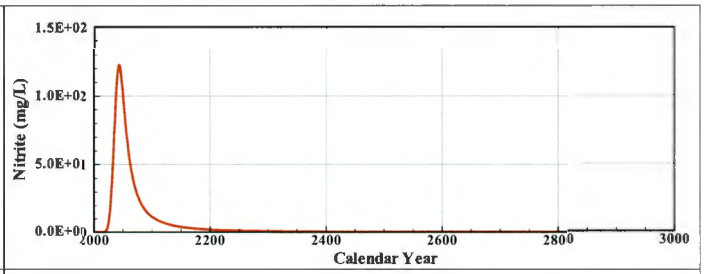
	No Shallow Releases within WMA T	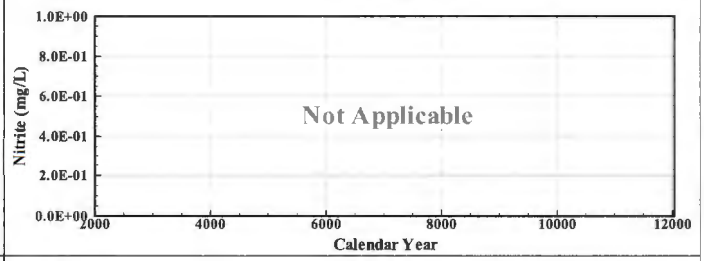
Residual Waste	**Tank Residuals SST Tank Row T-110 to T-112, T-203, T-204** Nitrite Inventory T-110 = 2.33E+2 kg T-111 = 9.90E+0 kg T-112 = 2.39E+0 kg T-203 = 4.00E-1 kg T-204 = 3.00E-1 kg Sum = 4.83E+2 kg Peak = 6.03E-3 mg/L Occurs in Year 8201	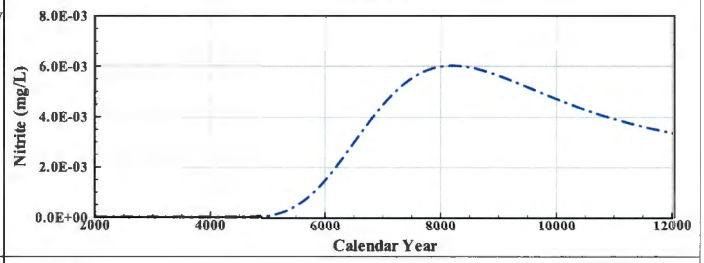
	Ancillary Equipment Pipeline Residuals No Blocked or Plugged Pipelines within WMA T	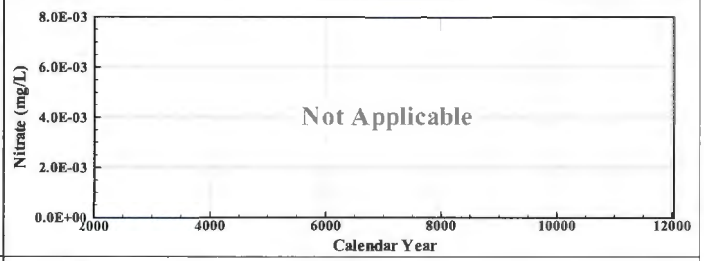
	Ancillary Equipment MUST in Tank Row T-110 to T-112, T-203, T-204 Nitrite Inventory T-301B = 3.70E+0 kg Peak = 4.6E-5 mg/L Occurs in Year 8201	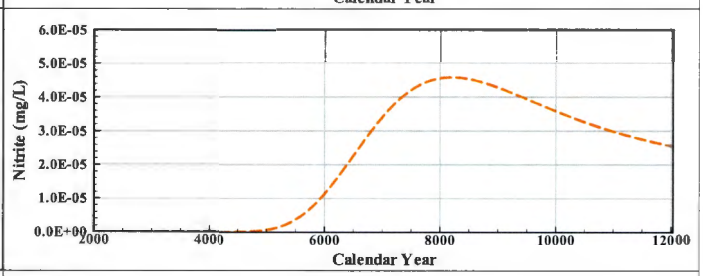
Maximum Impact Note: Shaded background indicates a change from a linear Y-Axis to a Log Y-Axis. This change in axis scale is necessary show all curves over the range of data in the same plot.		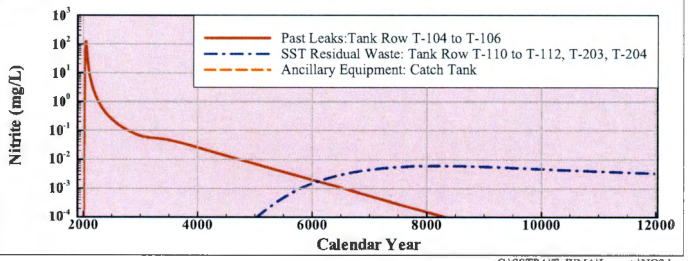

C:\SSTPA\T_WMA\Layouts\NO2.lay

Figure 4-15. Waste Management Area T Uranium Breakthrough Curves by Waste Source Component

Uranium K_d = 0.6 mL/g		
Past Releases	**Past Leaks from Tanks Tank Row T-104 to T-106** Uranium Inventory T-104 = 0.00E+0 kg T-105 = 0.00E+0 kg T-106 = 1.19E+1 kg Sum = 1.19E+1 kg Maximum < 1.0E-05 mg/L by End of Simulation	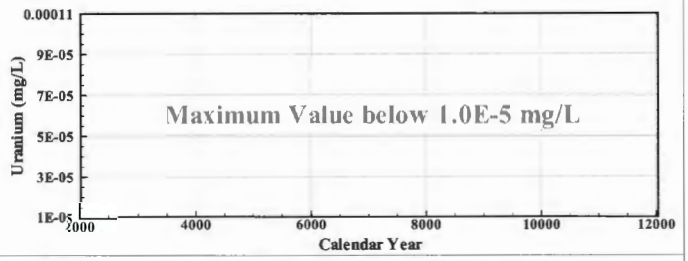
	No Shallow Releases within WMA T	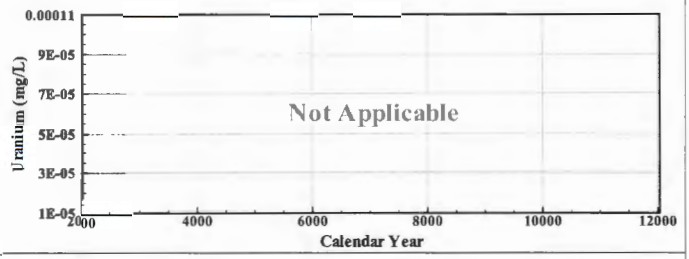
Residual Waste	**Tank Residuals SST Tank Row T-101 to T-103** Uranium Inventory T-101 = 1.64E+2 kg T-102 = 2.27E+2 kg T-103 = 1.40E+2 kg Sum = 5.31E+0 kg Maximum < 1.0E-05 mg/L by End of Simulation	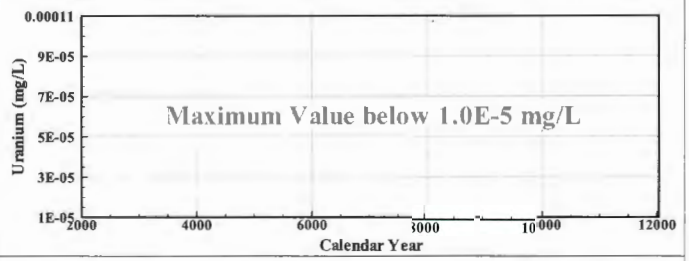
	Ancillary Equipment Pipeline Residuals No Blocked or Plugged Pipelines within WMA T	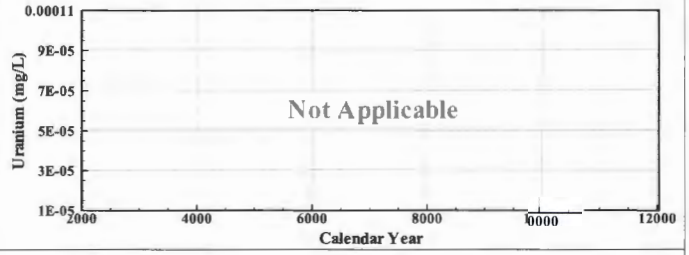
	Ancillary Equipment Catch Tank Uranium Inventory T-301B = 4.52E+0 kg Maximum < 1.0E-05 mg/L by End of Simulation	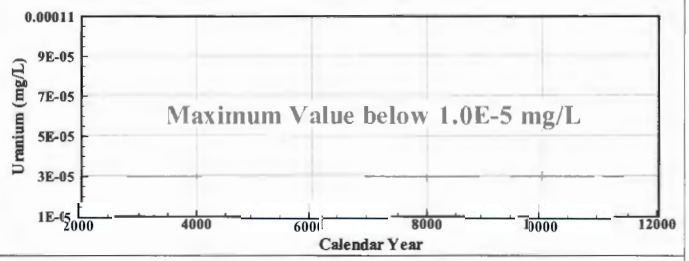
Maximum Impact Note: Shaded background indicates a change from a linear Y-Axis to a Log Y-Axis. This change in axis scale is necessary show all curves over the range of data in the same plot.		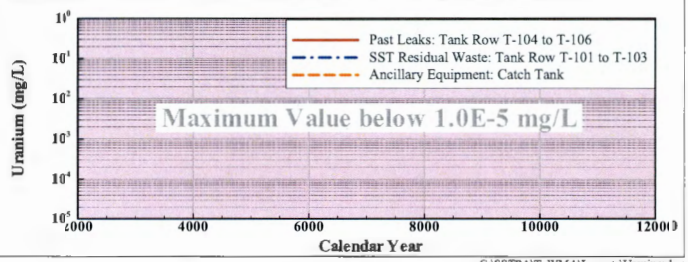

C:\SSTPA\T_WMA\Layouts\Uranium.lay

4.5 LONG-TERM CONTAMINANT CONCENTRATIONS FOR WASTE MANAGEMENT AREA TX-TY

This section presents the contaminant transport modeling results for indicator contaminants selected for WMA TX-TY. The numerical calculation point for this analysis is the WMA TX-TY fenceline. Impacts of individual source components (past releases, tank residuals, and ancillary equipment residuals) are identified.

Significant groundwater contamination driven by tank past leaks is predicted to reach the WMA TX-TY fenceline.

Contamination from tank residuals has minor groundwater concentration impacts late in the simulation.

The contaminant transport model developed for WMA S-SX is used as a template for WMA TX-TY.

WMA TX-TY has twenty-four 100-Series tanks (758,000 gal) aligned in eight rows that are effectively parallel with the groundwater flow (Figure 2-50). The 244-TXR vault and TX-302A catch tank constitute a ninth row parallel to groundwater flow located south of row TX-101. Reference case contaminant inventory estimates were developed for each row based on the information in Chapter 3.0. Impacts to groundwater from individual waste components were then evaluated on a row-by-row basis. This section presents the contaminant concentration estimates for the highest contributing row for each source component.

As noted in Section 3.2.2.1, contaminant transport models were developed for WMA C and WMA S-SX and are used as the templates for analyses for the 200 East Area and 200 West Area WMAs, respectively. The contaminant transport model designed for WMA S-SX was coupled with WMA TX-TY inventories to produce the results presented in this section. Subsequent versions of the SST PA will include WMA-specific contaminant transport models.

4.5.1 Previous Modeling Efforts for Waste Management Area TX-TY

The T and TX-TY FIR (Myers 2005) estimated long-term groundwater impact for past leaks in WMA TX-TY. The primary focus of the FIR modeling was to determine the effects of placing an interim surface barrier. A key contaminant source for WMA TX-TY is the TX–107 past tank leak. Peak concentration estimates resulting from past leaks reported in the FIR and those presented in this chapter are in close agreement (differing by less than 15%) for technetium-99, chromium, and nitrate. Uranium, both isotopic and total chemical, is not predicted to arrive at the WMA TX-TY fenceline during the simulation period for either model due to its less mobile nature (K_d value of 0.6 L/mg). The slight variation in peak concentrations is due to differences between the two modeling activities, including:

- A closure barrier is emplaced in year 2040 in the FIR, and in year 2032 in the SST PA modeling.
- The FIR uses the inventory from Jones et al. (2000a), while the inventory used for the SST PA is from Corbin et al. (2005). Differences in inventory account for most of the difference in magnitude of the reported peak concentrations.

- Based on borehole data, the FIR uses site-specific distribution of contaminants within the vadose zone, while the SST PA modeling uses a more generic distribution of contaminants within the vadose zone.

4.5.2 Waste Management Area TX-TY Fenceline Results

For the 10,000-year simulation period, twenty contaminants had their estimated concentrations above the effective zero at the WMA TX-TY fenceline. Table 4-9 defines the tank rows in WMA TX-TY and summarizes waste sources included in each row. The designation for each tank row is the lowest numbered tank in the sequence (e.g., TX-101 identifies the row consisting of tanks TX-101, TX-102, TX-103, and TX-104). Such a designation is used throughout Section 4.5. Table 4-10 lists the contaminants with fenceline concentrations above the effective zero indicating the dominant source term and the tank row resulting in the inventory responsible for the peak concentration.

Table 4-9. Waste Management Area TX-TY Tank Rows and Waste Components Included in the Modeling

Tank Row	Residual Waste		Past Releases	
	Tanks	Ancillary Equipment	Tank Leaks	Past Shallow Releases
TXR vault	None	244-TXR vault TX-302A catch tank	None	None
TX-101	241-TX-101 241-TX-102 241-TX-103 241-TX-104	TX-302XB catch tank	None	None
TX-105	241-TX-105 241-TX-106 241-TX-107 241-TX-108	None	241-TX-107 leak	UPR-200-W-100
TX-109	241-TX-109 241-TX-110 241-TX-111 241-TX-112	None	None	None
TX-113	241-TX-113 241-TX-114 241-TX-115	None	None	None
TX-116	241-TX-116 241-TX-117 241-TX-118	None	None	None
TY-101	241-TY-101 241-TY-102	241-TY-302B catch tank	241-TY-101 leak	None
TY-103	241-TY-103 241-TY-104	None	241-TY-103 leak 241-TY-104 leak	None
TY-105	241-TY-105 241-TY-106	241-TY-302A catch tank	241-TY-105 leak 241-TY-106 leak	None

Table 4-10. Estimated Concentrations of Contaminants from All Waste Components Appearing at the Waste Management Area TX-TY Fenceline

Radionuclides [a]				
Analyte Name	**Peak Concentration pCi/L**	**Dominant Component**	**Peak Year**	**Row with Peak Concentration**
Tritium	1.22E+03	Past releases	2040	TY-105
Carbon-14	1.37E+03	Past releases	2043	TX-105
Technetium-99	4.03E+04	Past releases	2043	TX-105
Iodine-129	1.37E-01	Past releases	12032	TX-105
Nonradionuclides [b]				
Analyte Name	**Peak Concentration mg/L**	**Dominant Component**	**Peak Year**	**Row with Peak Concentration**
Ammonia	5.66E-01	Past releases	2043	TX-105
Bismuth	7.19E-02	Past releases	2043	TY-105
Cerium	4.04E-05	Tank residuals	8201	TX-101
Chloride	6.47E+00	Past releases	2043	TY-105
Chromium	7.96E-01	Past releases	2043	TX-105
Fluoride	6.99E-01	Past releases	2043	TX-105
Hydroxide	1.47E-01	Tank residuals	8201	TX-101
Lanthanum	6.33E-05	Tank residuals	8201	TX-116
Neodymium	4.04E-05	Tank residuals	8201	TX-101
Nitrate	3.49E+02	Past releases	2043	TY-105
Nitrite	2.31E+01	Past releases	2043	TX-105
Oxalate	1.15E-02	Tank residuals	8201	TX-116
Phosphate	1.26E+01	Past releases	2043	TY-105
Sodium	1.75E+02	Past releases	2043	TY-105
Sulfate	2.24E+01	Past releases	2043	TY-105
n-Butyl Alcohol	1.95E-01	Past releases	2043	TX-105

[a] The following radionuclides reached the fenceline during the modeling period, but had concentrations below the effective zero (1.0E-02 pCi/L): tin-126, radium-226 + D, thorium 229 + D, thorium 232, uranium-233, uranium-234, uranium-235 + D, uranium-236, uranium-238 + D, and cobalt-60.

[b] The following nonradionuclides reached the fenceline during the modeling period, but had concentrations below the effective zero (1.0E-05 mg/L): aluminum, cobalt, manganese, uranium, and yttrium.

4.5.3 Results for Waste Management Area TX-TY Waste Components

The past releases component is the primary contributing source component to WMA TX-TY for fenceline concentrations for all the indicator contaminants described in Section 4.2.1. The past releases component consists of both SST past leaks and UPRs. Modeling of both source terms was the same except for the initial depth assignment (130 ft bgs for SST past leaks in the 200 East Area, 150 ft bgs for SST past leaks in the 200 West Area, and 30 ft bgs for UPRs). There are six total SST past leaks in the WMA, with one in TX tank farm and five in TY tank farm. There is one UPR in WMA TX-TY, residing along tank row TX-105 (Field and Jones 2005). Except for nitrate, tank row TX-105 is projected to contribute the highest past releases component concentration for all the indicator contaminants considered for WMA TX-TY. The peak past release nitrate concentration is from tank row TY-105.

For the tank residuals component, with the exception of nitrite, tank row TX-105 provides the highest fenceline concentrations for the indicator contaminants discussed in the following sections. Tank residual nitrite concentrations are highest from tank row TX-101. The tank residuals component consists of residuals in SSTs and ancillary equipment (i.e., MUSTs). The MUST residuals were incorporated into the tank residual calculations for each row because the SST and MUST residuals were modeled in the same manner (i.e., diffusion-limited release). The ancillary equipment residuals component in WMA TX-TY consists of plugged and blocked pipelines in the TX tank farm (Lambert 2005) and the following MUSTs:

- 244-TXR vault and TX-302A catch tank in the TXR vault row
- TX-302XB catch tank in the TX-101 row
- 241-TY-302B catch tank in the TY-101 row
- 241-TY-302A catch tank in the TY-105 row.

Ancillary equipment sources provide negligible contributions to the overall concentrations for each of the indicator contaminants considered in this chapter.

Table 4-11 shows peak fenceline concentrations for radionuclides by row, and Table 4-12 shows peak fenceline concentrations for nonradionuclides by row. Both tables show concentrations from past releases and tank residuals source terms relative to the peak contributing tank row. The past releases component consists of past tank leaks and UPRs. Since ancillary equipment residuals are modeled as tank residuals, the tank residuals portion of the tables include ancillary equipment that reside within a tank row. Although the peak concentrations from different source components occur at different times, Tables 4-11 and 4-12 show that, for any given contaminant, the peak concentration resulting from past leaks is between two and five orders of magnitude greater than that resulting from tank residuals.

Plugged and blocked pipelines do not fall within any one tank row and were evaluated separately. The plugged and blocked pipelines contribute to the following peak concentrations:

- Technetium-99: 2.17 pCi/L, peak year 2094
- Hexavalent chromium: 2.36×10^{-4} mg/L, peak year 2094
- Nitrate: 1.14×10^{-2} mg/L, peak year 2094
- Nitrite: 2.90×10^{-3} mg/L, peak year 2094.

Uranium and iodine-129 concentrations from the plugged and blocked pipeline residual components in WMA TX-TY are effectively zero.

Table 4-11. Waste Management Area TX-TY Tank Row Peak Radionuclide Concentrations [a]

Technetium-99				
	Past Releases Component, Peak Year: 2043		**Tank Residuals Component, Peak Year: 8191**	
Tank Row	**Peak Concentration pCi/L**	**Concentration Relative to Row TX-105**	**Peak Concentration pCi/L**	**Concentration Relative to Row TX-105**
TX-101	0.00E+00	NA	1.04E+02	73.76%
TX-105	4.03E+04	100.00%	1.41E+02	100.00%
TX-109	0.00E+00	NA	1.24E+02	87.94%
TX-113	0.00E+00	NA	1.28E+02	90.78%
TX-116	0.00E+00	NA	7.37E+01	52.27%
TXR vault	0.00E+00	NA	4.66E+00	3.30%
TY-101	4.09E+03	10.15%	1.52E+00	1.08%
TY-103	1.52E+04	37.72%	3.82E+00	2.71%
TY-105	7.16E+03	17.77%	8.11E-01	0.58%
Iodine-129				
	Past Releases Component, Max. Year: 12032		**Tank Residuals Component**	
Tank Row	**Peak Concentration pCi/L**	**Concentration Relative to Row TX-105**	**Max. Concentration pCi/L [b]**	**Concentration Relative to Row with Peak Concentration**
TX-101	0.00E+00	NA	0.00E+00	NA
TX-105	1.37E-01	100.00%	0.00E+00	NA
TX-109	0.00E+00	NA	0.00E+00	NA
TX-113	0.00E+00	NA	0.00E+00	NA
TX-116	0.00E+00	NA	0.00E+00	NA
TXR vault	0.00E+00	NA	0.00E+00	NA
TY-101	1.43E-02	10.44%	0.00E+00	NA
TY-103	5.15E-02	37.59%	0.00E+00	NA
TY-105	2.85E-02	20.80%	0.00E+00	NA

[a] Maximum values are shaded.

[b] Iodine-129 concentrations from the tank residuals component were not above effective zero (1.00E-02 pCi/L) for any row in the waste management area.

NA = not applicable

Table 4-12. Waste Management Area TX-TY Tank Row Peak Nonradionuclide Concentrations [a] (2 pages)

Hexavalent Chromium				
	Past Releases Component, Peak Year: 2043		**Tank Residuals Component, Peak Year: 8201**	
Tank Row	**Peak Concentration mg/L**	**Concentration Relative to Row TX-105**	**Peak Concentration mg/L**	**Concentration Relative to Row TX-105**
TX-101	0.00E+00	NA	2.63E-03	72.45%
TX-105	7.96E-01	100.00%	3.63E-03	100.00%
TX-109	0.00E+00	NA	2.12E-03	58.40%
TX-113	0.00E+00	NA	1.06E-03	29.20%
TX-116	0.00E+00	NA	1.79E-03	49.31%
TXR vault	0.00E+00	NA	9.17E-05	2.53%
TY-101	8.74E-02	10.98%	3.19E-04	8.79%
TY-103	2.99E-01	37.56%	2.63E-04	7.25%
TY-105	3.18E-01	39.95%	4.68E-05	1.29%
Nitrate				
	Past Releases Component, Peak Year: 2043		**Tank Residuals Component, Peak Year: 8201**	
Tank Row	**Peak Concentration mg/L**	**Concentration Relative to Row TY-105**	**Peak Concentration mg/L**	**Concentration Relative to Row TX-105**
TX-101	0.00E+00	NA	4.42E-02	96.93%
TX-105	5.99E+01	17.16%	4.56E-02	100.00%
TX-109	0.00E+00	NA	4.35E-02	95.39%
TX-113	0.00E+00	NA	3.64E-02	79.82%
TX-116	0.00E+00	NA	2.71E-02	59.43%
TXR vault	0.00E+00	NA	1.61E-03	3.53%
TY-101	6.70E+00	1.92%	2.75E-02	60.31%
TY-103	2.25E+01	6.45%	4.98E-03	10.92%
TY-105	3.49E+02	100.00%	4.60E-03	10.09%
Nitrite				
	Past Releases Component, Peak Year: 2043		**Tank Residuals Component, Peak Year: 8201**	
Tank Row	**Peak Concentration mg/L**	**Concentration Relative to Row TX-105**	**Peak Concentration mg/L**	**Concentration Relative to Row TX-101**
TX-101	0.00E+00	NA	5.42E-03	100.00%
TX-105	2.31E+01	100.00%	4.13E-03	76.20%
TX-109	0.00E+00	NA	3.33E-03	61.44%
TX-113	0.00E+00	NA	1.89E-03	34.87%
TX-116	0.00E+00	NA	1.68E-03	31.00%
TXR vault	0.00E+00	NA	1.34E-04	2.47%
TY-101	2.45E+00	10.61%	8.00E-04	14.76%
TY-103	8.66E+00	37.49%	5.49E-04	10.13%
TY-105	1.41E+01	61.04%	3.39E-04	6.25%

Table 4-12. Waste Management Area TX-TY Tank Row Peak Nonradionuclide Concentrations [a] (2 pages)

Uranium
Uranium concentrations from the past leak and tank residuals components were not above effective zero (1.00E-05 mg/L) for any row in the waste management area.

[a] Maximum values are shaded.

NA = not applicable

Figures 4-16 through 4-21 illustrate the BTCs for each of the six indicator contaminants. Each one of the first five plots in the figure is from a separate source component, with the bottom plot containing the previous five plots superimposed on each other to illustrate the maximum impact. Blank plots indicate cases where the concentration for a source component does not exceed the effective zero for any tank row for the 10,000-year simulation period. In those cases, the tank row with the greatest inventory is included. A linear scale (y-axis) is used for the individual source component plots, but in order to include the entire range of data, the maximum impact plot is shown using a logarithmic scale. Each plot represents the BTC for the tank row contributing the peak concentration estimate for that source component. Also given in each of the plots is the time of the peak and the inventory for each of the like source terms in the row. The tank row containing the largest inventory is shown even though the peak concentration falls below the effective zero.

4.5.4 Discussion of Results and Conclusions for Waste Management Area TX-TY

Estimated long-term groundwater impacts resulting from three contaminant source components (i.e., past releases inventory, tank residuals inventory, and ancillary equipment residuals inventory) in WMA TX-TY are modeled. Results of this analysis indicate that, except for nitrate and uranium, past releases along tank row TX-105 produce the maximum projected fenceline concentrations. Projected nitrate concentrations are the highest from the past releases component along tank row TY-105. Uranium is not projected to occur in concentrations above effective zero because of its lower mobility in the vadose zone.

Tank retrieval to the HFFACO prescribed volume and inventory estimates provided by Kirkbride et al. (2005) results in tank row TX-105 residual waste contributing the largest concentration during the latter half of the simulation period for all indicator contaminants, except for nitrate and uranium. The maximum residual waste nitrite concentration at the fenceline is attributed to tank row TX-101. Impacts from tank residuals are two to four orders of magnitude below those for past releases. Concentrations of mobile contaminants in the latter portion of the simulation are driven by residual waste inventories. Uranium concentrations at the fenceline are effectively zero for the entire simulation period.

Ancillary equipment, including plugged and blocked pipelines, has a negligible impact on the fenceline BTC for each contaminant. Impacts from ancillary equipment are three or more orders of magnitude less than those from past releases, with only four of the six indicator contaminants estimated to have concentrations above effective zero.

Figure 4-16. Waste Management Area TX-TY Technetium-99 Breakthrough Curves by Waste Source Component

Technetium-99
K_d = 0.0 mL/g

Past Releases

Past Leaks from Tanks Tank Row TX-105 to TX-108

^{99}Tc Inventory (Ci)

TX-105 = 0.00E+0
TX-106 = 0.00E+0
TX-107 = 4.37E+0
TX-108 = 0.00E+0
Sum = 4.37E+0

Peak = 4.03E+4 pCi/L
Occurs in Year 2043

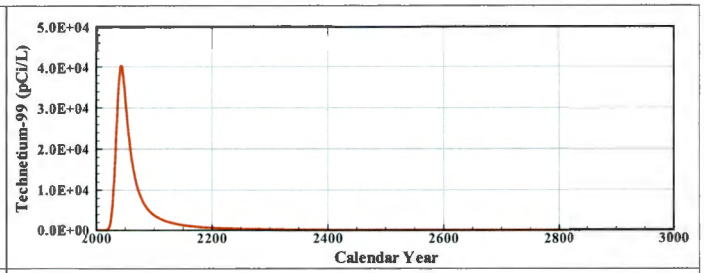

Past Shallow Release in Same Pathline

^{99}Tc Inventory (Ci)

UPR-200-W-100 = 1.96E-3

Peak = 6.05E-1 pCi/L
Occurs in Year 2094

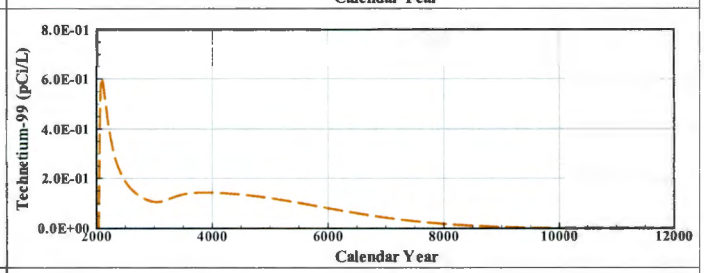

Residual Waste

Tank Residuals SST Tank Row TX-105 to TX-108

^{99}Tc Inventory (Ci)

TX-105 = 3.39E+0
TX-106 = 1.96E-1
TX-107 = 4.76E+0
TX-108 = 3.18E+0
SUM = 1.15E+1

Peak = 1.41E+2 pCi/L
Occurs in Year 8191

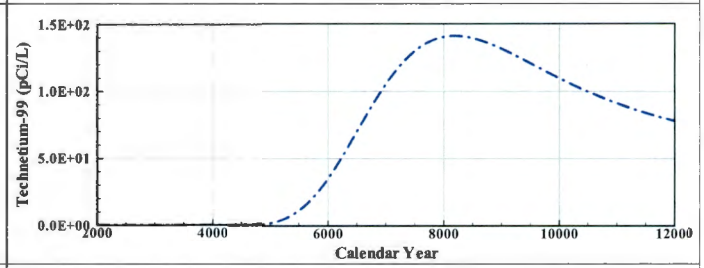

Ancillary Equipment Pipeline Residuals

^{99}Tc Inventory (Ci)

TX Pipelines = 7.03E-3

Peak = 2.17E+0 pCi/L
Occurs in Year 2094

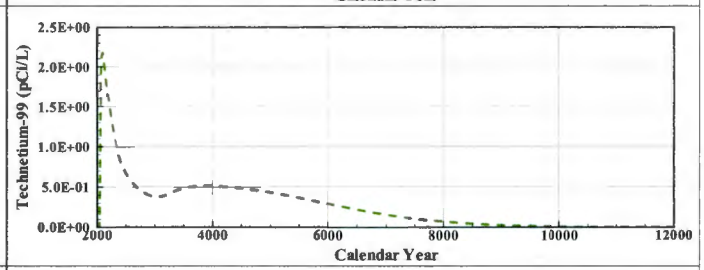

Ancillary Equipment MUST

^{99}Tc Inventory (Ci)

TXR-Vault = 3.09E-1

Peak = 3.78E+0 pCi/L
Occurs in Year 8191

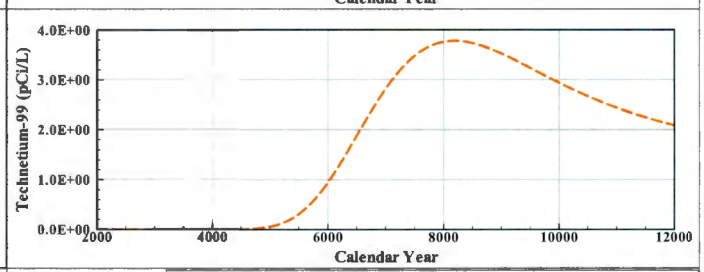

Maximum Impact

Note: Shaded background indicates a change from a linear Y-Axis to a Log Y-Axis. This change in axis scale is necessary show all curves over the range of data in the same plot.

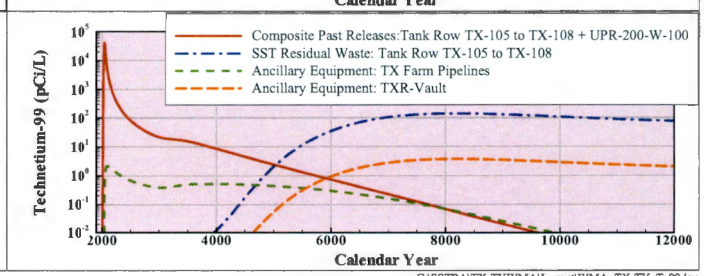

C:\SSTPA\TX-TYWMA\Layout\WMA_TX-TY_Tc99.lay

Figure 4-17. Waste Management Area TX-TY Iodine-129 Breakthrough Curves by Waste Source Component

Iodine-129
K_d = 0.2 mL/g

Past Releases

Past Leaks from Tanks Tank Row TX-105 to TX-108

^{129}Iodine Inventory (Ci)

TX-105 = 0.00E+0
TX-106 = 0.00E+0
TX-107 = 4.81E-3
TX-108 = 0.00E+0
Sum = 4.81E-3

Peak = 1.37E-1 pCi/L
Occurs in Year 12,032

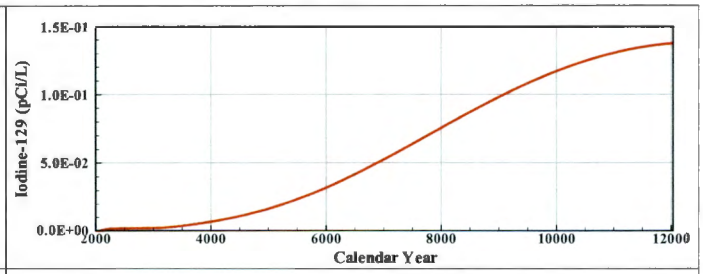

Past Shallow Release in Tank Row TX-105 to TX-108

^{129}Iodine Inventory (Ci)

UPR-200-W-100 = 2.5E-5 Ci

Max < 0.01 pCi/L
at End of Simulation

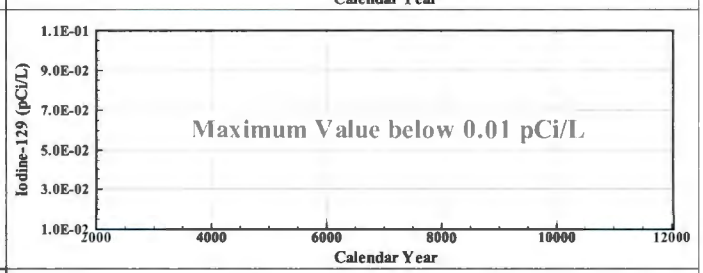

Residual Waste

Tank Residuals SST Tank Row TX-101 to TX-104

^{129}Iodine Inventory (Ci)

TX-101 = 5.96E-4
TX-102 = 2.27E-4
TX-103 = 2.16E-4
TX-104 = 2.02E-4
TX-302XB = 5.56E-6
Sum = 1.24E-3

Max < 0.01 pCi/L
at End of Simulation

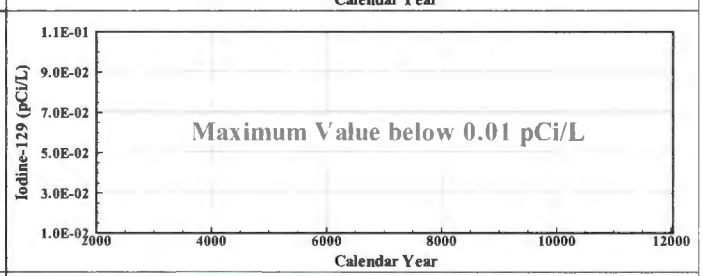

Ancillary Equipment Pipeline Residuals

^{129}Iodine Inventory (Ci)

TX Pipelines = 1.13E-05

Max < 0.01 pCi/L
at End of Simulation

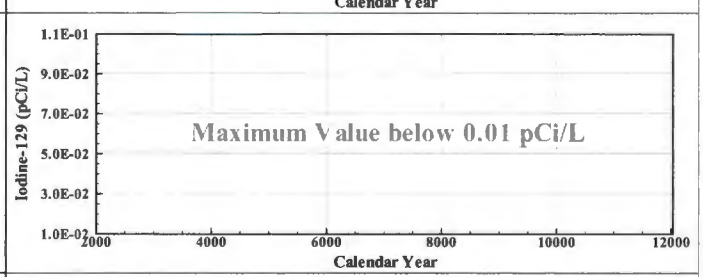

Ancillary Equipment MUST

^{129}Iodine Inventory

TXR-Vault = 2.39E-05

Max < 0.01 pCi/L
at End of Simulation

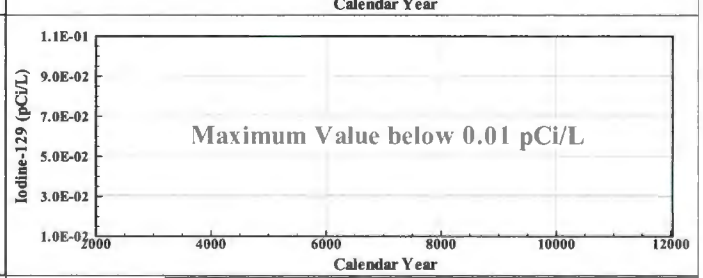

Maximum Impact

Note: Shaded background indicates a change from a linear Y-Axis to a Log Y-Axis. This change in axis scale is necessary show all curves over the range of data in the same plot.

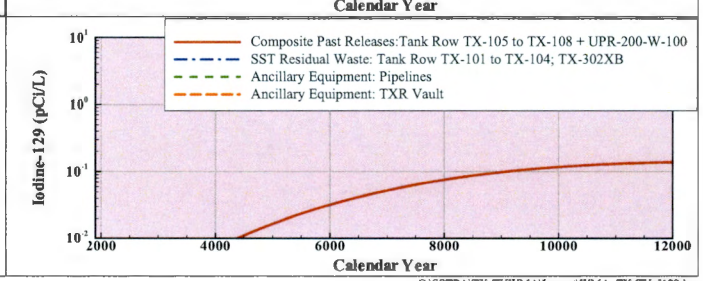

C:\SSTPA\TX-TYWMA\Layout\WMA_TX-TY_I129.lay

Figure 4-18. Waste Management Area TX-TY Hexavalent Chromium Breakthrough Curves by Waste Source Component

Chromium
K_d = 0.0 mL/g

Past Releases

Past Leaks from Tanks
SST Tank Row
TX-105 to TX-108

Chromium Inventory (kg)

TX-105 = 0.00E+0
TX-106 = 0.00E+0
TX-107 = 8.65E+1
TX-108 = 0.00E+0
Sum = 8.65E+1

Peak = 7.96E-1 mg/L
Occurs in Year 2043

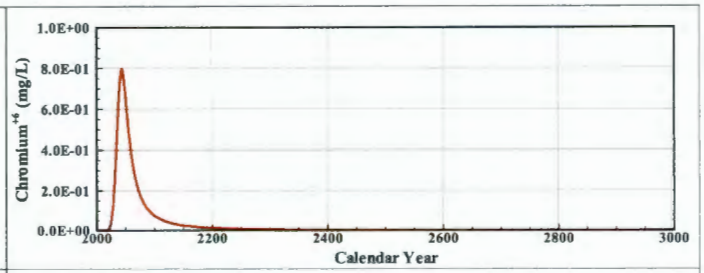

Past Shallow Release
SST Tank Row
TX-105 to TX-108

Chromium Inventory (kg)

UPR-200-W-100 = 3.45E+0

Peak = 1.07E-3 mg/L
Occurs in Year 2094

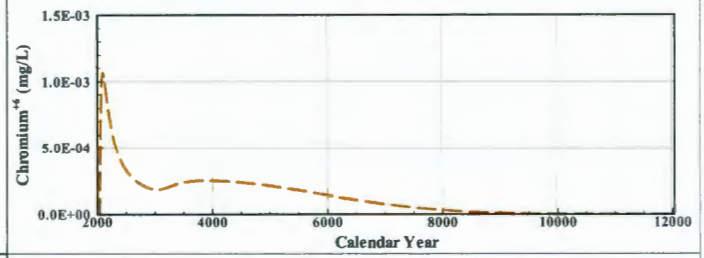

Residual Waste

Tank Residuals
SST Tank Row
TX-105 to TX-108

Chromium Inventory (kg)

TX-105 = 4.31E+1
TX-106 = 6.77E+1
TX-107 = 1.40E+2
TX-108 = 4.03E+1
SUM = 2.91E+2

Peak = 3.63E-3 mg/L
Occurs in Year 8201

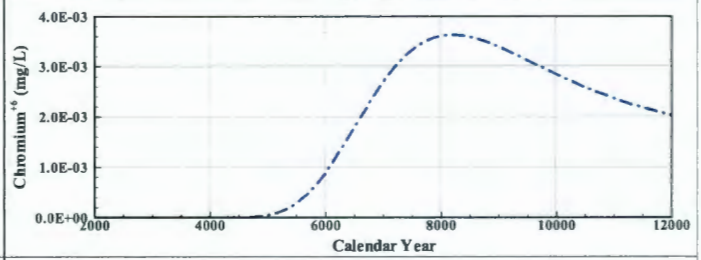

Ancillary Equipment
Pipeline Residuals

Chromium Inventory (kg)

TX Pipelines = 7.63E-01

Peak = 2.36E-4mg/L
Occurs in Year 2094

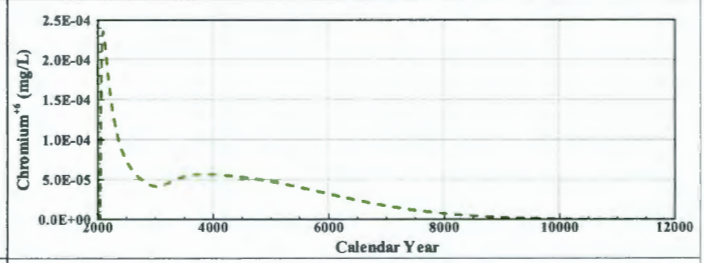

Ancillary Equipment
MUST

Chromium Inventory (kg)

TXR-Vault = 5.95E+0

Peak = 7.44E-5 mg/L
Occurs in Year 8201

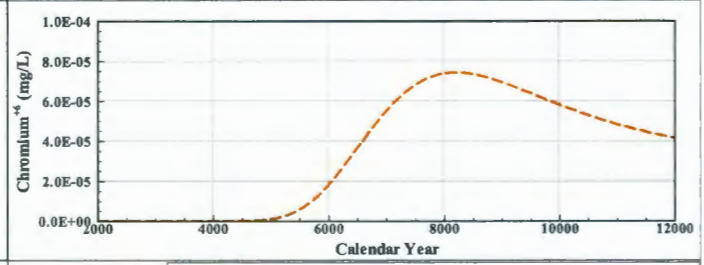

Maximum Impact

Note: Shaded background indicates a change from a linear Y-Axis to a Log Y-Axis. This change in axis scale is necessary show all curves over the range of data in the same plot.

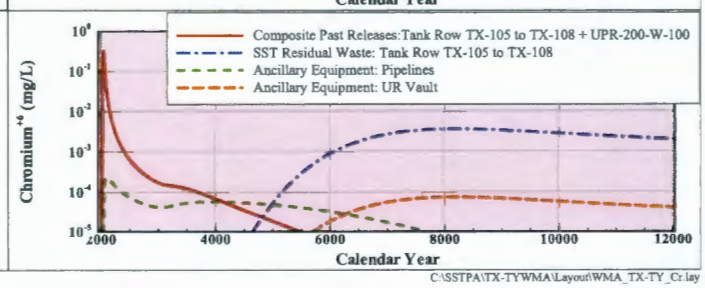

C:\SSTPA\TX-TY\WMA\Layout\WMA_TX-TY_Cr.lay

Figure 4-19. Waste Management Area TX-TY Nitrate Breakthrough Curves by Waste Source Component

Nitrate
K_d = 0.0 mL/g

Past Releases

Past Leaks from Tanks
SST Tank Row
TY-105 to TY-106

Nitrate Inventory (kg)
TY-105 = 2.41E+4
TY-106 = 1.38E+4
Sum = 3.79E+4

Peak = 3.49E+2 mg/L
Occurs in Year 2043

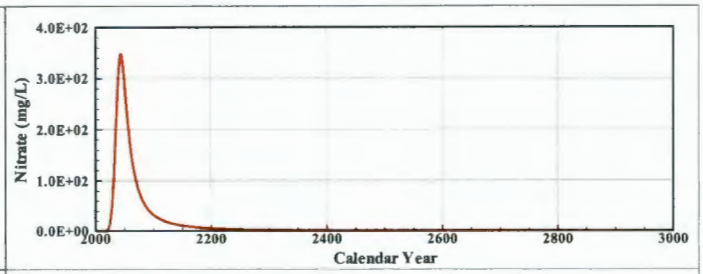

Past Shallow Release
SST Tank Row
TX-105 to TX-108

Nitrate Inventory (kg)
UPR-200-W-100 = 1.03E+3

Peak = 3.19E-1 mg/L
Occurs in Year 2094

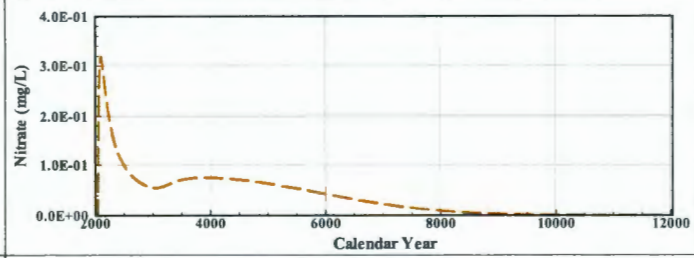

Residual Waste

Tank Residuals
SST Tank Row
TX-105 to TX-108

Nitrate Inventory (kg)
TX-105 = 9.49E+2
TX-106 = 8.30E+2
TX-107 = 9.40E+2
TX-108 = 9.29E+2
SUM = 3.65E+3

Peak = 4.56E-2 mg/L
Occurs in Year 8201

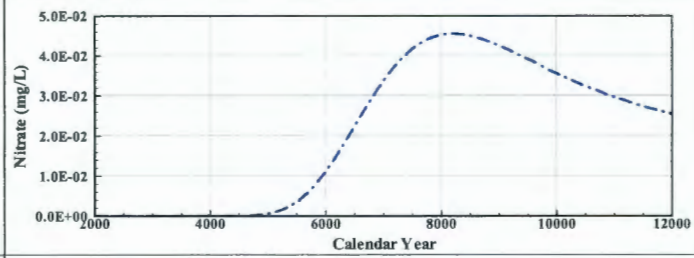

Ancillary Equipment
Pipeline Residuals

Nitrate Inventory (kg)
TX Pipelines = 3.70E+1

Peak = 1.14E-2 mg/L
Occurs in Year 2094

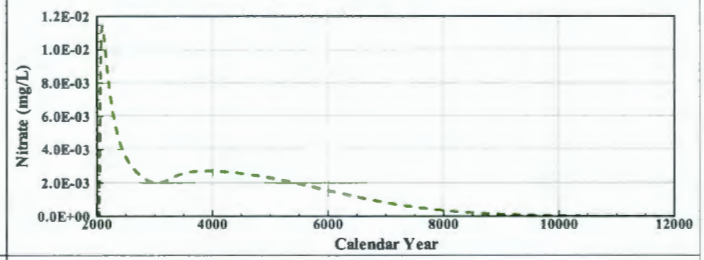

Ancillary Equipment
MUST

Nitrate Inventory (kg)
TXR-Vault = 1.04E+2

Peak = 1.30E-3 mg/L
Occurs in Year 8201

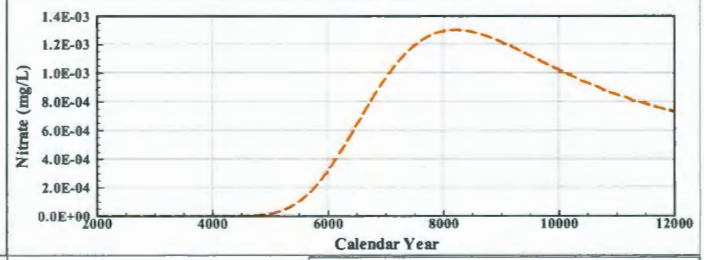

Maximum Impact

Note: Shaded background indicates a change from a linear Y-Axis to a Log Y-Axis. This change in axis scale is necessary show all curves over the range of data in the same plot.

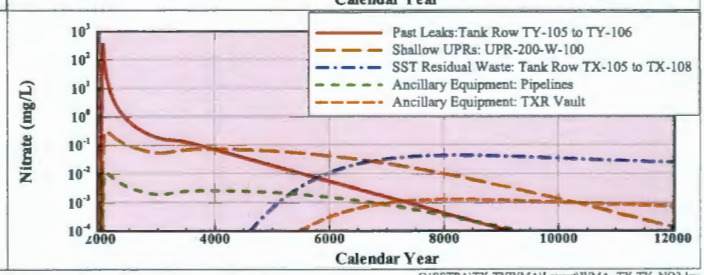

C:\SSTPA\TX-TYWMA\Layout\WMA_TX-TY_NO3.lay

Figure 4-20. Waste Management Area TX-TY Nitrite Breakthrough Curves by Waste Source Component

Nitrite
K_d = 0.0 mL/g

Past Releases

Past Leaks from Tanks
SST Tank Row
TX-105 to TX-108
Nitrite Inventory (kg)
TX-105 = 0.00E+0
TX-106 = 0.00E+0
TX-107 = 2.50E+3
TX-108 = 0.00E+0
Sum = 2.50E+3

Peak = 2.31E+1 mg/L
Occurs in Year 2043

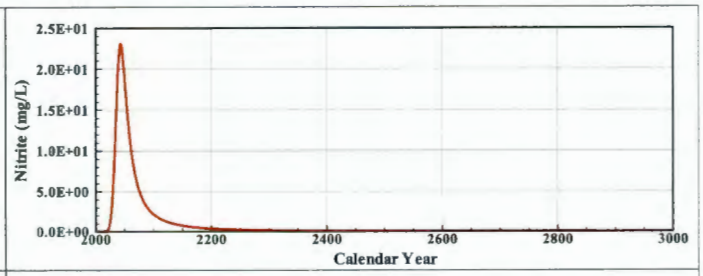

Past Shallow Release
SST Tank Row
TX-105 to TX-108
Nitrite Inventory (kg)
UPR-200-W-100 = 2.23E+1

Peak = 6.91E-3 mg/L
Occurs in Year 2094

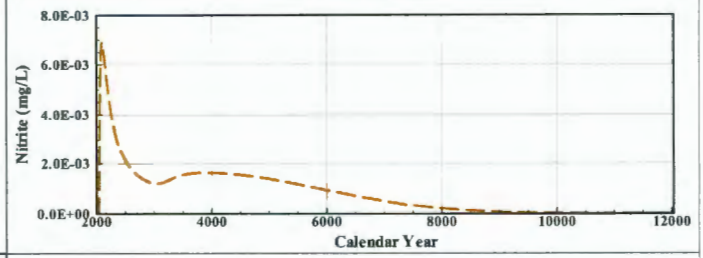

Residual Waste

Tank Residuals
SST Tank Row
TX-101 to TX-104
Nitrite Inventory (kg)
TX-101 = 1.41E+2
TX-102 = 9.20E+1
TX-103 = 8.71E+1
TX-104 = 1.12E+2
SUM = 4.32E+2

Peak = 5.42E-3 mg/L
Occurs in Year 8201

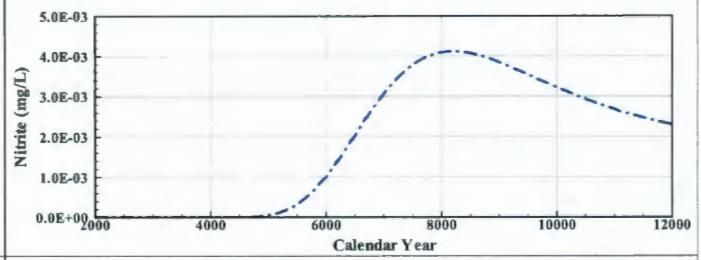

Ancillary Equipment
Pipeline Residuals

Nitrite Inventory (kg)

TX Pipelines = 9.38E+0

Peak = 2.90E-03 mg/L
Occurs in Year 2094

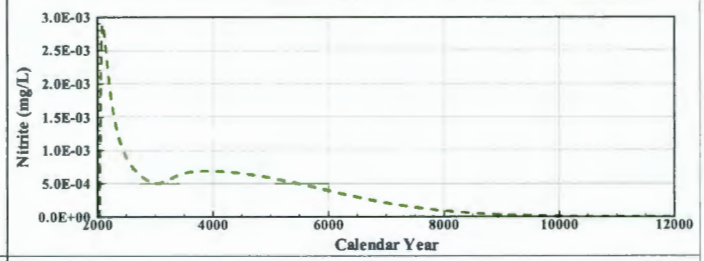

Ancillary Equipment
MUST
Nitrite Inventory (kg)

TXR-Vault = 8.72E+0

Peak = 1.09E-04 mg/L
Occurs in Year 8201

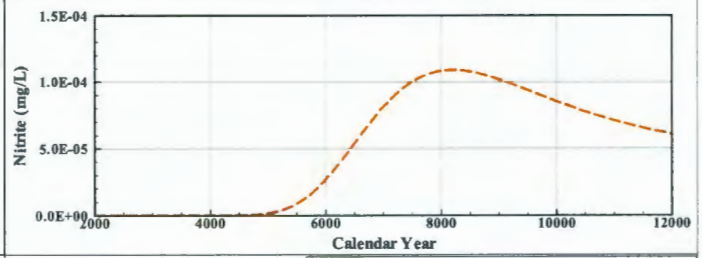

Maximum Impact

Note: Shaded background indicates a change from a linear Y-Axis to a Log Y-Axis. This change in axis scale is necessary show all curves over the range of data in the same plot.

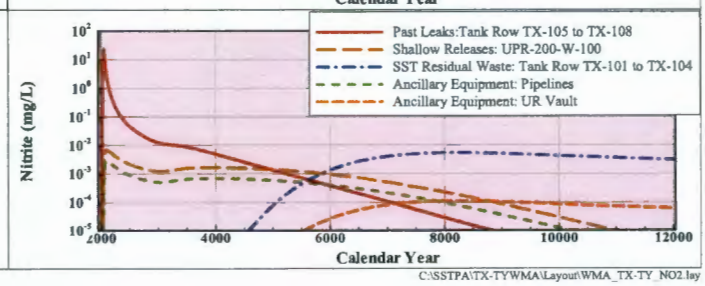

C:\SSTPA\TX-TYWMA\Layout\WMA_TX-TY_NO2.lay

Figure 4-21. Waste Management Area TX-TY Uranium Breakthrough Curves by Waste Source Component

Uranium
K_d = 0.6 mL/g

Past Releases

Past Leaks from Tanks
SST Tank Row
TY-105 to TY-106
Uranium Inventory (kg)
TY-105 = 4.11E+0
TY-106 = 2.35E+0
Sum = 6.46E+0

Max < 1.00E-5 mg/L
at End of Simulation

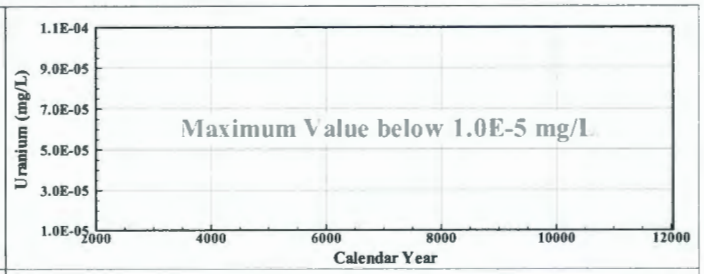

Past Shallow Release
SST Tank Row
TX-105 to TX-108
Uranium Inventory (kg)
UPR-200-W-100 = 3.00E-1

Max < 1.00E-5 mg/L
at End of Simulation

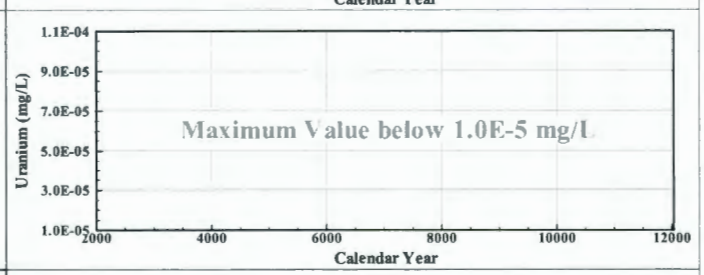

Residual Waste

Tank Residuals
SST Tank Row
TX-105 to TX-108
Uranium Inventory (kg)
TX-105 = 3.97E+2
TX-106 = 2.26E+2
TX-107 = 7.56E+1
TX-108 = 4.80E+2
SUM = 1.18E+3

Max < 1.00E-5 mg/L
at End of Simulation

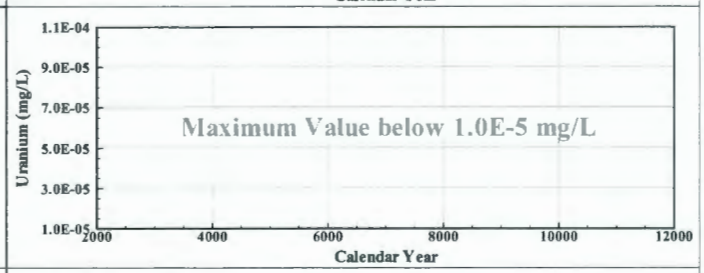

Ancillary Equipment
Pipeline Residuals

Uranium Inventory (kg)
TX Pipelines = 1.78E+01

Max < 1.00E-5 mg/L
at End of Simulation

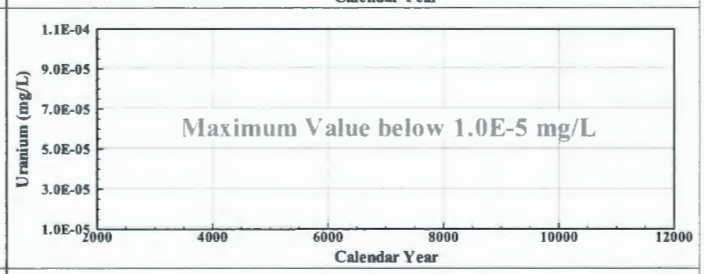

Ancillary Equipment
MUST

Uranium Inventory (kg)
TXR-Vault = 8.22E-03

Max < 1.00E-5 mg/L
at End of Simulation

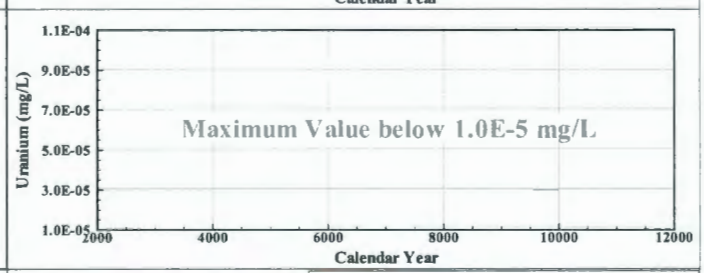

Maximum Impact

Note: Shaded background indicates a change from a linear Y-Axis to a Log Y-Axis. This change in axis scale is necessary show all curves over the range of data in the same plot.

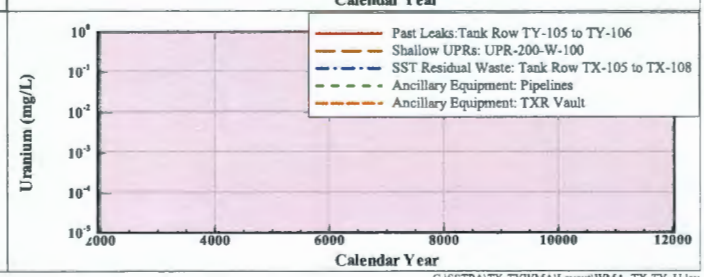

C:\SSTPA\TX-TYWMA\Layout\WMA_TX-TY_U.lay

4.6 LONG-TERM CONTAMINANT CONCENTRATIONS FOR WASTE MANAGEMENT AREA U

This section presents the results of contaminant transport modeling for the indicator contaminants selected for WMA U. The numerical calculation point for this analysis is the WMA U fenceline. Impacts of individual source components (past releases, tank residuals, and ancillary equipment residuals) are described.

Significant groundwater contamination driven by tank past leaks is predicted to reach the WMA U fenceline.

Contamination from tank residuals has minor groundwater concentration impacts late in the simulation.

The contaminant transport model developed for WMA S SX is used as a template for WMA U.

WMA U has sixteen 100-Series tanks (530,000 gal) aligned in four rows of four tanks each that are effectively parallel with the groundwater flow (Figure 2-57). In addition to the 100-Series tanks, there are four 200-Series tanks (55,000 gal) that are located approximately 100 ft to the west of the 100-Series SSTs. Tanks U-201 and U-202 are analyzed as part of the U-107 row, and tanks U-203 and U-204 are analyzed as part of the U-110 row. Reference case contaminant estimates were developed for each contaminant source component for each row based on the information in Chapter 3.0. Impacts to groundwater from individual waste components were then evaluated on a row-by-row basis. This section presents results for the indicator contaminants identified in Section 4.2.1 by the highest contributing row for each source component.

As noted in Section 3.2.2.1, contaminant transport models were developed for WMA C and WMA S-SX and are used as the templates for analyses for the 200 East Area and 200 West Area WMAs, respectively. The contaminant transport model designed for WMA S-SX was coupled with WMA U inventories to produce the results presented in this section. Subsequent versions of the SST PA will include WMA-specific contaminant transport models.

4.6.1 Previous Modeling Efforts for Waste Management Area U

No previous modeling efforts have been performed for WMA U. A draft FIR for WMA U is scheduled for publication in January 2007.

4.6.2 Waste Management Area U Fenceline Results

Sixteen contaminants in WMA U had fenceline concentrations above the effective zero within the 10,000-year simulation period. Table 4-13 defines the tank rows in WMA U and summarizes included waste sources in each row. The designation for each tank row is the lowest numbered tank in the sequence (e.g., U-101 identifies the row consisting of tanks U-101, U-102, and U-103). Such a designation is used throughout Section 4.6. The WMA U plugged and blocked pipelines are not listed in Table 4-13 because they do not coincide with a single tank row, and were therefore modeled as a separate source. Table 4-14 lists the contaminants with concentrations above the effective zero.

For all mobile contaminants, tank retrieval to the HFFACO prescribed volume and inventories estimated by Kirkbride et al. (2005) results in tank row U-107 providing the peak tank residuals fenceline concentration. Semi-mobile and less-mobile contaminants from tank residuals in WMA U are not projected to have fenceline concentrations above effective zero. The tank residuals component consists of residuals in SSTs and ancillary equipment (i.e., MUSTs). The MUST residuals were incorporated into the tank residual calculations for each row because the SST and MUST residuals were modeled in the same manner (i.e., diffusion-limited release). The ancillary equipment residuals component in WMA U consists of plugged and blocked pipelines (Lambert 2005), the 244-U double-contained receiver tank (DCRT), and the 244-UR vault. The 244-UR vault and 244-U DCRT have negligible impact on the overall fenceline BTC for the indicator contaminants discussed in this section.

Table 4-13. Waste Management Area U Tank Rows and Waste Components Included in Modeling

Tank Row	Residual Waste		Past Releases	
	Tanks	Ancillary Equipment	Tank Leaks	Past Shallow Releases
UR vault	None	244-UR vault	None	UPR 200-W-132 UPR 200-W-24
U-101	241-U-101 241-U-102 241-U-103	None	241-U-101 past leak	None
U-104	241-U-104 241-U-105 241-U-106	None	241-U-104 past leak	None
U-107	241-U-107 241-U-108 241-U-109 241-U-201 241-U-202	None	None	None
U-110	241-U-110 241-U-111 241-U-112 241-U-203 241-U-204	244-U double-contained receiver tank	241-U-110 past leak 241-U-112 past leak	None

Table 4-14. Estimated Concentrations of Contaminants from All Waste Components Appearing at the Waste Management Area U Fenceline

Radionuclides [a]				
Analyte Name	**Peak Concentration pCi/L**	**Dominant Component**	**Peak Year**	**Row with Peak Concentration**
Tritium	4.50E+03	Past releases	2040	U-104
Carbon-14	7.32E+02	Past releases	2043	U-104
Technetium-99	1.95E+04	Past releases	2043	U-104
Iodine-129	6.75E-02	Past releases	12032	U-104
Nonradionuclides [b]				
Analyte Name	**Peak Concentration mg/L**	**Dominant Component**	**Peak Year**	**Row with Peak Concentration**
Ammonia	1.32E-01	Past releases	2043	U-110
Bismuth	1.15E-01	Past releases	2043	U-104
Cerium	1.71E-04	Tank residuals	8201	U-104
Chloride	9.77E-01	Past releases	2043	U-110
Chromium	7.00E-01	Past releases	2043	U-110
Fluoride	1.52E-01	Past releases	2043	U-110
Hydroxide	1.06E-01	Tank residuals	8201	U-110
Lanthanum	6.62E-05	Tank residuals	8201	U-104
n-Butyl alcohol	1.63E-02	Past releases	2043	U-110
Neodymium	2.33E-04	Tank residuals	8201	U-104
Nitrate	3.94E+01	Past releases	2043	U-110
Nitrite	1.15E+01	Past releases	2043	U-110
Oxalate	1.38E-02	Tank residuals	8201	U-104
Phosphate	1.16E+01	Past releases	2043	U-104
Sodium	7.64E+01	Past releases	2043	U-104
Sulfate	2.07E+01	Past releases	2043	U-104

[a] The following radionuclides reached the fenceline during the modeling period, but had concentrations below the effective zero (1.0E-02 pCi/L): cobalt-60, tin-126, radium-226 + D, uranium-233, uranium-234, uranium-235 + D, uranium-236, and uranium-238 + D.

[b] The following nonradionuclides reached the fenceline during the modeling period, but had concentrations below the effective zero (1.0E-05 mg/L): aluminum, cobalt, manganese, uranium, and yttrium.

Table 4-15 provides peak fenceline concentrations for radionuclides for each tank row. Table 4-16 provides peak fenceline concentrations for nonradionuclides for each row. Both tables show concentrations from past releases and tank residuals source terms relative to the peak contributing tank row. The past releases component consists of past tank leaks and UPRs. Given that ancillary equipment residuals are modeled as tank residuals, the tank residuals portion of the tables include ancillary equipment that fall within a tank row. Although the peak concentrations from different source components occur at different times, Tables 4-15 and 4-16 show that, for any given contaminant, the peak concentration resulting from past leaks is between two and four orders of magnitude greater than that resulting from tank residuals.

The impact of mobile and semi-mobile indicator contaminants in plugged and blocked pipelines on the overall BTCs are of the same order of magnitude as the impact from residuals in some tank rows. Plugged and blocked pipelines do not fall within any one tank row and were evaluated separately. Plugged and blocked pipelines were modeled as a shallow release in the same manner as UPRs (i.e., initial depth of 30 ft bgs). Compared to contribution from either the 244-U DCRT or the 244-UR vault, plugged and blocked pipelines contribute higher concentrations for all the mobile contaminants. Semi-mobile and less-mobile contaminants from ancillary equipment residuals are not projected to occur above the effective zero concentration. Modeling results indicate that the plugged and blocked pipelines result in the following peak concentrations:

- Technetium-99: $3.15 \times 10^{+1}$ pCi/L, peak year 2094
- Hexavalent chromium: 7.50×10^{-4} mg/L, peak year 2094
- Nitrate: 3.67×10^{-2} mg/L, peak year 2094
- Nitrite: 1.69×10^{-2} mg/L, peak year 2094.

Uranium concentrations from the plugged and blocked pipeline residuals components in WMA U are effectively zero.

Table 4-15. Waste Management Area U Tank Row Peak Radionuclide Concentrations [a]

Technetium-99				
Tank Row	**Past Releases Component, Peak Year: 2043 Row UR-Vault, Peak Year: 2094**		**Tank Residuals Component, Peak Year: 8191**	
	Peak Concentration pCi/L	**Concentration Relative to Row U-104**	**Peak Concentration pCi/L**	**Concentration Relative to Row U-107**
UR vault	7.03E+00	0.04%	3.80E+00	1.89%
U-101	4.23E+03	21.69%	6.13E+01	30.50%
U-104	1.95E+04	100.00%	1.58E+01	7.86%
U-107	NA [b]	NA	2.01E+02	100.00%
U-110	9.14E+03	46.87%	7.79E+01	38.76%
Iodine-129				
Tank Row	**Past Releases Component, Max. Year: 12032**		**Tank Residuals Component**	
	Peak Concentration pCi/L	**Concentration Relative to Row U-104**	**Peak Concentration pCi/L [c]**	**Concentration Relative to Row with Peak Concentration**
UR vault	0.00E+00	0.00%	0.00E+00	NA
U-101	2.10E-02	31.11%	0.00E+00	NA
U-104	6.75E-02	100.00%	0.00E+00	NA
U-107	NA	NA	0.00E+00	NA
U-110	3.99E-02	59.11%	0.00E+00	NA

[a] Maximum values are shaded.

[b] No past releases occur in row U-107.

[c] Iodine-129 concentrations from the tank residuals component were not above effective zero (1.00E-02 pCi/L) for any row in the waste management area.

NA = not applicable

Table 4-16. Waste Management Area U Tank Row Peak Nonradionuclide Concentrations [a]

Hexavalent Chromium				
Tank Row	**Past Releases Component, Peak Year: 2043 Row UR Vault, Peak Year: 2094**		**Tank Residuals Component, Peak Year: 8201**	
	Peak Concentration mg/L	**Concentration Relative to Row U-110**	**Peak Concentration mg/L**	**Concentration Relative to Row U-107**
UR vault	1.16E-04	0.02%	2.95E-04	3.34%
U-101	4.60E-01	65.71%	7.42E-03	83.94%
U-104	3.22E-01	46.00%	6.15E-03	69.57%
U-107	NA [b]	NA	8.84E-03	100.00%
U-110	7.00E-01	100.00%	5.22E-03	59.05%
Nitrate				
Tank Row	**Past Releases Component, Peak Year: 2043 Row UR Vault, Peak Year: 2094**		**Tank Residuals Component, Peak Year: 8201**	
	Peak Concentration mg/L	**Concentration Relative to Row U-110**	**Peak Concentration mg/L**	**Concentration Relative to Row U-107**
UR vault	7.13E-03	0.02%	8.55E-04	2.79%
U-101	2.23E+01	56.60%	2.03E-02	66.12%
U-104	1.97E+01	50.00%	1.87E-02	60.91%
U-107	NA	NA	3.07E-02	100.00%
U-110	3.94E+01	100.00%	1.04E-02	33.88%
Nitrite				
Tank Row	**Past Releases Component, Peak Year: 2043 Row UR Vault, Peak Year: 2094**		**Tank Residuals Component, Peak Year: 8201**	
	Peak Concentration mg/L	**Concentration Relative to RowU-110**	**Peak Concentration mg/L**	**Concentration Relative to Row U-107**
UR vault	6.51E-04	0.01%	1.63E-04	3.34%
U-101	5.65E+00	49.13%	4.43E-03	90.78%
U-104	1.81E+00	15.74%	3.89E-03	79.71%
U-107	NA	NA	4.88E-03	100.00%
U-110	1.15E+01	100.00%	2.05E-03	42.01%
Uranium				
Uranium concentrations from the past leak and tank residuals components were not above effective zero (1.00E-05 mg/L) for any row in the waste management area.				

[a] Maximum values are shaded.

[b] No past releases occur in row U-107.

NA = not applicable

Figures 4-22 through 4-27 show the simulated BTCs for each of the six indicator contaminants. Each one of the first five plots in the figure represents a separate source component, with the bottom plot containing the previous five plots superimposed on each other to illustrate the maximum impact. Blank plots indicate cases where the concentration from a source component, for any tank row, does not exceed the effective zero over the 10,000-year simulation period. In those cases, the tank row with the greatest inventory is indicated. Again, a linear scale (y-axis) is used for the individual source component plots, but in order to include the range of data, the maximum impact plot is shown using a logarithmic scale. Each plot represents the BTC for the tank row contributing the peak concentration estimate for that source component. Also given in each of the plots is the time of the peak and the inventory for each of the like source terms in the row. The tank row containing the largest inventory is shown even though the peak concentration falls below the effective zero.

4.6.3 Discussion of Results and Conclusions for Waste Management Area U

Estimated long-term groundwater impacts resulting from three contaminant source components (i.e., past releases inventory, tank residuals inventory, and ancillary equipment residuals inventory) in WMA U are modeled. For WMA U, contamination at depth from tank row U-104 is projected to contribute to the highest past releases component concentration for all the radionuclides considered. Except for uranium, tank row U-110 is projected to contribute to the highest past releases component concentration for the nonradionuclides. Uranium is not projected to have a concentration above the effective zero for the duration of the simulation. Results also indicate that, regardless of contaminant mobility, concentrations resulting from contamination at depth are orders of magnitude higher than those resulting from the tank residuals component. For WMA U, tank row U-107 is responsible for the peak concentration for all contaminants having concentrations greater than the effective zero. Although the 244-UR vault and 244-U DCRT ancillary equipment residuals provide negligible contribution to the overall fenceline concentration for mobile and semi-mobile contaminants, plugged and blocked pipelines provide contributions equivalent in magnitude to some WMA U tank row residuals.

Tank retrieval to the HFFACO prescribed volume and inventories estimated by Kirkbride et al. (2005) results in an impact from tank residuals that is two to four orders of magnitude below that of past releases. Note that, for the tank residuals and for all indicator contaminants, only the row with the maximum impact is shown; the other tank rows are usually within a factor of 3 below the row with peak concentration, with tank row UR vault almost a factor of 30 lower (Tables 4-15 and 4-16).

Due to existing vadose zone contamination and the maximum operation recharge occurring during that period, contaminants with high mobility (K_d less than 0.2 mL/g) exhibit concentration peaks that occur early in the simulation and prior to emplacement of the Modified RCRA Subtitle C Barrier. Contaminants with lower mobility (K_d = 0.2 mL/g or greater) exhibit increasing concentrations at the end of the simulation period, dominated by the contamination at depth source component.

Figure 4-22. Waste Management Area U Technetium-99 Breakthrough Curves by Waste Source Component

Technetium-99
K_d = 0.0 mL/g

Past Releases

Past Leaks from Tanks Tank Row U-104 to U-106

^{99}Tc Inventory

U-104 = 2.1E+0 Ci
U-105 = 0.0E+0 Ci
U-106 = 0.0E+0 Ci
Sum = 2.1E+0 Ci

Peak = 1.95E+4 pCi/L
Occurs in Year 2043

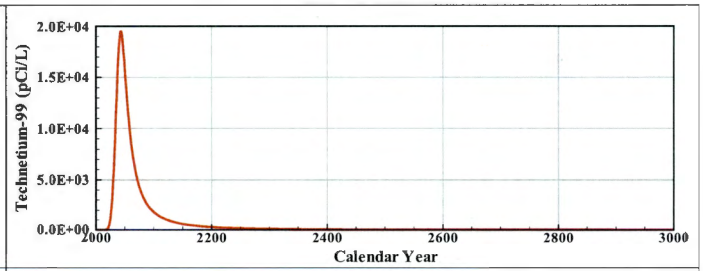

Past Shallow Release in Same Pathline

^{99}Tc Inventory

UPR-200-W-24 = 9.4E-4 Ci
UPR-200-W-132 = 2.2E-2 Ci
Sum = 2.3E-2 Ci

Peak = 7.03E+0 pCi/L
Occurs in Year 2094

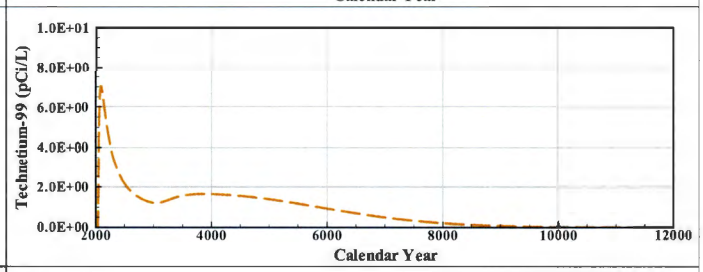

Residual Waste

Tank Residuals SST Tank Row U-107 to U-109, U-201, U-202

^{99}Tc Inventory
U-107 = 6.62E+0 Ci
U-108 = 3.07E+0 Ci
U-109 = 6.73E+0 Ci
U-201 = 3.80E-3 Ci
U-202 = 3.40E-3 Ci
Sum = 1.64E+1 Ci

Peak = 2.01E+2 pCi/L
Occurs in Year 8191

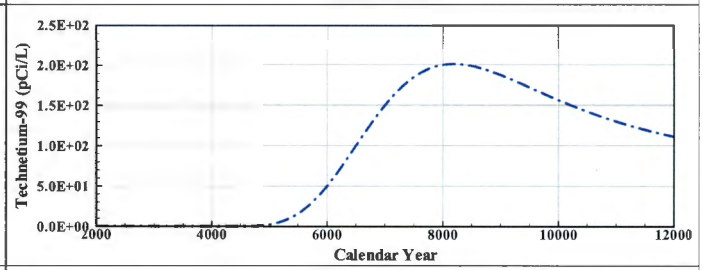

Ancillary Equipment Pipeline Residuals

^{99}Tc Inventory

U Pipelines = 1.0E-1 Ci

Peak = 3.15E+1 pCi/L
Occurs in Year 2094

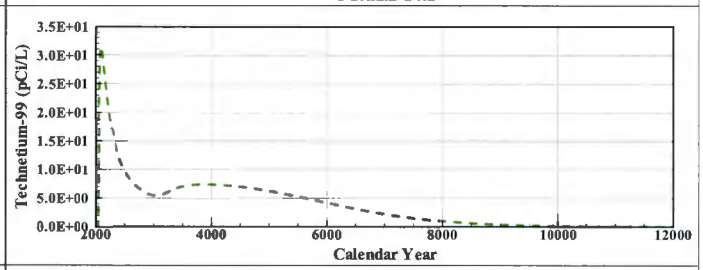

Ancillary Equipment MUST

^{99}Tc Inventory

UR-Vault = 3.0E-1 Ci

Peak = 3.8 pCi/L
Occurs in Year 8191

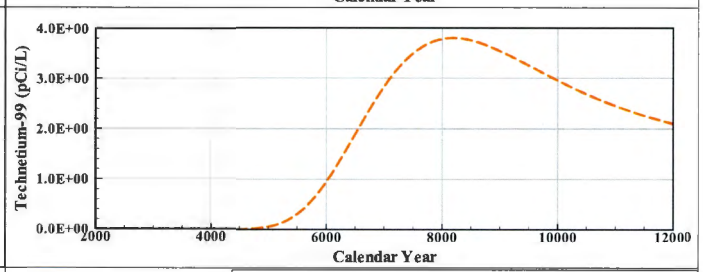

Maximum Impact

Note: Shaded background indicates a change from a linear Y-Axis to a Log Y-Axis. This change in axis scale is necessary show all curves over the range of data in the same plot.

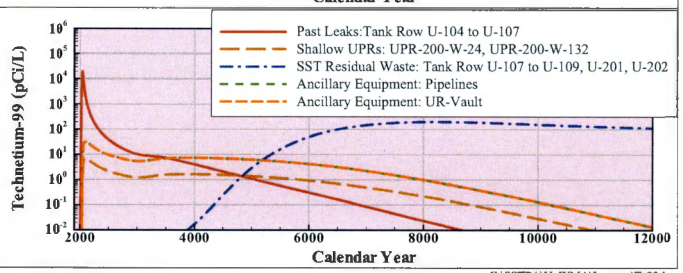

C:\SSTPA\U_WMA\Layouts\Tc99.lay

Figure 4-23. Waste Management Area U Iodine-129 Breakthrough Curves by Waste Source Component

Iodine-129 **K_d = 0.2 mL/g**		
Past Releases	**Past Leaks from Tanks Tank Row U-104 to U-106** ^{129}Iodine Inventory U-104 = 2.4E-3 Ci U-105 = 0.0 Ci U-106 = 0.0 Ci Sum = 2.4E-3 Ci Peak = 6.75E-2 pCi/L Occurs in Year 12,032	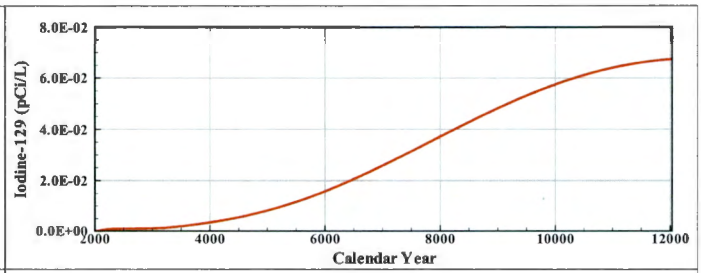
	Past Shallow Release in Same Pathline ^{129}Iodine Inventory UPR-200-W-24 = 4.2E-7 Ci UPR-200-W-132 = 2.5E-5 Ci Sum = 2.5E-5 Ci Max < 0.01 pCi/L Occurs in Year 12,032	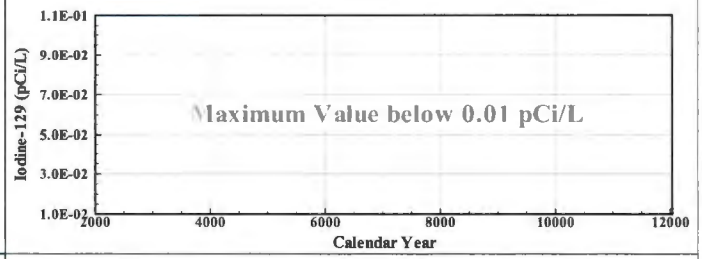
Residual Waste	**Tank Residuals SST Tank Row U-107 to U-109, U-201, U-202** ^{129}Iodine Inventory U-107 = 3.1E-4 Ci U-108 = 2.6E-4 Ci U-109 = 2.7E-4 Ci U-201 = 2.8E-7 Ci U-202 = 3.6E-7 Ci Sum = 8.4E-4 Ci Max < 0.01 pCi/L Occurs in Year 12,032	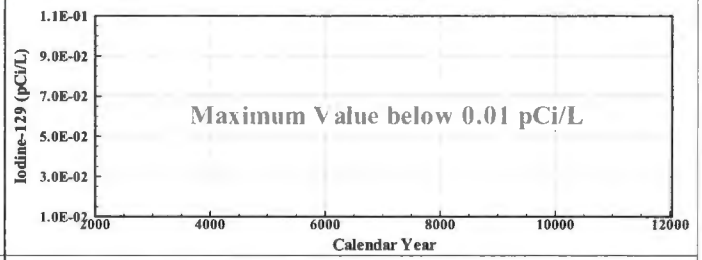
	Ancillary Equipment Pipeline Residuals ^{129}Iodine Inventory U Pipelines = 1.5E-4 Ci Max < 0.01 pCi/L Occurs in Year 12,032	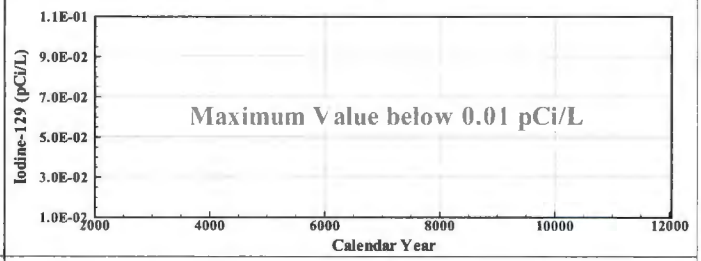
	Ancillary Equipment MUST ^{129}Iodine Inventory UR-Vault = 4.25E-5 Ci Max < 0.01 pCi/L Occurs in Year 12,032	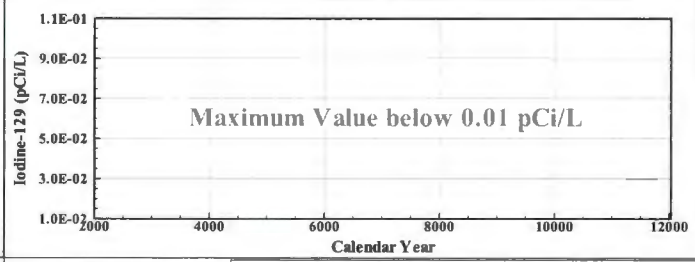
Maximum Impact Note: Shaded background indicates a change from a linear Y-Axis to a Log Y-Axis. This change in axis scale is necessary show all curves over the range of data in the same plot.		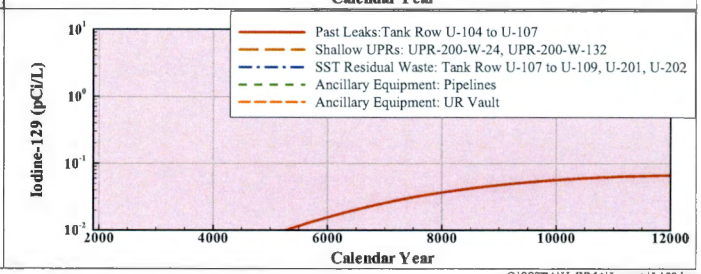

C:\SSTPA\U_WMA\Layouts\I-129.lay

Figure 4-24. Waste Management Area U Hexavalent Chromium Breakthrough Curves by Waste Source Component

Chromium
K_d = 0.0 mL/g

Past Releases

Past Leaks from Tanks
SST Tank Row
U-110 to U-112, U-203, U-204

Chromium Inventory
U-110 = 8.30E+0 kg
U-111 = 0.00E+0 kg
U-112 = 6.77E+1 kg
U-202 = 0.00E+0 kg
U-203 = 0.00E+0 kg
Sum = 7.6E+1 kg

Peak = 7.00E-1 mg/L
Occurs in Year 2043

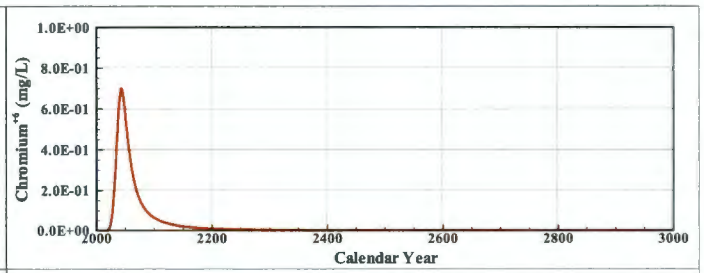

Past Shallow Release
in Same Pathline

Chromium Inventory
UPR-200-W-24 = 9.00E-3 kg
UPR-200-W-132 = 1.26E-1 kg
Sum = 1.35E-1 kg

Peak = 1.2E-4 mg/L
Occurs in Year 2094

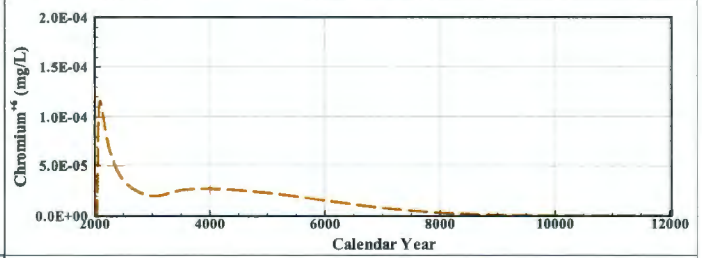

Residual Waste

Tank Residuals
SST Tank Row
U-107 to U-109, U-201, U-202

Chromium Inventory
U-107 = 2.45E+2 kg
U-108 = 1.72E+2 kg
U-109 = 2.89E+2 kg
U-201 = 4.00E-1 kg
U-202 = 3.00E-1 kg
Sum = 7.07E+2 kg

Peak = 8.84E-3 mg/L
Occurs in Year 8201

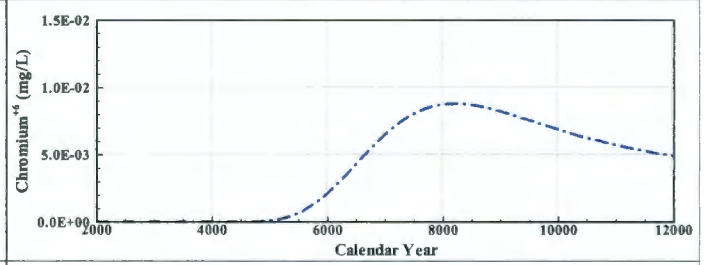

Ancillary Equipment
Pipeline Residuals

Chromium Inventory

U Pipelines = 2.42E+0 kg

Peak = 7.5E-4mg/L
Occurs in Year 2094

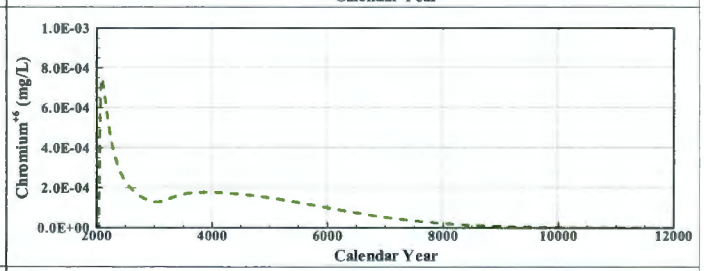

Ancillary Equipment
MUST

Chromium Inventory

UR-Vault = 2.36E+1 kg

Peak = 3.0E-4 mg/L
Occurs in Year 8201

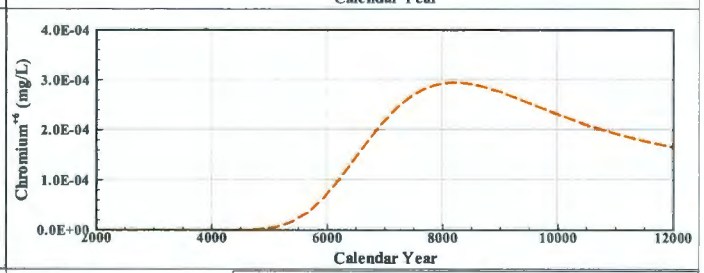

Maximum Impact

Note: Shaded background indicates a change from a linear Y-Axis to a Log Y-Axis. This change in axis scale is necessary show all curves over the range of data in the same plot.

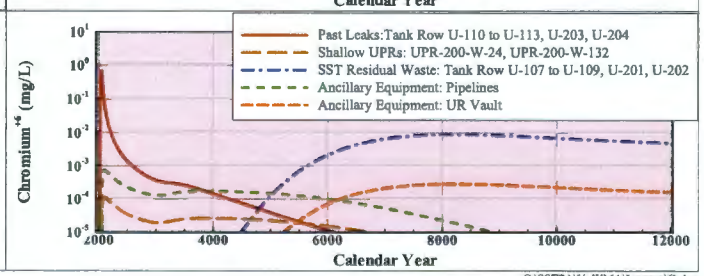

C:\SSTPA\U_WMA\Layouts\Cr.lay

Figure 4-25. Waste Management Area U Nitrate Breakthrough Curves by Waste Source Component

Nitrate K_d = 0.0 mL/g		
Past Releases	**Past Leaks from Tanks SST Tank Row U-110 to U-112, U-203, U-204** Nitrate Inventory U-110 = 6.92E+2 kg U-111 = 0.00E+0 kg U-112 = 3.59E+2 kg U-202 = 0.00E+0 kg U-203 = 0.00E+0 kg Sum = 4.28E+3 kg Peak = 3.94E+1 mg/L Occurs in Year 2043	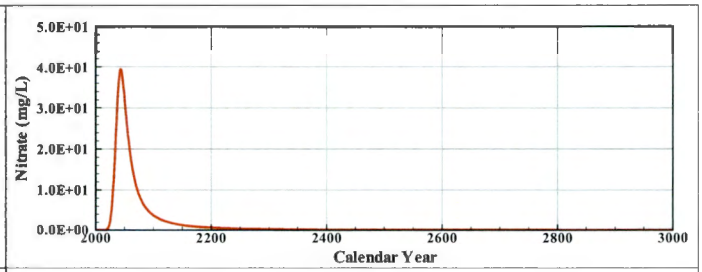
	Past Shallow Release in Same Pathline Nitrate Inventory UPR-200-W-24 = 1.6E+0 kg UPR-200-W-132 = 2.15E+1 kg Sum = 2.31E+1 kg Peak = 7.1E-3 mg/L Occurs in Year 2094	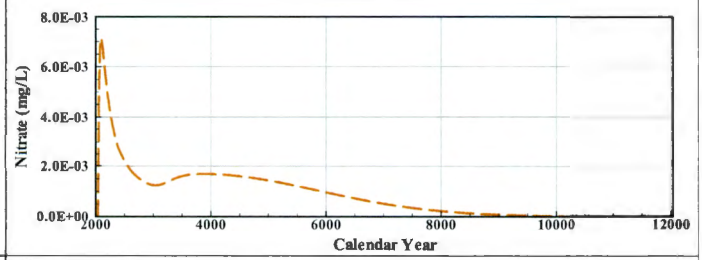
Residual Waste	**Tank Residuals SST Tank Row U-107 to U-109, U-201, U-202** Nitrate Inventory U-107 = 9.47E+2 kg U-108 = 7.39E+2 kg U-109 = 7.27E+2 kg U-201 = 2.38E+1 kg U-202 = 2.01E+1 kg Sum = 2.45E+3 kg Peak = 3.07E-2 mg/L Occurs in Year 8201	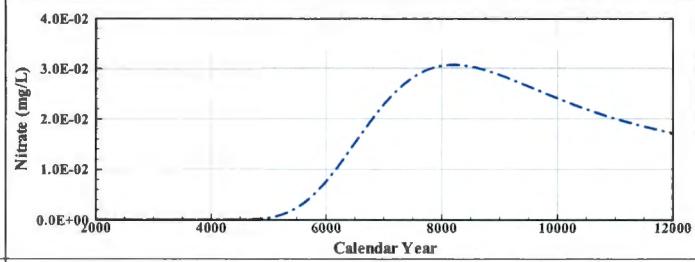
	Ancillary Equipment Pipeline Residuals Nitrate Inventory U Pipelines = 1.19E+2 kg Peak = 3.7E-2 mg/L Occurs in Year 2094	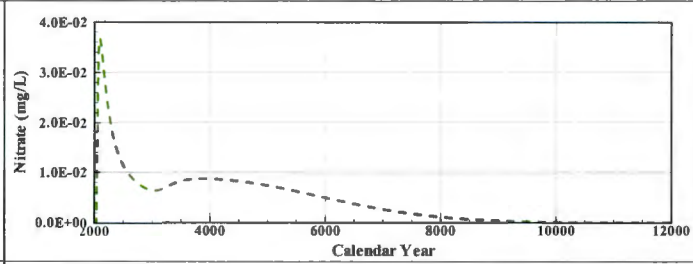
	Ancillary Equipment MUST Nitrate Inventory UR-Vault = 6.85E+1 kg Peak = 8.5E-4 mg/L Occurs in Year 8201	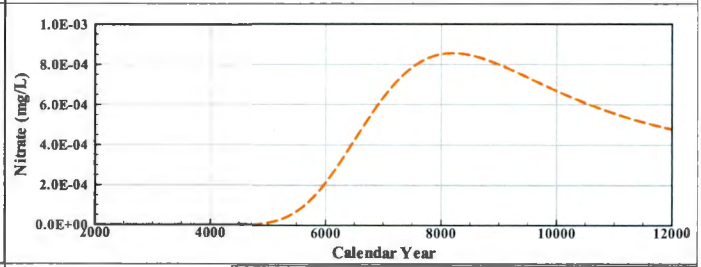
Maximum Impact Note: Shaded background indicates a change from a linear Y-Axis to a Log Y-Axis. This change in axis scale is necessary show all curves over the range of data in the same plot.		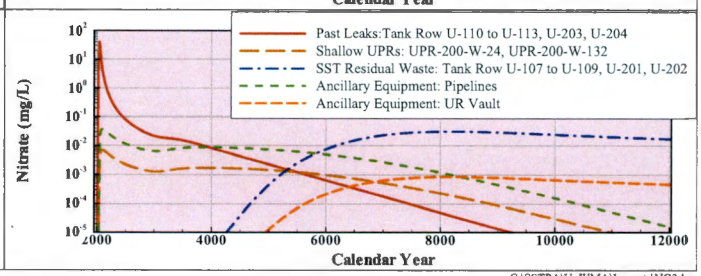

C:\SSTPA\U_WMA\Layouts\NO3.lay

Figure 4-26. Waste Management Area U Nitrite Breakthrough Curves by Waste Source Component

Nitrite
K_d = 0.0 mL/g

Past Releases

Past Leaks from Tanks
SST Tank Row
U-110 to U-112, U-203, U-204

Nitrite Inventory
U-110 = 3.47E+2 kg
U-111 = 0.00E+0 kg
U-112 = 9.05E+2 kg
U-202 = 0.00E+0 kg
U-203 = 0.00E+0 kg
Sum = 1.25E+3 kg

Peak = 1.15E+1 mg/L
Occurs in Year 2043

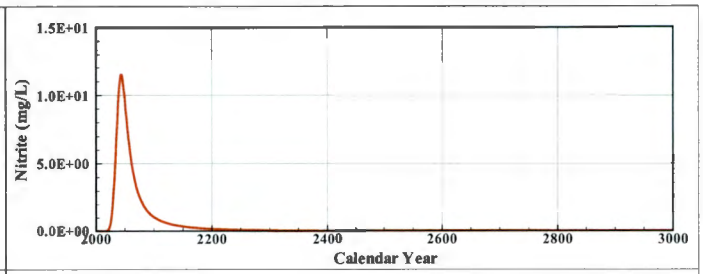

Past Shallow Release
in Same Pathline

Nitrite Inventory
UPR-200-W-24 = 1.0E-1 kg
UPR-200-W-132 = 2.0E+0 kg
Sum = 2.1E+0 kg

Peak = 6.5E-4 mg/L
Occurs in Year 2094

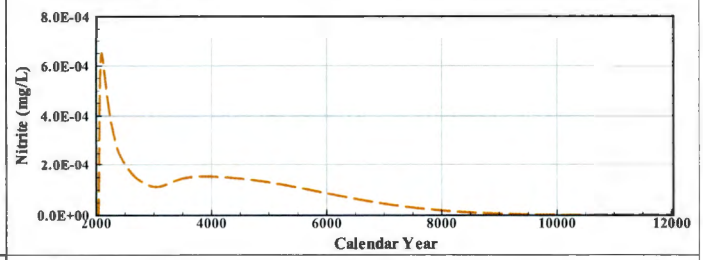

Residual Waste

Tank Residuals
SST Tank Row
U-107 to U-109, U-201, U-202

Nitrite Inventory
U-107 = 1.08E+2 kg
U-108 = 1.42E+2 kg
U-109 = 1.34E+2 kg
U-201 = 3.60E+0 kg
U-202 = 3.30E+0 kg
Sum = 3.91E+2 kg

Peak = 4.9E-3 mg/L
Occurs in Year 8201

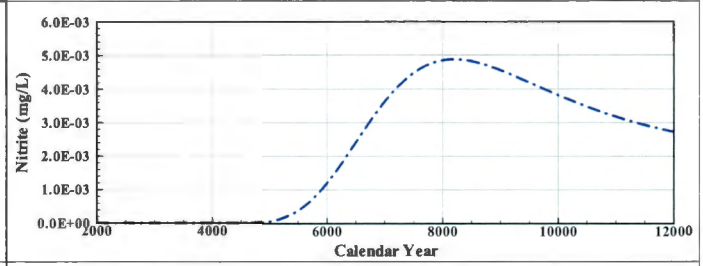

Ancillary Equipment
Pipeline Residuals

Nitrite Inventory

U Pipelines = 5.45E+1 kg

Peak = 1.7E-2 mg/L
Occurs in Year 2094

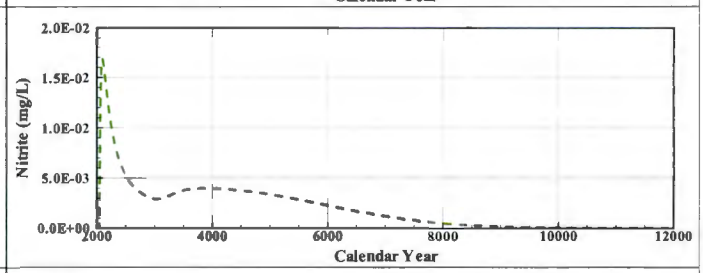

Ancillary Equipment
MUST

Nitrite Inventory

UR-Vault = 1.3E+1 kg

Peak = 1.6E-4 mg/L
Occurs in Year 8201

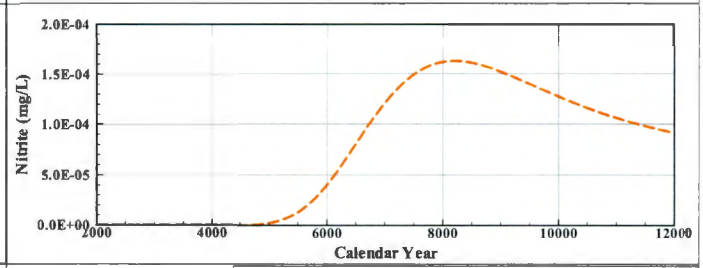

Maximum Impact

Note: Shaded background indicates a change from a linear Y-Axis to a Log Y-Axis. This change in axis scale is necessary show all curves over the range of data in the same plot.

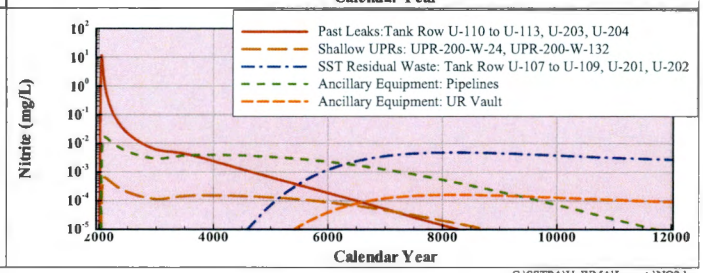

C:\SSTPA\U_WMA\Layouts\NO2.lay

Figure 4-27. Waste Management Area U Uranium Breakthrough Curves by Waste Source Component

Uranium
K_d = 0.6 mL/g

Past Releases

Past Leaks from Tanks
SST Tank Row
U-104 to U-106

Uranium Inventory

U-104 = 1.79E+2 kg
U-105 = 0.00E+0 kg
U-106 = 0.00E+0 kg
Sum = 1.79E+2 kg

Max < 1e-5 mg/L
by End of Simulation

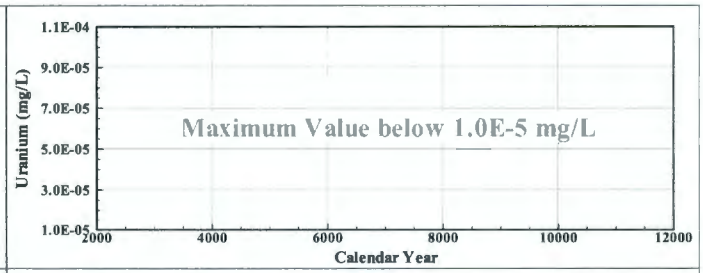

Past Shallow Release
in Same Pathline

Uranium Inventory

UPR-200-W-24 = 1.30E-1 kg
UPR-200-W-132 = 1.80E+0 kg
Sum = 1.93E+0 kg

Max < 1e-5 mg/L
by End of Simulation

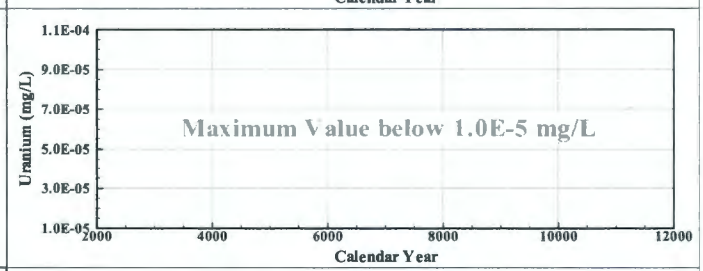

Residual Waste

Tank Residuals
SST Tank Row
U-104 to U-106

Uranium Inventory

U-104 = 4.82E+1 kg
U-105 = 3.42E+2 kg
U-106 = 8.96E+1 kg
Sum = 4.80E+2 kg

Max < 1e-5 mg/L
by End of Simulation

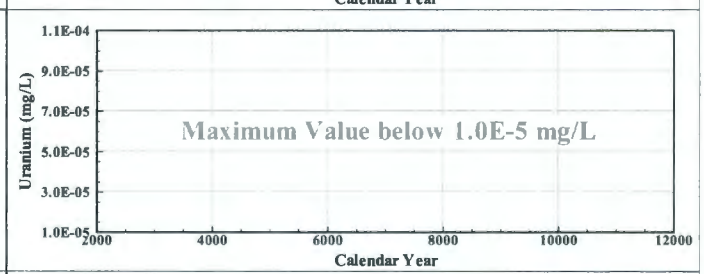

Ancillary Equipment
Pipeline Residuals

Uranium Inventory

U Pipelines = 1.40E-1 kg

Max < 1e-5 mg/L
by End of Simulation

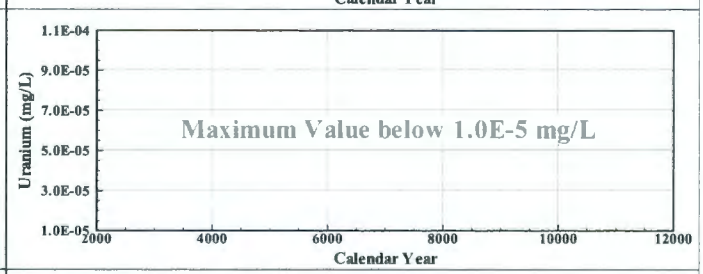

Ancillary Equipment
MUST

Uranium Inventory

UR-Vault = 1.32E+1 kg

Max < 1e-5 mg/L
by End of Simulation

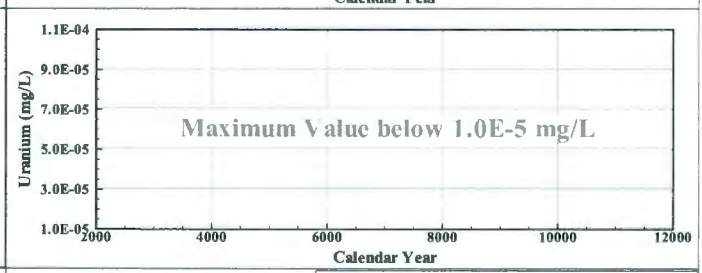

Maximum Impact

Note: Shaded background indicates a change from a linear Y-Axis to a Log Y-Axis. This change in axis scale is necessary show all curves over the range of data in the same plot.

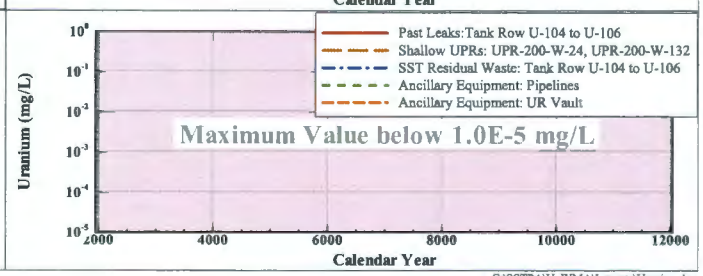

C:\SSTPA\U_WMA\Layouts\Uranium.lay

4.7 LONG-TERM CONTAMINANT CONCENTRATIONS FOR WASTE MANAGEMENT AREA C

This section presents the results of contaminant transport modeling for the indicator contaminants selected for WMA C. The numerical calculation point for this analysis is the WMA C fenceline. Impacts of individual source components (past releases, tank residuals, and ancillary equipment residuals) are described.

> Significant groundwater contamination driven by tank past leaks is predicted to reach the WMA C fenceline.
>
> Contamination from tank residuals has minor groundwater concentration impacts late in the simulation.

WMA C has sixteen primary tanks: twelve 100-Series tanks (530,000 gal) arranged in three rows of four, and four 200-Series tanks (55,000 gal) arranged in a single row (Figure 2-63). Reference case contaminant estimates were developed for each row based on the information in Chapter 3.0. Impacts to groundwater from individual waste components were then evaluated on a row-by-row basis. For the indicator contaminants identified in Section 4.2.1, this section presents results for the tank row contributing the maximum impact for each source component.

4.7.1 Previous Modeling Efforts for Waste Management Area C

Long-term contaminant fate and transport modeling was conducted for WMA C and presented in *Single-Shell Tank System Closure Plan* (Lee 2004). The same six primary contaminants from Lee (2004) were evaluated in this SST PA. The physical conceptual model developed in Lee (2004) is the pre-cursor to the model presented here in the SST PA. Notable differences between the modeling efforts used in Lee (2004) and in this SST PA include the following:

- **Degraded RCRA Subtitle C Barrier Recharge Rate**: Lee (2004) used a conservative degraded barrier recharge rate of 3.5 mm/yr (i.e., after year 2550), the same rate as estimated for the pre-disturbance (i.e., pre-Hanford Site) time period. The degraded barrier recharge rate used in the SST PA is 1.0 mm/yr. The lower degraded barrier recharge rate has a profound effect on delaying the arrival of peak fenceline groundwater concentrations from residual tank waste components. The difference in peak arrival times for residual tank waste components (i.e., diffusional release mechanism) is approximately 5,000 years.
- **Lower Diffusion Coefficient for Release of Tank Residuals**: Both models use a diffusional release mechanism for modeling release of contaminants from stabilized residual waste forms (i.e., residual tank waste stabilized with grout). Lee (2004) used a diffusion coefficient of 6.0×10^{-7} cm^2/s, while the SST PA uses a lower value of 1.0×10^{-9} cm^2/s based on results presented in Harbour et al. (2004).
- **Discussion of Peak Groundwater Concentrations and Included Sources**: Lee (2004) presents estimated peak fenceline groundwater concentrations as the cumulative contribution from all waste sources averaged across the entire fenceline. In the SST PA, peak fenceline concentrations are discussed on a row-by-row analysis basis focusing on the subset of waste components and source types aligned in a row that contribute

the highest groundwater concentrations projected over a 40-m section of the WMA fenceline.

Estimated peak fenceline groundwater concentrations from both past releases sources and residual waste components are generally within an order of magnitude despite the differences noted above. The biggest difference lies in the arrival of peak groundwater concentrations attributed to stabilized residual waste forms. Simulated peak concentrations resulting from tank residuals occur much later in the SST PA due to the use of a lower recharge estimate for the degraded barrier and the use of a lower diffusion coefficient. Differences in inventory assigned to each waste component are another contributing factor to resulting in differences in the magnitude and timing of peak fenceline concentrations.

4.7.2 Waste Management Area C Fenceline Results

Twenty-seven contaminants in WMA C had fenceline concentrations above the effective zero within the 10,000-year simulation period. Table 4-17 defines the tank rows in WMA C and summarizes included waste sources in each row. The designation for each tank row is the lowest numbered tank in the sequence (e.g., C-101 identifies the row consisting of tanks C-101, C-104, C-107, and C-110). Such a designation is used throughout Section 4.7. The WMA C plugged and blocked pipelines are not listed in Table 4-17 because they do not coincide with a single tank row and were therefore modeled as a separate source. Table 4-18 lists the contaminants with fenceline concentrations above the effective zero indicating the dominant source term and the tank row resulting in the peak concentration.

Table 4-17. Waste Management Area C Tank Rows and Waste Components Included in Modeling

Tank Row	Residual Waste		Past Releases	
	Tanks	Ancillary Equipment	Tank Leaks	Past Shallow Releases
C-101	241-C-101 241-C-104 241-C-107 241-C-110	None	241-C-101 past leak 241-C-110 past leak	UPR-200-E-107
C-102	241-C-102 241-C-105 241-C-108 241-C-111	None	241-C-105 past leak 241-C-111 past leak	None
C-103	241-C-103 241-C-106 241-C-109 241-C-112	241-C-301 catch tank	None	None
C-201	241-C-201 241-C-202 241-C-203 241-C-204	None	241-C-201 past leak 241-C-202 past leak 241-C-203 past leak 241-C-204 past leak	None
CR vault	None	241-CR vault	None	UPR-200-E-81 UPR-200-E-82 UPR-200-E-86